Mechanochemistry as an Enabling Technology for Synthesis and Catalysis

Matthew Thomas James Williams

This thesis is submitted for the degree of Doctor of Philosophy (PhD) at Cardiff University

December 2022

Abstract

This thesis describes the investigations into solvent-minimised catalytic transformations, under mechanochemical conditions.

Initially, the aza-Morita-Baylis-Hillman reaction was explored under ball-milling conditions, which built upon pioneering work from Mack and co-workers. This study revealed that the reaction could be carried out with decreased reaction times in comparison to solution-phase analogues and with the elimination of bulk reaction solvent, as toluene was used in liquid-assisted grinding quantities. A broad substrate scope was demonstrated, along with a scale up to 3 mmol. Additionally, asymmetric induction was performed using a cinchona-alkaloid derived tertiary amine catalyst. Finally, comparisons of the protocol to neat and solution-phase processes revealed the superiority of the reaction compared to these other techniques.

Next, a nickel-catalysed cross-electrophile coupling reaction between heteroaryl halides and alkyl halides was investigated. This built on previous research within the Browne group, where cross-electrophile coupling was carried out mechanochemically. The key benefits of this previous work were the circumvention of inert atmospheres and mechanical activation of the terminal metal reductant (zinc or manganese). The previous work was expanded to tolerate this new class of substrate, due to the importance of heteroaromatic compounds in drug discovery. This process required a re-optimisation of the previous reaction conditions, revealing that an amidine ligand was best for effective cross-coupling. Broad scope of a variety of *N*-heteroaryl halides was demonstrated, along with a scale up to 6 mmol. Solution-phase comparisons revealed the vast improvements of the protocol, including the aforementioned circumvention of inert atmospheres and terminal reductant activation. Additionally, the process was shown to be effective irrespective of the form of the zinc reductant used, which can be an issue encountered in large-scale processes.

The final research chapter describes the investigation into the nickel-catalysed intramolecular dicarbofunctionalisation of alkenes, which built on the previous cross-electrophile coupling work and was an unexplored type of reactivity under mechanochemical conditions. This reactivity allowed synthesis of 3,3-disubsituted heterocyclic compounds, namely oxindoles, using alkyl halides as a second coupling partner. Manganese was found to be a more effective terminal reductant than zinc and a higher filling degree of the milling jar had a positive effect on the product yield. Good substrate scope was demonstrated, including the tolerance of bromobenzene as an sp^2 electrophile. The process was scaled up to 10 mmol, also, and asymmetric induction was demonstrated by using a chiral ligand, giving moderate enantioinduction. Finally, solution-phase comparisons revealed that the process is largely ineffective without the explicit activation of the manganese reductant, which was demonstrated by mechanochemically grinding the manganese before adding it to a solution reaction.

Preface

Some of the work presented within this thesis can also be found in the following publications:

1. **Expedient Organocatalytic Aza-Morita–Baylis–Hillman Reaction through Ball-Milling** Matthew T. J. Williams, Louis C. Morrill*, and Duncan L. Browne*, *ACS Sustainable Chem. Eng.*, 2020, **8**, 17876–17881. *Presented in Chapter 2.*

2. **Mechanical Activation of Zero-Valent Metal Reductants for Nickel-Catalyzed Cross-Electrophile Coupling** Andrew C. Jones†, Matthew T. J. Williams†, Louis C. Morrill*, and Duncan L. Browne*, *ACS Catal.*, 2022, **12**, 13681–13689. *Presented in Chapter 3.*

†: Joint-first authors

*: Corresponding author

Acknowledgements

The work carried out in this thesis would not have been possible without the guidance and support I have received from several people over the past 4 years. This includes my two supervisors Dr Louis Morrill and Dr Duncan Browne, who have nurtured and helped develop my skills as a researcher and chemist. I am very grateful for the support that has been given to me by these two and the pressure-free environment they have instilled, allowing me the freedom to carry out the research that has interested me the most.

Another special mention goes out to my mum who has always supported me and believed in me no matter what I have done in life. I would not be where I am today without her love and support.

Additionally, I would like to thank the members of the Morrill and Browne research groups, past and present, for all their help, guidance, and plenty of laughs along the way. This includes Alex and Andy, who have been there since day one of my undergraduate. James, Albara, Hussain, Deepak, Betty, Salma, Dan, Will, Tom, and Abdulbari, who I have shared large amounts of my PhD time with at Cardiff. Additionally, I would like to thank the remaining Browne group members in London, Harry, Rob, Sarah, Jamie, and Lorenzo, who gave me a very enjoyable two months at UCL. I wish each and every one of you the very best in the future.

Finally, I would like to thank my funders and the staff at Cardiff University's School of Chemistry for allowing me to conduct research.

Abbreviations

3-HQD – 3-hydroxyquinuclidine

AE – atom economy

BHT – 2,6-Di-*tert*-butyl-4-methylphenol

cod – 1,5-cyclooctadiene

d.r. – diastereomeric ratio

DABCO – 1,4-diazabicyclo[2.2.2]octane

DCF – dicarbofunctionalisation

DCM – dichloromethane

DMA – *N*,*N*-dimethylacetamide

DME – dimethoxyethane

DMF – *N*,*N*-dimethylformamide

DMSO – dimethylsulfoxide

EDG – electron donating group

ee – enantiomeric excess

E-factor – environmental factor

equiv. – equivalents

EWG – electron withdrawing group

FDA – Food and Drug Administration

GC – gas chromatography

HOMO – highest-occupied molecular orbital

HPLC – high performance liquid chromatography

IUPAC - International Union of Pure and Applied Chemistry

LAG – liquid-assisted grinding

LR-MS – low resolution mass spectrometry

LUMO – lowest-occupied molecular orbital

MBH – Morita-Baylis-Hillman

MOF – metal-organic framework

NCTS – *N*-cyano-*N*-phenyl-4-(methylbenzene)sulfonamide

NHC – nucleophilic heterocyclic carbene

NMP – *N*-methyl-2-pyrrolidinone

NMR – nuclear magnetic resonance

phen – phenanthroline

PID – proportional–integral–derivative

PMHS – polymethylhydrosiloxane

PMI – process mass intensity

rpm – revolutions per minute

rt – room temperature

SET – single-electron transfer

TBAB – tetrabutylammonium bromide

TDAE – tetrakis(dimethylaminoethylene)

TEMPO – 2,2,6,6-tetramethylpiperidine 1-oxyl, free radical

THF – tetrahydrofuran

TSE – Twin-screw extruder

XEC – cross-electrophile coupling

α-IC – α-isocupreine

β-ICD – β-isocupreidine

Table of Contents

Chapter 1: Mechanochemistry as an Enabling Technology

1. Introduction

1.1. What is Mechanochemistry?

The International Union of Pure and Applied Chemistry (IUPAC) has defined mechanochemistry as a "chemical process that is induced by the direct absorption of mechanical energy".[1] This mechanical energy can be imparted by a variety of forces, such as shearing, stretching, and grinding forces. These energy inputs contrast with that which are typically encountered in solution-phase processes, where thermal energy is generally accepted to be the most relevant energy input. Many techniques exist for applying mechanical forces, such as atomic-force microscopes,[2–4] sonicators,[5] ultrasound,[6–9] grinding by hand using a mortar and pestle, ball-mills,[10–17] and twin-screw extruders.[18,19] All mechanochemical techniques offer the ability to carry out reactions in the absence of reaction solvent. This is an important benefit as the reliance on solvents is a huge issue, especially in large scale processes, where the disposal of the solvent waste is required after a process, which can be expensive and labour intensive.[20] This has resulted in an increased use of 'green solvents', however, these more environmentally benign solvents still require treatment to dispose of or recycle.[21–23] This has culminated in mechanochemistry being identified as a "Chemical innovation that will change our world" by IUPAC, in 2019.[24] Hence, the exploration and development of mechanochemical processes and its assessment by the mainstream chemistry community is important for the future of sustainable methodologies. Herein, the previously highlighted mechanochemical techniques will be described, focusing on the important parameters of each method and a selection of synthesis-based literature examples for each technique.

1.2. Mechanochemical Techniques

1.2.1. Mortar and Pestle Grinding

Manual grinding of materials can be traced back thousands of years; however, the use of a mortar and pestle as a technique for synthesis is a relatively recent development, with most historical examples involving mechanical alloying.[25] A recent example of mortar and pestle grinding being utilised for organic synthesis was reported by Kapoor

and co-workers, where they successfully synthesised dihydropyridine derivatives in a multi-component reaction starting from aldehydes, dimedone, ammonium acetate, and either β-ketoesters or α-cyano compounds (Scheme 1.1.).[26] Grinding these reagents by hand, in the absence of solvent, they were able to obtain excellent yields of their products in reaction times as short as 12 minutes. The removal of reaction solvent and these short reaction times were the key advancements of this report over solution-phase examples.

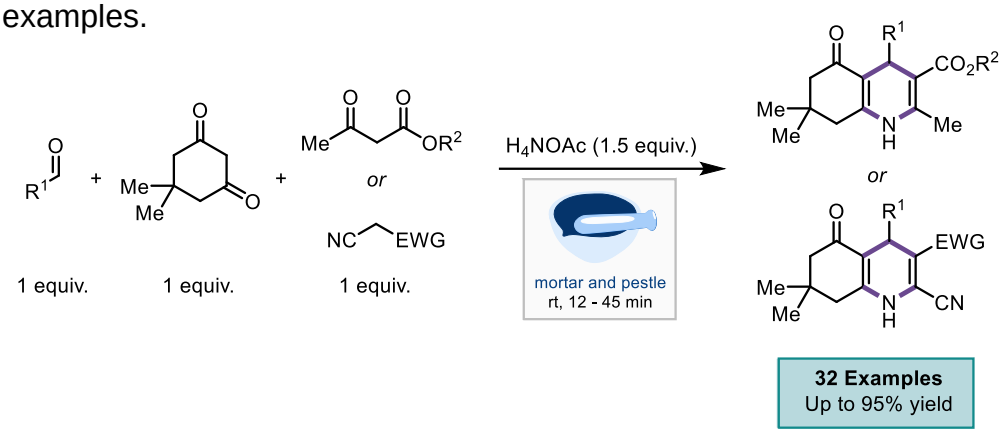

Scheme 1.1. Kapoor and co-workers' report on the synthesis of dihydropyridine derivatives in a mortar and pestle.

However, one of the main drawbacks to manual grinding is reproducibility issues, due to the varying amount of grinding forces input between users and within the same user for different experimental runs. Therefore, methods to improve reproducibility and to input consistent amounts of mechanical energy are more attractive, which has mostly come in the form of ball-mills.

1.2.2. Ball-mills

Ball-mills have been utilised in the last few decades as a reliable source of inputting mechanical energy into processes, due to the fully automated nature of the devices.[10–17] While a variety of automated grinding techniques have been developed and utilised, some of the more common devices are mixer ball-mills and planetary ball-mills, which were initially designed for decreasing the particle size of materials (Figure 1.1.). These devices both input kinetic energy to a grinding ball/balls, which in turn transfers the energy to the reagents via mechanical means. However, the mechanical forces imparted to the materials and the motion of the device is different between the

two ball-mills. Mixer mills utilise grinding jars, containing grinding balls, which can be fabricated from a variety of materials, such as stainless steel, zirconia, copper, and tungsten carbide. The jars are mounted horizontally on the device, which is then oscillated in a shallow figure of eight at high frequency, with typical frequencies up to 30 Hz (1800 rpm, Figure 1.2.). This high frequency oscillation has led to some researchers referring to milling using a mixer-ball mill as high-speed ball-milling (HSBM). The forces imparted by these mixer mills comes from the high energy impact of the grinding balls with both the material and the jar walls. The inception of commercially available Retsch and IST mixer mills has aided their popularity in research labs.

Planetary mills, on the other hand, contain grinding bowls, rather than jars, and grinding balls fabricated from the same materials available to mixer mills. These bowls are then mounted on a central disc, and are then rotated in a counter-directional manner to this central disc; aptly named the ‘sun wheel’ (Figure 1.1.). These devices operate at lower frequencies than mixer mills, typically up to 800 rpm (~13 Hz) and impart lower energy shearing forces to the reagents. Additionally, planetary mills typically utilise many smaller grinding balls per bowl, whereas mixer mills utilise only one larger grinding ball or a couple of grinding balls in some cases. Another difference between mixer and planetary mills is the scale that the reaction processes can be carried out at, typically up to a few grams for mixer mills, whereas planetary mill processes can tolerate up to a hundred grams of material. However, to carry out even larger scale processes, a different technique has been utilised, known as reactive extrusion. These extrusion processes operate via a similar concept to solution flow chemistry, allowing for continuous processing of materials in a mechanochemical manner. Twin-screw extruders (TSEs) are the most common extrusion devices that have been utilised for synthesis. This will be discussed in detail later.

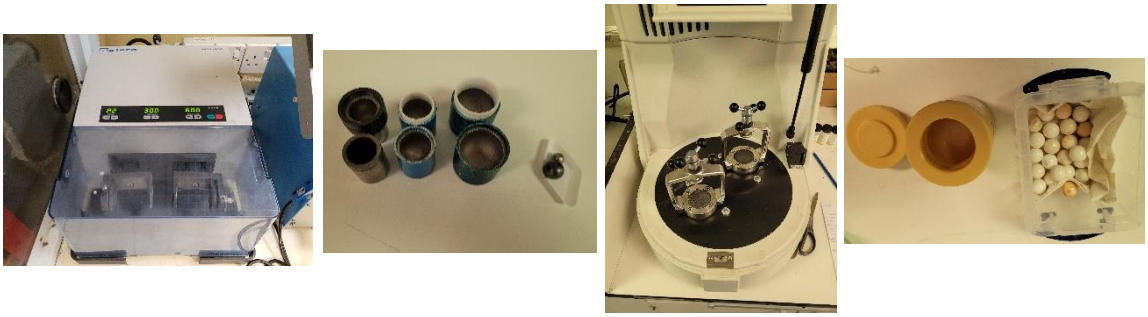

Figure 1.1. Images of ball-milling equipment (from left to right): Retsch 400 mixer mill, examples of stainless steel milling jars and grinding balls, Fritsch planetary mill, zirconia grinding bowl and grinding balls.

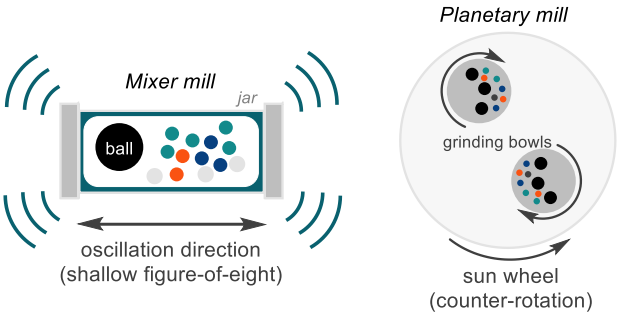

Figure 1.2. Schematic representation of mixer and planetary mills.

1.2.2.1. Ball-Milling Specific Parameters

Within ball-milling there are specific parameters that need to be considered that can influence the success and outcome of a given reaction. This includes variables that have already been discussed such as the material the jar and grinding balls are fabricated from, the volume of the jar, the size and number of the balls, and the frequency of milling. All of these factors can influence the amount of energy transmitted to the reagents, with the size of the balls and reaction frequency having one of the largest impacts on the energy imparted.[27] The jar material can influence the mechanical energy too, as harder materials such as stainless steel can potentially transfer the mechanical energy back into the reaction mixture more efficiently than softer materials such as copper. Additionally, the filling degree of the jar, i.e., the volume of the jar taken up by reagents and grinding balls, can influence the process, as higher energy impacts can occur with a lower filling degree, however, a lower number of successful impacts take place with less material in the jar.[28] A filling degree

between a third and a half full is recommended by the manufacturer, such as Retsch, for the grinding of materials to reduce their particle size. It is also possible that pressure and heat generation within the jar can be affected by the filling degree, where a higher filling degree could lead to increased jar pressure and temperature.

Another important consideration within ball-milling is the use of additives, which can improve reaction efficiency and, in some cases, alter the reactivity and/or selectivity observed. These additives can be solids or liquids, termed grinding auxiliaries and liquid-assisted grinding (LAG) agents, respectively. Grinding auxiliaries are typically relatively inert materials, such as sand or sodium chloride; however, potentially reactive materials such as silica or titania have also been used. The main role of these solid additives is to improve the mixing efficiency of the reaction mixture, especially in processes involving liquid reagents, where the mixture is sticky in nature. An example of a process being vastly improved by the addition of a grinding auxiliary is the report on the palladium-catalysed cross-coupling of aryl halides with thiols and disulfides by Browne and co-workers. During the optimisation of this process, it was found that the addition of sand as a grinding auxiliary was imperative for successful reactivity (Scheme 1.2A).[29] Without sand, the process was completely ineffective, whereas a 90% isolated yield of the cross-coupled product was obtained using 2 mass equivalents (with respect to the other reagents) of sand as a grinding auxiliary. It is postulated that the improved mixing efficiency and mass transfer enabled by the sand grinding auxiliary was responsible for this vast yield increase. Another process enhanced using a grinding auxiliary is the work of Bolm and co-workers, where a Biginelli-type multi-component reaction with sulfonimidamides was performed in a planetary ball-mill (Scheme 1.2B).[30] This work utilised silica as the grinding auxiliary, which likely has a less innocent role than the previous examples, due to the Brønsted acidity of the silica surface aiding the process. Without the addition of silica, a 28% yield of the cyclised product was obtained, compared to a 98% yield obtained with the addition of 1 g/mmol of silica with respect to the sulfonimidamide.

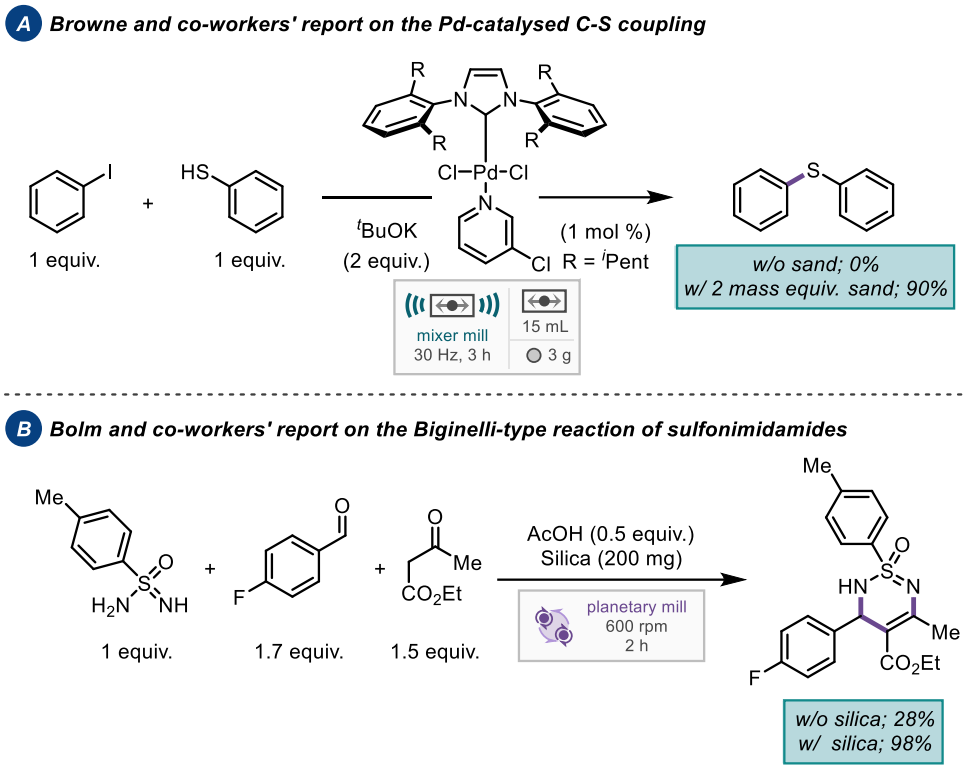

Scheme 1.2. A) Browne and co-workers' C-S coupling reaction improved by the addition of sand as a grinding auxiliary; B) Bolm and co-workers' report on the Biginelli-type reaction of sulfonimidamides improved by the addition of silica as a grinding auxiliary.

LAG agents are typically small amounts of common organic solvents that are added to a mechanochemical process.[31–34] The amount of liquid additive in a process is quantified by the variable η, which is defined as the volume of liquid additive per total mass of reagents, in units of µL/mg, with different values of η corresponding to different physical states of the reaction mixture (Scheme 1.3A). An η value of 0 corresponds to neat grinding of materials, whereas LAG is defined as an η value between 0 and 1. An η value between 1 and 10 can be described as a slurry, where the process is on the limit of what can be considered mechanochemical. Finally, an η value above 10 can simply describe a solution-phase process. Recently, Friščić and co-workers have described an η_{max} value, whereby the amount of liquid additive is reduced to its minimal value (<0.1 µL/mg) while maintaining effective reactivity.[35] LAG agents' exact role in processes can vary, such as improving the mixing efficiency of a gummy mixture, however, it is possible that their role is similar to bulk solvent in solution-phase processes, where they are able to improve reactions by stabilising transition states and/or reaction intermediates.

Some examples of the use of LAG agents to drastically improve a process includes the work by Kubota, Ito and co-workers, where they found that the addition of liquid alkenes in LAG quantities was able to increase the product yield in the palladium-catalysed Buchwald-Hartwig amination reaction between solid aryl halides and amines.[36] Without the addition of a LAG agent, their reaction only gave 33% yield of the cross-coupled product; however, when 1,5-cyclooctadiene (1,5-cod) was used in LAG quantities (η = 0.20 µL/mg), a 99% yield of the cross-coupled product was obtained (Scheme 1.3B). Their rationale for this is that the alkene LAG agent can coordinate to the palladium catalyst, which helps prevent the palladium particles from aggregating to form catalytically inactive palladium black. Thus, the LAG agent was described as a dispersant. Friščić and co-workers reported ruthenium-catalysed alkene metathesis reactions in a mixer ball-mill, enabled by use of LAG conditions and a grinding auxiliary.[37] They found that employing ethyl acetate as the LAG agent provided more consistent results, especially for solid alkene substrates, and that a solid grinding auxiliary such as sodium chloride was necessary to prevent aggregation of the reaction mixture around the grinding ball (Scheme 1.3C). For a ring-closing metathesis reaction, the reaction was ineffective in the absence of LAG and grinding auxiliary but could be improved to 39% yield under LAG conditions and improved further to 94% yield with the addition of the grinding auxiliary.

An example of altered product selectivity using LAG conditions was reported by Browne and co-workers, where the outcome of the reaction between a difluorinated 1,3-diketone and diphenyl disulfide could be altered using different LAG agents (Scheme 1.3D).[38] When polar LAG agents, such as dimethylsulfoxide (DMSO) were used, a sulfenylated product could be obtained in 56% yield. When non-polar LAG agents such as hexane were used, a β-hydroxyketone product was obtained in 72% yield. It was postulated that the β-hydroxyketone product was the kinetic product and that the addition of a polar LAG agent was able to supress its formation and favour the sulfenylated product. These examples demonstrate the power of LAG conditions in organic synthesis, both for improving processes and for switching reactivity.

LAG conditions have also been successfully applied to the formation of co-crystals, under mechanochemical conditions.[39,40]

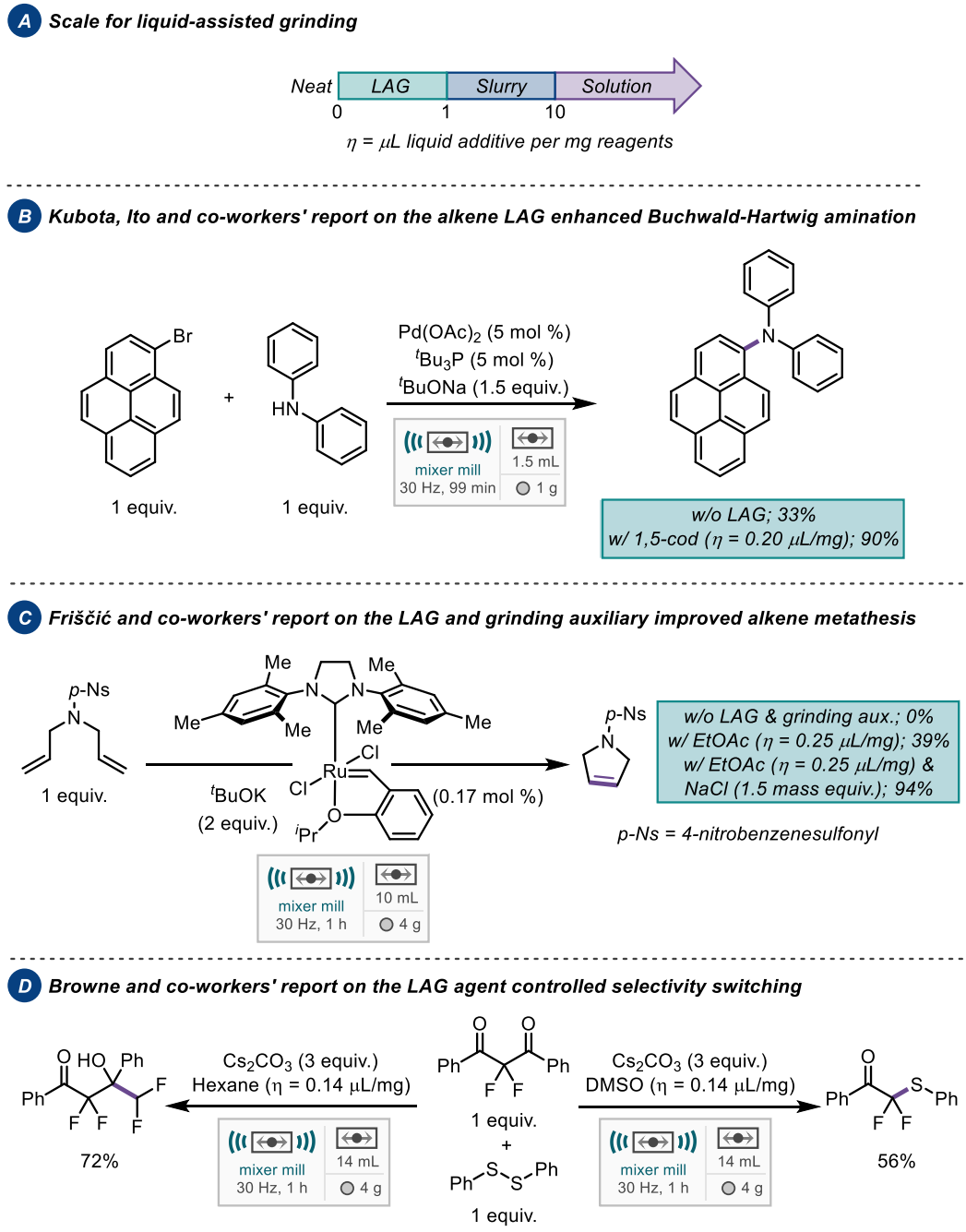

Scheme 1.3. A) Scale for LAG conditions; B) Kubota, Ito and co-workers' report on the LAG enhanced Buchwald-Hartwig amination; C) Friščić and co-workers' report on the LAG and grinding auxiliary enhanced alkene metathesis; D) Browne and co-workers' report on the LAG controlled selectivity switching of difluorinated 1,3-diketones.

1.2.2.3. Established Benefits of Ball-Milling

While the use of solid and liquid additives to enhance or alter product formation is a useful tool in the armoury of mechanochemistry, there are a host of other benefits that are more general to mechanochemical processes. These include the previously stated ability to: carry out reactions in the absence of bulk solvent, drastically decrease the reaction time of a process compared to solution-phase analogues,[41–48] carry out 'air sensitive' reactions without the requirement for inert gas protection,[29,49–54] and utilise substrates that are poorly soluble or completely insoluble in common organic solvents.[55]

Many examples of drastic decreases in reaction time exist; however, one such example is the report by Xu and co-workers, where they demonstrated palladium-catalysed C-H functionalisation of aryl rings using oximes as directing groups (Scheme 1.4A).[56] Using their method, they were able to obtain the desired product in 81% yield after only 1 hour of milling in a planetary mill. A comparable solution-phase analogue gave 33% yield of the product after 24 hours of stirring at 40 °C. Additionally, the solution-phase example required the coupling partner (toluene) to be used in vast excess, whereas the milled process required 3 to 6 equivalents of the coupling partner.

There are many examples of mechanochemical processes circumventing the requirement for inert atmospheres, mainly concerning transition-metal catalysed processes, some of which have already been described. However, an early example was reported by Mack and co-workers, where they carried out palladium-catalysed Sonogashira cross-coupling in a mixer ball mill, under an air atmosphere (Scheme 1.4B).[57] Additionally, they demonstrated the use of copper jars and balls as catalyst sources, hence avoiding the addition of copper metal. The circumvention of inert atmospheres is a useful benefit to mechanochemistry, as the use of gloveboxes and Schlenk lines for setting up reactions can be tedious and laborious.[58]

Perhaps the most impressive benefit of mechanochemistry is the ability to elicit reactions of poorly soluble substrates, as there is no need for the solubilisation of materials in the absence of bulk solvent. Kubota, Ito and co-workers have demonstrated many examples of this, including their work on the palladium-catalysed Suzuki-Miyaura cross-coupling of poorly soluble aryl halides under ball-milling conditions (Scheme 1.4C).[55] They found that these substrates were unsuitable for solution-phase processes, but underwent efficient reaction when applying heat to the milling jar. They applied this heat using a heat gun mounted to the mixer mill and measured the internal temperature of the jar using a thermographic camera. Short reaction times of 5 minutes could be used, and a heat gun set to a temperature of 250 °C (corresponding to an internal jar temperature of 120 °C) was used. For their model system, they obtained a quantitative yield of the desired cross-coupled product, compared to a 68% yield obtained in a solution-phase comparison. Additionally, the solution-phase reaction required a relatively large volume of reaction solvent (0.1 M) to combat the poor solubility of the aryl halide, although full solubility was not achieved. These examples serve to demonstrate the general benefits that mechanochemistry and ball-milling can provide for synthetic chemists.

Other key examples of mechanochemical benefits include its application to organocatalytic transformations[59–62] and the activation of zero-valent metals, such as zinc, manganese, and magnesium.[63] However, these will be discussed in much greater detail in the subsequent chapters.

1.2.2.4. Miscellaneous Ball-Milling Specific Benefits

1.2.2.4.1. Direct Mechanocatalysis

Briefly mentioned in Section 1.2.2.3. is the use of catalytically active grinding jars and balls, termed ‘direct mechanocatalysis’.[64] An example of this is the report by Borchardt and co-workers, where they carried out Suzuki-Miyaura cross-coupling using a palladium coated milling ball as the palladium source and a jar fabricated from a polyamide (Scheme 1.5).[65] They found that the use of ethanol as a LAG agent was

critical for effective reactivity. Additionally, abrasion and leeching experiments revealed that palladium from the ball was not contaminating the products. These mechanocatalytic processes are useful as the catalyst (jar and/or balls) are easily recoverable and reusable.

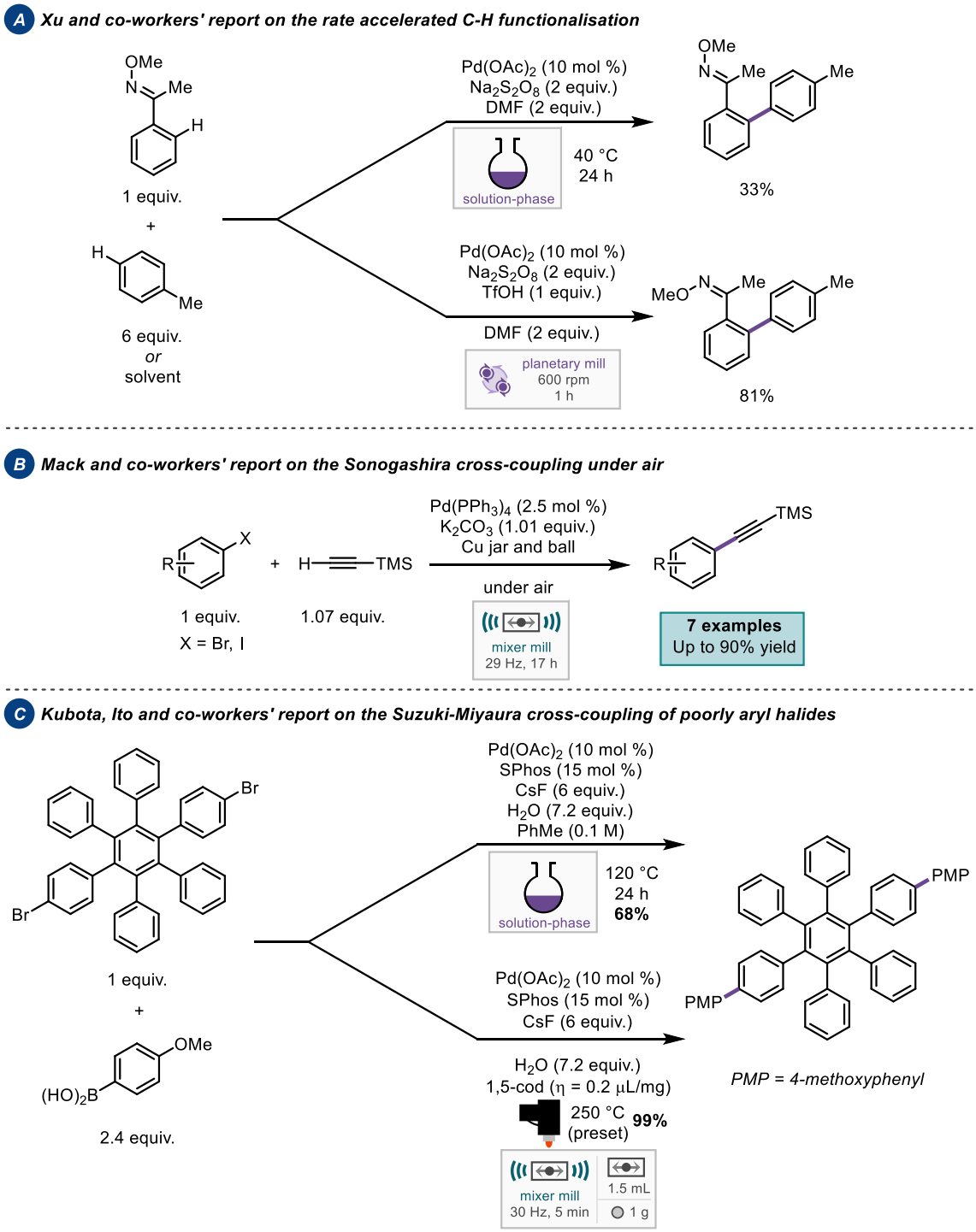

Scheme 1.4. A) Xu and co-workers' report on the rate accelerated palladium-catalysed C-H functionalisation of aryl oximes; B) Mack and co-workers' report on the inert atmosphere-free Sonogashira cross-coupling; C) Kubota, Ito and co-workers' report on the Suzuki-Miyaura cross-coupling of poorly soluble aryl halides.

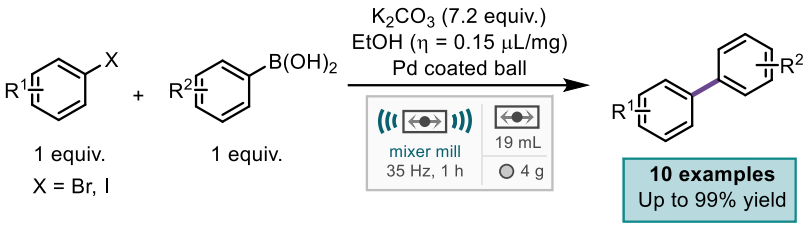

Scheme 1.5. Borchardt and co-workers' report on the direct mechanocatalytic Suzuki-Miyaura cross-coupling reaction.

1.2.2.4.2. Mechanoredox Reactions

Another interesting type of reactivity that is specific to ball-milling and, more broadly, mechanochemistry, is mechanoredox reactions.[66] This has been realised in recent years using piezoelectric materials, where the mechanical impact of ball-milling distorts the organised crystal lattice of these materials, which creates a highly polarised material that can elicit redox chemistry. This type of reactivity has been utilised recently,[67–70] including the report by Kubota, Ito and co-workers, where trifluoromethylation of electron-rich arenes, using Umemoto's trifluoromethylating agent was performed (Scheme 1.6).[71] This work utilised barium titanate ($BaTiO_3$) as the piezoelectric material and the authors also demonstrated that the material could be recovered and re-used in the process multiple times, without a decrease in the yield of the product.

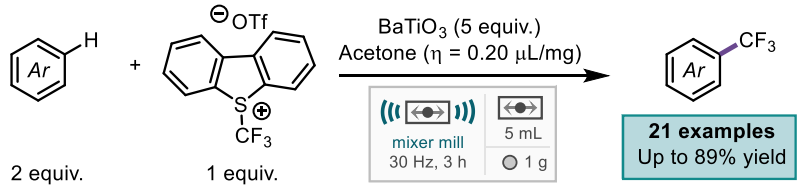

Scheme 1.6. Kubota, Ito and co-workers' report on the mechanoredox trifluoromethylation of electron-rich arenes.

1.2.3. Twin-Screw Extrusion

Planetary and mixer ball-milling techniques are limited in scalability up to tens of grams of material, however, large scale ball-mills such as tumbling mills can be used on up to ton scales. These large scale mills can suffer from poor heat dissipation, therefore extensive efforts to develop reactive extrusion as a continuous method to rapidly scale up mechanochemical processes have taken place in recent years, which would allow for improved temperature control over ball-milling methods.[18,19]

TSEs are based on a horizontal barrel containing two screws, which can accommodate a mixture of conveying, kneading, and sometimes reverse elements (Figure 1.4.). Screw elements can be manually configured, allowing the user to fine-tune the reaction process. Further to this, elements within the kneading sections can be arranged at 30° or 60° orientations (in either forward or reverse orientation) or at 90° to maximize mixing and mechanical energy transfer. Within this context, it is largely regarded that the predominant amount of the mechanical forces elicited by an extruder on a given material is in the kneading sections, imparting shearing and compression forces akin to a planetary mill. Additionally, reverse sections can be introduced to hold the material in these high-force kneading sections for longer periods of time. The reaction materials can either be added via solid additions through gravimetric/volumetric feeders, or via liquid additions from HPLC/syringe pumps, and often a combination of both. The barrel is generally split into multiple different sections which can be individually heated to independent temperatures.

Figure 1.3. Twin-screws in the barrel of the extruder (left) and full set up of extruder (right).

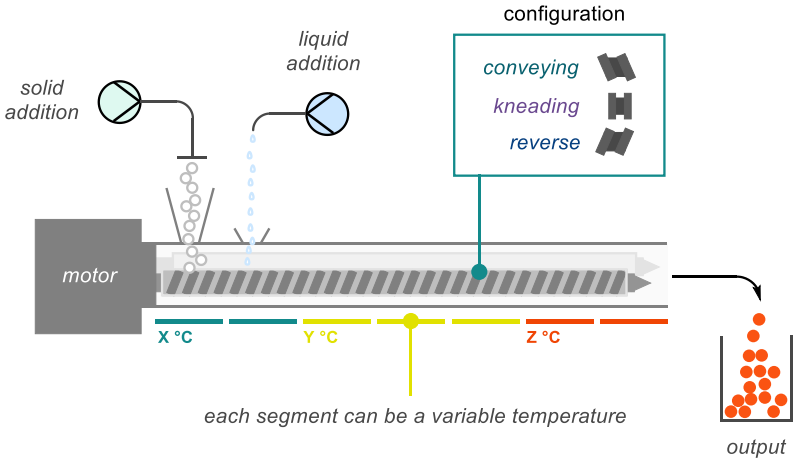

Figure 1.4. Schematic of a twin-screw extruder.

Extrusion processes bring with them their own unique parameters that are worth considering, such as the screw rotational speed, the feed rate of the solids and liquids, and the residence time of the material along the barrel. The residence time is an important consideration, especially when moving from a ball-milled process to extrusion, as there will be a large difference in the reaction time between the two. Lowering the screw speed and feed rate, as well as introducing reverse sections, can increase the residence time and thus the reaction time, which is useful for slow reactions or those with an initiation period i.e., catalyst activation. Additionally, recirculating extrusion can be carried out to continuously feed the output material back into the extrusion barrel. However, an increased residence time can come at the cost of reduced torque exerted on the reactants at kneading sections.

Another benefit of continuous extrusion processes over batch mechanochemistry processes is the ability to control temperature more precisely at each heating zone

(heating or cooling). This can be an issue in ball-milling processes, due to the poorer heat dissipation compared to solution-phase processes, where the reaction solvent can function as a heat sink. However, reports of temperature-controlled ball-milling protocols do exist.[72–77] Additionally, the ability to circumvent the handling of reactive intermediates and gaseous reagents, such as organolithium species and gaseous hydrogen has been demonstrated in solution-phase continuous flow processes.[78–80] While examples of reactive intermediate generation *in situ* and the use of pressurised milling equipment for gaseous reagents do exist,[81] the concept of circumventing the handling of hazardous substances by using continuous mechanochemistry is an attractive concept that is likely to be explored soon.

Most examples concerning the use of TSEs in synthesis have involved the formation of materials such as metal-organic frameworks (MOFs) and polymers, which have commercial applications.[82,83] However, more recently, applications of TSEs in organic synthesis have emerged in the literature, including pioneering work by Crawford, James and co-workers. This included Knoevenagel condensation of barbituric acid with aromatic aldehydes, where the temperature of the extruder was set to 160 °C and a screw speed of 55 rpm was used (Scheme 1.7A).[18] In residence times as short as 2 minutes, 100% conversion to the product was observed, giving up to 520 g/h of material.

More recently, Browne and co-workers demonstrated the use of TSE for the large-scale synthesis of a biaryl compound via the nickel-catalysed Suzuki-Miyaura type coupling of aryl sulfamates with aryl boronic acids. This process was optimised in a mixer mill and then successfully translated to the extruder by increasing the reaction scale 200-fold (to 100 mmol, Scheme 1.7B).[77] This process utilised a temperature gradient along the barrel, where the first two heating zones were set to 25 °C, the third and fourth heating zones were set to 63 °C, and the final three heating zones were set to 100 °C. This heating profile was carried over from the optimised milled process. A screw speed of 50 rpm was utilised, giving a residence time of approximately 3 minutes. This process gave over 13 grams of the cross-coupled product, at a throughput rate of 5.35 g/h. This example served as the first transition-metal catalysed

process successfully translated to an extruder. These extrusion process demonstrate the power of large-scale synthesis under the solvent-free conditions enabled by mechanochemistry.

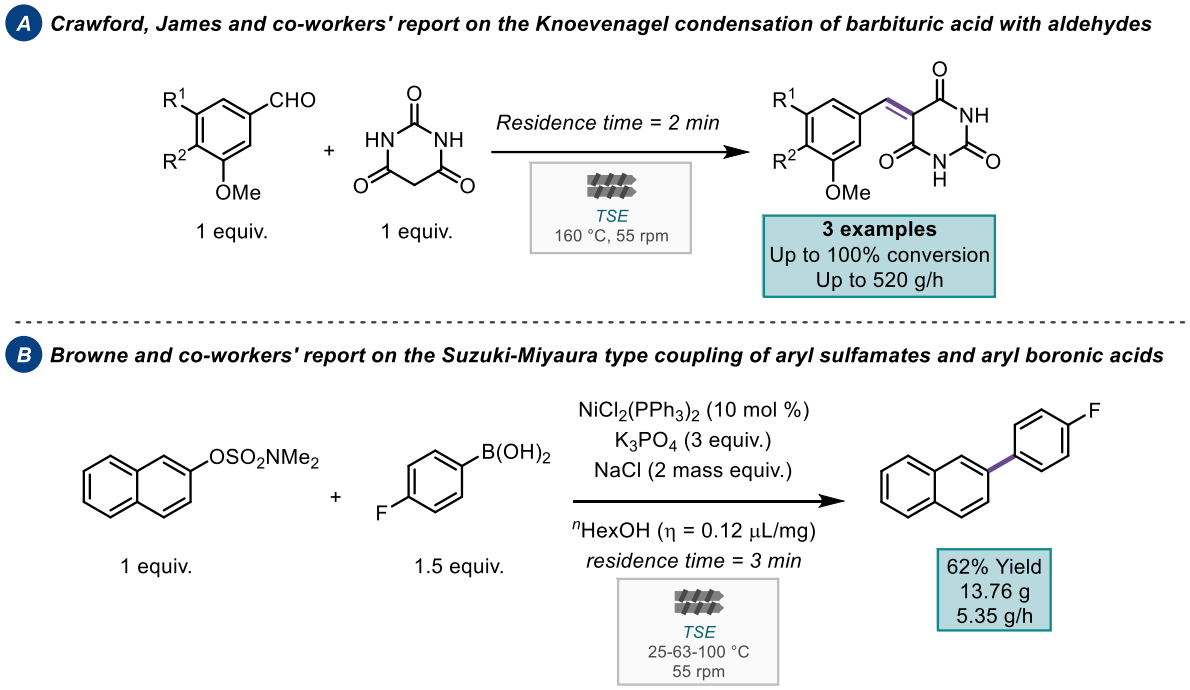

Scheme 1.7. Examples of TSE in synthesis, A) Crawford, James and co-workers' report on the Knoevenagel condensation reaction; B) Browne and co-workers report on the nickel-catalysed Suzuki-Miyaura type cross-coupling.

1.3. Sustainability Assessment

Mechanochemistry adheres to the '12 principles of green chemistry',[84] hence efforts to demonstrate the improved sustainability of mechanochemical processes have taken place. This has included the use of green metrics to assess the sustainability of processes, such as environmental factor (*E*-factor), atom economy (AE), and process mass intensity (PMI). *E*-factor is defined as the total amount of waste produced in a process, in kilograms, divided by the amount of product produced, in kilograms i.e., a smaller *E*-factor corresponds to a less wasteful process. AE is defined as the percentage of atoms from the input materials that are incorporated into the desired material. PMI is defined as the total mass of materials used in a process, in kilograms, divided by the mass of the product produced, in kilograms.[85–87] Colacino, Porcheddu

and co-workers carried out a detailed study on the sustainability assessment of the mechanochemical preparation of hydantoin-based active pharmaceutical ingredients (APIs).[88] This included Nitrofurantoin and Dantrolene, which are antibacterial and myorelaxant agents, respectively. These compounds were synthesised via Knoevenagel condensation of the respective hydantoin derivative onto a suitable aromatic aldehyde, in both a mixer and planetary ball-mill. Reaction times as short as 15 minutes were demonstrated, along with the absence of an external base and reaction solvent. They carried out green metric calculations for the formation of Nitrofurantoin and Dantrolene, comparing these values to a suitable solution-phase example (Table 1.1.). This revealed that the mechanochemical protocol is more sustainable than the solution-phase processes, with an *E*-factor of 0.29 and 0.30 for the mechanochemical synthesis of Nitrofurantoin and Dantrolene, respectively (entries 1 and 3) compared to 16 and 239 calculated for the solution-phase comparisons, respectively (entries 2 and 4). A similar trend is observed for the PMI of the processes.

Table 1.1. Colacino, Porcheddu and co-workers' report on the green metric calculations for the mechanochemical synthesis of hydantoin-derived APIs.

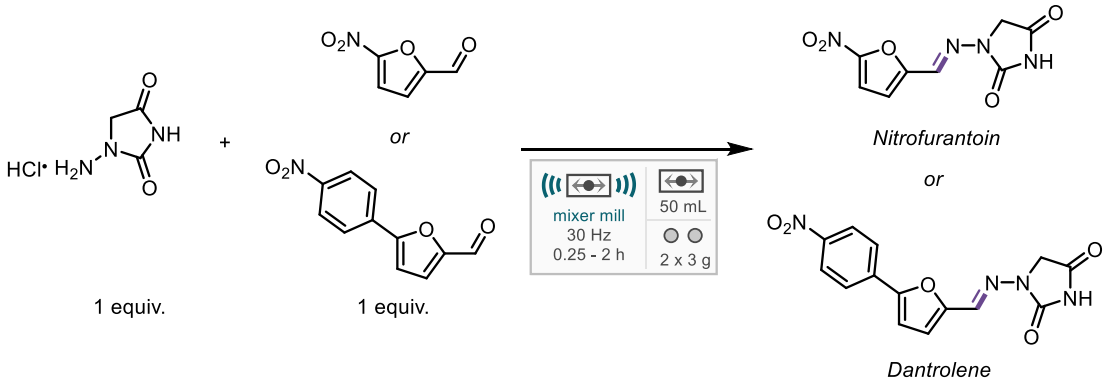

Entry	Compound	Method	Reaction time (h)	Yield (%)	AE (%)	*E*-factor	PMI (%)
1	**Nitrofurantoin**	Ball-mill	0.25	95	81	0.29	1.29
2		Solution	8	95	81	16	17
3	**Dantrolene**	Ball-mill	2	90	85	0.30	1.30
4		Solution	1	95	85	239	240

1.4. Conclusions and Outlook

Mechanochemistry has grown in popularity in recent years, due to the ability to carry out reactions under solvent-free or solvent-minimised conditions. Most contemporary

research has involved the use of ball mills as automated devices for carrying out mechanochemical processes, allowing for consistent energy inputs compared to manual grinding using a mortar and pestle, for example. Additional benefits to using mechanochemistry have been uncovered, including faster reactions, the use of LAG conditions to influence product yield and selectivity, the circumvention of inert atmospheres for sensitive protocols, and the utilisation of poorly soluble/insoluble materials. These benefits have attracted industrial interest, as the ability to reduce costs and time for industrial processes is appealing. This can be seen for the use of reactive extrusion, which allows for continuous processing of materials on a large scale and in a short amount of time. However, these extrusion processes perform best when the process has already been investigated and optimised in a ball-mill, hence further understanding and adoption of ball-milling within the scientific community is as important as ever.

Additionally, the safety implications of mechanochemical processes are coming under increased scrutiny, due to the increased publicity of the technology, therefore safety issues such as heat generation/dissipation and reactive intermediate generation are important considerations moving forward. Further investigation into the use of mechanochemistry as an enabling technology for synthesis is required, so that one day mechanochemistry can be considered a genuine alternative to solution-phase techniques.

1.5. Thesis Aims and Objectives

The aims of this thesis are to develop a deeper understanding of mechanochemical processes, in the form of utilising ball-milling for catalysis. All the previously discussed benefits of mechanochemistry will be targeted, however, the possibility for interesting observations, such as altered product selectivity or reactivity of starting materials that is not observed in the solution-phase, will be sought. There will be a focus on a range of catalytic techniques, namely organocatalysis and transition-metal catalysis, to cover a breadth of transformations. A deeper understanding of the processes studied will be achieved by carrying out detailed mechanistic investigations, where relevant, along

with carrying out comparisons of the mechanochemical techniques to suitable solution-phase analogues. Additionally, where applicable, the utility of the developed mechanochemical methodologies will be expanded to include the potential for starting material synthesis and asymmetric induction.

1.6. Bibliography

1 K. Horie, M. Barón, R. B. Fox, J. He, M. Hess, J. Kahovec, T. Kitayama, P. Kubisa, E. Maréchal, W. Mormann, R. F. T. Stepto, D. Tabak, J. Vohlídal, E. S. Wilks and W. J. Work, *Pure Appl. Chem.*, 2004, **76**, 889–906.

2 G. R. Gossweiler, G. B. Hewage, G. Soriano, Q. Wang, G. W. Welshofer, X. Zhao and S. L. Craig, *ACS Macro Lett.*, 2014, **3**, 216–219.

3 D. A. Davis, A. Hamilton, J. Yang, L. D. Cremar, D. Van Gough, S. L. Potisek, M. T. Ong, P. V. Braun, T. J. Martínez, S. R. White, J. S. Moore and N. R. Sottos, *Nature*, 2009, **459**, 68–72.

4 M. M. Caruso, D. A. Davis, Q. Shen, S. A. Odom, N. R. Sottos, S. R. White and J. S. Moore, *Chem. Rev.*, 2009, **109**, 5755–5798.

5 T. K. Achar, A. Bose and P. Mal, *Beilstein J. Org. Chem.*, 2017, **13**, 1907–1931.

6 S. L. Potisek, D. A. Davis, N. R. Sottos, S. R. White and J. S. Moore, *J. Am. Chem. Soc.*, 2007, **129**, 13808–13809.

7 B. Lee, Z. Niu and S. L. Craig, *Angew. Chem. Int. Ed.*, 2016, **55**, 13086–13089.

8 R. Stevenson and G. De Bo, *J. Am. Chem. Soc.*, 2017, **139**, 16768–16771.

9 M. Zhang and G. De Bo, *J. Am. Chem. Soc.*, 2018, **140**, 12724–12727.

10 S. L. James, C. J. Adams, C. Bolm, D. Braga, P. Collier, T. Frišcic, F. Grepioni, K. D. M. Harris, G. Hyett, W. Jones, A. Krebs, J. Mack, L. Maini, A. G. Orpen, I. P. Parkin, W. C. Shearouse, J. W. Steed and D. C. Waddell, *Chem. Soc. Rev.*, 2012, **41**, 413–447.

11 G. W. Wang, *Chem. Soc. Rev.*, 2013, **42**, 7668–7700.

12 L. Takacs, *Chem. Soc. Rev.*, 2013, **42**, 7649–7659.

13 J. L. Do and T. Friščić, *ACS Cent. Sci.*, 2017, **3**, 13–19.

14 J. G. Hernández and T. Friščić, *Tetrahedron Lett.*, 2015, **56**, 4253–4265.

15 J. L. Howard, Q. Cao and D. L. Browne, *Chem. Sci.*, 2018, **9**, 3080–3094.

16 A. Porcheddu, E. Colacino, L. De Luca and F. Delogu, *ACS Catal.*, 2020, **10**, 8344–8394.

17 J. Andersen and J. Mack, *Green Chem.*, 2018, **20**, 1435–1443.

18 D. E. Crawford, C. K. G. Miskimmin, A. B. Albadarin, G. Walker and S. L. James, *Green Chem.*, 2017, **19**, 1507–1518.

19 R. R. A. Bolt, J. A. Leitch, A. C. Jones, W. I. Nicholson and D. L. Browne, *Chem. Soc. Rev.*, 2022, **51**, 4243–4260.

20 D. J. C. Constable, C. Jimenez-Gonzalez and R. K. Henderson, *Org. Process Res. Dev.*, 2007, **11**, 133–137.

21 A. D. Curzons, D. C. Constable and V. L. Cunningham, *Clean Technol. Environ. Policy*, 1999, **1**, 82–90.

22 D. Prat, O. Pardigon, H. W. Flemming, S. Letestu, V. Ducandas, P. Isnard, E. Guntrum, T. Senac, S. Ruisseau, P. Cruciani and P. Hosek, *Org. Process Res. Dev.*, 2013, **17**, 1517–1525.

23 C. M. Alder, J. D. Hayler, R. K. Henderson, A. M. Redman, L. Shukla, L. E. Shuster and H. F. Sneddon, *Green Chem.*, 2016, **18**, 3879–3890.

24 F. Gomollón-Bel, *Chem. Int.*, 2019, **41**, 12–17.

25 C. Suryanarayana, *Mater. Res. Lett.*, 2022, **10**, 619–647.

26 S. Kumar, P. Sharma, K. K. Kapoor and M. S. Hundal, *Tetrahedron*, 2008, **64**, 536–542.

27 R. Schmidt, C. F. Burmeister, M. Baláž, A. Kwade and A. Stolle, *Org. Process Res. Dev.*, 2015, **19**, 427–436.

28 H. Kulla, F. Fischer, S. Benemann, K. Rademann and F. Emmerling, *CrystEngComm*, 2017, **19**, 3902–3907.

29 A. C. Jones, W. I. Nicholson, H. R. Smallman and D. L. Browne, *Org. Lett.*, 2020, **22**, 7433–7438.

30 F. Krauskopf, K.-N. Truong, K. Rissanen and C. Bolm, *Org. Lett.*, 2021, **23**, 2699–2703.

31 P. Ying, J. Yu and W. Su, *Adv. Synth. Catal.*, 2021, **363**, 1246–1271.

32 L. Chen, M. Regan and J. Mack, *ACS Catal.*, 2016, **6**, 868–872.

33 J. L. Howard, Y. Sagatov, L. Repusseau, C. Schotten and D. L. Browne, *Green Chem.*, 2017, **19**, 2798.

34 Z. J. Jiang, Z. H. Li, J. B. Yu and W. K. Su, *J. Org. Chem.*, 2016, **81**, 10049–10055.

35 L. Gonnet, T. H. Borchers, C. Lennox, J. Vainauskas, Y. Teoh, H. M. Titi, C. J. Barrett, S. G. Koenig, K. Nagapudi and T. Friščić, *Faraday Discuss.*, 2022, DOI:10.1039/d2fd00131d.

36 K. Kubota, T. Seo, K. Koide, Y. Hasegawa and H. Ito, *Nat. Commun.*, 2019, **10**, 111.

37 J. L. Do, C. Mottillo, D. Tan, V. Štrukil and T. Friščić, *J. Am. Chem. Soc.*, 2015, **137**, 2476–2479.

38 J. L. Howard, M. C. Brand and D. L. Browne, *Angew. Chem. Int. Ed.*, 2018, **57**, 16104–16108.

39 S. Karki, T. Friščić, L. Fabián, P. R. Laity, G. M. Day and W. Jones, *Adv. Mater.*, 2009, **21**, 3905–3909.

40 D. Braga, L. Maini and F. Grepioni, *Chem. Soc. Rev.*, 2013, **42**, 7638–7648.

41 W. Riley, A. C. Jones, K. Singh, D. L. Browne and A. M. Stuart, *Chem. Commun.*, 2021, **57**, 7406–7409.

42 J. Mack and M. Shumba, *Green Chem.*, 2007, **9**, 328–330.

43 T. Rantanen, I. Schiffers and C. Bolm, *Org. Process Res. Dev.*, 2007, **11**, 592–597.

44 C. Schumacher, C. Molitor, S. Smid, K.-N. Truong, K. Rissanen and C. Bolm, *J. Org. Chem.*, 2021, **86**, 14213–14222.

45 K. Yoo, E. J. Hong, T. Q. Huynh, B. S. Kim and J. G. Kim, *ACS Sustainable Chem. Eng.*, 2021, **9**, 8679–8685.

46 E. Tullberg, D. Peters and T. Frejd, *J. Organomet. Chem.*, 2004, **689**, 3778–

3781.

47 M. O. Rasmussen, O. Axelsson and D. Tanner, *Synth. Commun.*, 1997, **27**, 4027–4030.

48 S. F. Nielsen, D. Peters and O. Axelsson, *Synth. Commun.*, 2000, **30**, 3501–3509.

49 Q. Cao, W. I. Nicholson, A. C. Jones and D. L. Browne, *Org. Biomol. Chem.*, 2019, **17**, 1722–1726.

50 L. Chen, B. E. Lemma, J. S. Rich and J. Mack, *Green Chem.*, 2014, **16**, 1101–1103.

51 J. G. Hernández and C. Bolm, *Chem. Commun.*, 2015, **51**, 12582–12584.

52 G. N. Hermann and C. Bolm, *ACS Catal.*, 2017, **7**, 4592–4596.

53 G. N. Hermann, P. Becker and C. Bolm, *Angew. Chem. Int. Ed.*, 2015, **54**, 7414–7417.

54 P. Shi, Y. Tu, D. Kong, P. Wu, D. Ma and C. Bolm, *Angew. Chem. Int. Ed.*, 2022, **61**, e202204874.

55 T. Seo, N. Toyoshima, K. Kubota and H. Ito, *J. Am. Chem. Soc.*, 2021, **143**, 6165–6175.

56 S. J. Lou, Y. J. Mao, D. Q. Xu, J. Q. He, Q. Chen and Z. Y. Xu, *ACS Catal.*, 2016, **6**, 3890–3894.

57 D. A. Fulmer, W. C. Shearouse, S. T. Medonza and J. Mack, *Green Chem.*, 2009, **11**, 1821–1825.

58 K. Kubota, R. Takahashi, M. Uesugi and H. Ito, *ACS Sustainable Chem. Eng.*, 2020, **8**, 16577–16582.

59 M. T. J. Williams, L. C. Morrill and D. L. Browne, *ChemSusChem*, 2022, **15**, e202102157.

60 D. Kristofikova, V. Modrocká, M. Mečiarová and R. Sebesta, *ChemSusChem*, 2020, **13**, 1–32.

61 P. Chauhan and S. S. Chimni, *Beilstein J. Org. Chem.*, 2012, **8**, 2132–2141.

62 A. Bruckmann, A. Krebs and C. Bolm, *Green Chem.*, 2008, **10**, 1131–1141.

63 A. C. Jones, J. A. Leitch, S. E. Raby-Buck and D. L. Browne, *Nat. Synth.*, 2022, **1**, 763–775.

64 W. Pickhardt, S. Grätz and L. Borchardt, *Chem. Eur. J.*, 2020, **26**, 12903–12911.

65 W. Pickhardt, C. Beaković, M. Mayer, M. Wohlgemuth, F. J. L. Kraus, M. Etter, S. Grätz and L. Borchardt, *Angew. Chem. Int. Ed.*, 2022, **61**, e202205003.

66 J. A. Leitch and D. L. Browne, *Chem. Eur. J.*, 2021, **27**, 9721–9726.

67 Y. Wang, Z. Zhang, L. Deng, T. Lao, Z. Su, Y. Yu and H. Cao, *Org. Lett.*, 2021, **23**, 7171–7176.

68 C. Schumacher, J. G. Hernández and C. Bolm, *Angew. Chem. Int. Ed.*, 2020, **59**, 16357–16360.

69 H. Lv, X. Xu, J. Li, X. Huang, G. Fang and L. Zheng, *Angew. Chem. Int. Ed.*, 2022, **61**, e202206420.

70 K. Kubota, Y. Pang, A. Miura and H. Ito, *Science*, 2019, **366**, 1500–1504.

71 Y. Pang, J. W. Lee, K. Kubota and H. Ito, *Angew. Chem. Int. Ed.*, 2020, **59**, 22570–22576.

72 K. Užarević, V. Štrukil, C. Mottillo, P. A. Julien, A. Puškarić, T. Friščić and I. Halasz, *Cryst. Growth Des.*, 2016, **16**, 2342–2347.

73 N. Cindro, M. Tireli, B. Karadeniz, T. Mrla and K. Užarević, *ACS Sustainable Chem. Eng.*, 2019, **7**, 16301–16309.

74 J. M. Andersen and H. F. Starbuck, *J. Org. Chem.*, 2021, **86**, 13983–13989.

75 G. Kaupp, M. R. Naimi-Jamal and V. Stepanenko, *Chem. Eur. J.*, 2003, **9**, 4156–4161.

76 J. G. Hernández and E. Juaristi, *J. Org. Chem.*, 2011, **76**, 1464–1467.

77 R. R. A. Bolt, S. Raby-Buck, K. Ingram, J. A. Leitch and D. L. Browne, *Angew. Chem. Int. Ed.*, 2022, **61**, e202210508.

78 M. Brzozowski, M. O'Brien, S. V. Ley and A. Polyzos, *Acc. Chem. Res.*, 2015,

48, 349–362.

79 M. Movsisyan, E. I. P. Delbeke, J. K. E. T. Berton, C. Battilocchio, S. V. Ley and C. V. Stevens, *Chem. Soc. Rev.*, 2016, **45**, 4892–4928.

80 D. E. Fitzpatrick, C. Battilocchio and S. V. Ley, *ACS Cent. Sci.*, 2016, **2**, 131–138.

81 C. Bolm and J. G. Hernández, *Angew. Chem. Int. Ed.*, 2019, **58**, 3285–3299.

82 D. E. Crawford and J. Casaban, *Adv. Mater.*, 2016, **28**, 5747–5754.

83 D. E. Crawford, *Beilstein J. Org. Chem.*, 2017, **13**, 65–75.

84 K. J. Ardila-Fierro and J. G. Hernández, *ChemSusChem*, 2021, **14**, 2145–2162.

85 R. A. Sheldon, *Green Chem.*, 2017, **19**, 18–43.

86 R. A. Sheldon, *ACS Sustainable Chem. Eng.*, 2018, **6**, 32–48.

87 D. J. C. Constable, A. D. Curzons and V. L. Cunningham, *Green Chem.*, 2002, **4**, 521–527.

88 E. Colacino, A. Porcheddu, I. Halasz, C. Charnay, F. Delogu, R. Guerra and J. Fullenwarth, *Green Chem.*, 2018, **20**, 2973–2977.

Chapter 2: Mechanochemical Aza-Morita-Baylis-Hillman Reaction

2.1. Introduction to Organocatalysis

Organocatalysis can be defined as a process that is catalysed by a sub-stoichiometric quantity of an organic compound. These metal-free methods to forge new chemical bonds are an attractive prospect and can be dated as far back as the 1800s.[1] An early example was reported by Hajos and Parrish, where they performed an (*S*)-proline catalysed asymmetric intramolecular aldol reaction, affording the corresponding cyclised product with high enantio- and diastereocontrol (Scheme 2.1.).[2] However, it was not until the turn of the millennium that organocatalysis truly increased in popularity, as indicated by a surge in the number of literature reports utilising organic compounds as catalysts.[3–6]

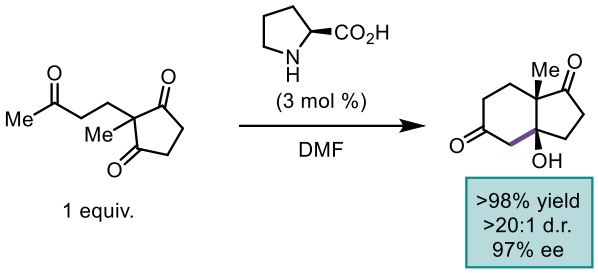

Scheme 2.1. Hajos and Parrish's (*S*)-proline catalysed intramolecular aldol reaction**.**

Two of the pioneers of modern organocatalysis are List and MacMillan, who concurrently reported an asymmetric intermolecular aldol reaction and an asymmetric Diels-Alder reaction, respectively.[7,8] Both processes were catalysed by a secondary amine organocatalyst, (*S*)-proline in List's report and an imidazolidinone-type catalyst in MacMillan's report, giving excellent yields and stereocontrol of the products (Scheme 2.2.).

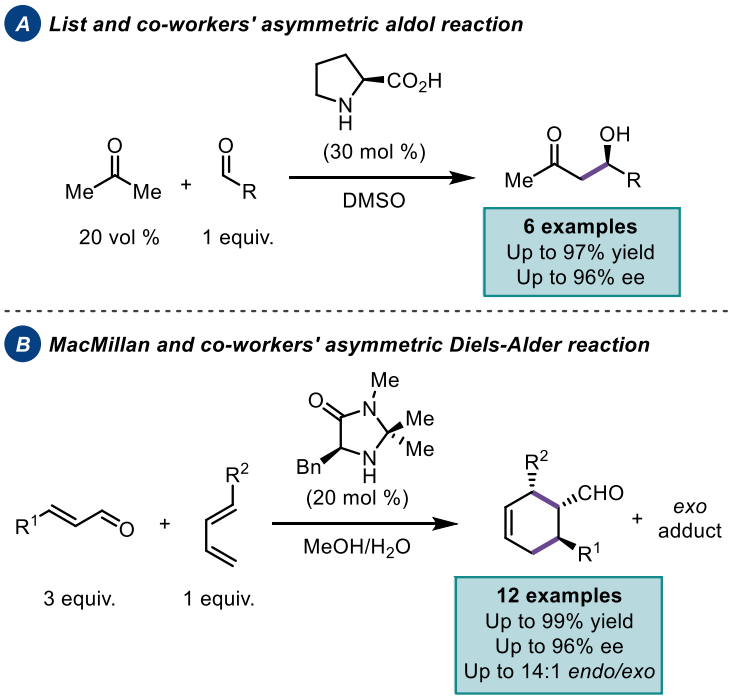

Scheme 2.2. A) List and co-workers' (*S*)-proline catalysed asymmetric aldol reaction; B) MacMillan and co-workers' imidazolidinone catalysed asymmetric Diels-Alder reaction.

MacMillan's report was also the first to coin the term 'organocatalysis'. This led to the aforementioned surge in literature reports of organocatalytic transformations and culminated in List and MacMillan sharing the Nobel prize in chemistry in 2021 for their contributions to metal-free asymmetric transformations. While a large quantity of the subsequent research from the groups of List and MacMillan have focused on secondary amine organocatalysis,[5] there have been many other catalyst types that have been extensively studied, including tertiary Lewis base catalysts (amines and phosphines),[6,9] Brønsted acid catalysts,[10] and nucleophilic-heterocyclic carbene (NHC) catalysts.[4]

Through combinations of organocatalyst classes and substrate types, different activation modes can be accessed (Scheme 2.3.). For example, secondary amine catalysts can either increase the energy of the highest-occupied molecular orbital (HOMO) or decrease the energy of the lowest-unoccupied molecular orbital (LUMO) of carbonyl compounds in oxidation level 2 depending on whether enolisable protons are present or not.[11] These interactions make the substrate either more nucleophilic or electrophilic, respectively. In the case of tertiary Lewis base catalysis, nucleophilic enolate intermediates are formed; for example, an acid chloride would form a so-called

C1-enolate. C2- and C3-enolates are also accessible from α-halo carbonyls and α,β-unsaturated carbonyls, respectively. NHC catalysts can access a unique intermediate when reacted with aldehydes, known as a Breslow intermediate,[12] which has umpolung reactivity at the carbonyl, allowing for reactions such as benzoin and Stetter reactions to be carried out (Scheme 2.3.).[13–15]

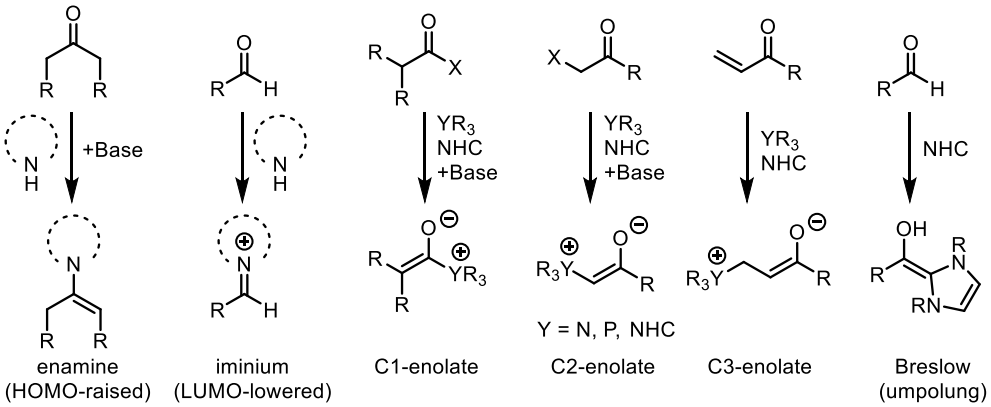

Scheme 2.3. Some common organocatalytic activation modes accessible by Lewis base organocatalysts.

2.1.1. Mechanochemical Organocatalysis

While most research relating to organocatalysis has taken place in the solution-phase, there have been many reports of using mechanochemistry as a solvent-free alternative.[16–22] This has included pioneering work by Bolm and co-workers, in 2006, where they carried out asymmetric aldol reactions between a variety of ketones and aryl aldehydes, using (*S*)-proline as the organocatalyst (Scheme 2.4.).[23] These reactions were carried out in a planetary ball-mill with no reaction solvent, furnishing the β-hydroxyketone products in high yields with excellent stereocontrol, and in decreased reaction times compared to solution-phase processes (5.5 h vs up to 48 h). This report reinforced the benefits of using mechanochemistry that were already established at the time, such as permitting reactions to be carried out in the absence of bulk reaction solvents and decreasing the reaction times for laborious processes. The report also demonstrated that the forceful conditions imparted by ball-milling do not hinder the stereocontrol, in comparison to milder solution-phase processes.

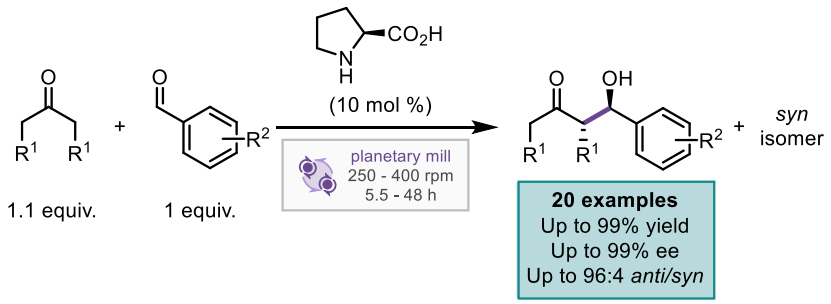

Scheme 2.4. Bolm and co-workers' (*S*)-proline catalysed asymmetric intermolecular aldol reaction, in a planetary ball-mill.

This pioneering report paved the way for subsequent examples of mechanochemical organocatalysis, most of which focused on secondary amine organocatalysis.[24–30] However, other catalyst types have been utilised too, such as hydrogen-bonding mediated thioureas,[31–33] NHCs,[34] and tertiary amines.[35] This included previous work from Morrill, Browne and co-workers, using NHC organocatalysis to carry out benzoin and Stetter reactions in a planetary ball-mill. This included inter- and intramolecular variants of each reaction, and a representative asymmetric example (Scheme 2.5.).[34]

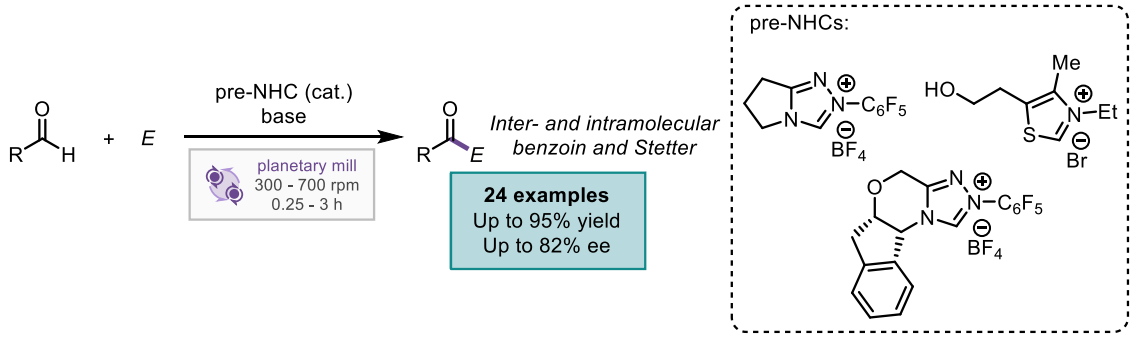

Scheme 2.5. Morrill, Browne and co-workers' NHC catalysed benzoin and Stetter reactions in a planetary ball-mill.

2.1.2. Tertiary Lewis Base Organocatalysis

2.1.2.1. The Morita-Baylis-Hillman Reaction

The Morita-Baylis-Hillman (MBH) reaction is a C-C bond forming reaction between an aldehyde and an α,β-unsaturated compound, such as an acrylate ester, catalysed by a tertiary Lewis base. It is named after the chemists that originally reported the reactivity; Morita and co-workers in 1968, followed by Baylis and Hillman in 1972,

using a tertiary phosphine or amine catalyst, respectively (Scheme 2.6A).[36,37] This process is atom economical and the products formed are allylic alcohols, which are useful synthetic motifs as they can be readily functionalised further. Mechanistic studies have allowed a mechanism to be deduced, which proceeds *via* the formation of a key C3-enolate intermediate formed from the 1,4-addition of the organocatalyst onto the α,β-unsaturated compound (Scheme 2.6B.).[38]

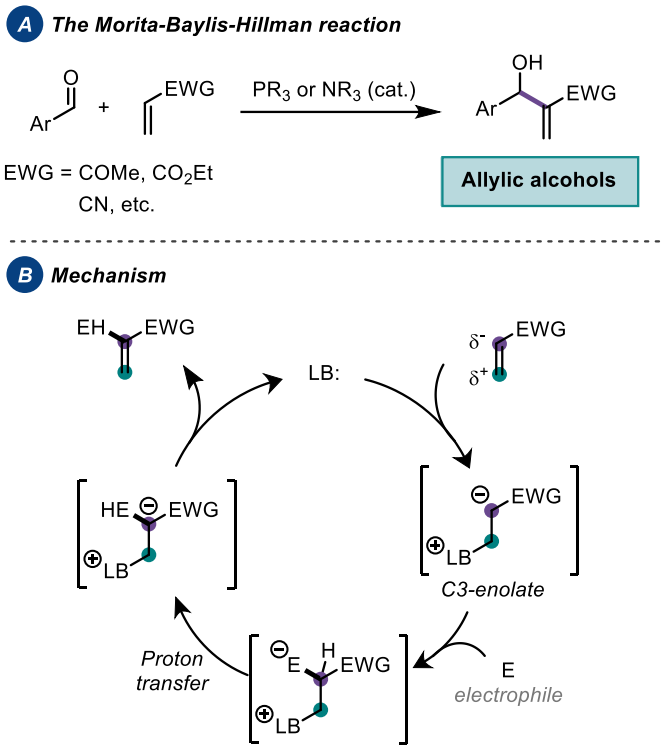

Scheme 2.6. A) The MBH reaction; B) mechanism.

Since these seminal reports, there have been a plethora of examples of the MBH reaction in the literature, with a keen interest on expanding the scope of the reaction to encompass asymmetric induction,[39,40] as well as an aza variant of the reaction (aza-MBH).[41] This aza-MBH reaction was first reported by Perlmutter and co-workers, in 1995, where a variety of *N*-tosyl aldimines were reacted with acrylate esters, using 1,4-diazabicyclo[2.2.2]octane (DABCO) as the organocatalyst (Scheme 2.7A). Interestingly, this process was carried out in the absence of reaction solvent, however, a sealed tube was used, hence it is likely that increased pressure within the tube was aiding the reaction. The products of the aza-MBH reaction are synthetically useful β-amino acid derivatives.[42,43] Following this initial report, many examples of aza-MBH reactions were reported,[44–48] including the work of Shi and co-workers, where a chiral

tertiary amine organocatalyst, β-isocupreidine (β-ICD), was utilised to furnish enantioenriched aza-MBH products in high yield and with high enantiocontrol (Scheme 2.7B).[49]

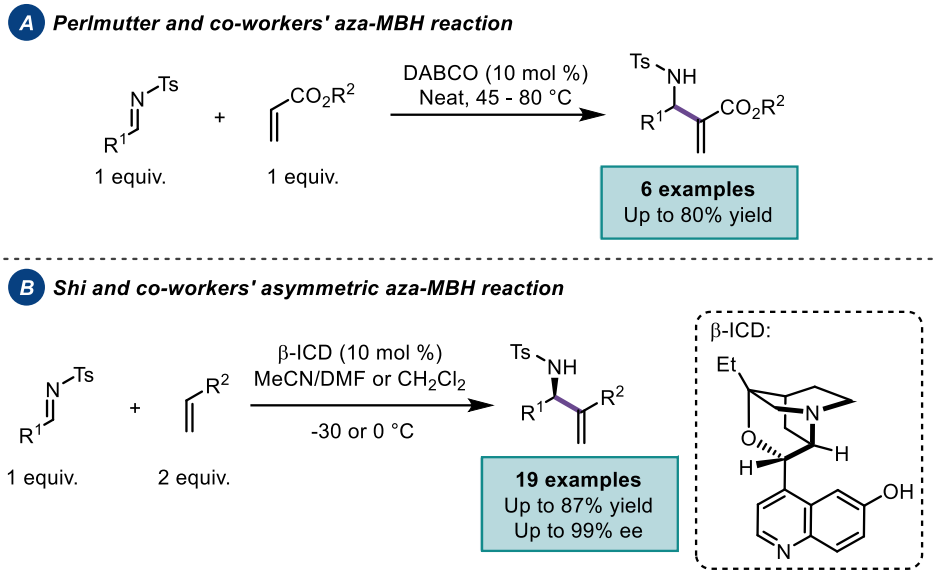

Scheme 2.7. A) The aza-MBH reaction; B) Asymmetric aza-MBH using a chiral tertiary amine organocatalyst.

One major drawback of both the MBH and aza-MBH reaction is the low reaction rate, where reaction times of up to a few days can be commonplace, especially for more challenging substrates, such as those with a large amount of steric encumbrance. Additionally, these processes often rely on toxic reaction solvents, such as dichloromethane, tetrahydrofuran, and *N,N*-dimethylformamide. Hence, this is a reaction that could potentially benefit from being translated to a solvent-free/minimised protocol, in addition to decreasing the reaction time and permitting tolerance of substrates that are ineffective in solution-phase reports.

2.1.2.2. The Mechanochemical Morita-Baylis-Hillman Reaction

With the potential benefits of translating processes to a mechanochemical set up in mind, Mack and co-workers were able to carry out the MBH reaction under ball-milling conditions.[35] They successfully achieved this by carrying out the MBH reaction between aryl aldehydes and methyl acrylate in a mixer ball-mill, using DABCO as the organocatalyst (Scheme 2.8.). This decreased reaction time was especially apparent

for their model aldehyde, 4-nitrobenzaldehyde, where a reaction time of only 30 minutes was required to achieve 98% yield of the allylic alcohol product, which demonstrates the time saving of their ball-milled process compared to solution-phase examples.

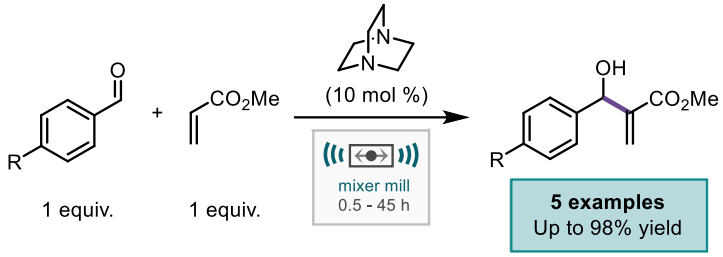

Scheme 2.8. Mack and co-workers' mechanochemical MBH reaction.

However, one of the drawbacks of this work was the lack of a universal time saving across the substrate scope, where all other examples had reaction times of at least 9 hours. Hence, there was still potential to explore the MBH further and develop a more general mechanochemical method for this process. Additionally, the process could be expanded to tolerate the aza-variant of this reaction, where the aldehyde starting material is replaced with an imine. Moreover, an asymmetric mechanochemical aza-MBH process would be an attractive method to form enantioenriched β-amino acid derived products.

To this end, it was envisaged that Mack and co-workers' seminal work could be expanded by investigating the aza-MBH reaction. A keen interest would be placed on developing a general process with a universal time-saving, and an investigation on the possibility for enantioinduction.

2.2. Results and Discussion

2.2.1. Reaction Optimisation

The investigations into the mechanochemical aza-MBH reaction commenced with the selection of *N*-tosyl imine (**3a**) as a model substrate. **3a** and other imines discussed in this chapter were typically prepared from the corresponding aldehydes and amines by a condensation reaction in refluxing toluene, using a catalytic amount of boron trifluoride diethyl etherate as a Lewis acid (Scheme 2.9.). Following this, a model

system of **3a** and ethyl acrylate **4a** was investigated under mechanochemical conditions.

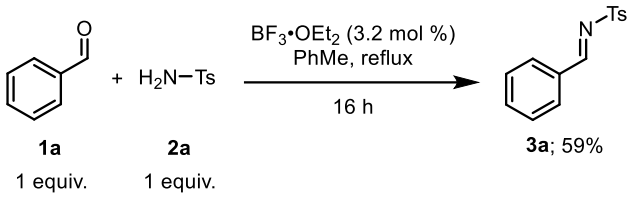

Scheme 2.9. Synthesis of *N*-tosyl imine **3a**.

Initial conditions of using 20 mol % of DABCO as the organocatalyst, 6 mass equivalents (with respect to reactants and catalyst) of sand as a grinding auxiliary, a 99 minute reaction time, and a milling frequency of 30 Hz were utilised. The reaction was carried out on a 0.25 mmol scale, furnishing the desired product (**5a**) in 23% yield by ^{1}H NMR analysis, which was isolated in 21% yield (Table 2.1., entry 1).

Following this initial result, a full optimisation of the reaction conditions was carried out, which included the immediate discovery that a small amount of liquid-assisted grinding (LAG) agent could greatly improve the reaction efficiency. In this case, adding 0.25 µL/mg (with respect to reactants and catalyst) of acetonitrile improved the yield to 52% (entry 2). As discussed in Chapter 1, the role of the LAG agent could be to improve the mixing efficiency of the reaction, however, stabilisation of reaction intermediates is possible, also. Next, a screen of the grinding auxiliary was carried out to elucidate whether using sand was optimal. This revealed that sodium chloride is a more adept grinding auxiliary and the amount of grinding auxiliary used could be decreased to 3 mass equivalents (entries 3 and 4). The latter provided **5a** in 57% isolated yield. This is likely due to the improved mixing efficiency of sodium chloride, in this instance, as sand would occasionally lead to aggregation of the reagents on the walls of the milling jar. Other solid additives such as magnesium sulfate and crushed molecular sieves largely inhibited to the reaction, likely due to their poorer solid uniformity leading to aggregation of materials (entries 5 – 7). It was then found that both quinuclidine and 3-hydroxyquinuclidine (3-HQD) are superior catalysts to DABCO, giving 78% and 81% yields as determined by ^{1}H NMR analysis, respectively (entries 8 and 9). The product was isolated in 71% yield from the use of quinuclidine. Decreasing the catalyst loading from 20 mol % to 10 mol % resulted in a significant

decrease in the product yield (entry 9). 3-HQD was taken forward as the optimal catalyst, due to its lower cost versus quinuclidine (£10/g vs £130/g).[50,51] Control reactions revealed that the reaction is less efficient in the absence of LAG agent and grinding auxiliary, and ineffective in the absence of organocatalyst (entries 11 – 14). The absence of both LAG agent and grinding auxiliary (entry 13) allows for the most comparable reaction conditions to Mack and co-workers' report, demonstrating the necessity to re-optimise the reaction parameters. Decreasing the reaction time to 30 minutes led to promising 71% yield of **5a** by ^{1}H NMR analysis, however, some **3a** remained, hence the 99 minutes reaction time was carried forward (entry 15). Increasing the amount of LAG agent did not improve the yield, likely due to having too much liquid in the jar, hence lowering the mixing efficiency (entry 16).

Finally, a LAG agent screen was carried out to elucidate if acetonitrile is the optimal liquid additive. Here, a variety of liquid additives ranging from non-polar (hexane) to polar (water) were tested (entries 18 – 25), revealing that toluene is the most effective LAG agent for this process, furnishing the product in 85% isolated yield (entry 19). It is apparent that this process favours non-polar aprotic LAG agents over polar protic LAG agents, however, the success of toluene as the additive could be a result of π-π interactions with the aromatic rings of the starting material. These conditions (entry 18) were taken forward as the optimal conditions, allowing the scope of the process to be evaluated.

Table 2.1. Optimisation of model aza-MBH reaction in a mixer ball-mill.

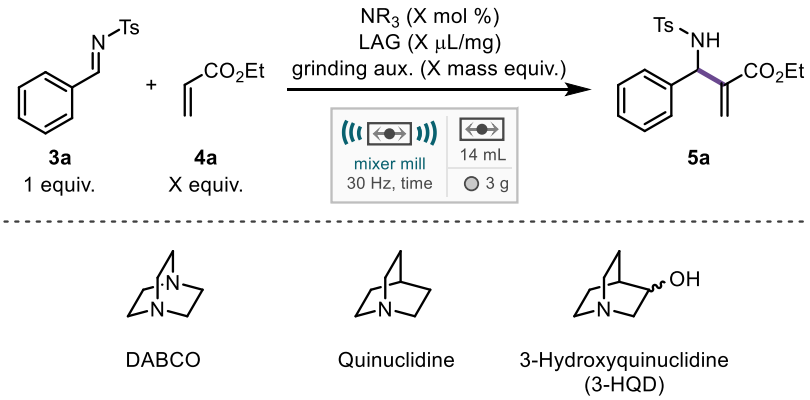

Entry[a]	3a (mmol)	4a (mmol)	Catalyst (mol %)	LAG agent (µL/mg)	Grinding aux. (mass equiv.)	Time (min)	5a (%)[b]
1	0.25	0.28	DABCO (20)	-	Sand (6)	99	23 (21)
2	0.25	0.28	DABCO (20)	MeCN (0.25)	*Sand (6)*	99	52
3	0.25	0.28	DABCO (20)	MeCN (0.25)	***NaCl (6)***	99	60
4	0.25	0.28	DABCO (20)	MeCN (0.25)	***NaCl (3)***	99	61 (57)
5	0.25	0.28	DABCO (20)	MeCN (0.25)	***$MgSO_4$ (3)***	99	32
6	0.25	0.28	DABCO (20)	MeCN (0.25)	***Na_2SO_4 (3)***	99	29
7	0.25	0.28	DABCO (20)	MeCN (0.25)	***Mol. sieves (3)***	99	12
8	0.25	0.28	***Quinuclidine (20)***	MeCN (0.25)	NaCl (3)	99	78 (71)
9	0.25	0.28	***Quinuclidine (10)***	MeCN (0.25)	NaCl (3)	99	45
10	0.25	0.28	***3-HQD (20)***	MeCN (0.25)	NaCl (3)	99	81
11	0.25	0.28	3-HQD (20)	-	NaCl (3)	99	67
12	0.25	0.28	3-HQD (20)	MeCN (0.25)	-	99	57
13	0.25	0.28	3-HQD (20)	-	-	99	61
14	0.25	0.28	-	MeCN (0.25)	NaCl (3)	99	<2
15	0.25	0.28	3-HQD (20)	MeCN (0.25)	NaCl (3)	***30***	71
16	0.25	0.28	3-HQD (20)	***MeCN (0.5)***	NaCl (3)	99	64
17	0.25	0.28	3-HQD (20)	***hexane (0.25)***	NaCl (3)	99	82
18	0.25	0.28	3-HQD (20)	***Toluene (0.25)***	NaCl (3)	99	89 (85)
19	0.25	0.28	3-HQD (20)	***EtOAc (0.25)***	NaCl (3)	99	86
20	0.25	0.28	3-HQD (20)	***CH_2Cl_2 (0.25)***	NaCl (3)	99	85
21	0.25	0.28	3-HQD (20)	***^{i}PrOH (0.25)***	NaCl (3)	99	71
22	0.25	0.28	3-HQD (20)	***MeOH (0.25)***	NaCl (3)	99	65
23	0.25	0.28	3-HQD (20)	***DMSO (0.25)***	NaCl (3)	99	63
24	0.25	0.28	3-HQD (20)	***H_2O (0.25)***	NaCl (3)	99	19

[a]Reactions were carried out in 14 mL stainless steel jars, equipped with a 3 g, 9 mm stainless steel grinding ball, under an air atmosphere.

[b]Yield determined by ^{1}H NMR analysis of the crude reaction mixture (after work-up), using mesitylene as an internal standard. Isolated yields are given in parentheses.

2.2.2. Substrate Scope

With these optimal conditions in hand, a range of imine starting materials were synthesised from the corresponding aldehydes and amines using a condensation reaction (Scheme 2.1.1., see Section 5.2.2. for experimental procedures). This included aldimines containing halogen substitution on the aromatic ring (**3b** – **3e**, **3n**, **3o**, **3q**, **3r**, **3u**), electron-withdrawing moieties on the aromatic ring (**3h** – **3k**), electron-donating moieties on the aromatic ring (**3l**, **3m**, **3v**), sterically encumbered substrates (**3s**, **3t**, **3w**), heteroaromatic substrates (**3y** – **3aa**), and ketimine substrates (**3ae**, **3af**).

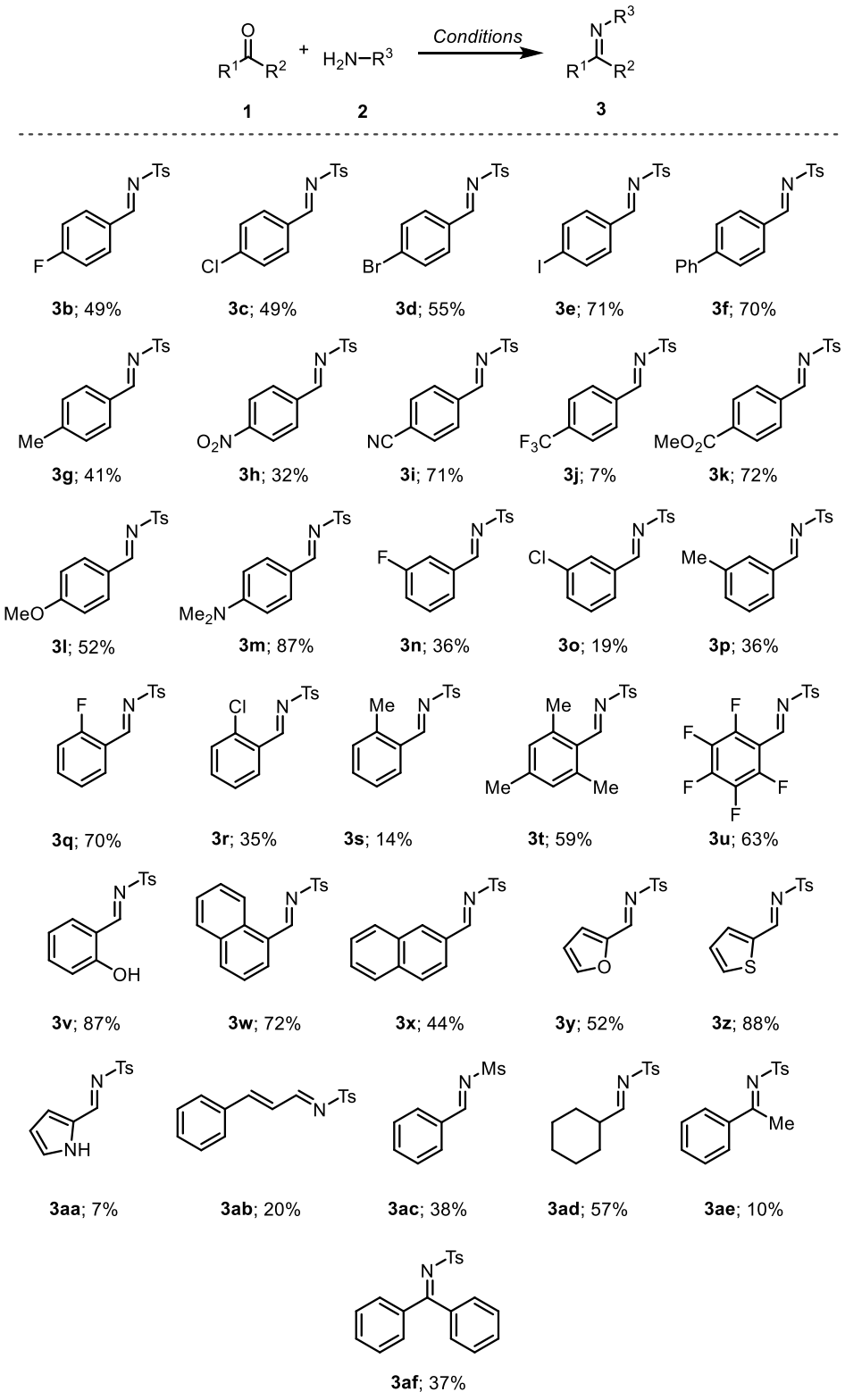

Scheme 2.1.1. Imines synthesised for the substrate scope.

Initial investigations into the scope of the aza-MBH reaction revealed that the 99 minute reaction time wouldn't be sufficient for all of the substrates, thus this was extended to 3 hours for most substrates. Additionally, a higher catalyst loading of 40 mol % was required for effective conversion of some substrates. These two factors

are likely because of poorer reactivity of some substrates, such as those containing electron-rich moieties or steric encumbrance.

The aza-MBH reaction proceeded effectively with a variety of halogen-substituted aromatic aldimines, namely 4-fluoro (**5b**; 68%), 4-chloro (**5c**; 61%), 4-bromo (**5d**; 51%), and 4-iodo (**5e**; 38%), as well as 3-fluoro (**5n**; 78%), 3-chloro (**5o**; 70%), 2-fluoro (**5q**; 49%), and 2-chloro (**5r**; 57%) substitution (Scheme 2.1.2.). Mildly electron donating 4-phenyl (**5f**; 68%) and 4-methyl (**5g**; 29%) substitution was tolerated in moderate to good yields. The low yield of **5g** is interesting as it does not appear to be because of the lower reactivity of the starting material, but as a consequence of the rheology of the reaction mixture. **3g** was synthesised as a low density solid, hence would aggregate to the walls of the milling vessel, causing poor mixing and the low yield. A more strongly electron donating 4-methoxy group (**5l**, 27%) was tolerated, with the lower yield likely due to the lower reactivity of the aldimine starting material. Methyl substitution at the 3- (**5p**, 70%) and 2-position (**5s**, 47%) of the aromatic ring was tolerated also. A variety of electron withdrawing groups were tolerated, including 4-nitro (**5h**; 46%), 4-cyano (**5i**, 44%), 4-trifluoromethyl (**5j**; 57%), and a methyl ester at the 4-position (**5k**; 51%). Sterically encumbered 1-naphthyl (**5w**; 25%) also participated in the reaction, albeit in lower yield. Perfluorination (**5u**; 31%) was tolerated on the aromatic ring in lower yield. Aromatic imine substrates which were not tolerated under these reaction conditions included strongly electron donating 4-dimethylamino (**5m**) and 2-hydroxy (**5v**) substitution and sterically encumbered 2,4,6-trimethyl (**5t**) substitution on the aromatic ring. This suggests that substrates with much lower reactivities, such as highly electron-rich substrates and sterically encumbered substrates, would likely require a major alteration to the reaction conditions to be tolerated.

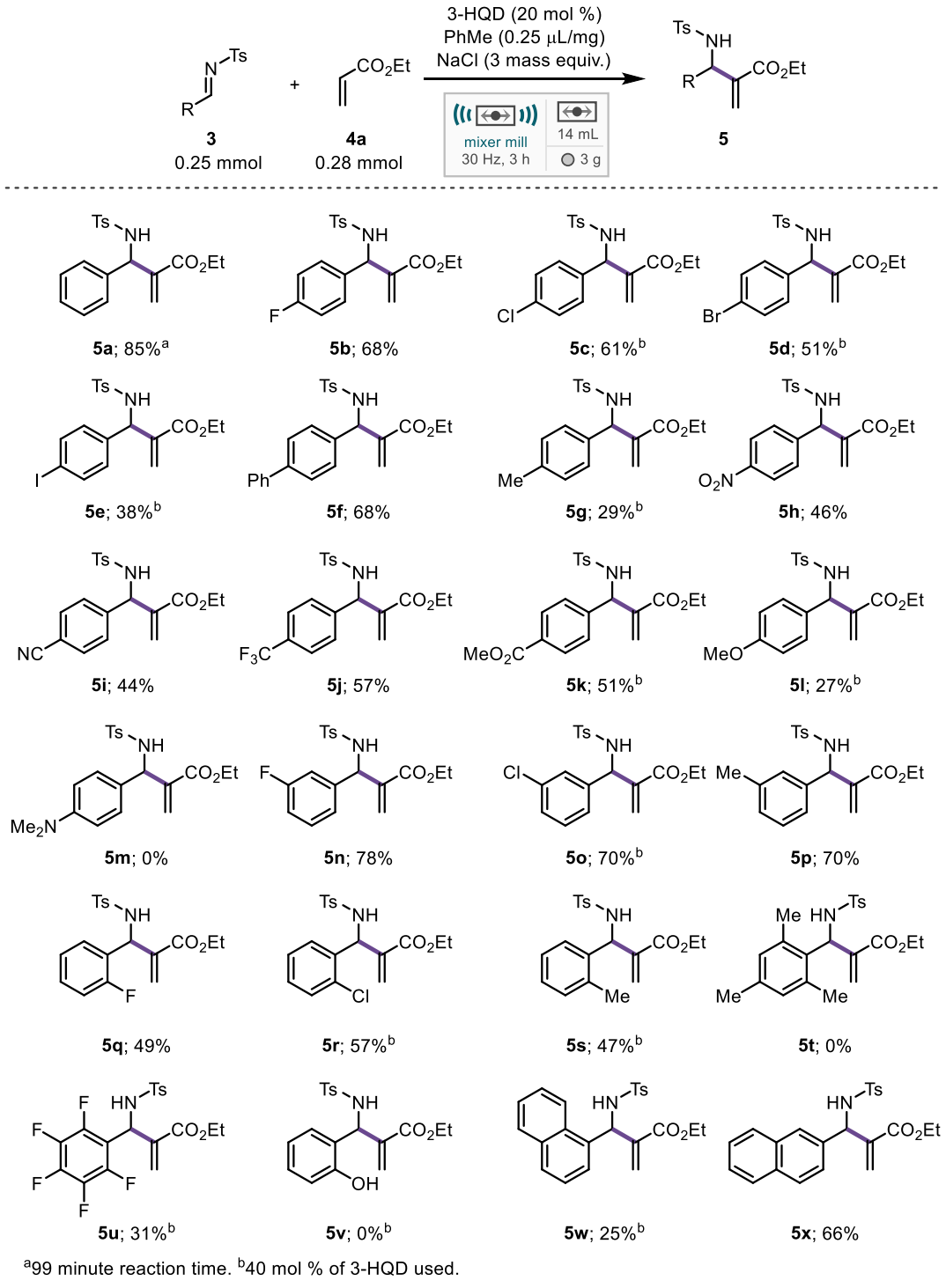

Scheme 2.1.2. Variation of aromatic system of the imine in the mechanochemical aza-MBH reaction.

Heteroaromatic 2-furanyl (**5y**; 60%) and 2-thiophenyl (**5z**; 35%) substitution was also tolerated (Scheme 2.1.3.). Interestingly, a cinnamyl substrate gave the 1,2-addition product (**5ab**; 40%) in moderate yield, with no competing 1,4-addition observed. It could be expected that the C3-enolate intermediate formed during the reaction is a

soft nucleophile, therefore 1,4-addition to this cinnamyl substrate could be envisaged as a side-reaction. Finally, a methanesulfonamide protected imine (**5ac**; 64%) furnished the desired product in good yield. 2-Pyrrole (**5aa**) substitution, possibly due to the presence of the reactive nitrogen atom of the pyrrole ring, was not tolerated. Additionally, the aza-MBH reaction with alkyl aldimines such as cyclohexyl aldimine (**5ad**) were unsuccessful, and acetophenone (**5ae**) and benzophenone (**5af**) based ketimines were also not tolerated. In the case of **5ad** and **5ae**, the imine starting materials are susceptible to isomerisation to their respective enamines, which may inhibit their ability to partake in the reaction. **5af** is a sterically encumbered ketimine, which could lead to poor reactivity in the aza-MBH reaction. Reaction conditions that tolerate this broader class of substrate would be of interest, however, as they are generally ineffective in solution-phase processes as well.

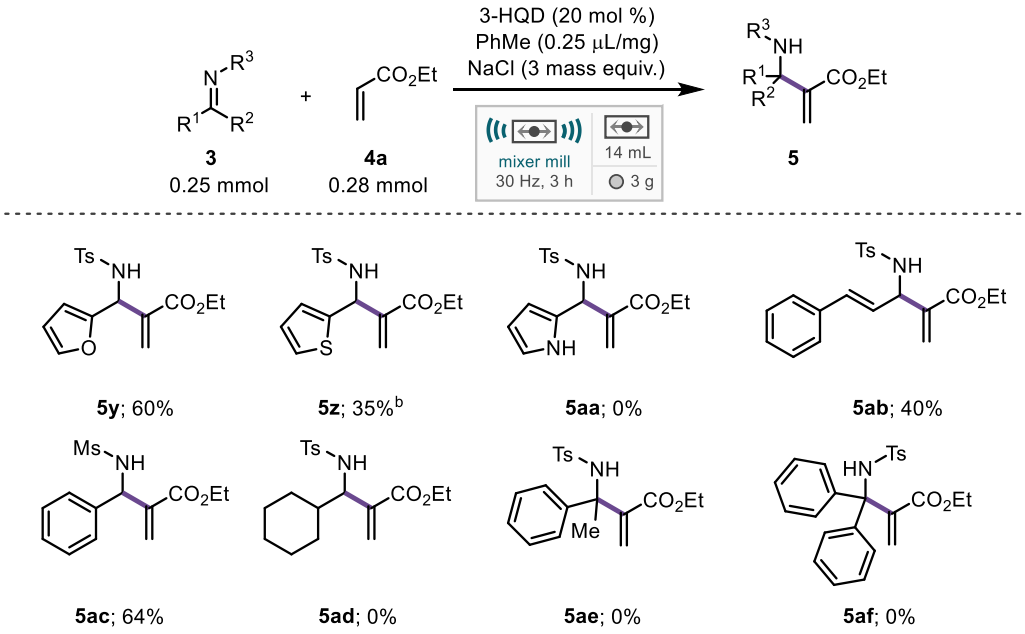

[a]99 minute reaction time. [b]40 mol % of 3-HQD used.

Scheme 2.1.3. Further imine scope of mechanochemical aza-MBH reaction.

A small selection of Michael acceptors also successfully reacted under these conditions, including acrylonitrile and methyl vinyl ketone, yielding products **5ag** and **5ah** in 60% and 31% yield, respectively (Scheme 2.1.4.). Interestingly, a reaction with the weak Michael acceptor acrylamide resulted in direct addition of the amide to the imine, giving the hemi-aminal product (**5ai**; 23%) in low yield. Incompatible substrates included β-substituted Michael acceptors such as ethyl crotonate and 2-cyclopentene-1-one, with neither of the corresponding products (**5aj**, **5ak**) being observed. These β-

substituted Michael acceptors are notoriously difficult substrates in the MBH reaction due to their increased steric demand, and typically require a new set of conditions to be successfully tolerated.[52]

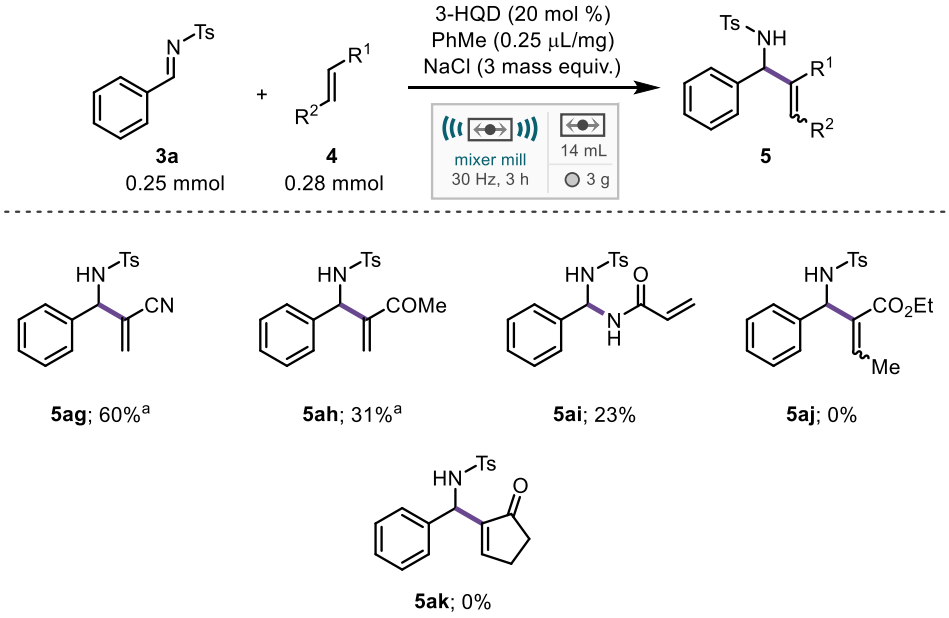

a99 minute reaction time.

Scheme 2.1.4. Scope of Michael acceptors for mechanochemical aza-MBH reaction.

2.2.3. Reaction Scale Up

It was then demonstrated that the process could be scaled up 12-fold, from a 0.25 mmol scale to a 3 mmol scale. This was done by simply increasing the milling jar and grinding ball size from 14 mL and 3 g to 25 mL and 12 g respectively. Using these conditions, the model system using imine **3a** and ethyl acrylate **4a** successfully yielded 0.86 g of product **5a** in 3 hours, with no significant drop in the isolated yield from the optimised process (80% vs. 85%) despite the changes in jar and ball size/mass (Scheme 2.1.5.).

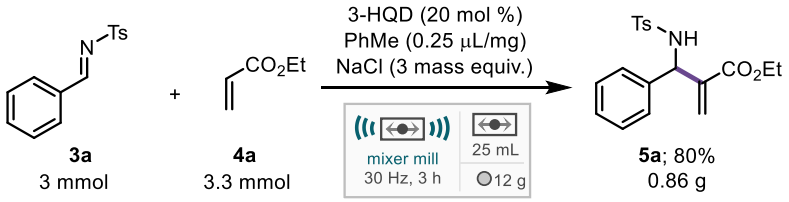

Scheme 2.1.5. Scale up of model mechanochemical aza-MBH reaction.

2.2.4. Comparison to Other Systems

Following completion of the substrate scope and subsequent scale up, the efficacy of the developed process was tested against other known processes, beginning with a comparison to the conditions developed previously by Mack and co-workers. To this end, the reaction of 4-nitrobenzaldehyde (**1b**) with ethyl acrylate (**4a**) under the optimised conditions furnished the desired allylic alcohol (**6a**) in 57% yield, in 99 minutes. This was compared to Mack and co-workers' system where 4-nitrobenzaldehyde (**1b**) was reacted with methyl acrylate (**4b**), using DABCO as the organocatalyst, yielding the allylic alcohol (**6b**) in 98% yield, in only 30 minutes (Scheme 2.1.6.). When 3-HQD was used in their work the allylic alcohol product (**6b**) was produced in 89% yield. While these results are not a 1:1 comparison with our process, it does demonstrate that our system is translatable to a different class of substrates, however, would likely require a small re-optimisation of the reaction conditions to provide better yields.

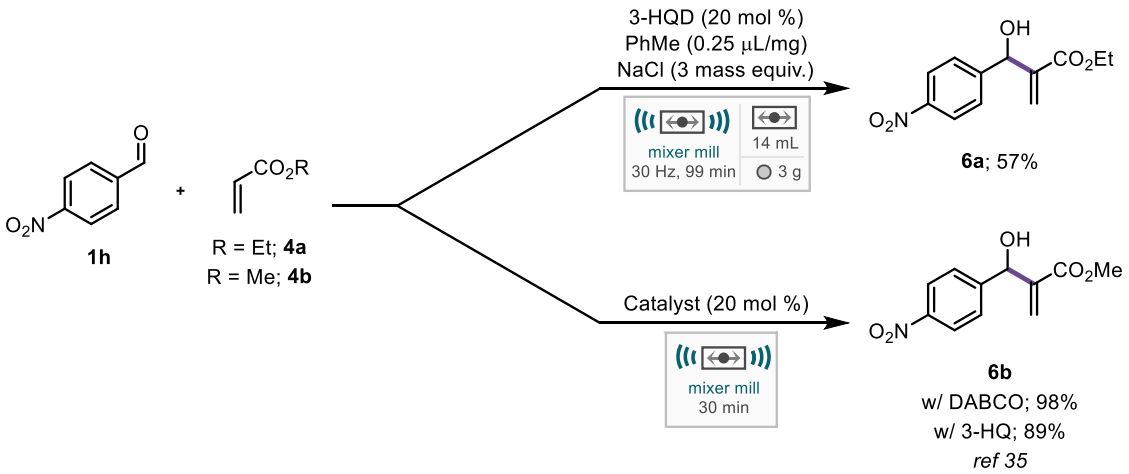

Scheme 2.1.6. Comparison of the developed reaction conditions to Mack and co-workers' conditions using 4-nitrobenzaldehyde as the substrate.

The next comparison conducted was between the ball-milled process and analogous solution-phase and neat-stirred processes. For this study three reactions were carried out using variations of the optimised reaction conditions: the ball-milled process, a solution process with 1 mL (0.25 M) of toluene, and a neat-stirred reaction with no toluene or grinding auxiliary (Scheme 2.1.7.). The solution-phase and neat-stirred processes were performed in microwave vials.

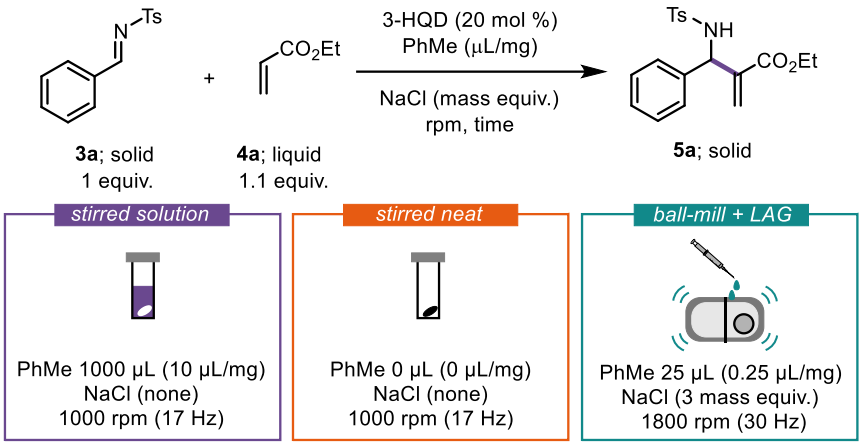

Scheme 2.1.7. Conditions used for the solution-phase and neat-stirred comparisons to the mechanochemical aza-MBH process.

The stirring speed of the solution-phase and neat-stirred reactions was set to 1000 rpm (~17 Hz), which was the highest it could be set to without losing control of the stirrer bar. These reactions were analysed at time points of 5, 30, 60, 120, and 180 minutes using ^{1}H NMR analysis, with mesitylene as an internal standard. The reactions were quenched with 1 M HCl to prevent further catalytic activity during the analysis process.

The solution-phase set of experiments reinforced that the aza-MBH reaction is slow, giving only 25% yield of **5a** by ^{1}H NMR analysis after the 180 minutes had elapsed (Figure 2.1.). For both the neat-stirred and ball-milled set of experiments, high yields of **5a** were observed within 30 minutes: 45% and 47% yield by ^{1}H NMR analysis, respectively. However, from 30 to 180 minutes, the ball-milled process was more efficient than the neat-stirred reaction, furnishing **5a** in 88% yield compared to 70% yield by ^{1}H NMR analysis after the 180 minutes had elapsed.

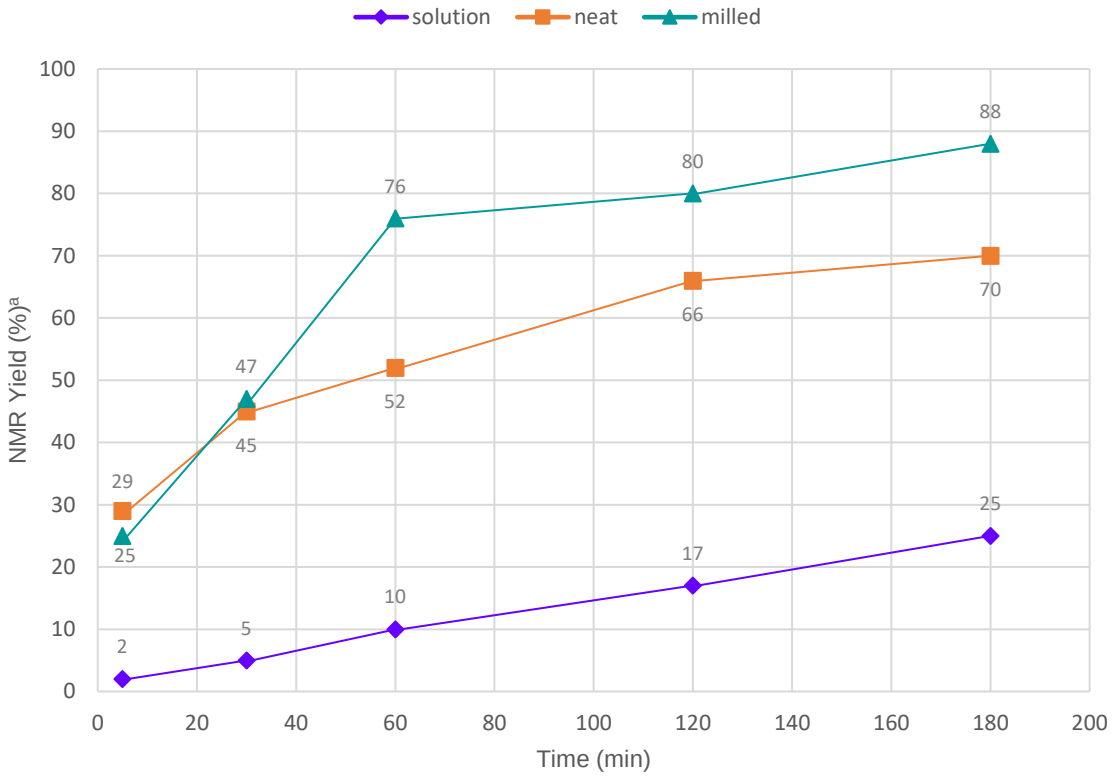

[a]Yield determined by ^{1}H NMR analysis of the crude reaction mixture (after 1 M HCl quench), using mesitylene as an internal standard.

Figure 2.1. Time gated analysis comparing the mechanochemical aza-MBH process to solution-phase and neat-stirred processes.

This contrast in the yields observed is likely due to the improved mixing efficiency of the mixer mill when compared to simple neat stirring in a flask/vial. Additionally, when the physical states of the starting materials and product are considered, where the imine (**3a**) and the product (**5a**) are both solid, and ethyl acrylate (**4a**) is a liquid, it is likely that as the product is formed, it becomes more difficult for effective stirring to occur in the vial. In contrast, the ball-milled process can continually mix effectively through the impact of the grinding ball against the contents of the jar and the jar walls.

2.2.5. One-Pot Procedure Investigations

While a decrease in the reaction time of the aza-MBH reaction and the removal of bulk reaction solvent has been demonstrated, the synthesis of the imine starting materials relies on traditional solution-phase methods. Therefore, the possibility of synthesising the imine starting materials mechanochemically and perhaps extending this to allow a one-pot procedure to be carried out was investigated. To this end, attempts to synthesise **3a** from benzaldehyde (**1a**) and 4-methylbenzenesulfonamide (**2a**) were carried out, with a variety of additives screened for this process (Table 2.2.). The simple milling of benzaldehyde and 4-methylbenzenesulfonamide, with and without sodium chloride as a grinding auxiliary, for 99 minutes, did not lead to any imine formation (entries 1 and 2), hence some common Lewis acids ($AlCl_3$, $CeCl_3$, $ZnCl_2$) were screened as additives. Both $AlCl_3$ and $CeCl_3$ gave poor yields of **3a**: 3% and 2% yield by ^1H NMR analysis, respectively (entries 3 and 4). Whereas $ZnCl_2$ gave a promising 14% yield of **5a** by ^1H NMR analysis (entry 5). Interestingly, when the organocatalyst for the aza-MBH process (3-HQD) was used in the reaction, a 25% yield of **5a** was observed (entry 6). Attempts to improve this yield further by increasing the amount of 3-HQD and extending the reaction time were unfruitful (entry 7). This observation can perhaps be rationalised by the ability of 3-HQD to behave as a Brønsted acid, due to the presence of the hydroxyl group, which could activate the aldehyde and facilitate nucleophilic attack from the amine. This result suggested that a one-pot aza-MBH procedure starting from the aldehyde and the amine was possible.

Table 2.2. Ball-milled synthesis of imine **3a**.

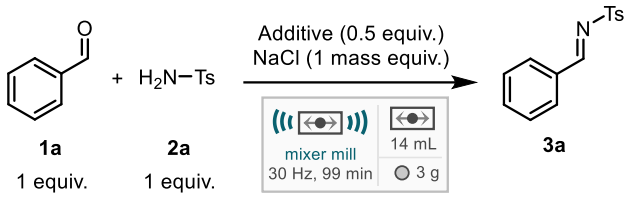

Entry[a]	Additive	3a (%)[b]
1	-	<2
2	None and no NaCl	<2
3	$AlCl_3$	3
4	$CeCl_3$	2
5	$ZnCl_2$	14
6	3-hydroxyquinuclidine (3-HQD)	25
7	3-HQD (1 equiv.) + 3 h reaction	24

[a]Reactions were carried out on a 1 mmol scale, in 14 mL stainless steel jars, equipped with a 3 g, 9 mm stainless steel grinding ball, under an air atmosphere.

[b]Yield determined by ^{1}H NMR analysis of the crude reaction mixture (after work-up), using mesitylene as an internal standard.

With these results in hand, a one-pot aza-MBH procedure was performed by milling benzaldehyde (**1a**), 4-methylbenzenesulfonamide (**2a**), and ethyl acrylate (**4a**), in the presence of 40 mol % 3-HQD as the organocatalyst (Scheme 2.1.8.). An increased catalyst loading was used to compensate for its expected dual role as a Brønsted acid and Lewis base. After 3 hours of milling, the aza-MBH product (**5a**) was isolated in 27% yield, however, the MBH product (**6c**) was also produced in 14% yield (^{1}H NMR analysis). The higher yield of **5a** compared to **6c** suggests that the *in situ* formation of the imine (**3a**) and its subsequent participation in the aza-MBH process is faster than **1a** participating in the MBH reaction. This result demonstrates that with further optimisation, the solution-based synthesis of the imine starting materials can be circumvented by carrying out a one-pot mechanochemical procedure.

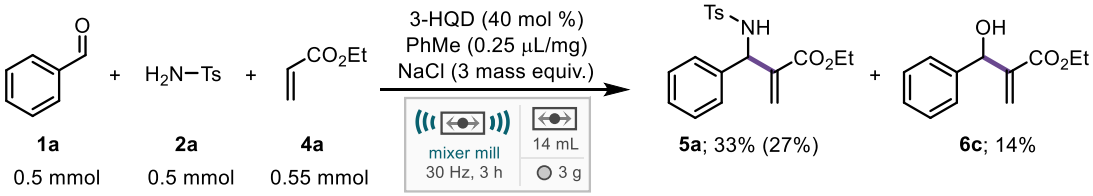

Scheme 2.1.8. One-pot mechanochemical aza-MBH reaction.

2.2.6. Asymmetric Investigations

The final part of this study concerned the potential for enantioinduction in the mechanochemical aza-MBH protocol, as this is an important development of both the MBH and aza-MBH reaction in solution-phase examples, as discussed in section 2.1.2. Initially, a small selection of chiral catalysts were identified as candidates to carry out these investigations, namely enantioenriched (*R*)-3-HQD, β-isocupreidine (β-ICD) and α-isocupreine (α-IC). α-IC can be considered a pseudo-enantiomer of β-ICD, hence these two catalysts are drawn in a way to more easily visualise this (Scheme 2.1.9). β-ICD and α-IC were synthesised from known procedures from the cinchona alkaloids quinidine and quinine, respectively.[39,53]

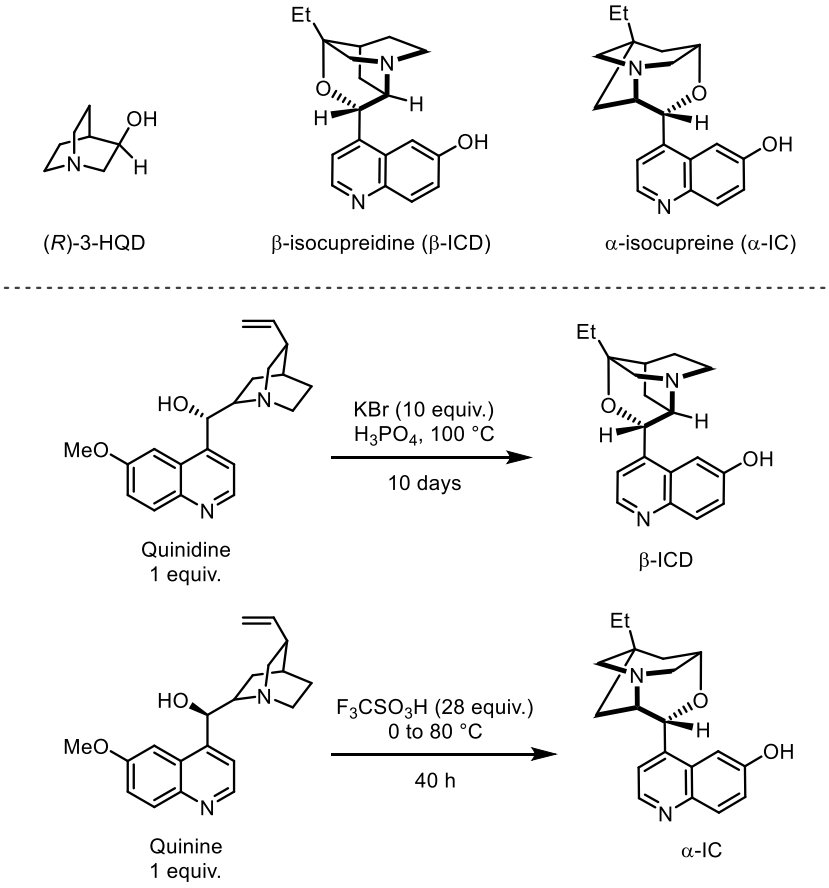

Scheme 2.1.9. Catalysts used for the asymmetric studies and the synthesis of β-ICD and α-IC.

With these catalysts in hand, they were applied to the mechanochemical aza-MBH reaction between imine **3a** and ethyl acrylate (**4a**). Utilising enantioenriched 3-HQD as the catalyst furnished the corresponding product (**5a**) in 76% yield, but with negligible

enantioinduction, (2% ee, Table 2.3., entry 1). However, both β-ICD and α-IC were able to impart moderate to good enantiocontrol, 64% and -26% ee, respectively, albeit in lower yield (both 20% yield, entries 2 and 3). α-IC produces the opposite enantiomer of the product to β-ICD, hence is assigned a negative ee value. For a direct comparison, the reaction with β-ICD was carried out under solution-phase conditions, furnishing the product (**5a**) in 24% yield and 78% ee, after stirring at room temperature in toluene (0.25 M) for 16 hours (entry 4). While the enantiocontrol of the ball-milled process is lower than that achieved in solution, this provides a proof-of-concept for asymmetric tertiary Lewis base organocatalysis to be carried out under mechanochemical conditions. An adjustment to the mechanochemical reaction conditions would likely be required to further improve this initial result.

Table 2.3. Asymmetric aza-MBH investigations.

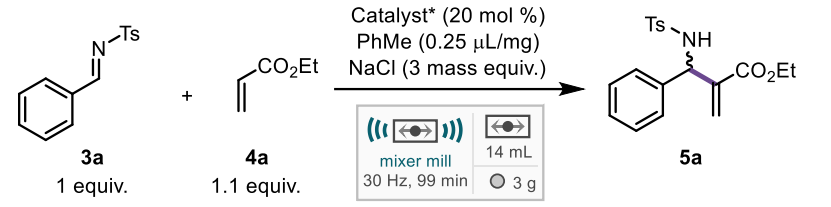

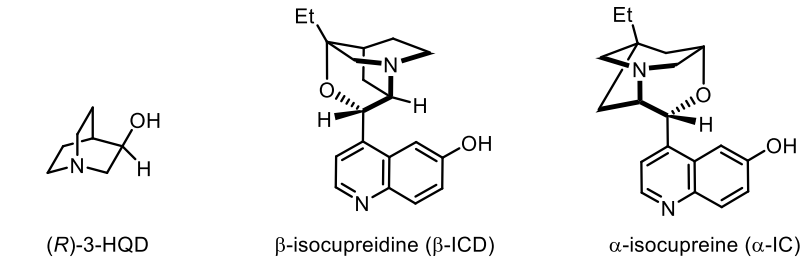

Entry[a]	Catalyst	5a (%)[b]	ee (%)[c]
1	(*R*)-3-HQD	76	2
2	β-ICD	20	64
3	α-IC	20	-26
4[d]	β-ICD	24	78

[a]Reactions were carried out on a 0.25 mmol scale, in 14 mL stainless steel jars, equipped with a 3 g, 9 mm stainless steel grinding ball, under an air atmosphere.

[b]Isolated yields are given.

[c]Determined by HPLC analysis, using a chiral stationary phase.

[d]Reaction carried out at room temperature, in 1 mL of toluene, with a 16 hour reaction time.

2.2.7. Conclusions and Future Work

In conclusion, a mechanochemical protocol for the aza-MBH reaction has been developed. This process demonstrates general time saving when compared to solution-phase examples and a good substrate scope. Additionally, bulk reaction solvent has been removed, and comparisons to solution-phase and neat-stirring analogues revealed the improved efficiency of the developed process. The process is also amenable to scale up, furnishing close to a gram of material in a short reaction time. Finally, it was demonstrated that enantioinduction is possible by utilising β-isocupreidine as the organocatalyst, furnishing providing 64% ee, which is only a small decrease in enantiocontrol compared to a solution-phase analogue.

Future work could involve exploration of other organocatalytic activation modes that have not yet been explored mechanochemically, such as Brønsted acid catalysis. This could be interesting in instances of fully solid-state behaviour, such as where one or more substrates have poor solubility and can only be utilised by mechanochemical means. Additionally, further exploration of asymmetric organocatalytic reactions, under mechanochemical conditions, could be of interest. The application of the developed aza-MBH process to a larger scale using extrusion is also a worthwhile consideration.

2.3. Bibliography

1 J. von Liebig, *Ann. Chem. Pharm.*, 1860, **113**, 246–247.

2 Z. G. Hajos and D. R. Parrish, *J. Org. Chem.*, 1974, **39**, 1615–1621.

3 A. G. Doyle and E. N. Jacobsen, *Chem. Rev.*, 2007, **107**, 5713–5743.

4 D. Enders, O. Niemeier and A. Henseler, *Chem. Rev.*, 2007, **107**, 5606–5655.

5 S. Mukherjee, J. W. Yang, S. Hoffmann and B. List, *Chem. Rev.*, 2007, **107**, 5471–5569.

6 M. J. Gaunt and C. C. C. Johansson, *Chem. Rev.*, 2007, **107**, 5596–5605.

7 B. List, R. A. Lerner and C. F. Barbas, *J. Am. Chem. Soc.*, 2000, **122**, 2395–2396.

8 K. A. Ahrendt, C. J. Borths and D. W. C. MacMillan, *J. Am. Chem. Soc.*, 2000, **122**, 4243–4244.

9 H. Guo, Y. C. Fan, Z. Sun, Y. Wu and O. Kwon, *Chem. Rev.*, 2018, **118**, 10049–10293.

10 D. Parmar, E. Sugiono, S. Raja and M. Rueping, *Chem. Rev.*, 2014, **114**, 9047–9153.

11 D. W. C. MacMillan, *Nature*, 2008, **455**, 304–308.

12 R. Breslow, *J. Am. Chem. Soc.*, 1958, **80**, 3719–3726.

13 J. R. De Alaniz, M. S. Kerr, J. L. Moore and T. Rovis, *J. Org. Chem.*, 2008, **73**, 2033–2040.

14 M. S. Kerr, J. R. De Alaniz and T. Rovis, *J. Am. Chem. Soc.*, 2002, **124**, 10298–10299.

15 H. Takikawa and K. Suzuki, *Org. Lett.*, 2007, **9**, 2713–2716.

16 A. Bruckmann, A. Krebs and C. Bolm, *Green Chem.*, 2008, **10**, 1131–1141.

17 P. Chauhan and S. S. Chimni, *Beilstein J. Org. Chem.*, 2012, **8**, 2132–2141.

18 C. G. Avila-Ortiz, M. Pérez-Venegas, J. Vargas-Caporali and E. Juaristi,

Tetrahedron Lett., 2019, **60**, 1749–1757.

19 D. Kristofikova, V. Modrocká, M. Mečiarová and R. Sebesta, *ChemSusChem*, 2020, **13**, 1–32.

20 M. Pérez-Venegas, E. Juaristi and E. Juaristi, *ACS Sustainable Chem. Eng.*, 2020, **8**, 8881–8893.

21 I. N. Egorov, S. Santra, D. S. Kopchuk, I. S. Kovalev, G. V. Zyryanov, A. Majee, B. C. Ranu, V. L. Rusinov and O. N. Chupakhin, *Green Chem.*, 2020, **22**, 302–315.

22 M. T. J. Williams, L. C. Morrill and D. L. Browne, *ChemSusChem*, 2022, **15**, e202102157.

23 B. Rodríguez, T. Rantanen and C. Bolm, *Angew. Chem. Int. Ed.*, 2006, **45**, 6924–6926.

24 G. Guillena, M. del Carmen Hita, C. Nájera and S. F. Viózquez, *Tetrahedron Asymmetry*, 2007, **18**, 2300–2304.

25 J. G. Hernández and E. Juaristi, *J. Org. Chem.*, 2011, **76**, 1464–1467.

26 J. G. Hernández and E. Juaristi, *Tetrahedron*, 2011, **67**, 6953–6959.

27 J. G. Hernández, V. García-López and E. Juaristi, *Tetrahedron*, 2012, **68**, 92–97.

28 E. Veverková, V. Poláčková, L. Liptáková, E. Kázmerová, M. Mečiarová, Š. Toma and R. Šebesta, *ChemCatChem*, 2012, **4**, 1013–1018.

29 E. Veverková, V. Modrocká and R. Šebesta, *Eur. J. Org. Chem.*, 2017, **2017**, 1191–1195.

30 D. Krištofíková, M. Mečiarová, E. Rakovský and R. Šebesta, *ACS Sustainable Chem. Eng.*, 2020, **8**, 14417–14424.

31 Y. F. Wang, R. X. Chen, K. Wang, B. Bin Zhang, Z. B. Li and D. Q. Xu, *Green Chem.*, 2012, **14**, 893–895.

32 M. Jörres, S. Mersmann, G. Raabe and C. Bolm, *Green Chem.*, 2013, **15**, 612–616.

33 M. Hestericová and R. Šebesta, *Tetrahedron*, 2014, **70**, 901–905.

34 W. I. Nicholson, A. C. Seastram, S. A. Iqbal, B. G. Reed-Berendt, L. C. Morrill and D. L. Browne, *ChemSusChem*, 2020, **13**, 131–135.

35 J. Mack and M. Shumba, *Green Chem.*, 2007, **9**, 328–330.

36 K.-I. Morita, Z. Suzuki and H. Hirose, *Bull. Chem. Soc. Jpn.*, 1968, **41**, 2815–2815.

37 A. B. Baylis and M. E. D. Hillman, *Chem. Abstr.*, 1972, **77**, 34174q.

38 R. Robiette, V. K. Aggarwal and J. N. Harvey, *J. Am. Chem. Soc.*, 2007, **129**, 15513–15525.

39 Y. Iwabuchi, M. Nakatani, N. Yokoyama and S. Hatakeyama, *J. Am. Chem. Soc.*, 1999, **121**, 10219–10220.

40 N. T. McDougal and S. E. Schaus, *J. Am. Chem. Soc.*, 2003, **125**, 12094–12095.

41 E. Campi, A. Holmes, P. Perlmutter and C. Teo, *Aust. J. Chem.*, 1995, **48**, 1535–1540.

42 S. Bhowmik and S. Batra, *Curr. Org. Chem.*, 2015, **18**, 3078–3119.

43 S. Bhowmik and S. Batra, *Eur. J. Org. Chem.*, 2013, **2013**, 7145–7151.

44 V. Declerck, J. Martinez and F. Lamaty, *Chem. Rev.*, 2009, **109**, 1–48.

45 N. Abermil, G. Masson and J. Zhu, *J. Am. Chem. Soc.*, 2008, **130**, 12596–12597.

46 F. Le Hu, Y. Wei, M. Shi, S. Pindi and G. Li, *Org. Biomol. Chem.*, 2013, **11**, 1921–1924.

47 X. Lu and U. Schneider, *Chem. Commun.*, 2016, **52**, 12980–12983.

48 S. Takizawa, E. Rémond, F. A. Arteaga, Y. Yoshida, V. Sridharan, J. Bayardon, S. Jugé and H. Sasai, *Chem. Commun.*, 2013, **49**, 8392–8394.

49 M. Shi and Y. M. Xu, *Angew. Chem. Int. Ed.*, 2002, **41**, 4507–4510.

50 3-Quinuclidinol price, https://www.sigmaaldrich.com/GB/en/product/aldrich/253340, (accessed 3

November 2022).

51 Quinuclidine price, https://www.sigmaaldrich.com/GB/en/product/aldrich/197602, (accessed 3 November 2022).

52 Y. L. Shi, Y. M. Xu and M. Shi, *Adv. Synth. Catal.*, 2004, **346**, 1220–1230.

53 Y. Nakamoto, F. Urabe, K. Takahashi, J. Ishihara and S. Hatakeyama, *Chem. Eur. J.*, 2013, **19**, 12653–12656.

Chapter 3: Mechanochemical Cross-Electrophile Coupling of Heteroaryl Halides and Alkyl Halides

3.1. Introduction to Cross-Electrophile Coupling

Over the last 50 years, transition metal-catalysed cross-coupling reactions have become a staple of organic synthesis, celebrated in 2010 with the award of the Nobel prize in chemistry to Heck, Suzuki, and Negishi, for the development of palladium-catalysed methods.[1–6] The development of these processes required many key breakthroughs from the wider chemistry community to deliver a versatile methodology capable of forging new C-C or C-heteroatom bonds from a variety of starting materials.[7] This has included substrates such as boronic acids and esters, organometallics (organozinc, organomagnesium, organotin), and amines. However, these substrates are all nucleophilic in nature i.e., favour transmetallation pathways, hence the observed selectivity in the corresponding cross-coupling reactions arises from the reactivity matching with the electrophile (Scheme 3.1A). Additionally, these substrates can be difficult to handle and often require point-of-use preparation, which can be troublesome during late-stage functionalisation processes. These drawbacks have been somewhat circumvented in recent years by the development of so-called cross-electrophile coupling (XEC) processes.[8–11] Here, two substrates that are electrophilic in nature, such as two aryl halides, are selectively coupled together to furnish the cross-coupled product (Scheme 3.1B). However, selectivity for these cross-coupled products is much more difficult to control than in traditional cross-coupling processes, due to the similar reactivity of the substrates, whereby oxidative addition is favoured over transmetallation pathways. For this reason, homo-coupling of either substrate can be a common issue to overcome.

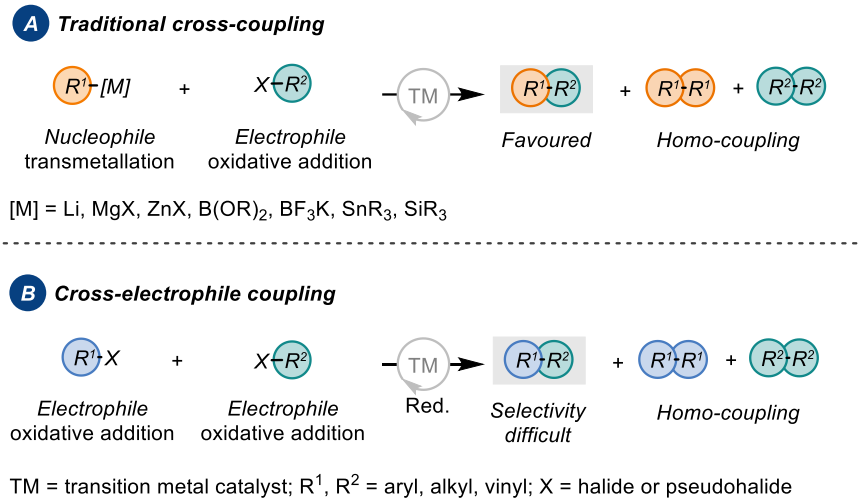

Scheme 3.1. A) Traditional cross-coupling; B) cross-electrophile coupling.

Many methods have been developed to overcome the selectivity issues that arise during XEC processes, which have typically been achieved by using two electrophiles with different reactivities, e.g., an aryl halide and an alkyl halide.[12] These XEC processes are typically performed in the presence of a terminal reducing species, such as a zero-valent metal (zinc, manganese, magnesium) which have been suggested to have multiple roles in these processes, including the generation and regeneration of the active metal catalyst species. The most common metal catalyst that has been utilised is earth-abundant nickel, due to its ability to access oxidation states that are not accessible to second and third row transition-metals such as palladium, including I and III oxidation states.[13–16] This enables metals like nickel to undergo catalytic steps involving single-electron transfer (SET), rather than the two-electron processes that are commonly encountered, such as oxidative addition and reductive elimination.

All of this considered, the four commonly proposed pathways for XEC are: *in situ* formation of an organometallic species from the reducing species and one of the electrophiles, transmetallation between two nickel species, sequential oxidation addition of the two electrophiles, and a radical chain process where an alkyl radical is formed via an SET between the nickel catalyst and an alkyl halide (Scheme 3.2A–D).[10] As previously mentioned, electronic reactivity differences between the two electrophilic species allow each mechanistic pathway to favour cross-coupling over homo-coupling. However, the pathway that has attracted the most interest over the last decade is the incitation of a radical chain pathway (Scheme 3.2D).

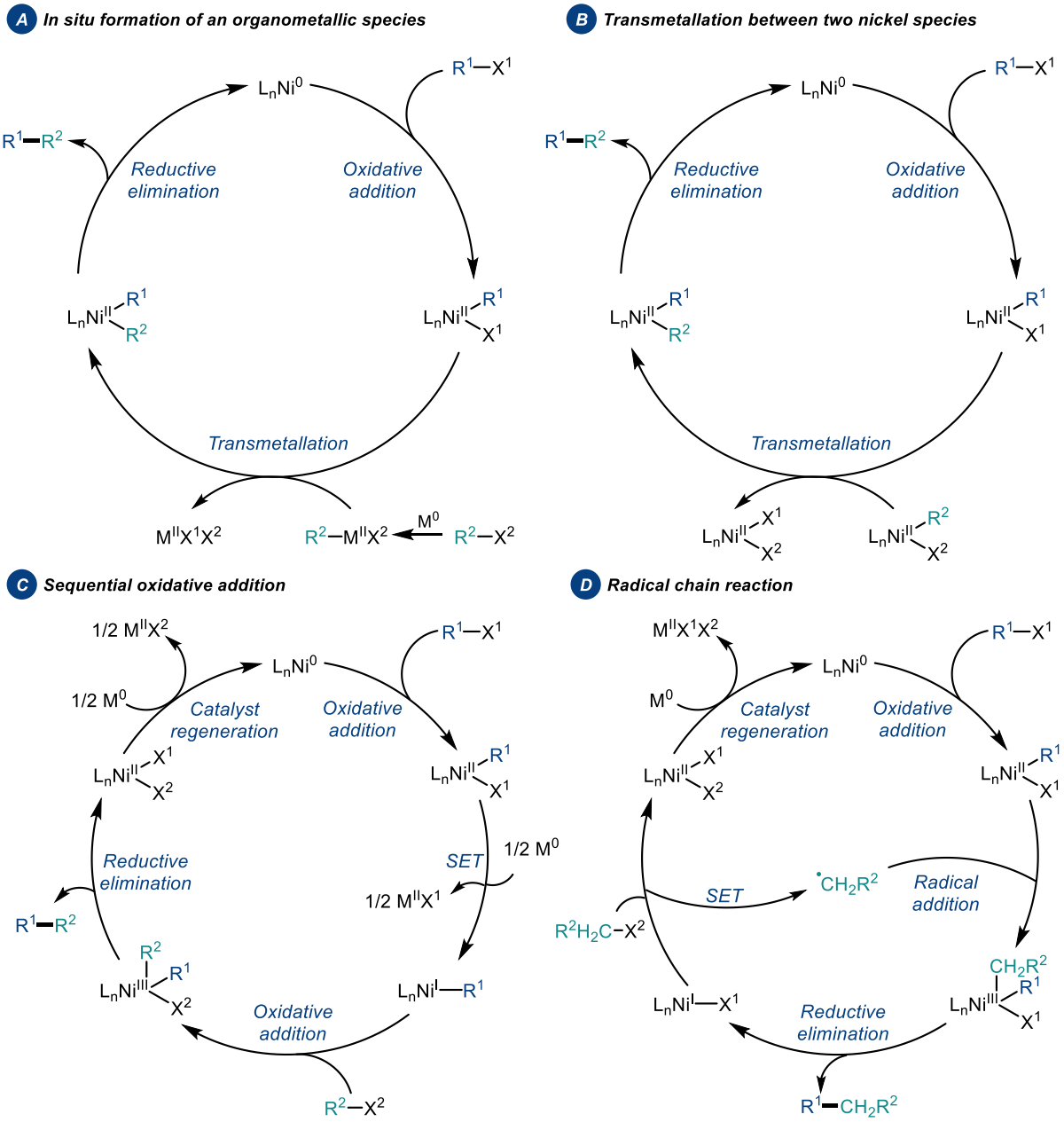

Scheme 3.2. XEC mechanisms: A) *in situ* formation of an organometallic species, B) transmetallation between two nickel species, C) sequential oxidative addition, D) radical chain reaction.

Weix and co-workers are one of the leading pioneers of using radical chain pathways for XEC. They reported one of the first examples of this type of chemistry between aryl halides and alkyl halides.[17] This work utilised nickel(II) iodide as the pre-catalyst and a mixed ligand system of a bipyridine (4,4'-di-*tert*-butyl-2,2'-bipyridine) and a biphosphine (*o*-$(Ph_2P)_2C_6H_4$), with manganese metal as the terminal reductant (Scheme 3.3A). This work demonstrated good functional group tolerance, including successful coupling of free alcohol and a boronic ester, which are not typically

tolerated using traditional cross-coupling methods. A major limitation of this work and many subsequent reports was the general intolerance of aryl or alkyl chlorides,[18] a functionality that would be desirable as they are much more commercially available than the bromide and iodide counterparts (~1.8 million organic chlorides are commercially available compared to ~841 000 organic bromides and <100 000 organic iodides). The C-Cl bond is less reactive than C-Br and C-I bonds, hence more specialised conditions have been employed to tolerate these substrates.[19] However, a later report by Weix and co-workers successfully utilised aryl chlorides and alkyl chlorides as substrates for XEC, with the key to overcoming the previous limitations coming in the form of an amidine based ligand and lithium chloride as an additive (Scheme 3.3B).[14,20] The authors suggested that key co-catalysis between the chloride additive and the nickel pre-catalyst (NiX_2) could lead to the formation of other lithium salts (LiBr or LiI). These could then undergo halide exchange with the alkyl chloride to form more reactive alkyl bromides or iodides *in situ*.

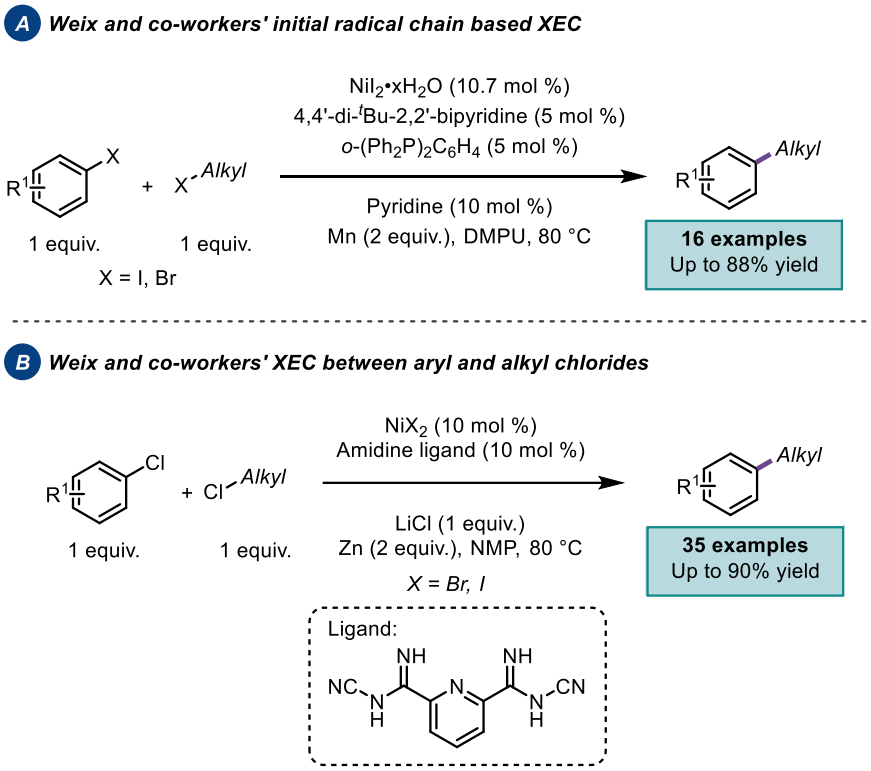

Scheme 3.3. A) Weix and co-workers' initial report on the radical chain-based XEC; B) Weix and co-workers' report on the XEC of aryl and alkyl chlorides.

However, while there have been great strides made in XEC processes over the past decade, there still remain some general limitations, such as the reliance on amide solvents (*N,N*-dimethylformamide, *N,N*-dimethylacetamide, *N*-methylpyrrolidinone),

which are typically difficult to remove and are highly regulated for their negative environmental and health impact. Examples using non-amide solvents do exist, but there is still a reliance on these solvents, in general.[21] In addition, these reactions can be slow and often require inert set ups, which is likely due to the poor air stability of the active nickel (0) species and the terminal reductant. Most notably, however, is the somewhat tedious requirement to activate the terminal reductant (zinc, manganese, magnesium) either *ex situ* or *in situ*, to remove the metal oxide layer that coats the material. This activation is typically achieved using harsh conditions, such as washing with concentrated acid (HCl) followed by drying under vacuum, or by the use of additives, such as an iodine crystal, chlorotrimethylsilane, or 1,2-dibromoethane, under inert conditions.[22] These methods require the point-of-use generation of the activated metal into the reaction system before the oxide layer reforms from exposure to air (Scheme 3.4A).[23] This activation step is particularly problematic on a large scale and the efficacy of the activation can vary between various forms and suppliers of the metal. For this reason, a method that avoids these tedious activation steps is an attractive prospect from a large-scale perspective. There have also been successful reports of using non-metal reductants, such as tetrakis(dimethylaminoethylene) (TDAE);[21] however, these organic reductants present their own limitations, such as their air instability and formation of insoluble iminium by-products.[24] Use of metal reductants has also been circumvented by using photo- or electrochemical techniques, but a general method does not exist (Scheme 3.4B).[25–32]

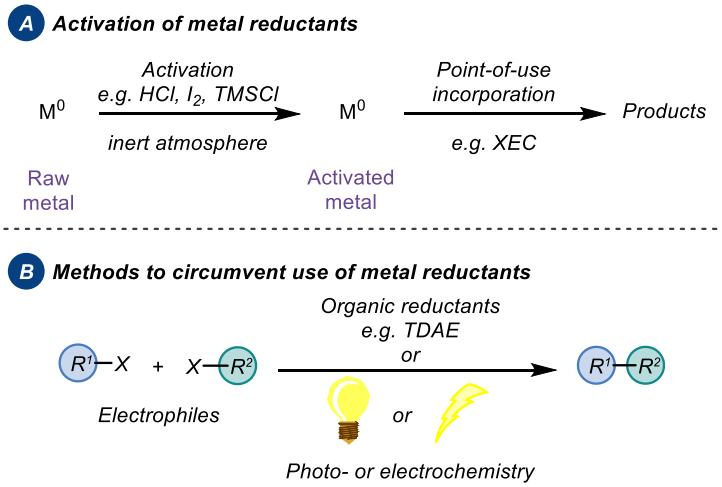

Scheme 3.4. A) Overview of traditional methods to activate metal reductants; B) common methods to circumvent usage of metal reductants.

Therefore, a technique to overcome the limitations encountered within traditional XEC processes is of great interest, and it is envisaged that mechanochemistry could enable this. Mechanochemistry could permit the efficient grinding and mixing of these metal reductants, resulting in the fine comminution of the materials, and revealing the desired active metal.[33]

3.2. Mechanochemical Activation of Zero-Valent Metals

The mechanochemical grinding of zero-valent metals to reveal the active metal form has been demonstrated many times in the literature, including an early example from Wan and co-workers, where they successfully functionalised fullerene using an *in situ* generated organozinc reagent formed from the insertion of zinc metal into α-bromoesters, albeit in low yield (Scheme 3.5A).[34] This report was also solvent-free, but an inert atmosphere was still required, in the form of a nitrogen bag encapsulating the milling vessel. More recent work has included work from Browne and co-workers on the mechanochemical activation of zinc metal and its application to both the Reformatsky and Negishi cross-coupling reactions, via an *in situ* generated organozinc reagent (Scheme 3.5B and 3.5C).[35,36] These reports proved to be more general than the previous report by Wan and co-workers, with a broad range of substrates tolerated and the demonstration that the raw form of the zinc metal was inconsequential to the efficiency of the process. A range of zinc forms were shown to be effective, including foil, dust, powder, and wire. Additionally, both systems were shown to be tolerant to an air atmosphere, making the protocol operationally simple. Following these reports and others of a similar nature,[37–41] it became apparent that the mechanochemical activation of zinc, along with other metals such as manganese and magnesium, could be applied to a range of systems, therefore, it was envisaged that this could be applied to XEC processes.

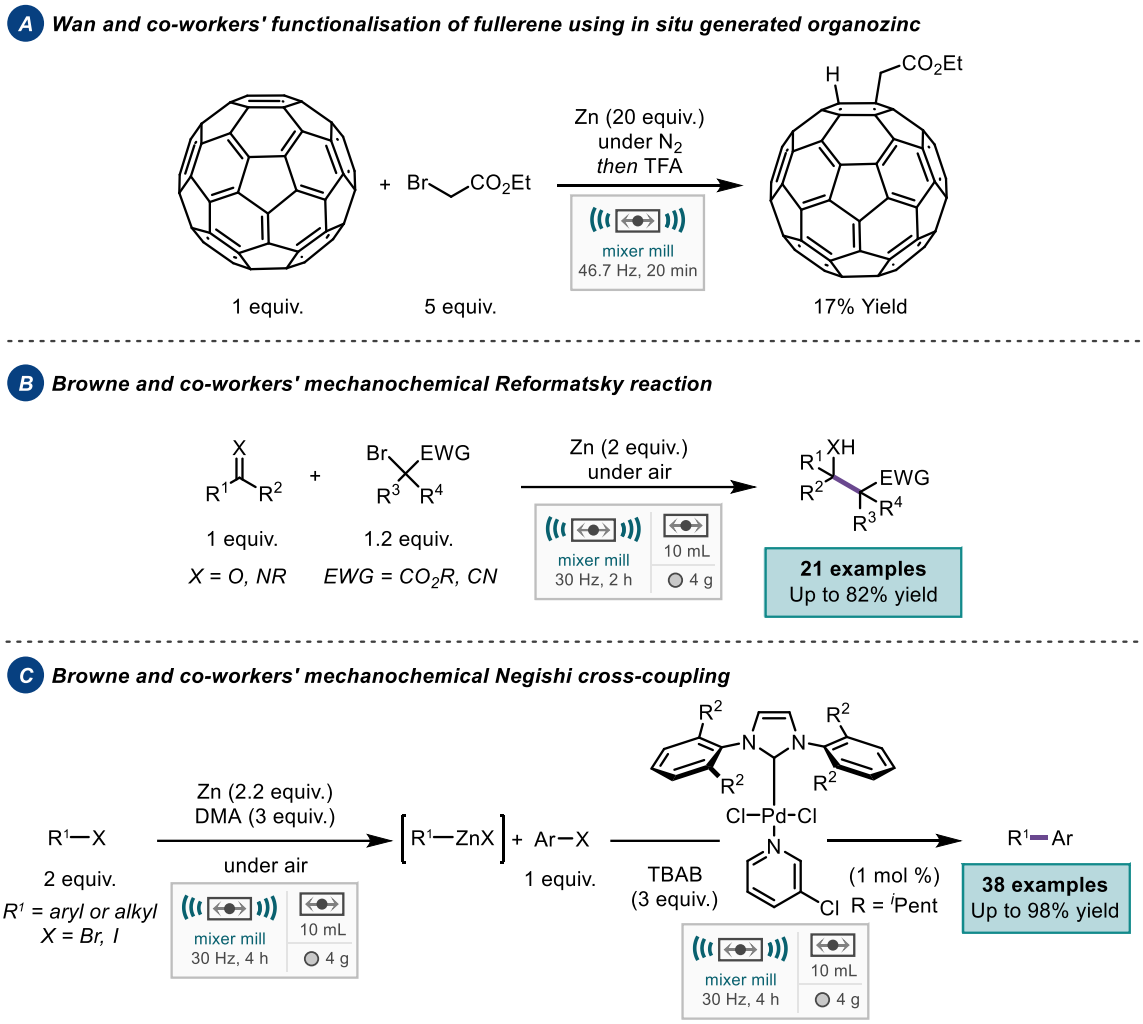

Scheme 3.5. A) Wan and co-workers' report on the mechanochemical functionalisation of fullerene via an *in situ* generated organozinc reagent; B) Browne and co-workers' mechanochemical Reformatsky reaction; C) Browne and co-workers' mechanochemical Negishi cross-coupling reaction.

3.2.1. Mechanochemical Cross-Electrophile Coupling

Mechanochemical XEC was fully realised in 2021 by concurrent reports from Browne and co-workers, along with Shi, Zou and co-workers, where a range of aryl halides and alkyl halides were successfully cross-coupled (Scheme 3.6A and 3.6B).[42,43] The key differences between these reports were the choice of metal reductant used, (zinc in Browne's report and manganese in Shi and Zou's report), the type of mill used, (a mixer ball-mill in Browne's report and a planetary ball mill in Shi and Zou's report), and the reaction atmosphere, (with Browne's report under an air atmosphere and Shi and

Zou's report under a nitrogen atmosphere). However, both reports demonstrated significantly decreased reaction time versus solution-phase techniques, the use of DMA as a liquid-assisted grinding agent, and the mechanochemical activation of the zinc and manganese reductants, respectively. Additionally, a range of both aryl and alkyl bromides and iodides were tolerated, along with a range of sensitive functional groups, such as aldehydes, alcohols, and boronic esters. However, one of the limitations of the zinc-mediated work was the poor tolerance of a wider class of substrate, such as heteroaryl halides. This included 2- and 3-bromopyridine, 3-bromofuran, and 3-bromothiophene, which were all poorly yielding under these reaction conditions.

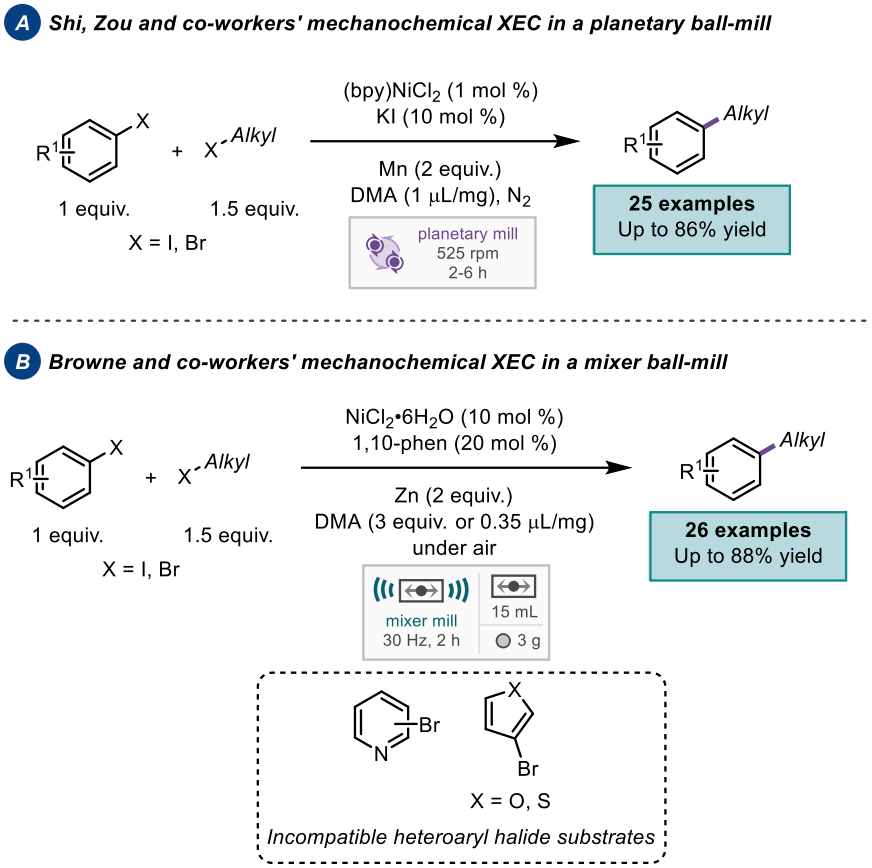

Scheme 3.6. Reports of mechanochemical XEC: A) Shi, Zou and co-workers' report in a planetary ball-mill; B) Browne and co-workers' report in a mixer ball-mill.

These heteroaryl halide class of substrates are of interest, especially the nitrogen-containing examples, as 60% of the Food and Drug Administration's (FDA) approved small molecule drugs contain a nitrogen-based heterocycle,[44] with a few examples of alkylated *N*-heterocycles displayed below. This includes Betahistine, which is used to treat Ménière's disease: a form of vertigo (Figure 3.1.).[45] Pyridine is the second most common nitrogen heterocycle present within these drugs. Therefore, it was proposed

that it would be of interest to follow up the previous work to develop a set of conditions to tolerate these heteroaryl halide substrates.

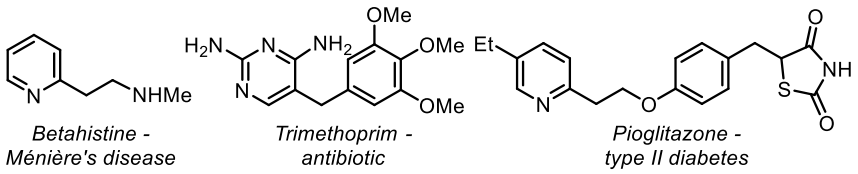

Figure 3.1. Examples of small molecule drugs containing nitrogen heterocycles.

3.3. Results and Discussion

3.3.1. Reaction Optimisation

Studies into the mechanochemical heteroaryl XEC process commenced with a demonstration that the previously developed reaction conditions (Scheme 3.6B) were incompatible with this class of substrate. To this end, 3-bromopyridine (**7a**) and 1-iodooctane (**8a**) were reacted under the previous conditions of 10 mol % nickel (II) chloride hexahydrate, 20 mol % of 1,10-phenanthroline (1,10-phen), 2 equivalents of zinc metal, and 3 equivalents (η = 0.33 µL/mg) of DMA as the LAG agent. The reaction was carried out in a mixer ball-mill, for 2 hours at 30 Hz, with no precautions to remove air or moisture (Scheme 3.7.). Under these conditions, the desired cross-coupled product (**9a**) was produced in 34% yield as determined by ^{1}H NMR spectroscopy and isolated in 28% yield. While this result shows that these conditions are moderately effective for this class of substrate, the relatively poor yield prevents the process from being considered a viable general method.

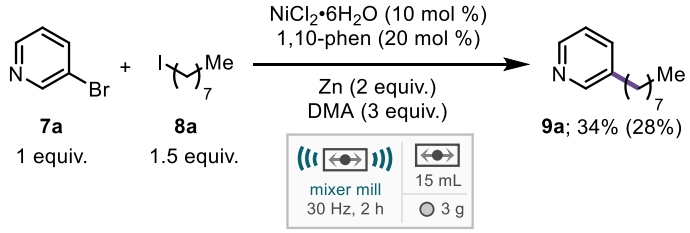

Scheme 3.7. Initial result for heteroaryl XEC using the optimal conditions from Browne and co-workers' previous report.

Following this, a survey of the literature revealed that these heteroaryl halide substrates typically require a re-optimisation of the established reaction conditions, where the ligand used is shown to have a profound effect on the efficacy of the reaction.[46] This can be rationalised by considering that *N*-heteroaryl halides are ligands themselves, hence can competitively coordinate to the metal catalyst, which may result in diminished catalytic activity. Consequently, a selection of amidine ligands developed by Weix and co-workers were identified as suitable candidates for the milled process, which were synthesised according to the procedures reported by Weix and co-workers, from the corresponding picolinonitrile starting materials (Scheme 3.8.).[20] The authors postulated that these amidine ligands are able to bind more strongly to the catalyst than typical nitrogen-based ligands (bipyridines, phenanthrolines), therefore, can more readily prevent competitive binding from the heteroaryl substrates. It is worth noting that the amidine ligands made using ammonium chloride (i.e., R = H), are formed as their hydrochloric acid salts.

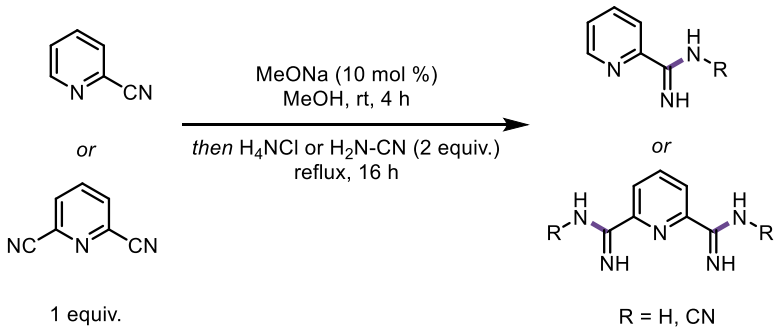

Scheme 3.8. Synthesis of amidine ligands.

These amidine ligands, along with some commonly used bi- and tridentate nitrogen-based ligands, were investigated for the mechanochemical heteroaryl XEC reaction. This ligand screen revealed that bipyridine, phenanthroline, and terpyridine based ligands (**L1** – **L7**) were largely ineffective for selective cross-coupling of 3-bromopyridine and 1-iodooctane, with 1,10-phenanthroline giving the highest yield of product, 34% of **9a** as determined by ^{1}H NMR analysis (Table 3.1., entries 1 – 7). Amongst the amidine ligands (**L8** – **L11**), **L8** proved to be the most effective ligand for cross-coupling, furnishing the product in 57% yield as determined by ^{1}H NMR analysis (entries 8 – 11). Hence, this ligand was carried forward as the most optimal for the process. Following this, the catalyst to ligand ratio was varied to determine if the 1:2 ratio used previously is optimal in this case. Ratios of 1:1 and 1:4 were tested, revealing that the 1:2 ratio was optimal (entries 12 and 13). In all cases, the mass

balance is relatively poor, which can potentially be rationalised by the formation of by-products that are difficult to observe, such as pyridine formed from the proto-debromination of **7a** and the possibility of **7a** to ligate to the nickel catalyst. Both these outcomes could result in mass being lost in the workup process.

Table 3.1. Ligand screen for mechanochemical XEC between 3-bromopyridine and 1-iodooctane.

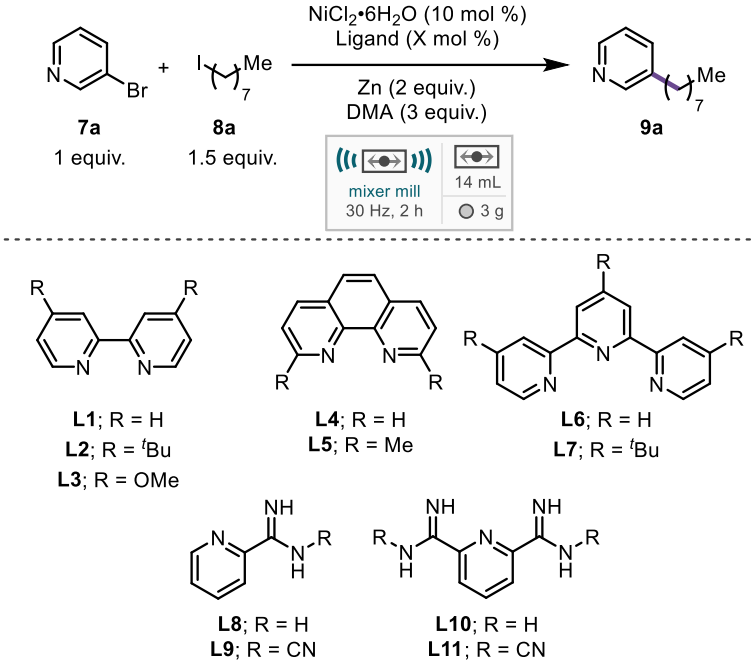

Entry[a]	Ligand (mol %)	7a (%)[b]	9a (%)[b]
1	**L1** (20)	39	8
2	**L2** (20)	23	26
3	**L3** (20)	21	29
4	**L4** (20)	3	34 (28)
5	**L5** (20)	55	<2
6	**L6** (20)	8	14
7	**L7** (20)	20	16
8	**L8** (20)	11	57
9	**L9** (20)	18	36
10	**L10** (20)	15	39
11	**L11** (20)	36	5
12	**L8** (10)	26	41
13	**L8** (40)	17	36

[a]Reactions were carried out on a 0.3 mmol scale in 14 mL stainless steel jars, equipped with a 3 g, 9 mm stainless steel grinding ball, under an air atmosphere.

[b]Yield determined by ^{1}H NMR analysis of the crude reaction mixture (after work-up), using mesitylene as an internal standard. Isolated yields are given in parentheses.

Subsequently, the remaining reaction parameters were varied, including the equivalents of alkyl halide, the nickel pre-catalyst, the metal reductant, and the reaction time (Table 3.2.). These investigations revealed that using a larger excess of alkyl halide coupling partner was more effective for product formation than a slight excess; 2 equivalents of **8a** gave 58% yield of **9a**, compared to 31% for the use of 1.1 equivalents (entries 1 – 3). This is potentially due to the alkyl halide participating in undesired side-reactions, such as elimination, protodehalogenation, and homocoupling, hence an excess of the reagent is necessary. Increasing or decreasing the catalyst loading proved to be unnecessary, furnishing **9a** in 39% and 62% yield, respectively for the use of 5 and 20 mol % of catalyst (entries 4 and 5). In addition, changing the nickel catalyst to a dimethoxy ethane (DME) ligated catalyst did not result in a significant change to the product yield, providing **9a** in 55% yield (entry 6). Using zinc as the reductant instead of manganese was optimal (entry 7), and the 2 hour reaction time was deemed to be sufficient (entry 8).

Table 3.2. Optimisation of XEC between 3-bromopyridine and 1-iodooctane.

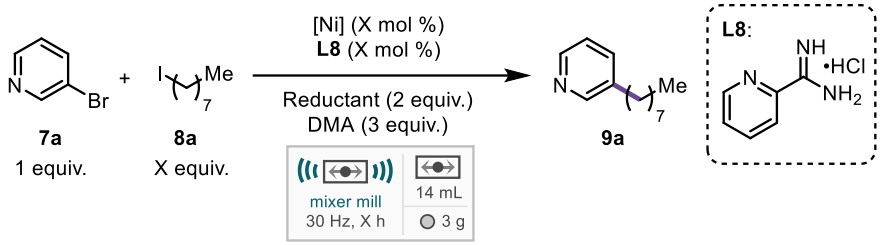

Entry[a]	8a (equiv.)	[Ni] (mol %)	L8 (mol %)	Reductant	Time (h)	7a (%)[b]	9a (%)[b]
1	1.5	$NiCl_2$•$6H_2O$ (10)	20	Zn	2	11	57
2	1.1	$NiCl_2$•$6H_2O$ (10)	20	Zn	2	8	31
3	2	$NiCl_2$•$6H_2O$ (10)	20	Zn	2	9	58
4	2	$NiCl_2$•$6H_2O$ (5)	10	Zn	2	22	39
5	2	$NiCl_2$•$6H_2O$ (20)	40	Zn	2	8	62 (48)
6	2	$NiBr_2$(DME) (10)	20	Zn	2	14	55
7	2	$NiCl_2$•$6H_2O$ (10)	20	Mn	2	59	1
8	2	$NiCl_2$•$6H_2O$ (10)	20	Zn	3	15	49

[a]Reactions were carried out on a 0.3 mmol scale in 14 mL stainless steel jars, equipped with a 3 g, 9 mm stainless steel grinding ball, under an air atmosphere.

[b]Yield determined by ^{1}H NMR analysis of the crude reaction mixture (after work-up), using mesitylene as an internal standard. Isolated yields are given in parentheses.

These results gave the impression that this was not the best system to optimise this process on, so 3-bromopyridine (**7a**) was substituted for 2-bromopyridine (**7b**) or 4-bromopyridine (**7c**) in the hope that these substrates would perform better in the process. Immediately, it was found that 2-bromopyridine was the more effective substrate, furnishing the XEC product (**9b**) in 65% yield by ^{1}H NMR analysis (Scheme 3.9.). The more effective reactivity of this substrate could be due to the 2-position of pyridines being more activated than the 3-position, because of inductive effects from the nitrogen atom. When 4-bromopyridine was used as the substrate 22% yield of the XEC product (**9c**) was produced, as determined by ^{1}H NMR analysis. Hence, 2-bromopyridine was carried forward as the substrate to finalise the optimisation of the XEC process.

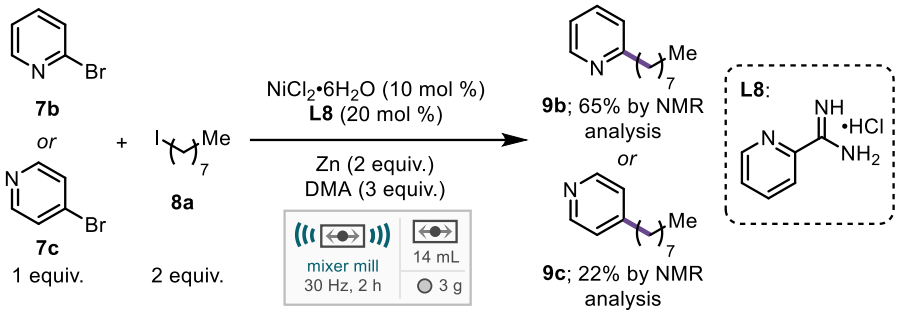

Scheme 3.9. Results from using 2- and 4-bromopyridine as alternative substrates in the XEC process.

To fully assess the reaction using 2-bromopyridine, a mini screen was carried out of the parameters that had previously been investigated for 3-bromopyridine (Table 3.3.). This included varying the equivalents of zinc reductant by testing a range of stoichiometries from 1.2 to 3 equivalents. This revealed that 2.5 equivalents were more effective than 2 equivalents, furnishing **9b** in 79% yield by ^{1}H NMR analysis and 72% isolated yield (entries 1 – 4). It is common to utilise a large excess of the terminal reductant in XEC processes, potentially due to the multiple roles that the reductants have in the reaction (e.g., catalyst generation and regeneration).[8,9] A small screen of the previously utilised ligands demonstrated that the bidentate amidine ligand **L8** was also optimal for this substrate (entries 5 – 8). Other nickel pre-catalysts were effective, however, they resulted in slightly decreased yields of **9b** (entries 9 and 10). Manganese proved to be an effective reductant for this system, however, **9b** was furnished in a decreased yield of 55% (entry 11). By contrast, the organic reductant TDAE was ineffective for this process with no product **9b** observed and 2-bromopyridine remaining (entry 12). TDAE is known to be intolerant to air and moisture, hence this is likely the cause of its ineffectiveness.[24] DMA was shown to be the optimal LAG agent and removing or decreasing the amount of DMA severely

hindered the reaction efficiency (entries 13 – 17). It is possible that amide additives, such as DMA, can stabilise intermediates in the process, for example by coordinating to the activated metal reductant, however this is conjecture. Unsurprisingly, the process is completely ineffective in the absence of nickel or reductant and is significantly inhibited without exogenous ligand (entries 20 – 22). The necessity for the exogenous ligand perhaps highlights the inhibition of the catalyst by coordination of the pyridine substrate. Additionally, homo-coupled **7b** was observed in a few instances (**10a**), especially when bipyridine ligands were utilised, demonstrating the superior cross-coupling selectivity enabled by the amidine ligand. **10a** could arise via sequential oxidative addition pathways of **7b**, followed by reductive elimination.[8] Finally, a reaction containing an external base (K_2CO_3, 20 mol %) was carried out to determine if deprotonation of the amidine ligand **L8** could improve the yield of the product. However, no improvement to the yield of **9b** was observed (70% by NMR analysis analysis) suggesting that formation of the free amidine is unnecessary for effective reactivity (entry 23). Hence, the conditions highlighted (entry 3) were taken forward as the optimal conditions.

Table 3.3. Optimisation of XEC between 2-bromopyridine and 1-iodooctane.

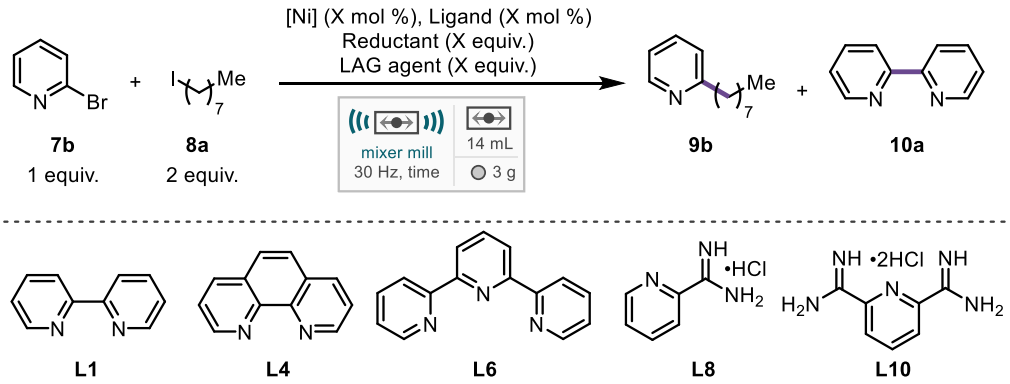

Entry[a]	[Ni] (mol %)	Ligand (mol %)	Reductant (equiv.)	LAG agent (equiv.)	Time (h)	9b (%)[b]	10a (%)[b]
1	$NiCl_2$•$6H_2O$ (10)	**L8** (20)	***Zn (1.2)***	DMA (3)	2	26	<2
2	$NiCl_2$•$6H_2O$ (10)	**L8** (20)	***Zn (2.0)***	DMA (3)	2	65	<2
3	$NiCl_2$•$6H_2O$ (10)	**L8** (20)	***Zn (2.5)***	DMA (3)	2	79 (72)	<2
4	$NiCl_2$•$6H_2O$ (10)	**L8** (20)	***Zn (3.0)***	DMA (3)	2	72	<2
5	$NiCl_2$•$6H_2O$ (10)	***L1 (20)***	Zn (2.5)	DMA (3)	2	38	10
6	$NiCl_2$•$6H_2O$ (10)	***L4 (20)***	Zn (2.5)	DMA (3)	2	34	3
7	$NiCl_2$•$6H_2O$ (10)	***L6 (20)***	Zn (2.5)	DMA (3)	2	27	5
8	$NiCl_2$•$6H_2O$ (10)	***L10 (20)***	Zn (2.5)	DMA (3)	2	63	<2
9	***$NiCl_2$(DME) (10)***	**L8** (20)	Zn (2.5)	DMA (3)	2	69	4
10	***$NiBr_2$(DME) (10)***	**L8** (20)	Zn (2.5)	DMA (3)	2	70	3
11	$NiCl_2$•$6H_2O$ (10)	**L8** (20)	***Mn (2.5)***	DMA (3)	2	52	11
12	$NiCl_2$•$6H_2O$ (10)	**L8** (20)	***TDAE (2.5)***	DMA (3)	2	<2	<2
13	$NiCl_2$•$6H_2O$ (10)	**L8** (20)	Zn (2.5)	***NMP (3)***	2	64	5
14	$NiCl_2$•$6H_2O$ (10)	**L8** (20)	Zn (2.5)	***DMF (3)***	2	62	5
15	$NiCl_2$•$6H_2O$ (10)	**L8** (20)	Zn (2.5)	**-**	2	7	6
16	$NiCl_2$•$6H_2O$ (10)	**L8** (20)	Zn (2.5)	***DMA (1)***	2	27	7
17	$NiCl_2$•$6H_2O$ (10)	**L8** (20)	Zn (2.5)	***DMA (4)***	2	77	<2
18	$NiCl_2$•$6H_2O$ (10)	**L8** (20)	Zn (2.5)	DMA (3)	***1***	52	7
19	$NiCl_2$•$6H_2O$ (5)	**L8** (10)	Zn (2.5)	DMA (3)	2	65	5
20	-	**L8** (20)	Zn (2.5)	DMA (3)	2	<2	<2
21	$NiCl_2$•$6H_2O$ (10)	**-**	Zn (2.5)	DMA (3)	2	10	7
22	$NiCl_2$•$6H_2O$ (10)	**L8** (20)	-	DMA (3)	2	<2	<2
23[c]	$NiCl_2$•$6H_2O$ (10)	**L8** (20)	Zn (2.5)	DMA (3)	2	70	<2

[a]Reactions were carried out on a 0.3 mmol scale in 14 mL stainless steel jars, equipped with a 3 g, 9 mm stainless steel grinding ball, under an air atmosphere.

[b]Yield determined by ^{1}H NMR analysis of the crude reaction mixture (after work-up), using mesitylene as an internal standard. Isolated yields are given in parentheses.

[c]K_2CO_3 (20 mol %) was added to the reaction.

Before commencing with the substrate scope of the process, the effectiveness of alkyl bromides to partake in the XEC process was assessed, as previous work in this area demonstrated that using iodide additives such as sodium iodide was paramount to successful reactivity.[42,43] The likely role of the iodide additive is to simply convert the alkyl bromide to the more reactive alkyl iodide *in situ*. However, it has been reported that iodide additives can reduce homo-coupling of aryl halides, also.[10] Replacing 1-iodooctane in the model system with (3-bromopropyl)benzene (**8b**) resulted in only 18% yield of the XEC product **9d**, determined by ^{1}H NMR analysis (Table 3.4., entry 1). Hence, sodium iodide was added in quantities between 0.25 and 3 equivalents to determine the optimal amount needed for effective XEC (entries 2 – 6). This small study revealed that 2 equivalents of sodium iodide are necessary for effective product formation, furnishing 59% yield by ^{1}H NMR analysis of **9d**, which was isolated in 56% yield (entry 5). 3 equivalents of sodium iodide led to a greater consumption of **7b**, but no significant change in the yield of **9d** was observed (entry 6). It is likely that side-reactions (homo-coupling, protodehalogenation) are accounting for the missing mass balance.

Table 3.4. Optimisation of sodium iodide additive in XEC process with alkyl bromides.

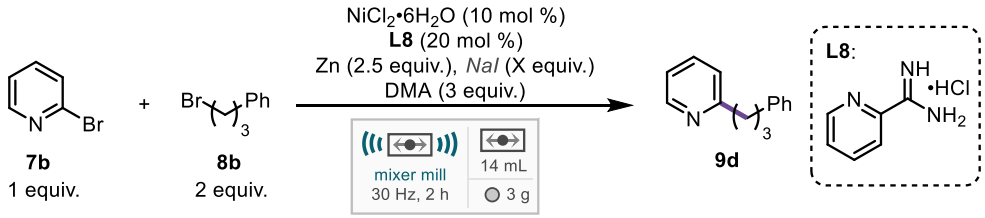

Entry[a]	Sodium iodide (equiv.)	7b (%)[b]	9d (%)[b]
1	-	<2	18
2	0.25	<2	39
3	0.50	23	36
4	1.0	21	43
5	2.0	16	59 (56)
6	3.0	<2	55

[a]Reactions were carried out on a 0.3 mmol scale in 14 mL stainless steel jars, equipped with a 3 g, 9 mm stainless steel grinding ball, under an air atmosphere.

[b]Yield determined by ^{1}H NMR analysis of the crude reaction mixture (after work-up), using mesitylene as an internal standard. Isolated yields are given in parentheses.

3.3.2. Substrate Scope

With optimal conditions for both alkyl iodide and bromide coupling partners in hand, the scope of the process was investigated. Firstly, a selection of heteroaryl bromides (**7**) were successfully coupled with 1-iodooctane, including a pyrimidine (**9e**; 43%), in moderate yield (Scheme 3.1.1.). Additionally, a variety of substitution at the 5-position of 2-bromopyridine was tolerated, including weakly electron-withdrawing fluoro (**9g**; 68%) and acetamido (**9n**; 46%) groups, along with more strongly electron-withdrawing cyano (**9h**; 46%) and trifluoromethyl (**9i**; 50%) groups; all in moderate to good yields. In terms of electron-donating moieties, a methoxy group (**9l**; 56%), a free alcohol (**9k**; 34%), and a free amine (**9m**; 40%) were tolerated, albeit in decreased yields. The tolerance for a free amine-containing substrate, which contains two sites that can competitively coordinate to the catalyst, is particularly pleasing. Interestingly, a chloro-substituted substrate reacted chemoselectively at the C-Br bond in the XEC process, furnishing the XEC product (**9j**; 62%) in good yield. This example would allow orthogonal cross-coupling to take place at the C-Cl bond to functionalise the molecule further. An aldehyde substituted 2-bromopyridine failed to furnish the corresponding XEC product (**9o**), potentially due to competitive coordination of the aldehyde to the nickel centre.

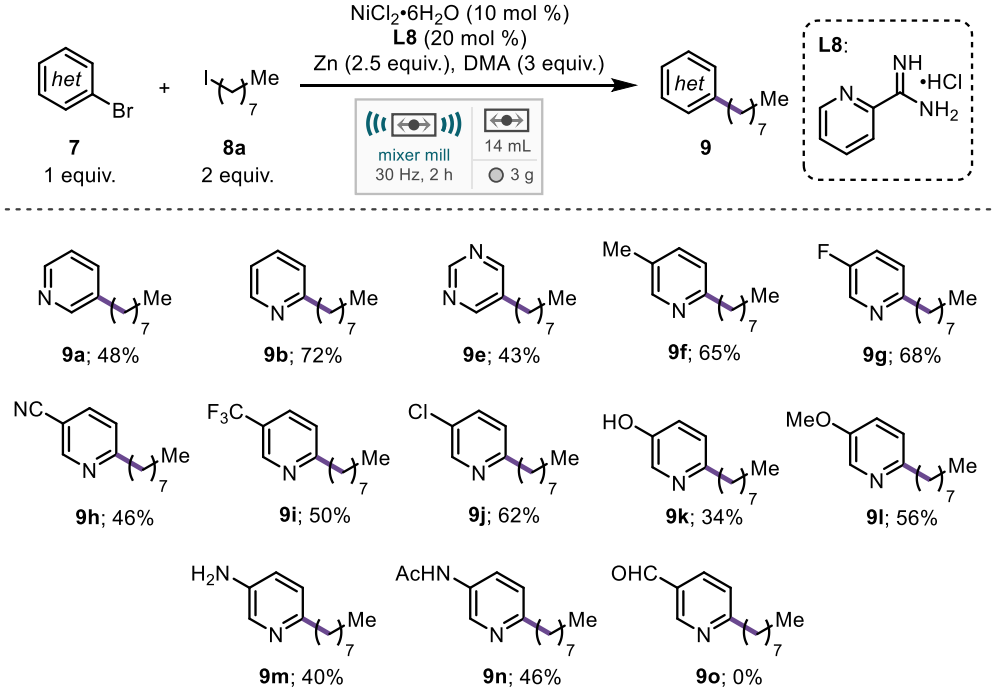

Scheme 3.1.1. Substrate scope of heteroaryl bromides with 1-iodooctane in XEC process.

Following this, a variety of heteroaryl bromides were tested, using ethyl 4-bromobutyrate (**8c**) as the alkyl bromide coupling partner, as the XEC products would exhibit more synthetic utility, due to the presence of the ester functionality (Scheme 3.1.2.). This included 2-, 3-, and 4-bromopyridine, furnishing the respective XEC products (**9p**; 72%, **9q**; 49%, **9r**; 25%) in moderate to good yield. 5- and 2-bromopyrimidine, along with 2-bromopyridazine were tolerated, furnishing the XEC products (**9s;** 67%, **9t**; 42%, **9u**; 23%) in moderate to good yields. 3-bromoquinoline was also tolerated, furnishing the XEC product in moderate yield (**9v**; 57%). An indole was tolerated under the reaction conditions, albeit in low yield (**9w**; 28%). This tolerance for this substrate containing a basic, unprotected nitrogen atom is pleasing. However, an isatin derived compound (**9x**) was not tolerated, potentially indicating it has lower reactivity than the indole or that the presence of multiple oxygen atoms can inhibit reactivity through competitive coordination. Attempts to utilise 5-membered heteroaryls, such as pyrazole, furan, and thiophene (**9y** – **9aa**) were unsuccessful. This is potentially due to the propensity of these substrates to partake in side-reactions such as protodehalogenation, or from competitive coordination to the nickel centre. These 5-membered heteroaryl halide substrates may require a major alteration to the reaction conditions to improve tolerance and selectivity.

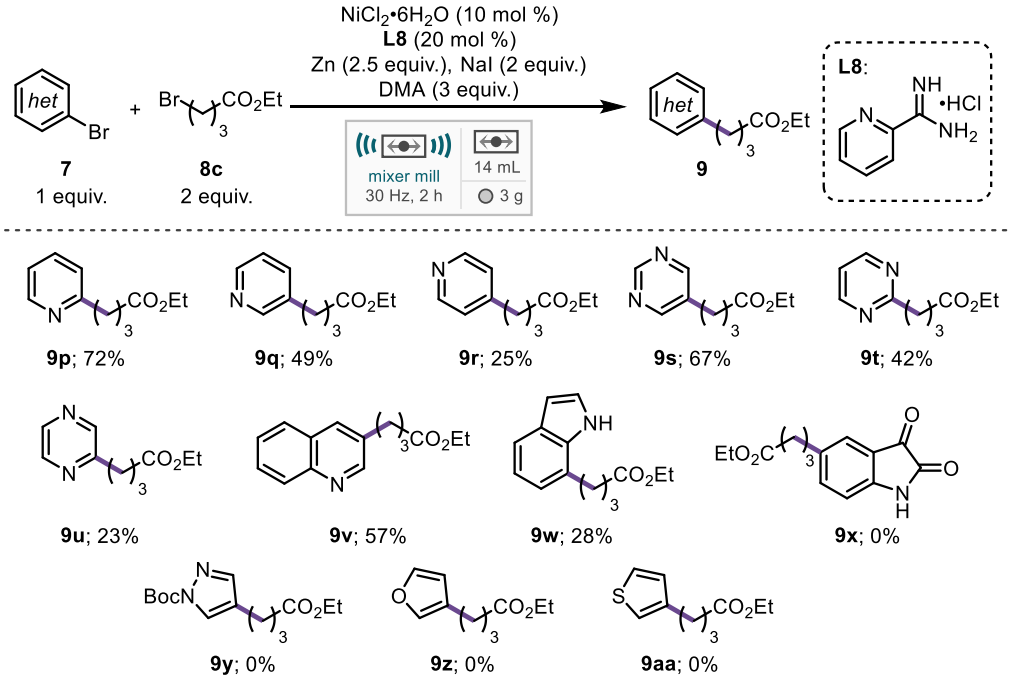

Scheme 3.1.2. Substrate scope of heteroaryl bromides with ethyl 4-bromobutyrate in XEC process.

Next, the scope of the alkyl halides was examined, including both alkyl bromides and iodides (Scheme 3.1.3.). This included formation of products containing a phthalimide (**9ac**; 63%), a homobenzyl group (**9ad**; 54%), and a cyclohexyl moiety (**9ag**; 30%), in moderate to good yields. Gratifyingly, functionalised alkyl groups, such as a protected alcohol and amine were tolerated (**9ae**; 27% and **9af**; 24%), in decreased yields. The latter compound is a structural analogue of the drug betahistine (*cf.* Figure 3.1.). An example containing an oxetane moiety was tolerated (**9ah**; 32%), although a low yield was obtained and a 4 hour reaction time was required for full conversion of the starting material. Oxetanes represent an important bioisosteric replacement for carbonyl groups in medical sciences, due to the spatial area occupied by the oxetane being similar to that of a carbonyl.[47] Hence, this example is important to highlight. Examples including a terminal alkene (**9ai**; 22%), which could also coordinate to the metal centre, and a neopentyl group (**9aj**; 42%), were tolerated in reduced yields. These two examples include the acetamido functionality at the 5-position of the pyridine, due to volatility issues encountered with the products from the unsubstituted pyridine. Unsuccessful examples included a protected piperidine (**9ak**), which is likely due to both the presence of an electron-rich moiety and the lower reactivity of secondary alkyl halides in comparison to primary alkyl halides. This is highlighted by the intolerance of the reaction to tertiary alkyl halides, such as *tert*-butyl iodide (**9al**), where the ease of alkyl radical addition to the nickel (II) centre is reduced due to steric encumbrance.

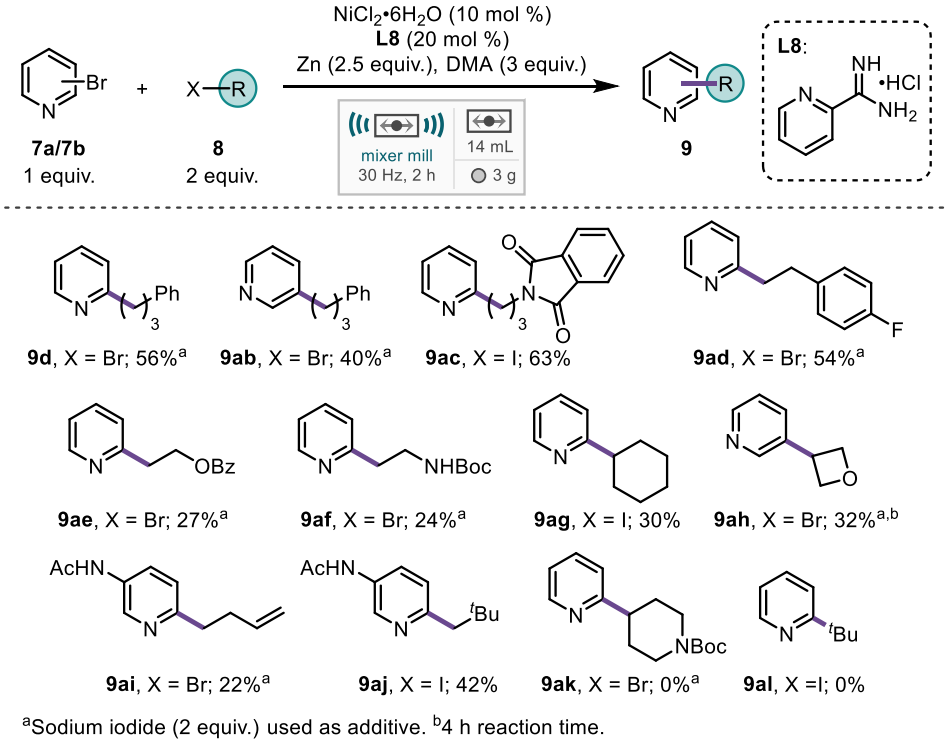

Scheme 3.1.3. Substrate scope of alkyl halides in XEC process.

The model system was shown to also tolerate 2-chloro and 2-iodopyridine, giving the XEC product (**9b**) in 31% and 36% yield by ^{1}H NMR analysis, respectively (Scheme 3.1.4.). These are much lower yielding than when 2-bromopyridine is used (*cf.* 79% by NMR analysis), however, the successful reactivity of 2-chloropyrdine is a marked improvement from previous reports, where aryl chlorides were ineffective.[48]

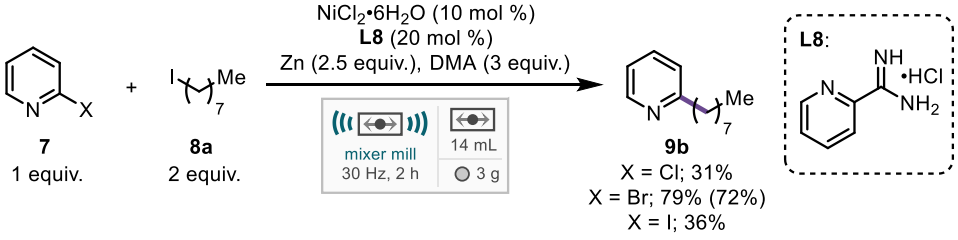

Scheme 3.1.4. Comparison of reactivity of 2-chloro, 2-bromo, and 2-iodopyridine in XEC process.

3.3.3. Reaction Scale Up

It was demonstrated that the mechanochemical XEC process is amenable to scale up, using 5-bromopyrimidine (**7d**) and ethyl 4-bromobutyrate (**8c**) as the substrates. This was achieved by increasing the reaction scale, jar size, and ball size to 6 mmol, 25 mL and 12 g, respectively. Under the optimised conditions, 0.73 g of the XEC product (**9s**) was furnished in 62% yield (Scheme 3.1.5.). This 20-fold increase in scale shows only a slight decrease in yield compared to the 0.3 mmol yield that was utilised throughout the study (*cf.* 67% yield).

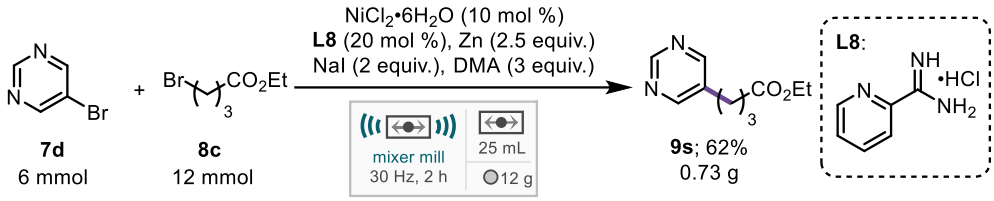

Scheme 3.1.5. Scale up of mechanochemical XEC process.

3.3.4. Solution-Phase Comparisons

To demonstrate the utility of the mechanochemical protocol versus traditional solution-phase processes, analogous solution-phase experiments were performed. This included an experiment in DMA, at room temperature, under an air atmosphere, for 16 hours, which only yielded 4% of XEC product (**9b**) by ^{1}H NMR analysis (Scheme 3.1.6A, condition A). The same experiment under a nitrogen atmosphere yielded 31% of **9b** by NMR analysis, demonstrating the requirement for an inert atmosphere in solution-phase examples (condition B). Finally, heating the reaction to 60 °C yielded 67% of **9b** by NMR analysis, which demonstrates the temperature dependence of these processes (condition C). In contrast, the milled process without external heating is expected to not exceed temperatures of 40 °C.[49] For these solution comparisons, the zinc reductant was used as is, with no activation step carried out, to allow a more direct comparison to the ball-milled process. However, for full transparency the result obtained by Weix and co-workers in their report on heteroaryl XEC is included (Scheme 3.1.6B). This report used (3-bromopropyl)benzene (**8b**) as the coupling

partner, furnishing the XEC product (**9d**) in 85% isolated yield, using similar conditions to the developed mechanochemical process. Comparing this to the ball-milled process, which yields 79% of **9b** after only 2 hours, it is clear to see the benefits of the mechanochemical approach over the solution-phase analogues (condition D). This is made even more apparent when it is considered that the process requires no precautions with inert atmospheres, no activation of the zinc reductant, and that DMA is only used in LAG quantities.

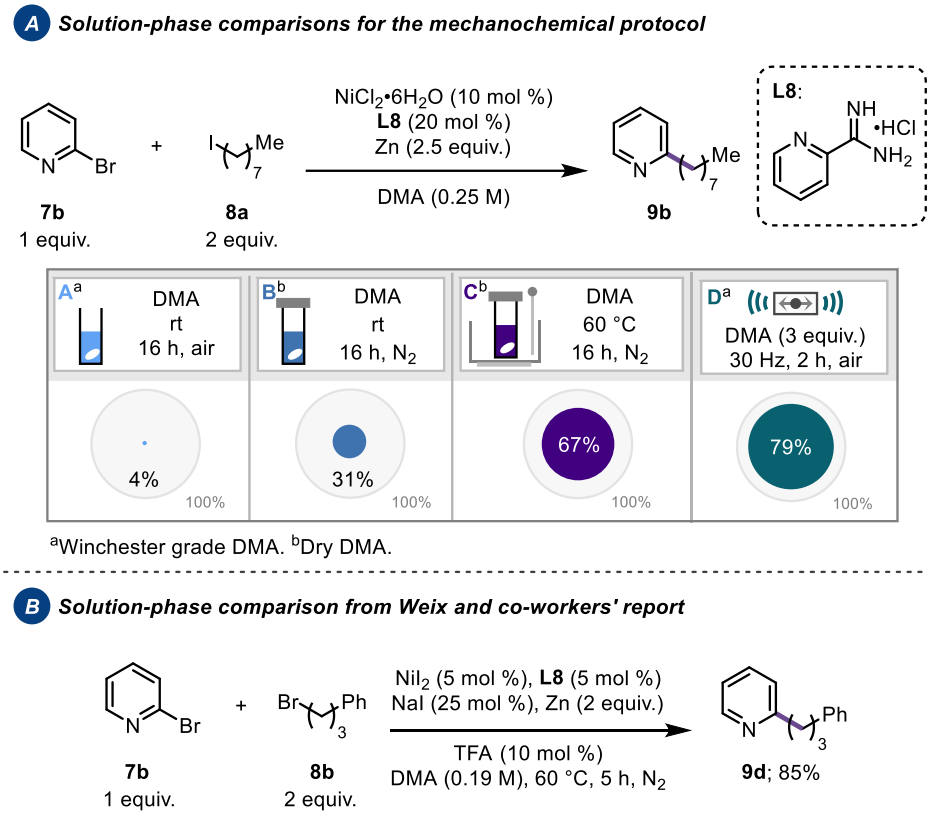

Scheme 3.1.6. A) Solution-phase comparisons carried out for the XEC process; B) Result obtained by Weix and co-workers for a similar XEC system.

3.3.5. Screen of Reductant Form

Throughout the study, a granular form of zinc was used as the reductant (Zn granular 20 – 30 mesh, supplier: Merck), however, an issue commonly encountered on larger scales is the irregularity in reaction efficiency when using different forms of reductant metal, whether that be zinc or manganese. Therefore, it would be ideal to demonstrate that the developed process is effective regardless of the form of zinc metal that is

used. To this end, a small selection of common zinc forms, including mossy, flakes, wire, and foil, were all successfully employed in the model system (2-bromopyridine and 1-iodooctane), where only slight deceases in product yield were observed from single runs of the experiments (Scheme 3.1.7.). Only zinc flakes gave a significantly lower yield of the XEC product **9b**, yielding 53% by NMR analysis, potentially due to the larger degree of zinc oxide existing because of the form's greater surface area. However, this study demonstrated that the protocol could tolerate a range of zinc reductant forms.

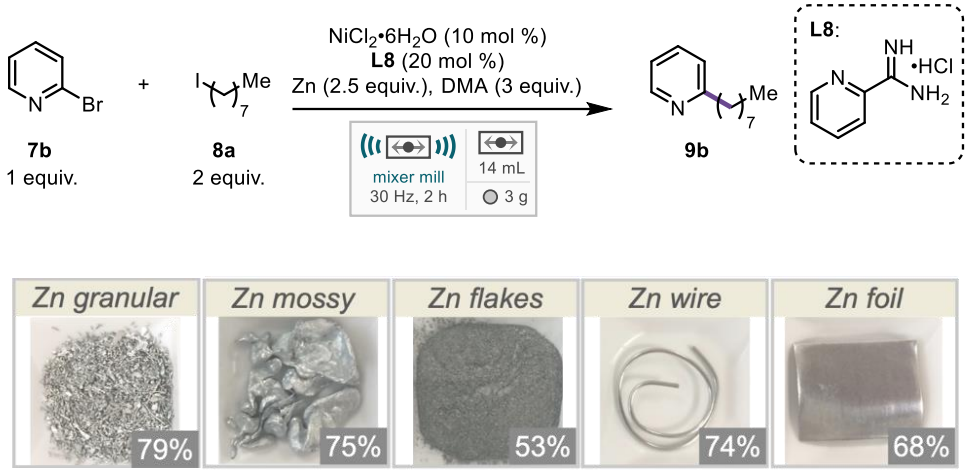

Scheme 3.1.7. Screen of different zinc forms in the XEC process.

3.3.6. Application of Heat

As shown in the solution-phase comparison reactions (Section 3.3.4.), these XEC processes are typically sensitive to temperature. To achieve temperature control under milling conditions, the XEC reaction between 2-bromopyridine and ethyl 4-bromobutyrate was carried out with the application of heat via a band heater that encases the milling jar, which is connected to a PID thermocouple to control the temperature.[49] Heating the jar to 80 °C, while milling for 30 minutes, resulted in a 60% yield by NMR analysis of the desired XEC product (**9q**), whereas the reaction with no external heating furnished **9q** in 49% yield by NMR analysis (Scheme 3.1.8.). Hence, heating the ball-milled process can have a small positive impact on the product yield in this example. However, due to the operational simplicity of the room temperature process, it was decided that it was not worth a re-investigation of the substrate scope.

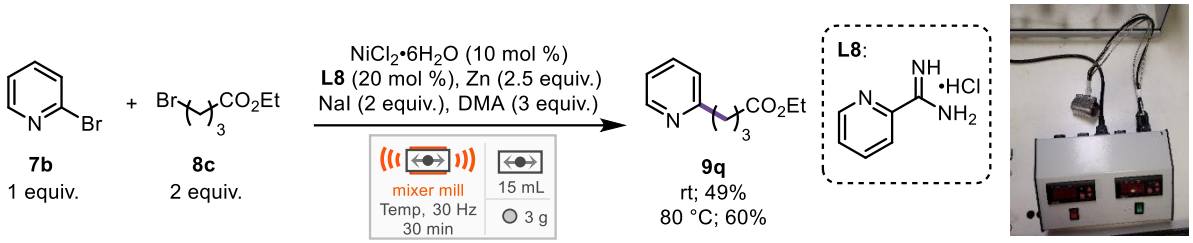

Scheme 3.1.8. Application of heat to the XEC process and the PID thermocouple controller used for the heated reaction.

3.3.7. Mechanistic Studies

3.3.7.1. Stainless Steel Free Reaction

To rule out the possibility of trace amounts of iron leaching into the reaction mixture from the stainless steel jars or balls and influencing the reaction, a stainless steel free reaction on a planetary ball-mill was performed. Iron from the stainless steel milling media has been shown to be synthetically relevant in previous mechanochemical protocols.[50] No non-steel jars were available for use on the mixer ball-mill, hence a planetary ball-mill was used. Here, the model reaction was carried out in a zirconia grinding bowl, containing six 3 g zirconia grinding balls. The mixture of 2-bromopyridine and ethyl 4-bromobutyrate was milled at 800 rpm (the highest setting on a planetary mill) for 2 hours, yielding 32% of the XEC product (**9q**) by ^{1}H NMR analysis (Scheme 3.1.9.). The lower yield is likely due to the lower energy forces imparted by a planetary mill in comparison to a mixer mill, as highlighted in Chapter 1, rather than the absence of iron. It is likely that the planetary system would require an adjustment to the conditions, for instance a longer reaction time or the addition of a grinding auxiliary.

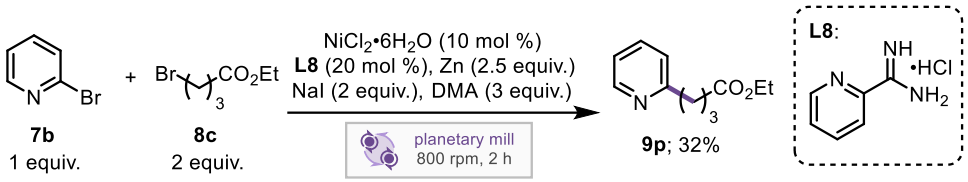

Scheme 3.1.9. Stainless steel free reaction in a planetary ball-mill.

3.3.7.2. Radical Clock Studies

As previously discussed (*cf* Section 3.1.), XEC processes between aryl halides and alkyl halides have been suggested to proceed via an alkyl radical formed in a radical chain mechanism. However, due to the change in reactor from solution-phase chemistry to a mechanochemical process, it is worth verifying this aspect for the developed system. Firstly, a radical clock experiment was carried out, using (bromomethyl)cyclopropane (**8d**) as the alkyl halide coupling partner with 3-bromoquinoline (**7e**), under the optimal conditions (Scheme 3.2.1.). This experiment would allow the fate of the alkyl halide to be determined, as the resulting radical formed (I) on this substrate would undergo rapid ring-opening of the cyclopropyl ring to give the terminal alkene intermediate (II), which would furnish the rearranged XEC product (**9am**). An organozinc reagent formed *in situ* from the reaction of the zinc with the alkyl halide would be expected to give the unrearranged, Negishi-type product (**9an**). However, it is possible that the organozinc reagent could initiate ring-opening of the cyclopropyl ring to give the rearranged XEC product (**9am**), as reported by Rieke and co-workers,[51] hence the experiment was carried out with manganese as the reductant as well. Such a rearrangement has not been reported via an organomanganese reagent, likely due to the slower rate of insertion of manganese into C-X bonds. However, Kubota, Ito and co-workers have recently reported manganese insertion into aryl halides using mechanochemistry.[52] The experiment using zinc as the reductant gave exclusive formation of the rearranged product (**9am**) in 58% yield by ^{1}H NMR analysis (49% isolated yield), No observable amount of the unrearranged product was obtained, giving credence to the previously established radical chain mechanism (**9an**). To further fortify this argument, the reaction using manganese as the reductant also gave exclusive formation of **9am** in 48% yield by ^{1}H NMR analysis, with no **9an** observed.

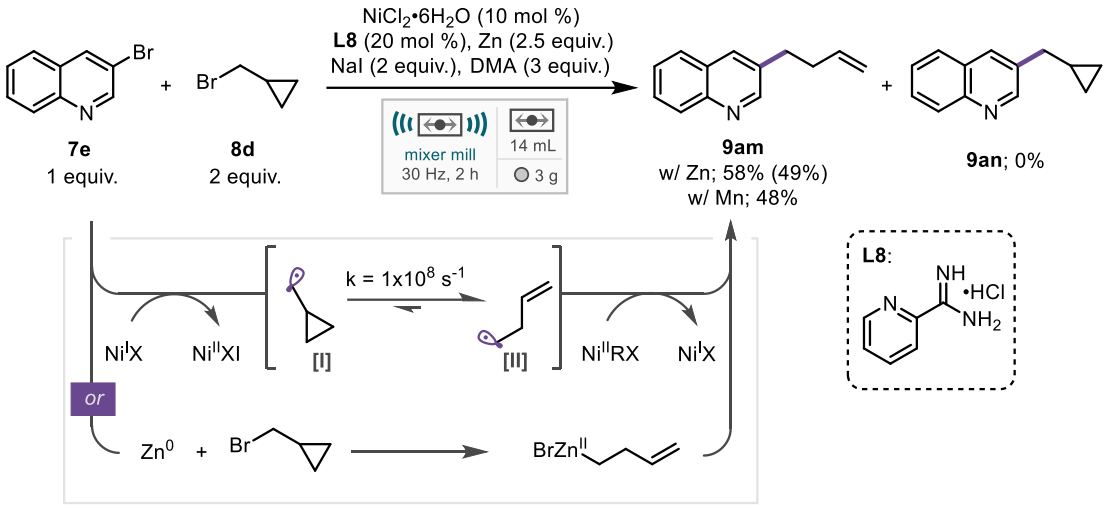

Scheme 3.2.1. Radical clock experiments using (bromomethyl)cyclopropane as the alkyl halide coupling partner and the mechanistic routes to the rearranged product.

3.3.7.3. Organozinc and Organomanganese Formation

The results from the radical clock studies suggest that radical intermediates are likely present, however, to further probe the presence of organozinc or manganese reagents forming *in situ* some additional control experiments were performed. Previous work has demonstrated that the mechanochemical formation of organozinc reagents from alkyl bromides and iodides is possible, hence this was not repeated here (Scheme 3.2.2A).[36] However, this had not been demonstrated for the corresponding organomanganese formation, hence (3-bromopropyl)benzene (**8b**) was subjected to ball-milling conditions with manganese metal and DMA. The reaction was run for 4 hours, followed by an acid quench, which would furnish the hydrocarbon product (**11a**) if an organomanganese intermediate was formed. This process was carried out with and without sodium iodide, with both reactions furnishing **11a** after the acid quench, in 31% and 60% yield by ^{1}H NMR analysis, respectively (Scheme 3.2.2B). These results show that organomanganese formation is possible under these reaction conditions, therefore, a Negishi-type mechanism cannot be completely ruled out.

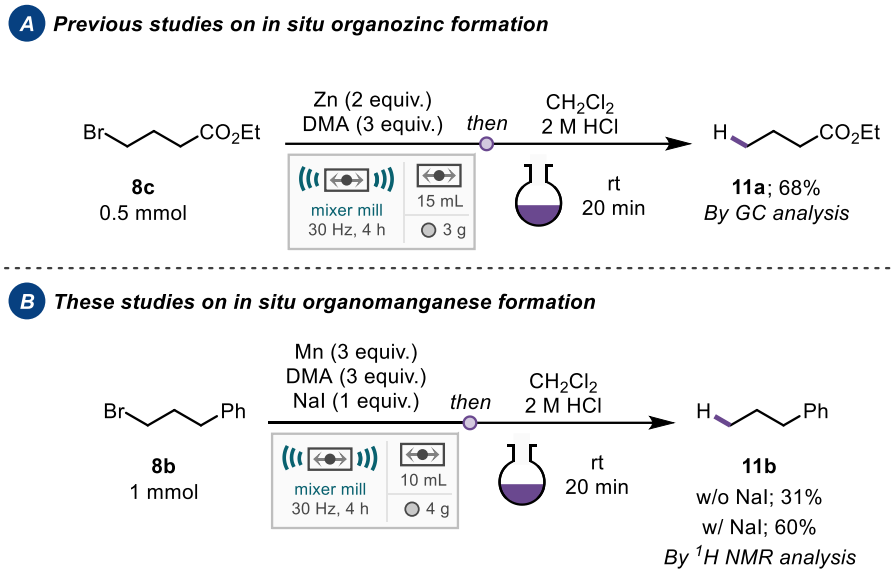

Scheme 3.2.2. A) Previous work on the generation organozinc intermediates; B) These studies on the generation of organomanganese intermediates.

3.3.7.4. Radical Trapping Experiments

Finally, radical trapping experiments were carried out to intercept any potential radical intermediates present, using common radical inhibitors; 2,2,6,6-tetramethylpiperidine 1-oxyl (TEMPO) and butylated hydroxytoluene (BHT). Adding 2 equivalents of each of these radical inhibitors to the model system, resulted in nullification of the process in the case of TEMPO and a significantly reduced yield of 54% by ^{1}H NMR analysis in the case of BHT (Scheme 3.2.3.). Additionally, the TEMPO adduct that could arise from radical trapping (**12a**) was observed by mass spectroscopy (LR-MS) of the crude reaction mixture (Figure 3.2.). However, it is possible that **12a** could be produced because of single-electron reduction of the TEMPO radical to an *N*-oxide, followed by a nucleophilic attack onto the alkyl halide. Moreover, nullification of reactivity could occur because of direct attack of TEMPO onto the nickel centre. Also, only a minor suppression of the reaction using BHT could suggest that the mechanism is not solely radical based and there could be a mixture of mechanistic pathways in operation. However, reaction inhibition due to changes in the jar filling or reaction mixture rheology cannot be ruled out.

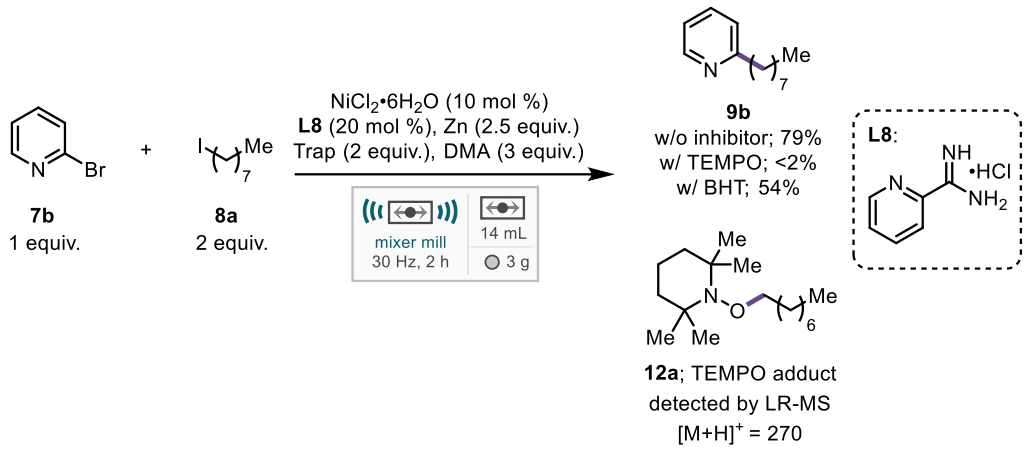

Scheme 3.2.3. Radical trapping experiments using TEMPO and BHT.

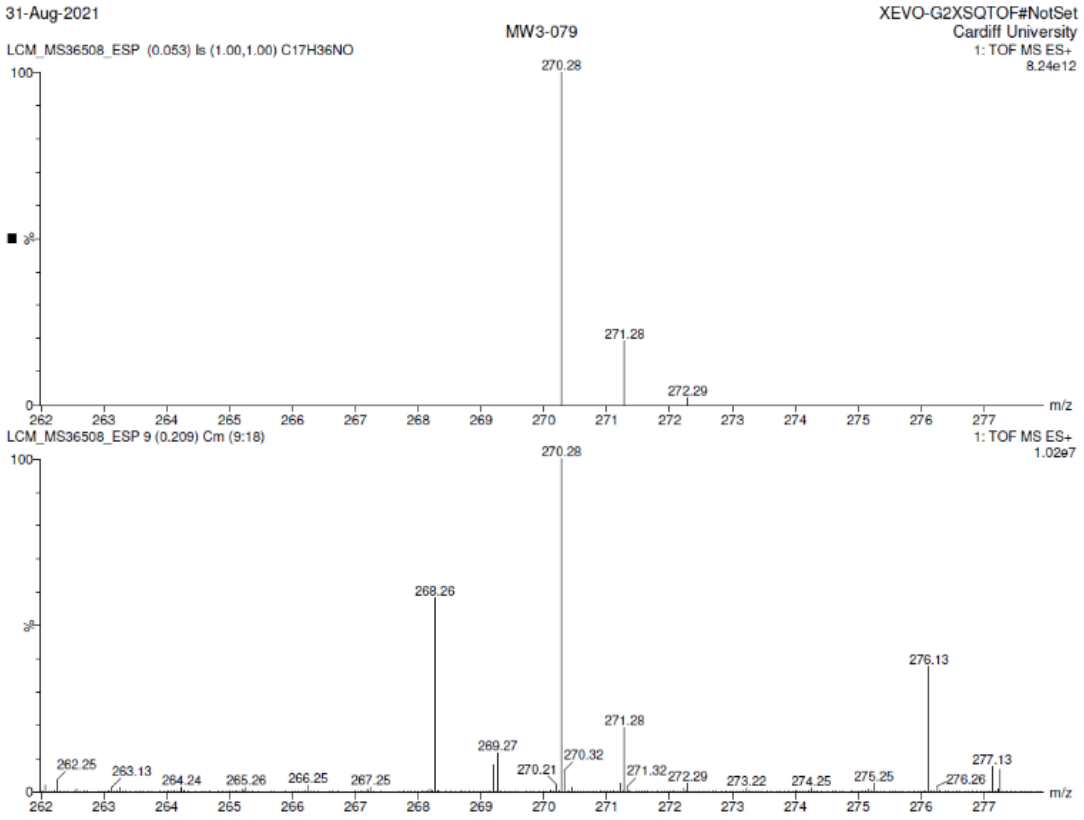

Figure 3.2. Section of LR-MS showing TEMPO trapped adduct detection at m/z 270.

3.3.7.5. Proposed Mechanism

With all the observations and results collected throughout the mechanistic study, two plausible reaction pathways can be proposed; one involving an alkyl radical intermediate, as suggested in solution-phase XEC processes, or the other involving

an *in situ* generated organozinc intermediate (Scheme 3.2.4A and 3.2.4B). It is difficult to elucidate which mechanism is solely operating, however, it is plausible that a mixture of the two reaction pathways is operating in the XEC process.

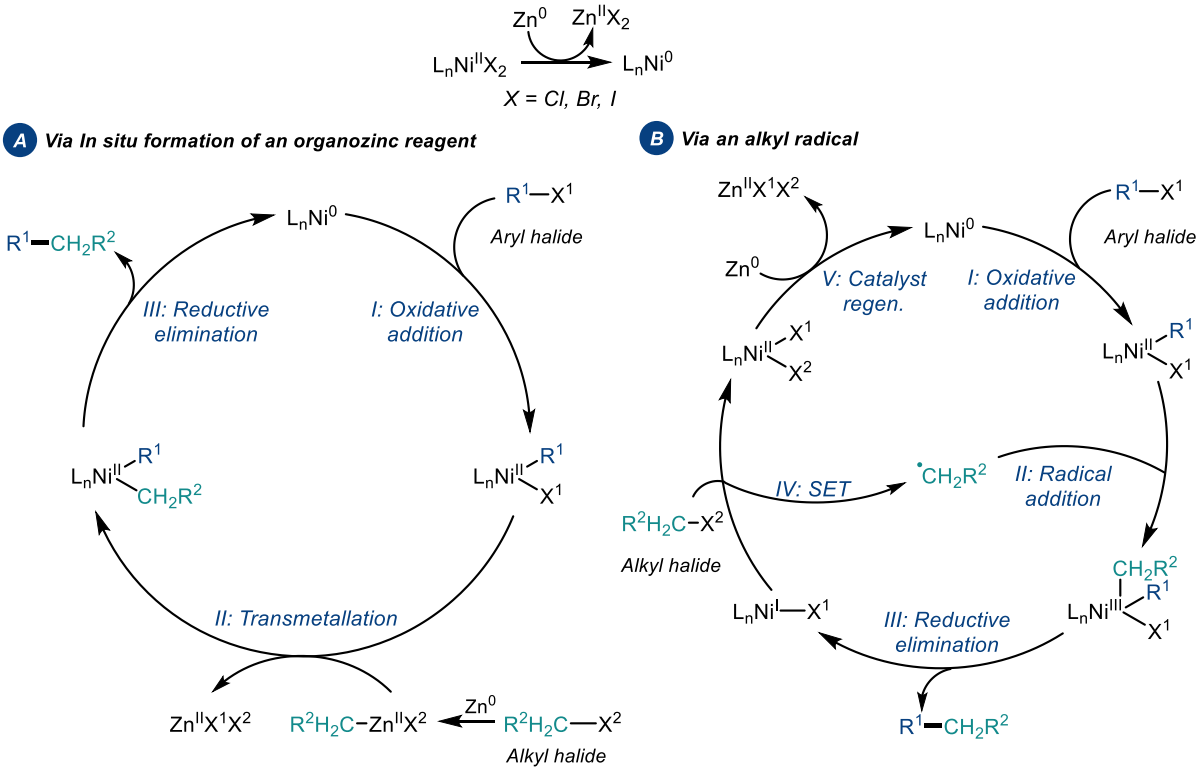

Scheme 3.2.4. Plausible reaction pathways, A) via transmetallation from an organozinc reagent; B) via an alkyl radical intermediate.

3.4. Conclusions and Future Work

In conclusion, a mechanochemical protocol for the XEC of heteroaryl halides and alkyl halides has been developed. This built upon previous XEC work from Browne and co-workers where heteroaryl substrates were not tolerated under the optimised reaction conditions. Key to the success of the process described within this chapter was the employment of an amidine ligand, which allowed good selectivity of the cross-coupled product to be achieved over homo-coupling and proto-dehalogenation pathways. The developed process shows good substrate scope for a variety of *N*-heteroaryl compounds and has several benefits over solution-phase analogues, such as shorter reaction times, no requirement for inert reaction atmospheres, and needing only LAG

quantities of DMA. Additionally, the process has no requirement for activation of the terminal reductant (zinc), where the mechanical forces imparted by the ball-mill are sufficient to activate the metal. It was also demonstrated that the process is amenable to scale up and that a variety of raw zinc forms can be employed, without a depreciable drop in process efficiency. Finally, through extensive control reactions and mechanistic studies, it has been deduced that the process likely operates either via an *in situ* generated organozinc reagent, or via an alkyl radical intermediate, or potentially a mixture of both pathways operating at a given point.

Future work could involve applying the developed protocol to more challenging substrate classes, such as substrates with high degrees of functionality or solubility issues, for example natural product analogues and precursors to organic dyes. Additionally, other bond forming XEC processes, such as C-Si or C-Ge, could be of interest. Also of interest is the large-scale application of the XEC process by extrusion, as no examples of zero-valent metal activation on a TSE exist to date, however transition-metal catalysed extrusion processes are beginning to emerge.

3.5. Bibliography

1 R. F. Heck, *J. Am. Chem. Soc.*, 1968, **90**, 5518–5526.

2 R. F. Heck, *J. Am. Chem. Soc.*, 1968, **90**, 5531–5534.

3 K. F. Heck and J. P. Nolley, *J. Org. Chem.*, 1972, **37**, 2320–2322.

4 E. ichi Negishi, A. O. King and N. Okukado, *J. Org. Chem.*, 1977, **42**, 1821–1823.

5 N. Miyaura and A. Suzuki, *J. Chem. Soc. Chem. Commun.*, 1979, 866–867.

6 N. Miyaura, K. Yamada and A. Suzuki, *Tetrahedron Lett.*, 1979, **20**, 3437–3440.

7 C. C. C. Johansson Seechurn, M. O. Kitching, T. J. Colacot and V. Snieckus, *Angew. Chem. Int. Ed.*, 2012, **51**, 5062–5085.

8 D. A. Everson and D. J. Weix, *J. Org. Chem.*, 2014, **79**, 4793–4798.

9 D. J. Weix, *Acc. Chem. Res.*, 2015, **48**, 1767–1775.

10 D. A. Everson, B. A. Jones and D. J. Weix, *J. Am. Chem. Soc.*, 2012, **134**, 6146–6159.

11 J. Gu, X. Wang, W. Xue and H. Gong, *Org. Chem. Front.*, 2015, **2**, 1411–1421.

12 A. Ariafard and Z. Lin, *Organometallics*, 2006, **25**, 4030–4033.

13 K. A. Johnson, S. Biswas and D. J. Weix, *Chem. Eur. J.*, 2016, **22**, 7399–7402.

14 S. Kim, M. J. Goldfogel, M. M. Gilbert and D. J. Weix, *J. Am. Chem. Soc.*, 2020, **142**, 9902–9907.

15 S. Biswas, B. Qu, J. N. Desrosiers, Y. Choi, N. Haddad, N. K. Yee, J. J. Song and C. H. Senanayake, *J. Org. Chem.*, 2020, **85**, 8214–8220.

16 M. Xing, H. Cui and C. Zhang, *Org. Lett.*, 2021, **23**, 7645–7649.

17 D. A. Everson, R. Shrestha and D. J. Weix, *J. Am. Chem. Soc.*, 2010, **132**, 920–921.

18 D. J. Weix, *Acc. Chem. Res.*, 2015, **48**, 1767–1775.

19 T. Li, X. Cheng, J. Lu, H. Wang, Q. Fang and Z. Lu, *Chinese J. Chem.*, 2022, **40**, 1033–1038.

20 E. C. Hansen, D. J. Pedro, A. C. Wotal, N. J. Gower, J. D. Nelson, S. Caron and D. J. Weix, *Nat. Chem.*, 2016, **8**, 1126–1130.

21 L. L. Anka-Lufford, K. M. M. Huihui, N. J. Gower, L. K. G. Ackerman and D. J. Weix, *Chem. Eur. J.*, 2016, **22**, 11564–11567.

22 G. Picotin and P. Miginiac, *J. Org. Chem.*, 1987, **52**, 4796–4798.

23 S. Huo, *Org. Lett.*, 2003, **5**, 423–425.

24 D. J. Charboneau, H. Huang, E. L. Barth, C. C. Germe, N. Hazari, B. Q. Mercado, M. R. Uehling and S. L. Zultanski, *J. Am. Chem. Soc.*, 2021, **143**, 21024–21036.

25 L. Yi, T. Ji, K. Q. Chen, X. Y. Chen and M. Rueping, *CCS Chem.*, 2022, **4**, 9–30.

26 R. J. Perkins, D. J. Pedro and E. C. Hansen, *Org. Lett.*, 2017, **19**, 3755–3758.

27 B. L. Truesdell, T. B. Hamby and C. S. Sevov, *J. Am. Chem. Soc.*, 2020, **142**, 5884–5893.

28 M. C. Franke, V. R. Longley, M. Rafiee, S. S. Stahl, E. C. Hansen and D. J. Weix, *ACS Catal.*, 2022, **15**, 12617–12626.

29 J. Cornella, J. T. Edwards, T. Qin, S. Kawamura, J. Wang, C.-M. Pan, R. Gianatassio, M. Schmidt, M. D. Eastgate and P. S. Baran, *J. Am. Chem. Soc*, 2016, **138**, 14.

30 J. Yi, S. O. Badir, L. M. Kammer, M. Ribagorda and G. A. Molander, *Org. Lett.*, 2019, **21**, 3346–3351.

31 S. H. Lau, M. A. Borden, T. J. Steiman, L. S. Wang, M. Parasram and A. G. Doyle, *J. Am. Chem. Soc.*, 2021, **143**, 15873–15881.

32 P. Zhou, X. Li, D. Wang and T. Xu, *Org. Lett.*, 2021, **23**, 4683–4687.

33 A. C. Jones, J. A. Leitch, S. E. Raby-Buck and D. L. Browne, *Nat. Synth.*, 2022, **1**, 763–775.

34 G. W. Wang, Y. Murata, K. Komatsu and T. S. M. Wan, *Chem. Commun.*, 1996, 2059–2060.

35 Q. Cao, R. T. Stark, I. A. Fallis and D. L. Browne, *ChemSusChem*, 2019, **12**, 2554–2557.

36 Q. Cao, J. L. Howard, E. Wheatley and D. L. Browne, *Angew. Chem. Int. Ed.*, 2018, **57**, 11339–11343.

37 S. Wada, N. Hayashi and H. Suzuki, *Org. Biomol. Chem.*, 2003, **1**, 2160–2163.

38 J. X. Yin, R. T. Stark, I. A. Fallis and D. L. Browne, *J. Org. Chem.*, 2020, **85**, 2347–2354.

39 R. Takahashi, A. Hu, P. Gao, Y. Gao, Y. Pang, T. Seo, J. Jiang, S. Maeda, H. Takaya, K. Kubota and H. Ito, *Nat. Commun.*, 2021, **12**, 6691.

40 C. Wu, T. Ying, X. Yang, W. Su, A. V. Dushkin and J. Yu, *Org. Lett.*, 2021, **23**, 6423–6428.

41 R. A. Haley, A. R. Zellner, J. A. Krause, H. Guan and J. Mack, *ACS Sustainable Chem. Eng.*, 2016, **4**, 2464–2469.

42 A. C. Jones, W. I. Nicholson, J. A. Leitch and D. L. Browne, *Org. Lett.*, 2021, **23**, 6337–6341.

43 S. Wu, W. Shi and G. Zou, *New J. Chem.*, 2021, **45**, 11269–11274.

44 E. Vitaku, D. T. Smith and J. T. Njardarson, *J. Med. Chem.*, 2014, **57**, 10257–10274.

45 M. Baumann and I. R. Baxendale, *Beilstein J. Org. Chem.*, 2013, **9**, 2265–2319.

46 E. C. Hansen, C. Li, S. Yang, D. Pedro and D. J. Weix, *J. Org. Chem.*, 2017, **82**, 7085–7092.

47 G. Wuitschik, E. M. Carreira, B. Wagner, H. Fischer, I. Parrilla, F. Schuler, M. Rogers-Evans and K. Müller, *J. Med. Chem.*, 2010, **53**, 3227–3246.

48 A. C. Jones, W. I. Nicholson, J. A. Leitch and D. L. Browne, *Org. Lett.*, 2021, **23**, 6337–6341.

49 R. R. A. Bolt, S. Raby-Buck, K. Ingram, J. A. Leitch and D. L. Browne, *Angew.*

Chem. Int. Ed., 2022, **61**, e202210508.

50 D. Kong, M. M. Amer and C. Bolm, *Green Chem.*, 2022, **24**, 3125–3129.

51 A. Guijarro, D. M. Rosenberg and R. D. Rieke, *J. Am. Chem. Soc.*, 1999, **121**, 4155–4167.

52 R. Takahashi, P. Gao, K. Kubota and H. Ito, *Chem. Sci.*, 2023, **14**, 499-505.

Chapter 4: Mechanochemical Nickel-Catalysed Alkene Difunctionalisation

4.1. Nickel-Catalysed Alkene Difunctionalisation

Alkene difunctionalisation processes can be described as a reaction where two new components are added across an alkene. These processes can be as simple as dihalogenation using molecular bromine, or hydrohalogenation using hydrobromic acid, for example. However, in recent years there has been a keen interest in developing transition-metal catalysed alkene difunctionalisation processes, due to the milder reaction conditions that can be employed. Hence, a broader range of substrates can be tolerated and better selectivity can be achieved.[1–4] An early example was demonstrated by Knochel and co-workers, in 1996, where tetrahydrofuran derivatives were synthesised from the corresponding alkyl halide tethered allylic ethers, using nickel catalysis (Scheme 4.1.).[5] The authors suggested that the diethyl zinc was utilised to form an organozinc intermediate *in situ* which was capable of generating radical intermediates akin to that discussed for XEC processes in Chapter 3. Good yields with excellent diastereocontrol were achieved in this process, with a variety of electrophiles tolerated, such as α-haloacrylate esters, acid chlorides, and benzaldehydes.

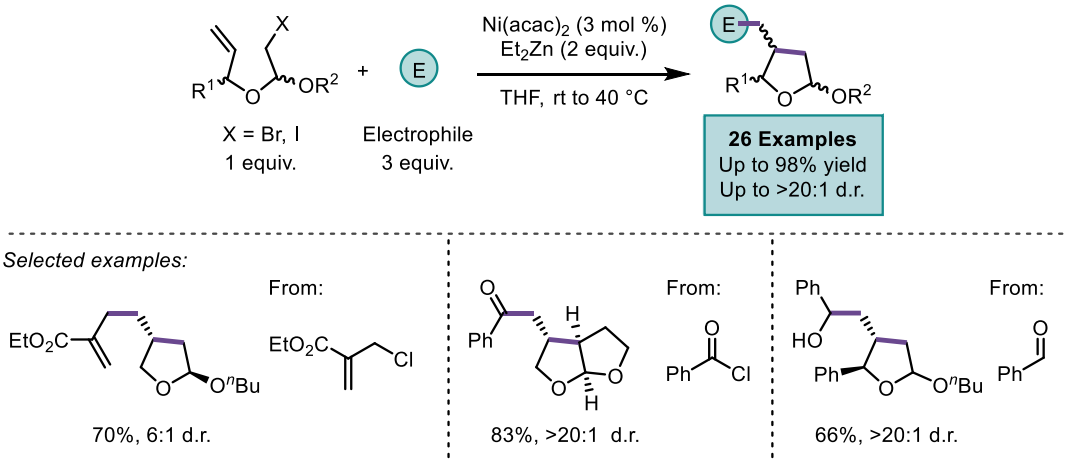

Scheme 4.1. Knochel and co-workers' nickel-catalysed intramolecular alkene difunctionalisation of alkyl halide tethered allylic ethers.

Following this, subsequent reports involved expanding the scope of transition-metal catalysed alkene difunctionalisation, through the development of both inter- and intramolecular processes and the induction of enantioselectivity.[6–10] This has been pioneered in recent years by the likes of Nevado, Kong and co-workers for inter- and

intramolecular processes, respectively. Nevado and co-workers, in 2017, reported a three-component alkene difunctionalisation reaction between activated alkenes, such as acrylate esters, with an aryl iodide and an alkyl iodide (Scheme 4.2A).[11] This process was catalysed by nickel and used TDAE as the terminal reductant. This report showed broad substrate scope and functional group tolerance, due to the relatively mild reaction conditions, including a boronic-ester containing compound and a steroid-derived compound. The regioselectivity of the reaction can be rationalised by considering the proposed reaction mechanism, where an alkyl radical generated from the alkyl iodide via SET with a nickel(I) species, is the first species to react with the alkene, resulting in the formation of the more stable carbon-centred radical intermediate (Scheme 4.2B). The subsequent elementary steps are comparable to the radical chain-type mechanisms proposed for XEC processes. Later work from the same group demonstrated improved tolerance for 'unactivated' alkenes.[12]

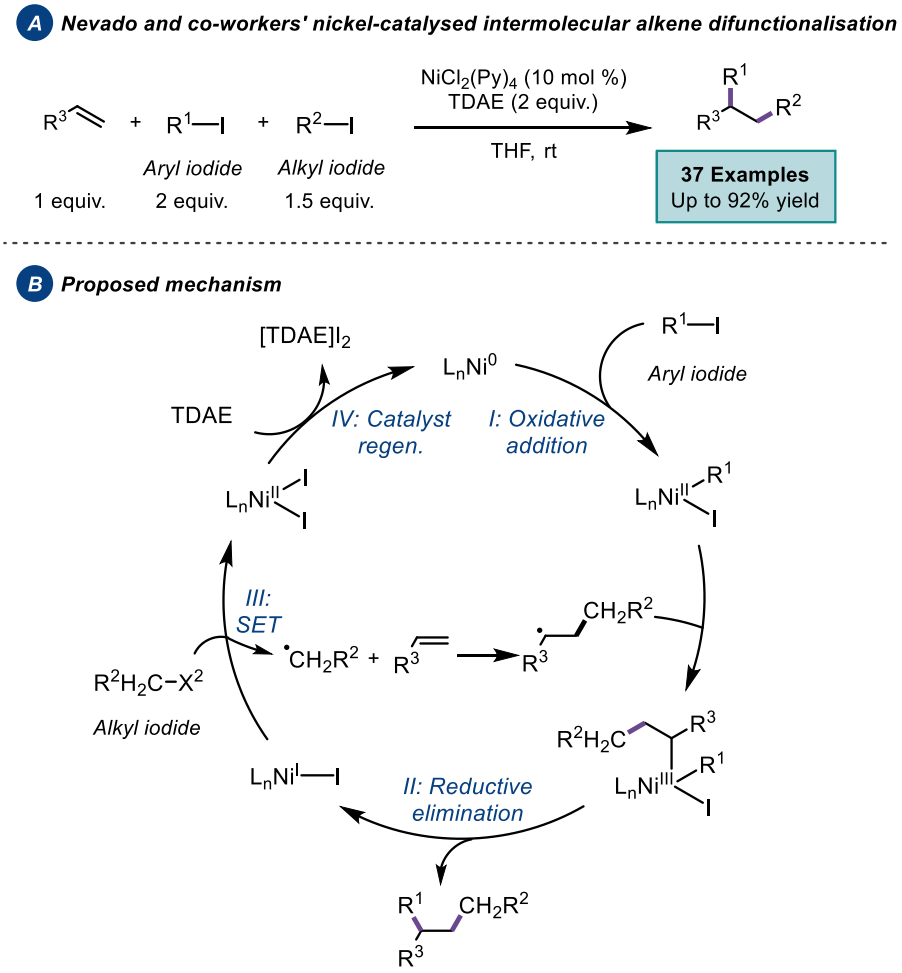

Scheme 4.2. A) Nevado and co-workers' report on the nickel-catalysed intermolecular alkene difunctionalisation reaction; B) Proposed mechanism.

These processes have been dubbed 'dicarbofunctionalisation' (DCF) or conjunctive coupling, due to the addition of two C-C bonds across the alkene substrate.[13,14] However, other difunctionalisation processes do exist, such as those incorporating both a new C-C and a new C-H bond across the alkene substrate (hydrocarbofunctionalisation).[15–18] An example of this is the report from Xue, Engle, Zhao, and co-workers, where a range of alkenes were hydrocarbofunctionalised using an alcohol as the proton source and an aryl boronic acid as the source of the carbon-containing unit, respectively (Scheme 4.3.).[19] This process was catalysed by a nickel (0) species and involved an 8-aminoquinoline moiety as a directing group on the alkene, which was required for effective reactivity. These hydrocarbofunctionalisation processes are postulated to involve a nickel-hydride intermediate species, arising from the interaction between the nickel(0) species and the alcohol, in this example.

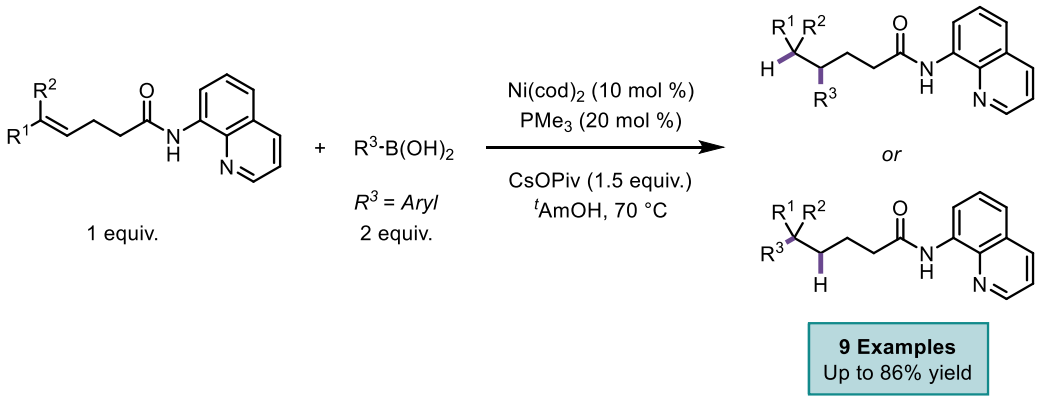

Scheme 4.3. Xue, Engle, Zhao, and co-workers' report on the hydrocarbofunctionalisation of aminoquinoline tethered alkenes.

Additionally, utilisation of other metals for alkene difunctionalisation reactions have been reported, however, use of nickel is common due to its versatile reactivity.[20–24]

Within intramolecular alkene dicarbofunctionalisation, Kong and co-workers reported the synthesis of 3,3-disubstituted oxindoles from acrylamide-tethered aryl bromides and aryl bromides, catalysed by nickel (Scheme 4.4A).[25] This process employed a chiral ferrocene-based phosphine ligand, and led to enantioenriched reaction products with excellent stereocontrol. This process utilised zinc as the terminal reductant and bis(pinacolato)diboron was suggested to act as a co-reductant. The proposed mechanism involves a 1,2-migratory insertion step from a nickel(II) species onto the

alkene portion of the acrylamide to form the new 5-membered ring. It is likely that steric effects control the formation of the 5-membered ring over 6-membered ring formation, as the 6-memberd intermediate formed from 1,2-migratory is more sterically encumbered around the nickel centre than the 5-membered intermediate. This is preceded by oxidative addition of a nickel(0) species into the C-Br bond of the acrylamide tethered aryl bromide and followed by reductive elimination to give the product (Scheme 4.4B). It is suggested that single-electron reduction of the nickel(II) to nickel(I), by zinc, occurs after the migratory insertion step, however, it is possible that this reduction takes place before the migratory insertion.

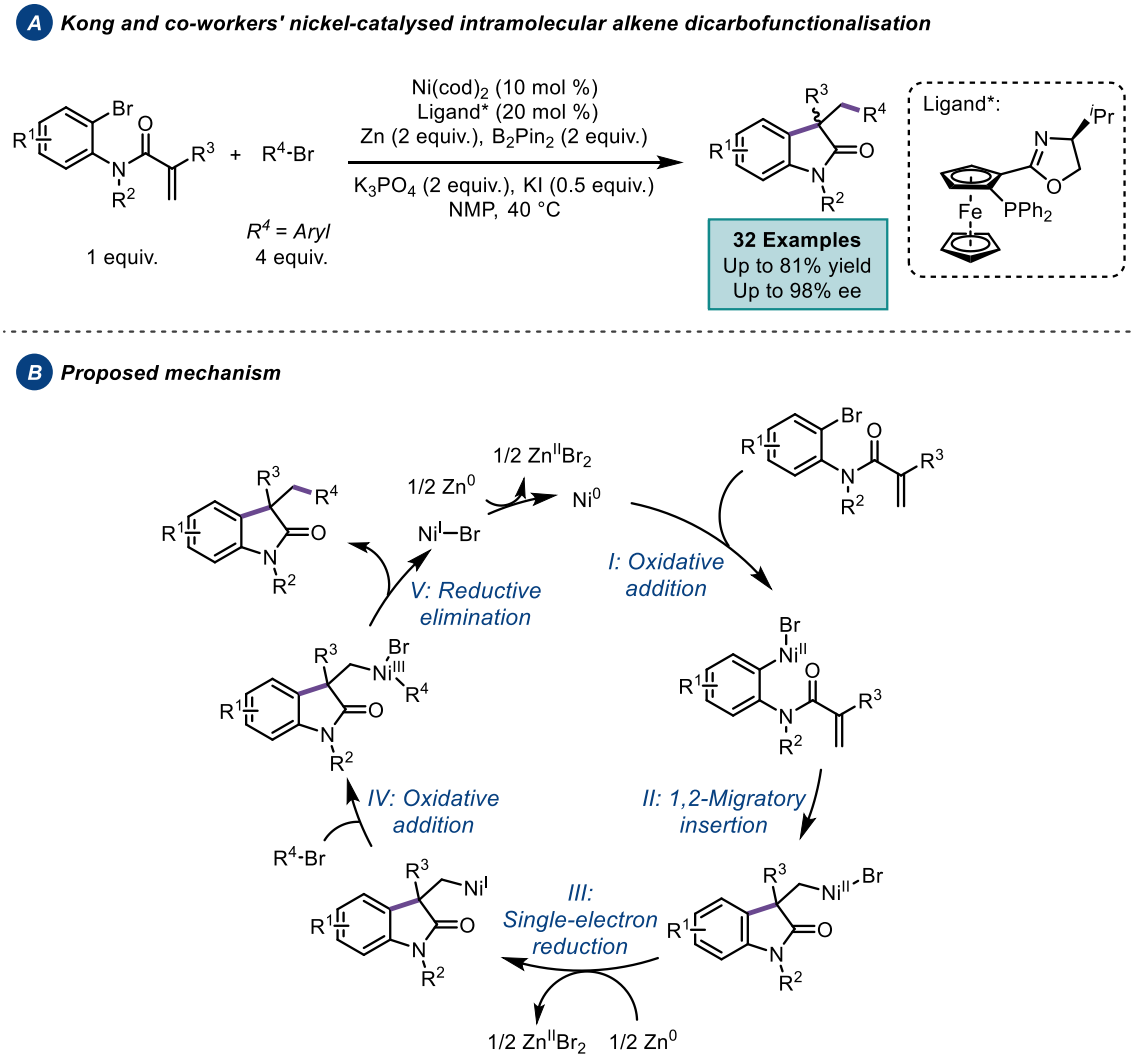

Scheme 4.4. A) Kong and co-workers' report on the nickel-catalysed asymmetric intramolecular alkene dicarbofunctionalisation; B) Proposed mechanism.

This report served as a first example of synthesising such 3,3-disubstitiuted oxindole structures via nickel-catalysed difunctionalisation of alkenes. This represented an important advance as most of the previous literature utilised more-expensive and less-

abundant palladium-based catalytic systems. Additionally, using reductive conditions (i.e., in the presence of a terminal reductant) allows for broader functional group tolerance, such as acid sensitive groups, compared to examples using palladium catalysis that typically require basic conditions. These 3,3-disubstitiuted oxindole products and their derivatives are of interest, as this is a motif present in many pharmaceutically relevant compounds, with some examples shown (Figure 4.1.).[26,27] More recently, 3,3-disubstituted oxindoles and other *N*-heterocycles were synthesised using mechanoredox chemistry.[28,29]

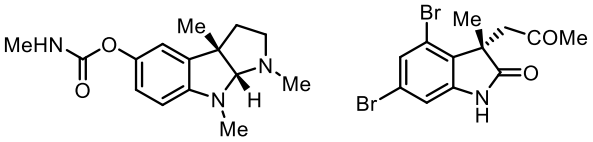

Physostigmine
Alzheimer's disease

Convolutamydine A
Leukemia

Figure 4.1. Drug molecules containing a 3,3-disubstituted oxindole derived core.

There has been a sustained effort to develop these intramolecular alkene difunctionalisation process further to tolerate a broader range of electrophiles, such as alkyl halides,[30,31] alkenyl halides,[32,33] isocyanates,[34] and cyanating agents.[35,36] Methods that furnish other heterocyclic cores, such as indoles,[37] indanes,[38,39] and pyrrolidines[40] have also been developed. However, these processes typically suffer from the same drawbacks that hinder XEC processes, such as the reliance on undesired amide solvents (DMA, NMP), the requirement for inert atmospheres, and the *ex situ* activation of the terminal reductant when zinc or manganese are employed. Therefore, it was envisaged that these limitations could be overcome by applying the established mechanochemical XEC protocol from the Browne research group to these alkene difunctionalisation processes, which is yet to be reported under mechanochemical conditions. Such methodology would allow rapid construction of complex molecules in a facile, sustainable, and operationally simple fashion.

4.2. Results and Discussion

4.2.1. Reaction Optimisation

To commence the investigations into the nickel-catalysed difunctionalisation of alkenes, a model system encompassing intramolecular reactivity, namely acrylamide tethered aryl bromide (**13a**) and 1-iodooctane (**8a**), was selected. **13a** was synthesised from the corresponding aniline and methacryloyl chloride, followed by methylation of the secondary amide using methyl iodide (Scheme 4.5A). Following this, the optimal conditions previously developed i.e., nickel chloride(II) hexahydrate as the pre-catalyst, 1,10-phenanthroline as the ligand, zinc as the reductant, and DMA in LAG quantities (3 equivalents or η = ~0.30 μL/mg) were applied to this system. The presence of a fluorine atom on the aromatic ring of **13a** allowed for simpler analysis of the crude reaction mixture by utilising ^{19}F NMR spectrometry, instead of ^{1}H NMR spectrometry. This mixture was then milled at 30 Hz for 2 hours, furnishing both the dicarbofunctionalisation (DCF) product (**14a**) and the XEC product (**15a**) in 24% yield by ^{19}F NMR analysis, which were isolated in 23% and 22% yield, respectively (Scheme 4.5B). The formation of the XEC product was unsurprising considering these conditions were optimised for a similar XEC process.

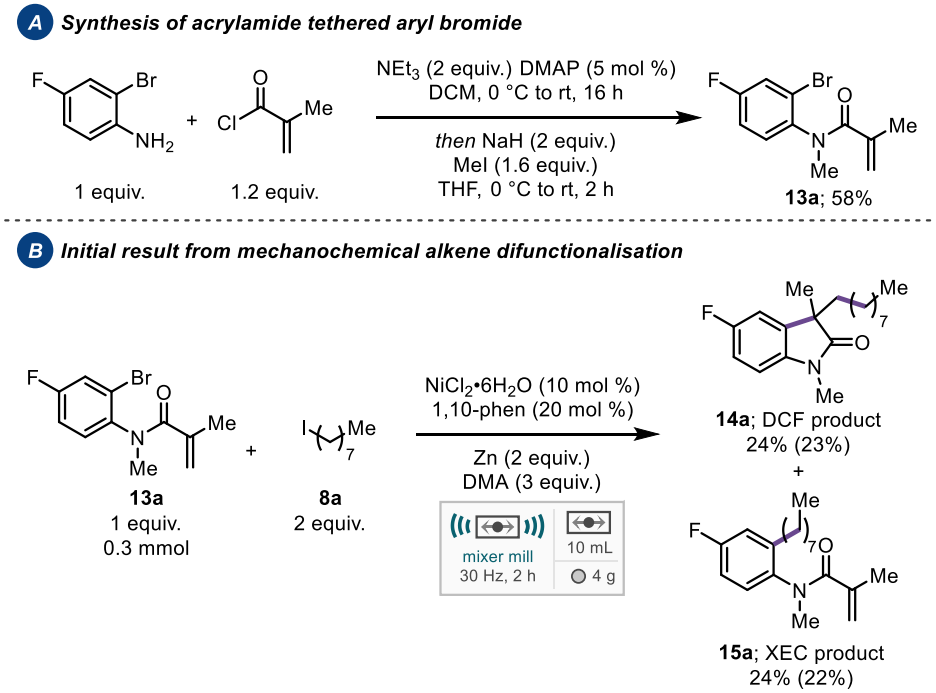

Scheme 4.5. A) Synthesis of acrylamide tethered aryl bromide (**13a**); B) Initial hit in mechanochemical alkene difunctionalisation investigations.

Following this initial result, a full screen of the reaction parameters, including the ligand, reductant, and the LAG agent was carried out (Table 4.1.A.). It was immediately discovered that utilising manganese as the reductant, instead of zinc, gave a much-improved selectivity for the DCF product (**14a**) over the XEC product (**15**); 21% and 2% yield by ^{19}F NMR analysis, respectively (entry 2). It is possible that the increased propensity of zinc to form organometallic species is influencing this selectivity. Additionally, increasing the equivalents of manganese from 2 to 3 led to a noticeable increase in DCF product yield; 36% by ^{19}F NMR analysis (entry 3). Increasing the equivalents of manganese further did not result in an increase in the product yield (entry 4). Varying the ligand to other phenanthroline-type ligands or varying the LAG agent did not have a positive impact on the product yield (entries 5 – 9). Increasing the reaction time from 2 hours to 4 hours led to a slight increase in product yield, giving 39% of **14a** by ^{19}F NMR analysis (entry 10).

Peculiarly, when the scale of the reaction, with respect to **13a**, was increased from 0.3 mmol of **13a** to 1 mmol, a large increase in yield was observed, furnishing 75% yield of **14a** by ^{19}F NMR analysis, which was isolated in 67% yield and with only a small amount of **15a** observed (entry 11). It is known that the jar filling degree can influence the reaction efficiency, however, the exact cause for this dramatic yield increase is unknown.[41,42]

To probe this further, the scale of the reaction was increased to 2 mmol, along with decreasing and increasing the size of both the grinding ball and milling jar (Table 4.1.B.). To this end, no additional increase in product yield was observed, therefore, it is possible that the jar filling ratio is already optimal (entries 1 – 5). Additionally, it is possible that increased temperature generation from a >3-fold increase in the amount of material in the jar could be assisting the process in some way. Following this, a few other ligands, namely bipyridines and terpyridine, were tested at the increased reaction scale, however these all returned poorer product yields than with 1,10-phenanthroline (entries 6 – 8). Other nickel(II) pre-catalysts were equally as effective or slightly less effective than nickel(II) chloride hexahydrate, as was the case with decreasing or increasing the catalyst loading of nickel and changing the 1:2

nickel/ligand ratio to 1:1 or 1:3 (entries 9 – 14). Changing the reductant to zinc resulted in a an approximately 1:1 mixture of DCF product (**14a**) and XEC product (**15a**), whereas an organic reductant (TDAE) gave very poor product yields (entries 15 and 16), likely due to the poor air stability of TDAE as previously discussed.

Finally, control reactions revealed that the reaction is ineffective in the absence of catalyst, ligand, reductant, and LAG agent (entries 17 – 20). Hence, the conditions highlighted (Table 4.1.A., entry 11) were carried forward as the optimal conditions.

Table 4.1.A. Optimisation of nickel-catalysed intramolecular alkene dicarbofunctionalisation.

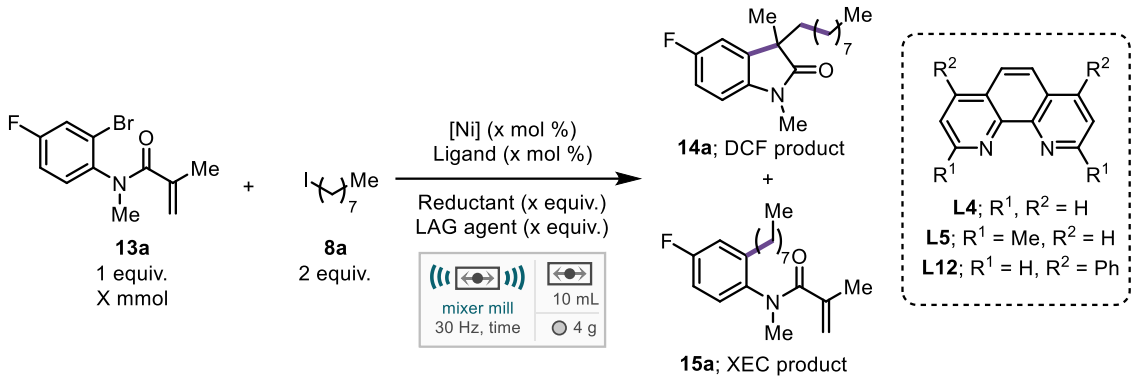

Entry[a]	Scale (mmol)	[Ni] (mol %)	Ligand (mol %)	Red. (equiv.)	LAG agent (equiv.)	Time (h)	14a[b] (%)[a]	15a[b] (%)[a]
1	0.3	$NiCl_2•6H_2O$ (10)	**L4** (20)	***Zn (2)***	DMA (3)	2	24 (23)	24 (22)
2	0.3	$NiCl_2•6H_2O$ (10)	**L4** (20)	***Mn (2)***	DMA (3)	2	21	2
3	0.3	$NiCl_2•6H_2O$ (10)	**L4** (20)	***Mn (3)***	DMA (3)	2	36	4
4	0.3	$NiCl_2•6H_2O$ (10)	**L4** (20)	***Mn (4)***	DMA (3)	2	35	3
5	0.3	$NiCl_2•6H_2O$ (10)	***L5 (20)***	Mn (3)	DMA (3)	2	<2	<2
6	0.3	$NiCl_2•6H_2O$ (10)	***L12 (20)***	Mn (3)	DMA (3)	2	21	3
7	0.3	$NiCl_2•6H_2O$ (10)	**L4** (20)	Mn (3)	***DMF (3)***	2	24	3
8	0.3	$NiCl_2•6H_2O$ (10)	**L4** (20)	Mn (3)	***THF (3)***	2	<2	<2
9	0.3	$NiCl_2•6H_2O$ (10)	**L4** (20)	Mn (3)	***MeCN (3)***	2	<2	<2
10	0.3	$NiCl_2•6H_2O$ (10)	**L4** (20)	Mn (3)	DMA (3)	***4***	39	3
11	***1***	$NiCl_2•6H_2O$ (10)	**L4** (20)	Mn (3)	DMA (3)	4	75 (67)	3

[a]Reactions were carried out on the stated reaction scale in 10 mL stainless steel jars, equipped with a 4 g, 10 mm stainless steel grinding ball, under an air atmosphere.

[b]Yield determined by ^{19}F NMR analysis of the crude reaction mixture (after work-up), using (trifluoromethyl)benzene as an internal standard. Isolated yields are given in parentheses.

Table 4.1.B. Further optimisation of nickel-catalysed intramolecular alkene dicarbofunctionalisation.

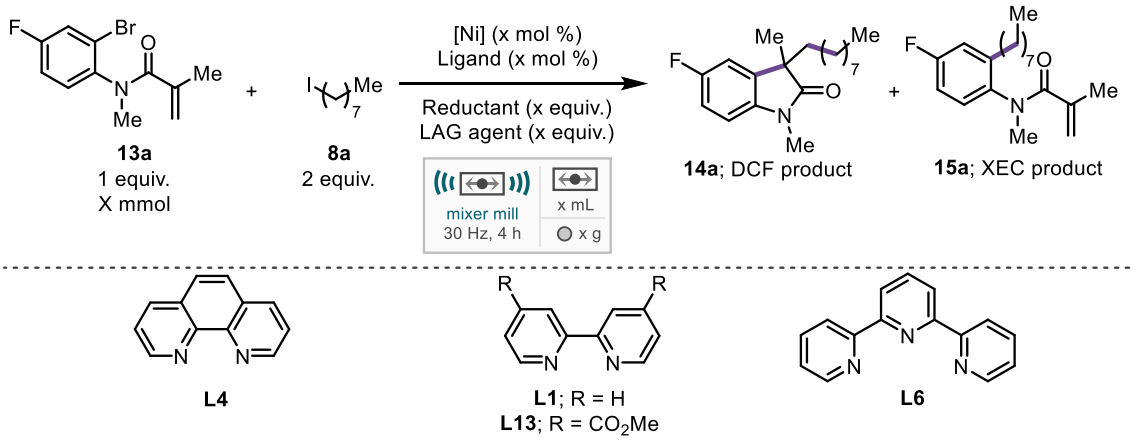

Entry[a]	Scale (mmol)	[Ni] (mol %)	Ligand (mol %)	Red. (equiv.)	LAG agent (equiv.)	Jar (mL) and ball (g)	14a[b] (%)[a]	15a[b] (%)[a]
1	***2***	$NiCl_2•6H_2O$ (10)	**L4** (20)	Mn (3)	DMA (3)	10, 4	69	4
2	1	$NiCl_2•6H_2O$ (10)	**L4** (20)	Mn (3)	DMA (3)	***10, 2***	73	4
3	1	$NiCl_2•6H_2O$ (10)	**L4** (20)	Mn (3)	DMA (3)	***10, 8***	71	4
4	1	$NiCl_2•6H_2O$ (10)	**L4** (20)	Mn (3)	DMA (3)	***5, 4***	72	2
5	1	$NiCl_2•6H_2O$ (10)	**L4** (20)	Mn (3)	DMA (3)	***25, 4***	68	2
6	1	$NiCl_2•6H_2O$ (10)	***L1 (20)***	Mn (3)	DMA (3)	10, 4	59	3
7	1	$NiCl_2•6H_2O$ (10)	***L13 (20)***	Mn (3)	DMA (3)	10, 4	31	6
8	1	$NiCl_2•6H_2O$ (10)	***L6 (20)***	Mn (3)	DMA (3)	10, 4	15	7
9	1	***$NiCl_2$(DME) (10)***	**L4** (20)	Mn (3)	DMA (3)	10, 4	74	<2
10	1	***$NiBr_2•4H_2O$ (10)***	**L4** (20)	Mn (3)	DMA (3)	10, 4	41	2
11	1	***$NiCl_2•6H_2O$ (5)***	**L4** (10)	Mn (3)	DMA (3)	10, 4	75	<2
12	1	***$NiCl_2•6H_2O$ (20)***	**L4** (40)	Mn (3)	DMA (3)	10, 4	61	2
13	1	$NiCl_2•6H_2O$ (10)	***L4 (10)***	Mn (3)	DMA (3)	10, 4	67	2
14	1	$NiCl_2•6H_2O$ (10)	***L4 (40)***	Mn (3)	DMA (3)	10, 4	73	3
15	1	$NiCl_2•6H_2O$ (10)	**L4** (20)	***Zn (3)***	DMA (3)	10, 4	41	31
16	1	$NiCl_2•6H_2O$ (10)	**L4** (20)	***TDAE (3)***	DMA (3)	10, 4	8	<2
17	1	-	**L4** (20)	Mn (3)	DMA (3)	10, 4	<2	<2
18	1	$NiCl_2•6H_2O$ (10)	-	Mn (3)	DMA (3)	10, 4	<2	<2
19	1	$NiCl_2•6H_2O$ (10)	**L4** (20)	-	DMA (3)	10, 4	<2	<2
20	1	$NiCl_2•6H_2O$ (10)	**L4** (20)	Mn (3)	-	10, 4	<2	<2

[a]Reactions were carried out on the stated reaction scale in 10 mL stainless steel jars, equipped with a 4 g, 10 mm stainless steel grinding ball, under an air atmosphere, unless stated otherwise.

[b]Yield determined by ^{19}F NMR analysis of the crude reaction mixture (after work-up), using (trifluoromethyl)benzene as an internal standard. Isolated yields are given in parentheses.

4.2.2. Substrate Scope

Before commencing with an evaluation of the scope of the reaction, a range of alkene tethered aryl halides were synthesised from the corresponding anilines, phenols, or thiophenols, using the standard synthetic procedure (Scheme 4.6.).

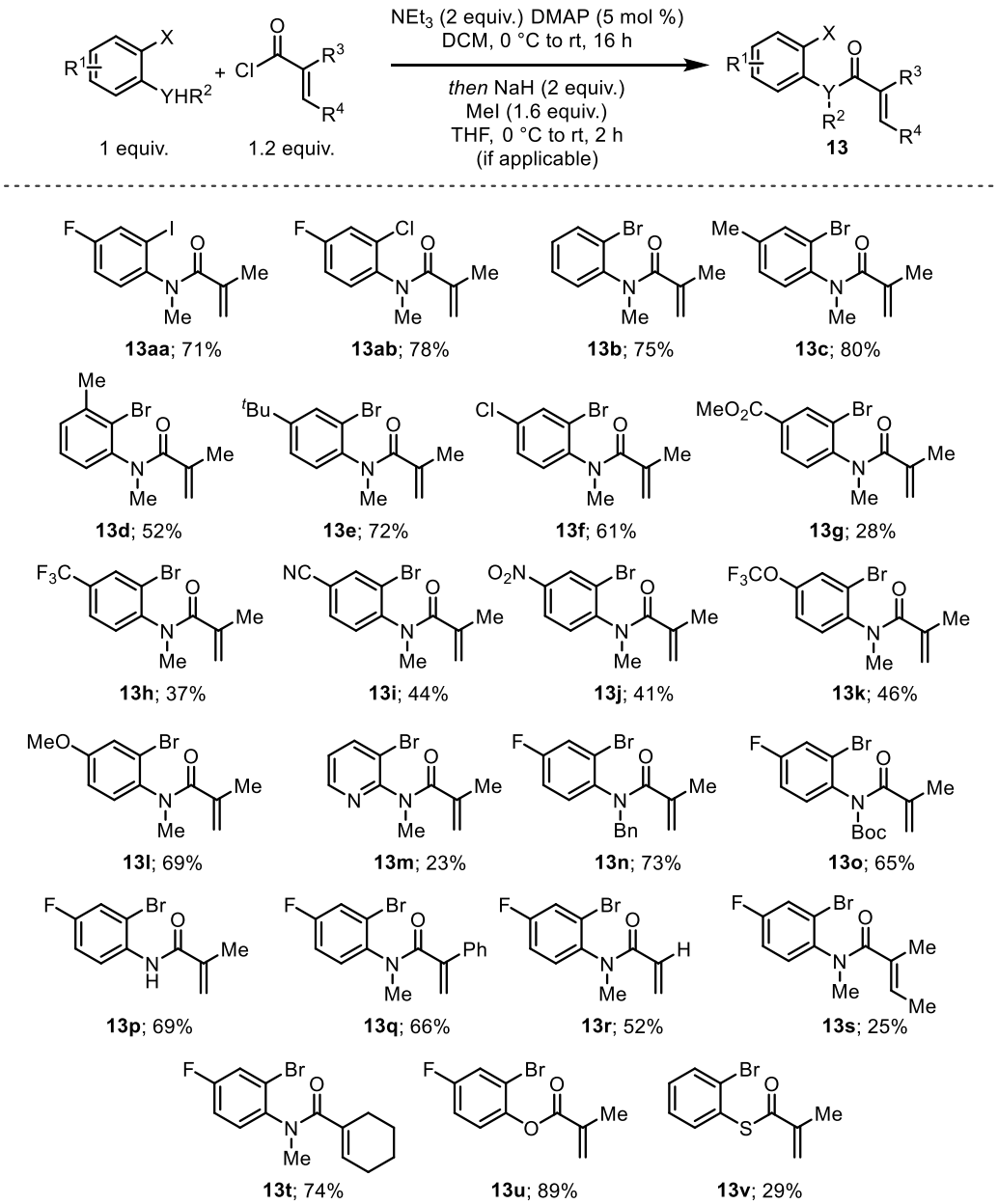

Scheme 4.6. Alkene tethered aryl halides synthesised in this study.

The substrate scope studies began with an evaluation of the alkyl halide coupling partners. A small selection of alkyl iodides were tolerated, including neopentyl iodide and 1-iodocyclohexane, furnishing the respective DCF products (**14c** and **14d**) in 76% and 55% isolated yields (Scheme 4.7.). Some unsuccessful alkyl iodides included a

phthalimide (**14e**), *tert*-butyl iodide (**14f**), and an oxetane (**14g**). This could be due to the lower reactivity of these substrates, because of the presence of electron-rich moieties in the case of the phthalimide and oxetane, or steric encumbrance in the case of the *tert*-butyl iodide.

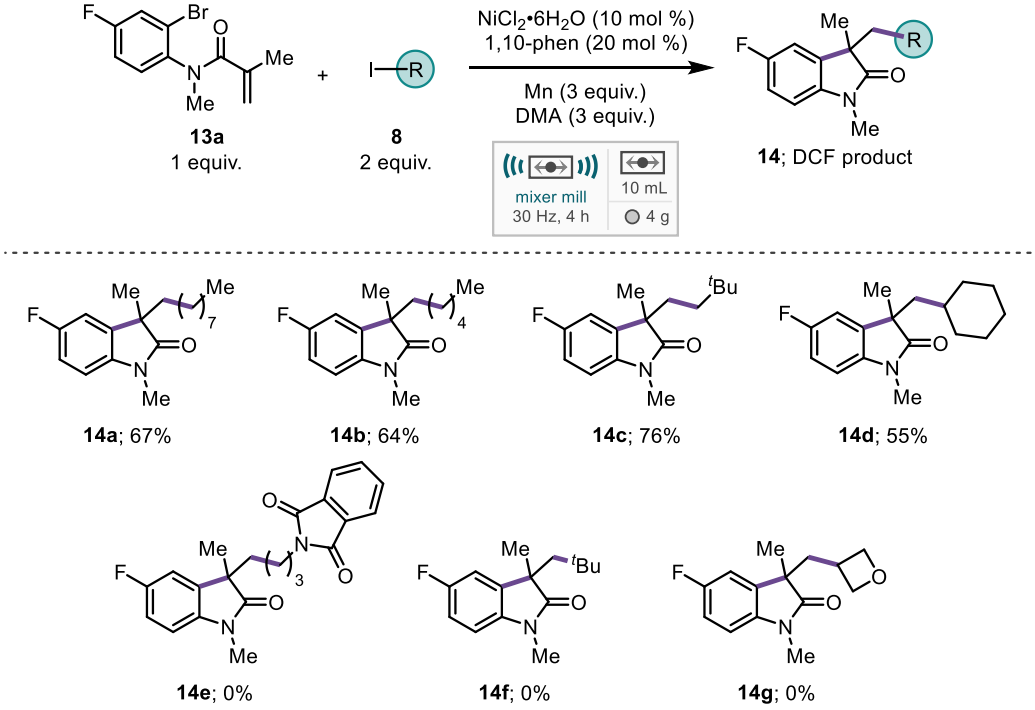

Scheme 4.7. Scope of alkyl iodide coupling partners for intramolecular alkene dicarbofunctionalisation.

Following this, the scope of the alkyl bromide coupling partners was explored, however, as with the XEC process (Chapter 3) it was found that using sodium iodide as an additive was required for effective reactivity. To this end, 1 equivalent of sodium iodide was sufficient for effective product formation, using a model system of acrylamide **13a** and ethyl 4-bromobutyrate (Table 4.2.).

Table 4.2. Optimisation of sodium iodide additive in intramolecular alkene dicarbofunctionalisation process.

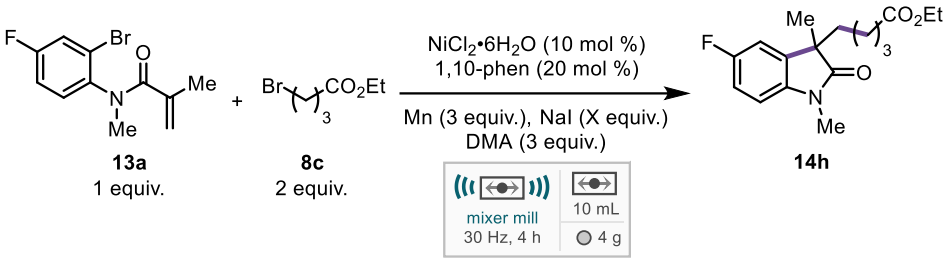

Entry	Sodium iodide (equiv.)	14h (%)[a]
1	0	12
2	1	66 (56)
3	2	62

[a]Yield determined by ^{19}F NMR analysis of the crude reaction mixture (after work-up), using (trifluoromethyl)benzene as an internal standard. Isolated yields are given in parentheses.

With these conditions for alkyl bromide coupling partners in hand, a variety of alkyl bromides were screened (Scheme 4.8.). This included functionalised alkyl groups, such as those containing a methyl ether (**14i**; 50%) and a cyano group (**14k**; 44%). A selection of cycloalkyl rings were also incorporated, including a cyclobutane (**14m**; 72%), cyclohexane (**14n**; 51%), and a cyclopentane (**14o**; 47%) in moderate to good yields. A product containing an alkenyl chain (**14p**; 51%), derived from (*S*)-citronellyl bromide, was furnished as a 1:1 mixture of diastereomers. Some unsuccessful examples included alkyl chains containing a benzoate ester (**14q**), a protected amine (**14r**), a protected piperidine (**14s**), a tetrahydropyran (**14t**), and a prenyl group (**14u**). The intolerance of the reaction to these alkyl halides is likely due to their lower reactivities from the presence of electron-rich moieties.

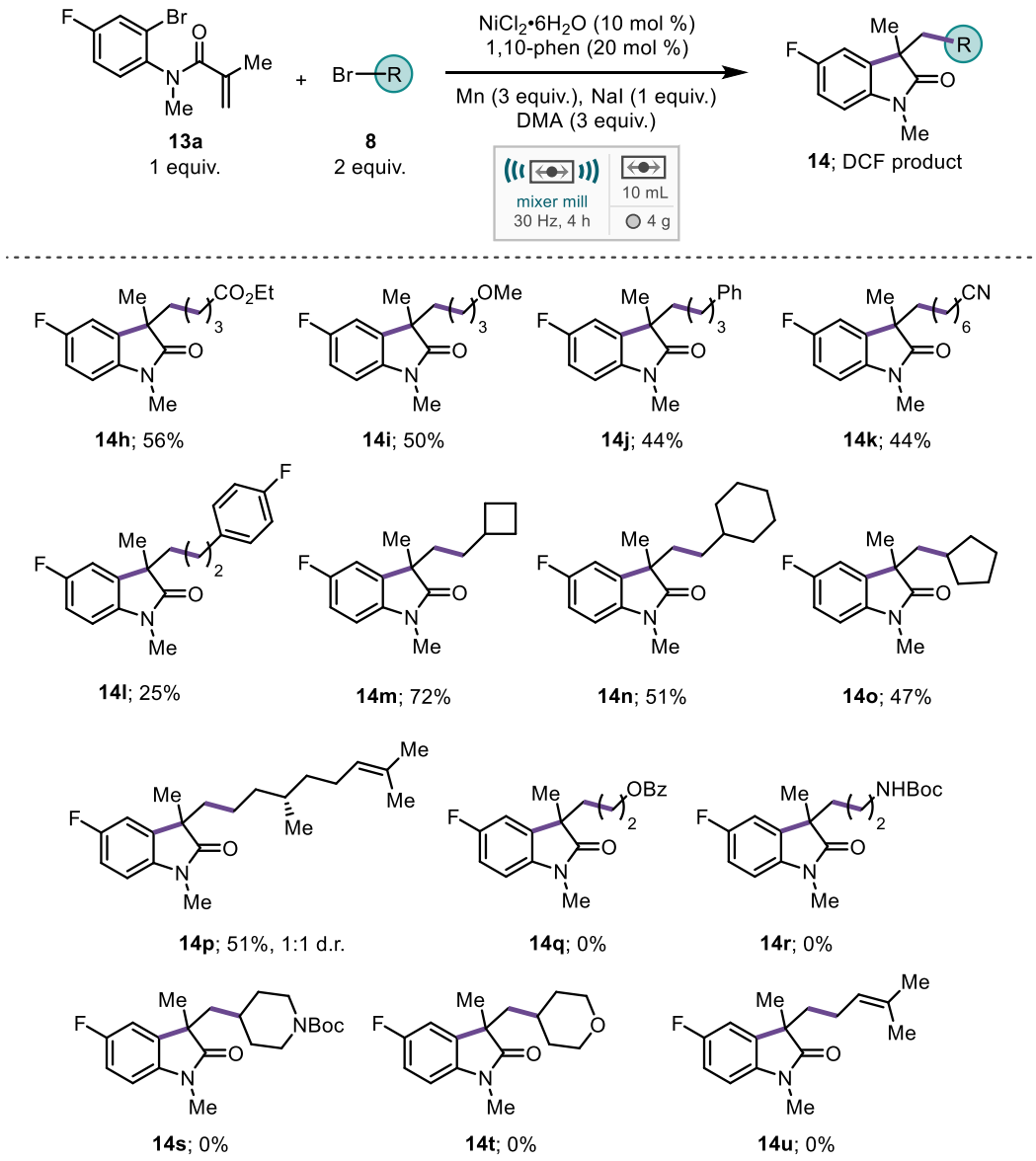

Scheme 4.8. Scope of alkyl bromide coupling partners for intramolecular alkene dicarbofunctionalisation.

Subsequently, the scope of the alkene tethered aryl halide was explored, using neopentyl iodide (**8e**) as the coupling partner (Scheme 4.9.). This included the tolerance of a range of functionality on the aromatic ring, such as sterically hindered *tert*-butyl substitution at the 4-position (**14x**; 52%) and methyl substitution at the 3-position of the aromatic ring (**14ae**; 35%), albeit in lower yields. Electron-withdrawing groups were also tolerated, including a methyl ester (**14y**; 49%), trifluoromethyl substitution (**14z**; 69%), and cyano substitution (**14aa**; 65%). Additionally, an electron-rich methoxy substituent was tolerated in good yield (**14ac**; 71%). Interestingly, a chloro substituted example was tolerated with chemoselectivity at the C-Br bond, in

good yield (**14ab**; 65%), allowing for further functionalisation to take place. An 'aza'-oxindole type compound (**14af**; 56%) was successfully furnished in moderate yield, demonstrating tolerance for basic *N*-heteroaromatics.

Finally, substitution on the acrylamide was varied, which included changing the *N*-substitution from a methyl to a benzyl group (**14ag**; 63%), changing the methacrylamide to a phenacrylamide (**14ah**; 34%), and utilising a trisubstituted acrylamide derived from tiglic acid (**14ai**; 16%), which was produced as a 3:1 mixture of diastereomers. The low yield of the latter example is likely due to the increased steric demand around the alkene. Some unsuccessful examples included a strongly electron-withdrawing nitro substitution on the aromatic ring (**14aj**). Other substitution on the nitrogen, such as a *tert*-butyloxycarbonyl (Boc, **14ak**) protecting group and a free oxindole (**14al**) were not tolerated. This could suggest that *N*-substitution is necessary to prevent poisoning of the catalyst via nitrogen coordination, however, electron-withdrawing protecting groups can inhibit reactivity, also. Additionally, an unsubstituted acrylamide (**14am**) was not tolerated, along with attempts to synthesise a spiro-substituted oxindole (**14an**). Steric effects are most likely preventing successful reactivity of this latter example. Finally, attempts to synthesise other fused heterocycles using this methodology, namely benzofuranone (**14ao**) and benzothiophenone (**14ap**), were unsuccessful, suggesting that the presence of the nitrogen atom is important.

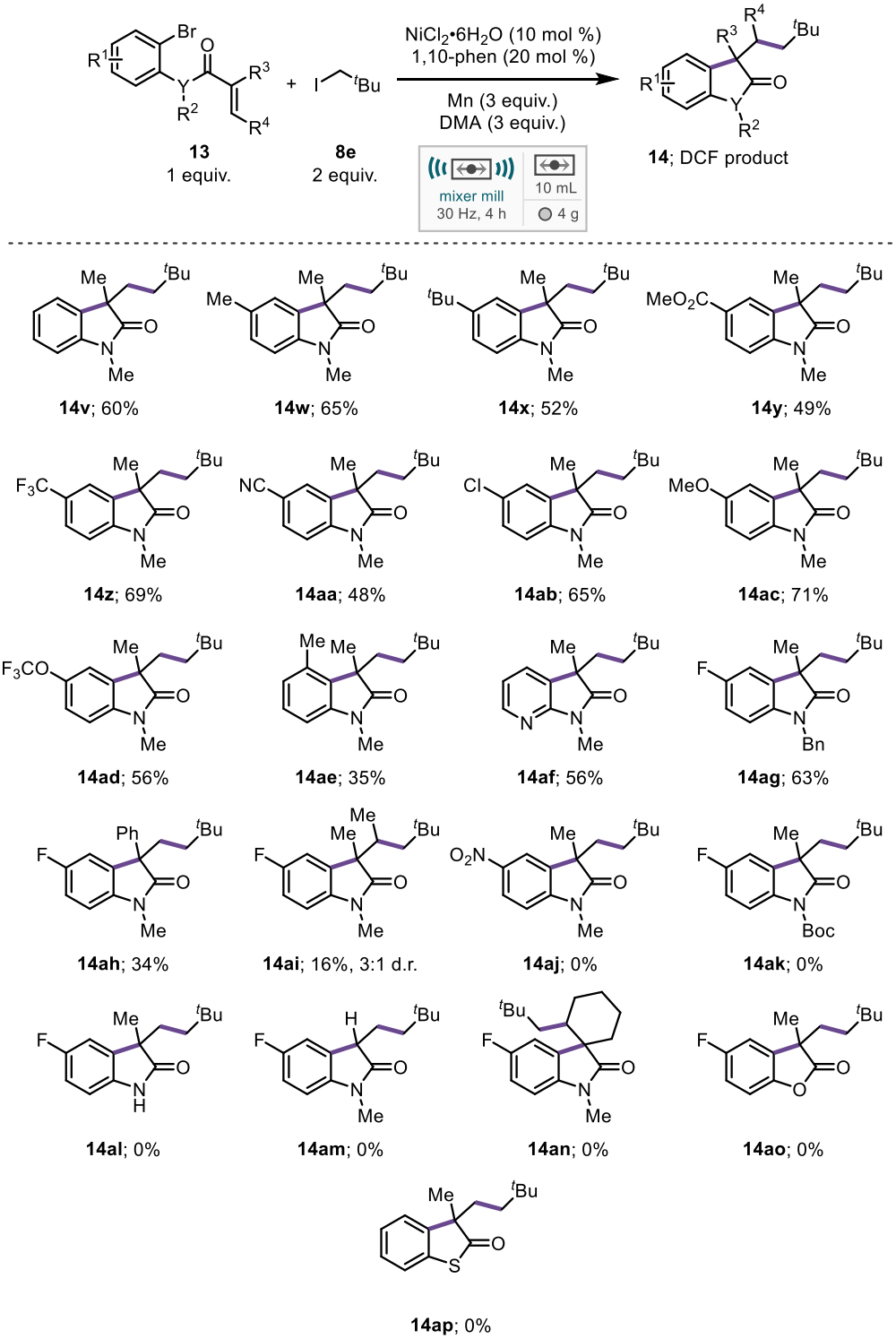

Scheme 4.9. Scope of alkene tethered aryl bromides for intramolecular alkene dicarbofunctionalisation.

Following this, a small selection of alternative electrophiles were screened in the dicarbofunctionalisation process, including bromobenzene (**8f**), *N*-cyano-*N*-phenyl-4-(methylbenzene)sulfonamide (NCTS, **8g**), and 4-nitrobenzene isocyanate (**8h**). The reaction with bromobenzene was successful, furnishing the desired product (**14aq**;

11%) in low yield (Scheme 4.1.1.). However, it is worth noting that this is an sp^2-sp^2 coupling, compared to the sp^2-sp^3 coupling normally in effect in the process, hence this substrate class would likely require an alteration of the reaction conditions to provide better yields. The cyano (**14ar**) and amido (**14as**) substituted oxindole products that would be furnished from the reactions with NCTS and the isocyanate, respectively, were not observed. These electrophiles may also require different reaction conditions to be tolerated.

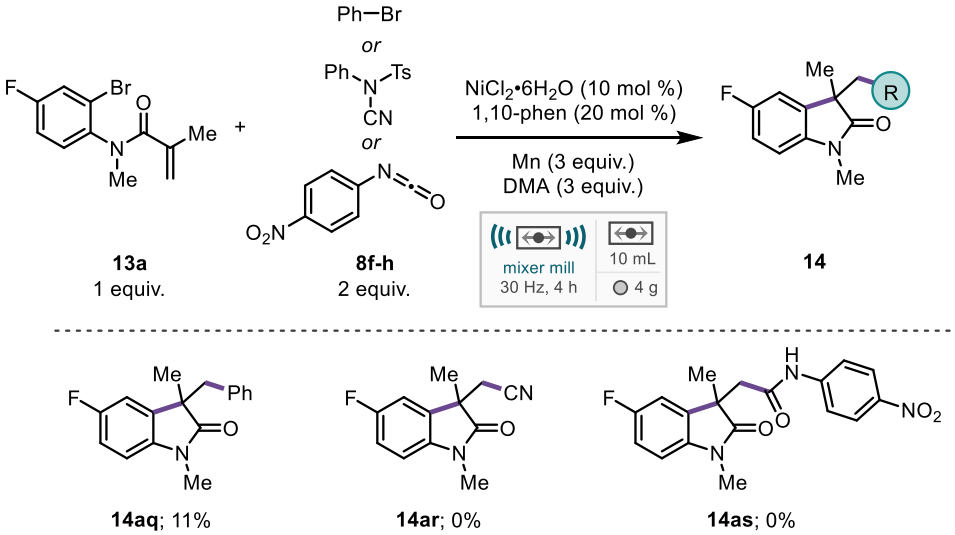

Scheme 4.1.1. Screen of alternate electrophiles for intramolecular alkene difunctionalisation.

Following this, it was demonstrated that the chloro and iodo substituted analogues of the parent alkene tethered aryl bromide (**13a**) could be utilised, under the optimal conditions, furnishing the oxindole product (**14a**) in decreased yields of 36% and 58% by ^{19}F NMR analysis, respectively (Scheme 4.1.2.). This is a marked improvement over previous mechanochemical XEC reports, where aryl chlorides were not tolerated.[43]

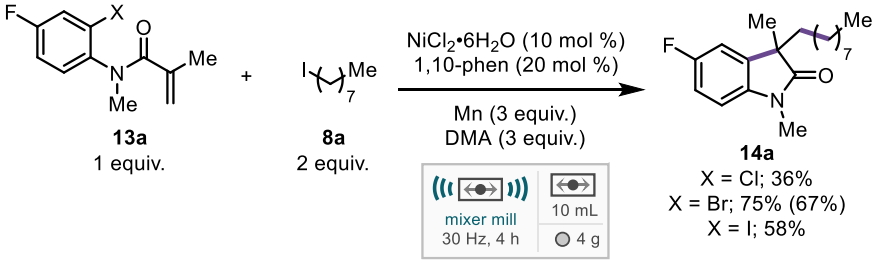

Scheme 4.1.2. Comparison of reactivity of 2-chloro, 2-bromo, and 2-iodopyridine in XEC process.

4.2.3. Nickel-Hydride Investigations

When 4-bromo-but-1-ene (**8i**) was used as the coupling partner during the substrate scope, the expected DCF product was observed as an approximately 1:1 inseparable mixture of alkene isomers (**14ata** and **14atb**), in 30% isolated yield (Scheme 4.1.3.). The presence of the 'chain-walked' product **14atb** could suggest that a nickel-hydride species is present in the mechanism; although the origin of this is unknown, a plausible pathway to this product is shown.

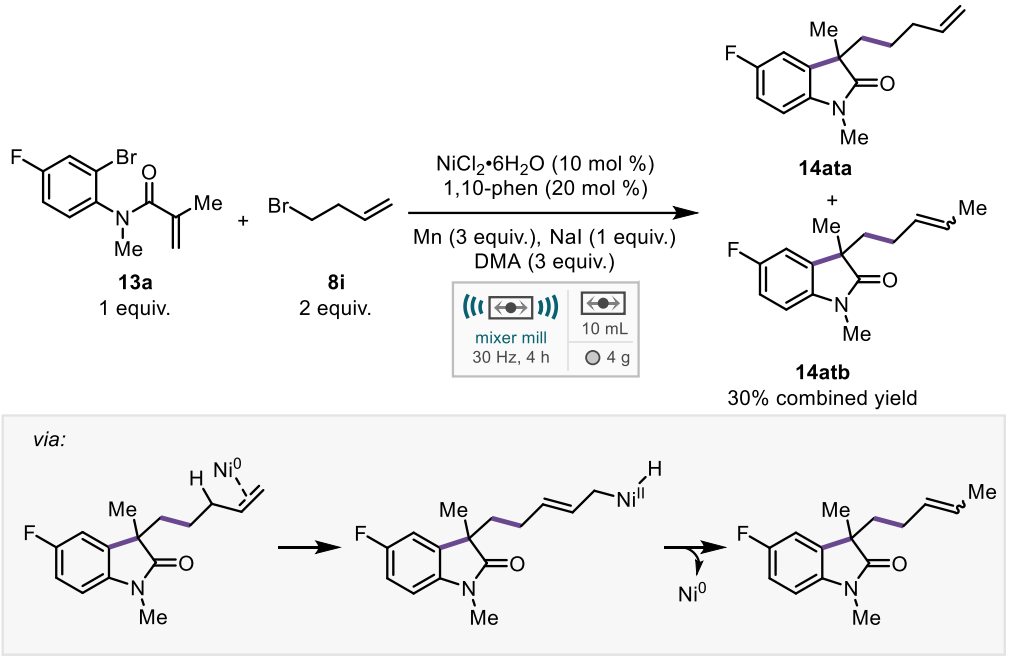

Scheme 4.1.3. Result obtained from reaction of **13a** and 4-bromo-but-1-ene, under the optimal conditions and a plausible pathway for the formation of the chain-walked product.

Additionally, a side product was occasionally observed during the evaluation of the alkyl bromide scope: a so-called reductive Heck product (**16a**). This product is reported as a side product in solution-phase intramolecular dicarbofunctionalisation processes and further implies the presence of a nickel-hydride intermediate. The formation of **16a** was particularly predominant in examples with poor desired reactivity, such as using 4-bromotetrahydropyran (**8j**) as the coupling partner. As stated previously, this example did not furnish any of the desired product; however, did furnish 53% yield of the Heck side product by ^{19}F NMR analysis (33% isolated, Scheme 4.1.4.).

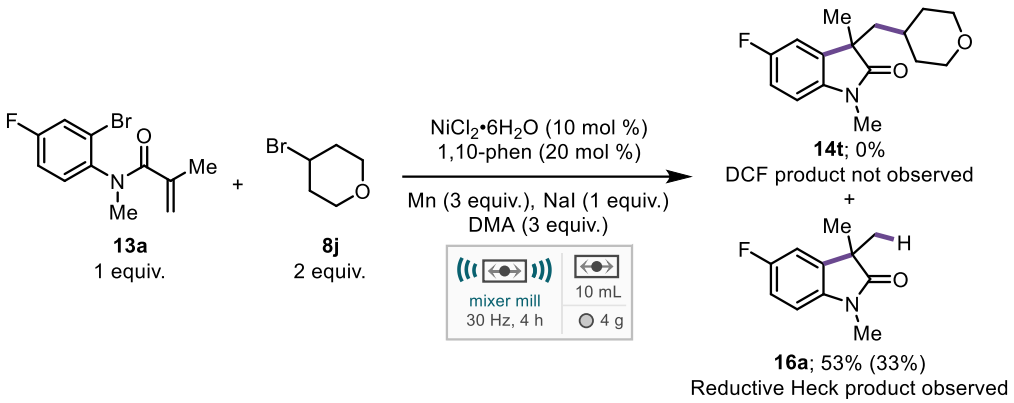

Scheme 4.1.4. Formation of reductive Heck product (**16a**) during alkyl bromide scope.

To probe this aspect further, the reaction was carried out without the addition of the second electrophile (alkyl halide) and with sodium iodide either added or omitted, to help determine the cause of the formation of **16a** (Table 4.3.). Without sodium iodide, only a trace amount of **16a** was produced, however, with sodium iodide **16a** was produced in 55% yield by NMR analysis and isolated in 48% yield (entries 1 and 2). Additionally, adding a mild hydride source to the reaction mixture, polymethylhydrosiloxane (PMHS), resulted in 34% yield of **16a** by NMR analysis, which was increased to 62% yield when an equivalent of sodium iodide was added, also (entries 3 and 4). While the cause of a nickel-hydride intermediate is still unknown, the reaction with sodium iodide using an alternative nickel pre-catalyst was carried out to exclude the possibility of a nickel-hydride species arising from an interaction with the water ligands of nickel(II) chloride hexahydrate with sodium iodide. To this end, the Heck product **16a** was furnished in 32% yield by NMR analysis, using nickel(II) chloride dimethoxyethane as the nickel source (entry 5). This suggests that any potential nickel-hydride species are not arising from the presence of water in the nickel catalyst, however, the presence of water in the remaining reagents is possibly resulting in a nickel-hydride species. Trace amounts of water, in the presence of sodium iodide, could lead to the formation of hydroiodic acid *in situ*, which could permit formation of a nickel-hydride, also. Hence, a plausible mechanism for the formation of the reductive Heck product can be suggested based on these observations and implications (Scheme 4.1.5.).

Table 4.3. Investigations into the formation of Heck product **16a**.

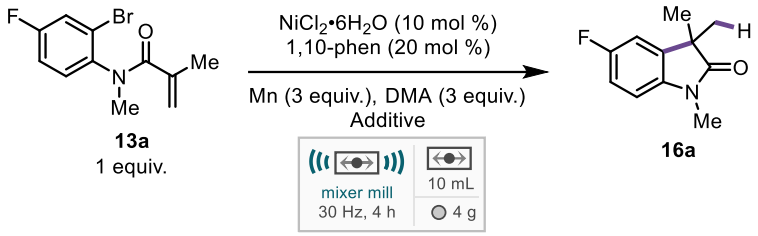

Entry	Additive	16a (%)[a]
1	None	3
2	NaI (1 equiv.)	55 (48)
3	PMHS (4 equiv.)	34
4	NaI (1 equiv.) & PMHS (4 equiv.)	62
5	$NiCl_2$(DME) as catalyst and NaI (1 equiv.)	32

[a]Yield determined by ^{19}F NMR analysis of the crude reaction mixture (after work-up), using (trifluoromethyl)benzene as an internal standard. Isolated yields are given in parentheses.

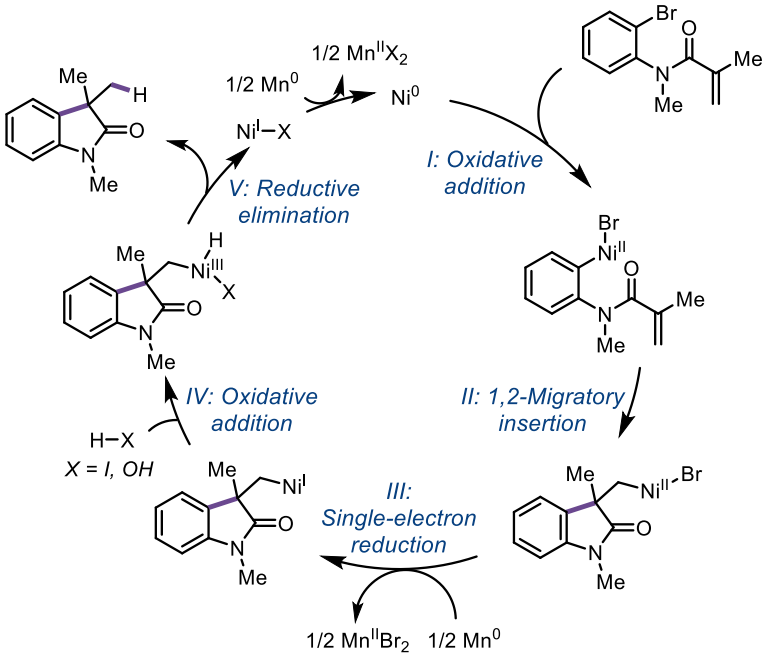

Scheme 4.1.5. Plausible pathway for the formation of the reductive Heck side-product.

4.2.4. Reaction Scale Up

4.2.4.1. Scale Up by Ball-Milling

To demonstrate that the mechanochemical process is amenable to scale up, a 10-fold increase in scale for the reaction between acrylamide tethered aryl bromide (**13a**) and 1-iodooctane (**8a**) was carried out, by increasing the jar and ball size to 30 mL and 12 g, respectively (Scheme 4.1.6.). This experiment furnished 1.60 g of dicarbofunctionalised product (**14a**) in 52% isolated yield. The process is not optimised for the increased jar and ball size, hence the decrease in yield is somewhat expected.

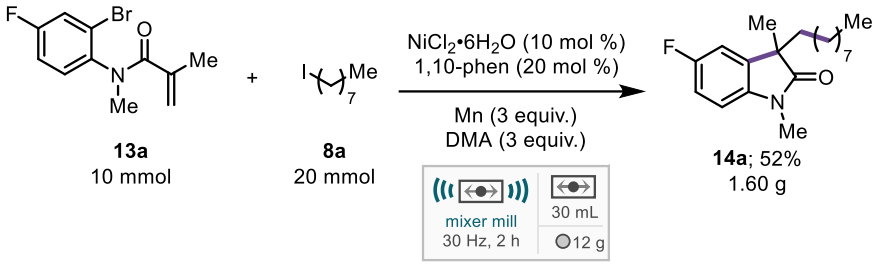

Scheme 4.1.6. Scale up of mechanochemical alkene dicarbofunctionalisation process.

However, the possibility of increasing the reaction scale even further by utilising extrusion is attractive, particularly for a process that requires activation of the terminal reductant, such as this. No such activation using extrusion has been reported to date.

4.2.4.2. Scale Up by Extrusion

Before commencing with studying the alkene dicarbofunctionalisation process on the twin-screw extruder, it was necessary to decrease the amount of liquid in the reaction mixture and to study the effect of temperature on the process. If the mixture has too much liquid in it, then there is the risk that the screws of the extruder can become blocked by the clumping of solid and liquid reagents. If these blockages occur, the screws are unable to continue rotating and the motor ceases its operation. This phenomenon is known as ‘torquing out’ i.e., the energy required for the motor to turn the screws again is too great. Grinding auxiliaries can be utilised to reduce the fluidity of reaction mixtures, also. The aims were to decrease the volume of liquid reagents used in the process and to introduce a grinding auxiliary. Additionally, due to the much

faster reaction time of extrusion processes (residence time <10 minutes) compared to the ball-milled process (2 – 4 hours), it was necessary to try and decrease the total reaction time by introducing heat into the process to provide the best opportunity for success in translating from the mixer mill to the extruder.

These studies were carried out for the reaction between acrylamide tethered aryl bromide (**13a**) and 1-iodopentane (**8k**), where it was found that the equivalents of the alkyl halide and DMA LAG agent could be reduced to 1.2 and 2, respectively, along with the addition of 1 g of sodium chloride (1 g/mmol of **13a**) as a grinding auxiliary (Table 4.4., entry 1). This furnished the product **14b** in 63% yield by ^{19}F NMR analysis, compared to the 71% yield obtained using the standard conditions (2 and 3 equivalents of alkyl halide and DMA, respectively and no grinding auxiliary; entry 2). However, approximately 13% of the Heck side product (**16a**) was also produced. Following this, the effect of temperature on the reaction was investigated, revealing that a temperature of 100 °C, in combination with a 30-minute reaction time, could be utilised to give 35% yield of the product **14b** by ^{19}F NMR analysis (entry 3). Interestingly, increasing the amount of grinding auxiliary to 2 g/mmol led to inhibition of the reaction (entry 4). This is potentially due to an overfilling of the jar preventing efficient mixing, rather than any nefarious influence from the sodium chloride. However, to rule out any inhibition from the sodium chloride, sand was substituted in as the grinding auxiliary, furnishing **14b** in 40% and 29% yield by ^{19}F NMR analysis when 1 and 2 g of sand were used, respectively (entries 5 and 6). These results show that sand is a superior grinding auxiliary, hence this was carried forward. Carrying out the reaction at room temperature, 50 °C and 75 °C all produced decreased yields of **14b** (entries 7 – 9). With these conditions in hand, attempts to translate the process to the extruder were carried out.

Table 4.4. Adjustment of reaction conditions for translation to the extruder.

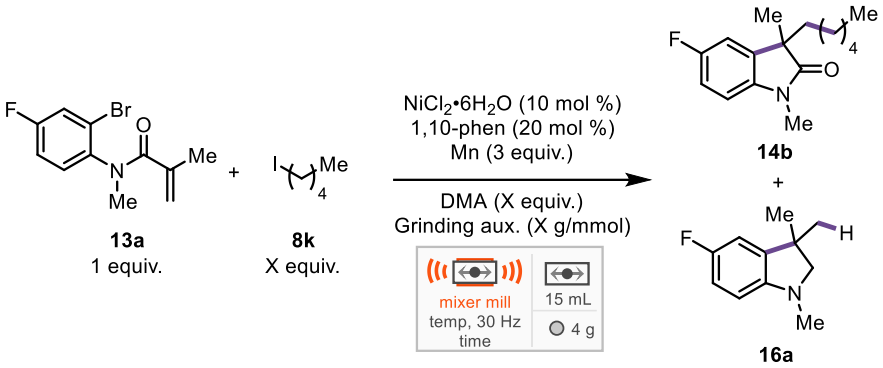

Entry[a]	8k (equiv)	DMA (equiv.)	Grinding auxiliary (g/mmol)	Temperature (°C)	Time (h)	14b (%)[b]	16a (%)[b]
1	1.2	2	NaCl (1)	rt	4	63	13
2	2	3	-	rt	4	71 (64)	8
3	1.2	2	NaCl (1)	100	0.5	35	17
4	1.2	2	NaCl (2)	100	0.5	<2	<2
5	1.2	2	Sand (1)	100	0.5	40	13
6	1.2	2	Sand (2)	100	0.5	29	10
7	1.2	2	Sand (1)	75	0.5	25	4
8	1.2	2	Sand (1)	50	0.5	13	<2
9	1.2	2	Sand (1)	rt	0.5	2	<2

[a]Reactions were carried out in 15 mL stainless steel jars encased in a band heater, equipped with a 4 g, 10 mm stainless steel grinding ball.

[b]Yield determined by ^{19}F NMR analysis of the crude reaction mixture (after work-up), using (trifluoromethyl)benzene as an internal standard. Isolated yields are given in parentheses.

For the extrusion experiment, reverse sections along the screws were used to maximise the mechanical energy input and increase the residence time of the reaction. The solid reagents were hand mixed in a mortar and pestle to obtain a relatively smooth solid mixture. The solids were fed into the extruder using a gravimetric feeder, with a feed-rate of approximately 3 g/min. The liquids were fed into a liquid addition port via a syringe pump, with a feed-rate of 0.92 mL/min. The screw speed was set to 300 rpm and all the heating zones were set to 100 °C. A residence time of around 6 minutes was observed and the extrudate was collected for workup and ^{19}F NMR analysis (Scheme 4.1.7.). Unfortunately, no product formation was observed, and the

starting material remained. It is difficult to determine the cause of the poor reactivity, however, some possible reasons are the poor activation of the manganese metal under extrusion conditions, hence the inability to reduce the nickel(II) pre-catalyst to the catalytically active nickel(0). Therefore, future investigations would likely involve attempts to ensure successful activation of the manganese metal through milling prior to the extrusion process, for example. Additionally, utilising an all-solid system would improve the chances of successful reactivity, hence switching to a solid alkyl halide coupling partner and developing a method to remove the DMA could be envisaged.

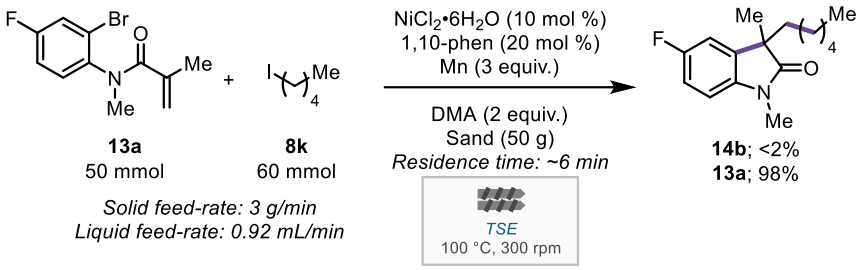

Scheme 4.1.7. Attempted large scale reaction by extrusion.

4.2.5. Solution-Phase Comparisons

As with the mechanochemical XEC process, solution-phase experiments were performed to compare the mechanochemical alkene difunctionalisation process to traditional methods. For these comparisons, acrylamide tethered aryl bromide (**13a**) and neopentyl iodide (**8e**) were used as the substrates (Scheme 4.1.8.). Two sets of conditions were initially examined: a room temperature reaction, in DMA, under a nitrogen atmosphere, for 16 hours and the same conditions, however, heated to 80 °C (conditions A and B). However, conditions A did not furnish any product (**14c**) and conditions B only furnished 11% yield of **14c** by ^{19}F NMR analysis. It was envisaged that the slow activation of the manganese metal reductant could be partly responsible for the poor reactivity, therefore, a separate reaction where the manganese metal was milled for 5 minutes before being added to the solution-phase reaction was carried out (conditions C). This experiment furnished a much-improved 40% yield of **14c** by ^{19}F NMR analysis, highlighting the necessity to activate the metal reductant in these processes and demonstrating the operational simplicity of this activation by ball-

milling. Additionally, the result obtained from the ball-milled process, 79% of **14c** by ^{19}F NMR analysis, in only 4 hours, is a vast improvement over these solution-phase analogues (conditions D).

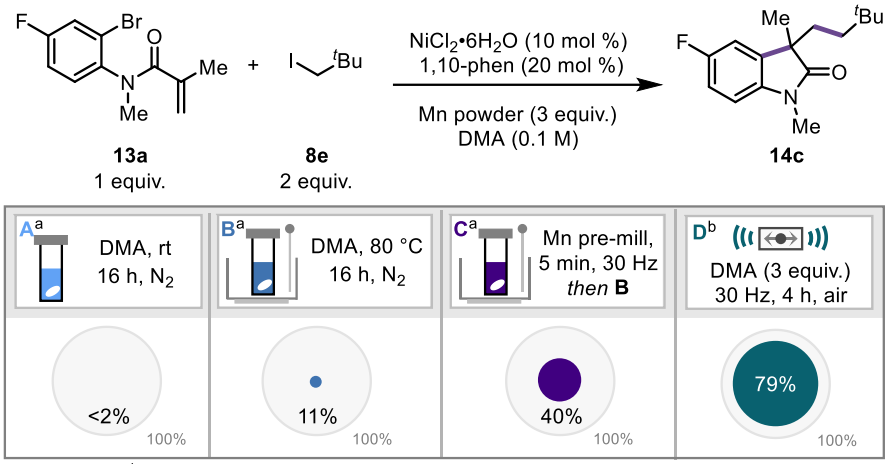

[a]Dry DMA. [b]Winchester grade DMA.

Scheme 4.1.8. Solution-phase comparisons for alkene dicarbofunctionalisation process.

4.2.6. Asymmetric Studies

As the 3,3-disubtituted oxindole products are chiral, there is the possibility for asymmetric induction. Hence, a small selection of chiral ligands were screened in place of 1,10-phenanthroline. This included a bis(oxazoline)-2-pyridine ligand (**L1***), an oxazoline-2-pyridine ligand (**L2***), and a ferrocene-based phosphine ligand (**L3***). However, only **L2*** gave an appreciable amount of the product, furnishing **14a** in 34% isolated yield and with 46% ee (Scheme 4.1.9.). This enantiocontrol is modest, but is a promising initial result. Additionally, there are currently no reports of asymmetric nickel catalysis under mechanochemical conditions, hence this provides a proof-of-concept for future work. Further screening of additives, ligands and adjusting the reaction parameters would likely be required to achieve improved enantiocontrol.

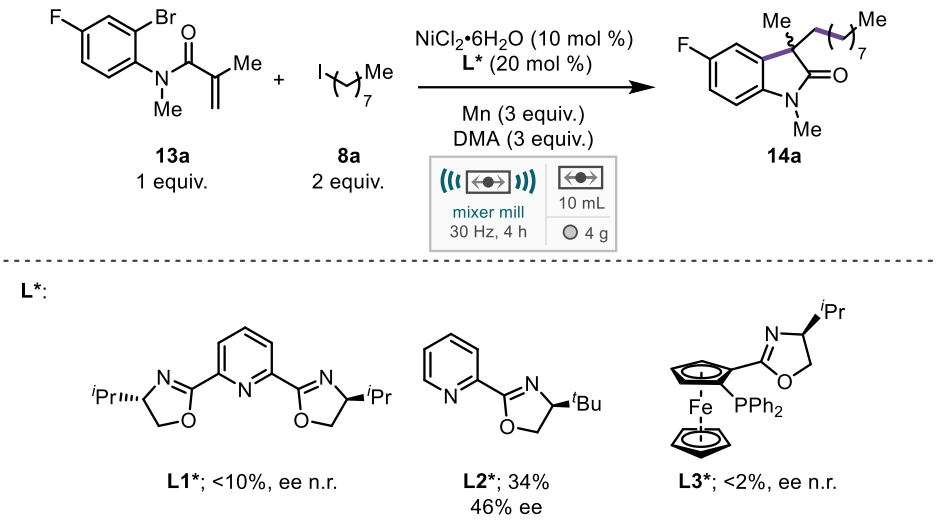

Scheme 4.1.9. Investigations into asymmetric alkene dicarbofunctionalisation.

4.2.7. Mechanochemical Synthesis of Starting Material

The developed mechanochemical protocol can be defined as a blended approach, in the sense that the starting materials for the process are synthesised according to solution-based methods, while the alkene difunctionalisation takes place by mechanochemical means. A method to synthesis the starting material mechanochemically was investigated. With this in mind, a previous report from Browne and co-workers was taken as inspiration, whereby the direct amidation of esters was successfully accomplished, in a ball-mill, using potassium *tert*-butoxide as the base.[44] Applying this to the synthesis of acrylamide **13p**, 2-bromo-4-fluoroaniline (**17a**) was reacted with methyl methacrylate (**18a**) in the presence of potassium *tert*-butoxide, for 2 hours on a mixer mill, furnishing a 33% isolated yield of **13p** (Scheme 4.2.1A). This yield is moderate, however, poorly nucleophilic amines such as anilines, were found to be low yielding during the original study. Comparing this to the solution-based method that was used to synthesise the starting materials in this study, where methacryloyl chloride (**18b**) is used in place of methyl methacrylate, a much greater 69% isolated yield of **13p** was obtained (Scheme 4.2.1B). However, the solution method requires the use of much more toxic reagents, namely acid chlorides, 4-(dimethylamino)pyridine, and dichloromethane as the solvent, in addition to requiring

an inert atmosphere and longer reaction times. Therefore, the mechanochemical approach is much more environmentally benign, as well as being operationally simple.

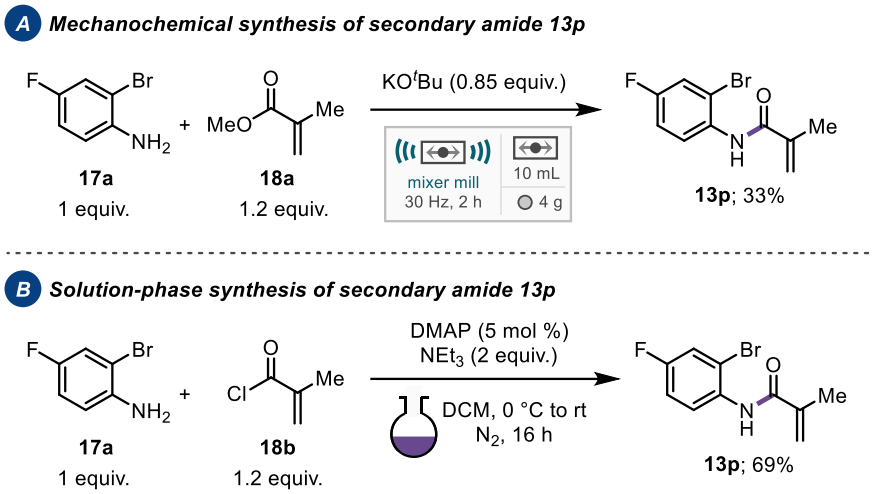

Scheme 4.2.1. A) Mechanochemical synthesis of the starting material; B) Solution-phase synthesis of the starting material.

4.2.8. Mechanistic Studies

4.2.8.1. Stainless Steel Free Reaction

As with the XEC process (Chapter 3), a stainless steel free reaction was carried out to demonstrate that iron from the stainless steel milling jars and balls was not influencing the process. The model reaction between acrylamide tethered aryl bromide (**13a**) and 1-iodooctane (**8a**) was carried out in a planetary ball-mill, using a zirconia grinding bowl and balls (Scheme 4.2.2.). This reaction furnished the product (**14a**) in 48% yield by ^{19}F NMR analysis, which implies that the presence of iron in the stainless steel is not imperative to successful reactivity. As previously stated, the lower yield is likely due to the lower energy impacts imparted by the planetary mill, compared to the mixer mill.

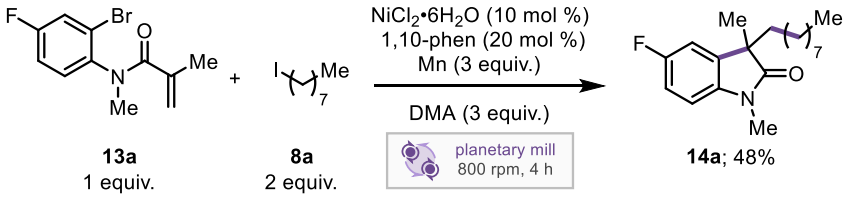

Scheme 4.2.2. Stainless steel free reaction in a planetary ball-mill.

4.2.8.2. Radical Clock Studies

To probe the mechanism of the reaction and to determine whether the process is operating via alkyl radical intermediates or via *in situ* generated organomanganese reagents, akin to XEC processes, a radical clock experiment using (bromomethyl)cyclopropane (**8d**) as the alkyl halide coupling partner was carried out. Using the optimal conditions and acrylamide tethered aryl bromide (**13a**), the rearranged products (**14ata** and **14atb**) were obtained exclusively, with no observable amount of the unrearranged product (**14au**, Scheme 4.2.3.). These rearranged products were obtained as an inseparable mixture, in an approximately 3:1 ratio and isolated in 43% yield. As previously discussed in Section 3.3.7.2., the rearranged products likely arise from an alkyl radical intermediate, however rearrangement via an organomanganese reagent cannot be ruled out.[45] Additionally, it was shown in Section 3.3.7.3. that organomanganese formation from the alkyl halide electrophile is possible under these conditions.

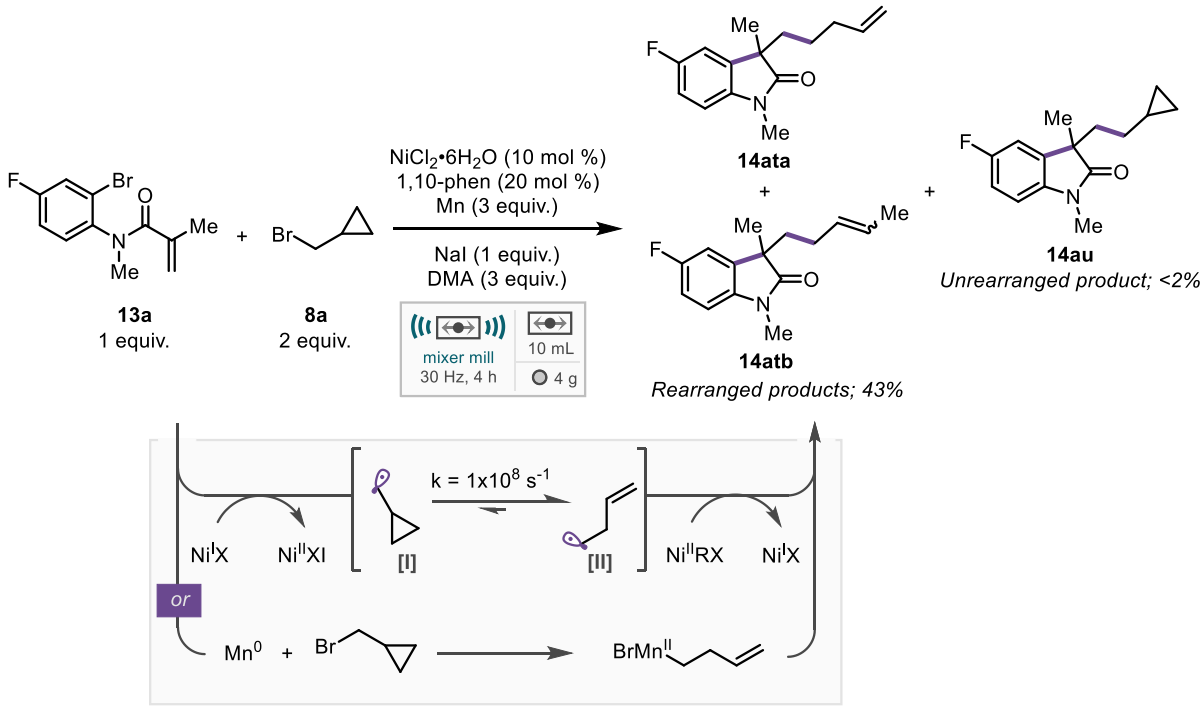

Scheme 4.2.3. Radical clock experiment.

4.2.8.3. Radical Trapping Experiments

Radical trapping experiments were carried out to potentially intercept any radical intermediates present, using 2,2,6,6-tetramethylpiperidine 1-oxyl (TEMPO) and butylated hydroxytoluene (BHT) as the radical inhibitors. 2 equivalents of each radical trap were added to the model reaction system, which resulted in no product formation when TEMPO was used, which could suggest that radical intermediates were intercepted by TEMPO, nullifying effective reactivity (Scheme 4.2.4.). However, adducts resulting from TEMPO intercepting radical intermediates were not detected by either NMR or mass spectrometry. When BHT was used, the product was obtained in 45% yield by NMR analysis, which could suggest suppression of radical intermediates, however, changes in the rheology and jar filling cannot be ruled out as causes for the reduced yield in both instances.

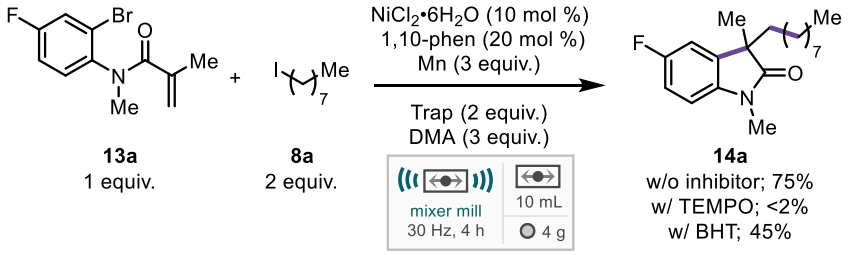

Scheme 4.2.4. Radical trapping experiments using TEMPO and BHT.

4.2.8.4. Proposed Mechanism

With all the results obtained during the mechanistic studies, two distinct mechanistic pathways can be proposed, involving either an alkyl radical formed from an SET event or via an *in situ* generated organomanganese reagent (Scheme 4.2.5.). While it is not possible to unambiguously rule out either mechanism, some of the results thus far suggest that one mechanistic pathway may dominate in a particular circumstance. For example, the exclusive formation of the rearranged products during the radical clock experiment suggests that the pathway involving a radical intermediate may predominate for alkyl halide electrophiles (*cf.* Section 4.2.8.2.). The success from employing bromobenzene as the second electrophile, albeit in low yield, suggests that

the organomanganese pathway could predominate for these sp^2 hybridised electrophiles (*cf.* Section 4.2.2.). However, solution-phase reports utilising sp^2 electrophiles, such as aryl halides, suggest that neither radical nor organometallic intermediates are present in the reaction mechanism.[25] The single-electron process is postulated to occur between the reductant and a nickel (II) species (*cf* Scheme 4.4.). Although there is little experimental evidence to support this.

4.3. Conclusions and Future Work

In conclusion, a mechanochemical protocol for the intramolecular difunctionalisation of alkenes has been developed. This process allows for facile construction of heterocyclic rings, namely 3,3-disubstituted oxindoles, with a broad range of acrylamide tethered aryl halides and alkyl halide coupling partners tolerated. This process is amenable to scale up, yielding over 1.5 grams of product, and it was shown that enantioinduction is possible by utilising a chiral ligand. The mechanochemical process has several key benefits over solution-phase examples, such as shorter reaction times, no requirement for an inert atmosphere, the use of DMA in only liquid-assisted grinding quantities, and the circumvention of terminal reductant (manganese) activation. These benefits were accentuated when carrying out solution-phase comparisons, which were sluggish and could be aided by mechanical grinding of the manganese metal prior to the reaction. Additionally, mechanistic studies permitted the proposal of two mechanistic pathways involving either an alkyl radical intermediate or an *in situ* generated organomanganese reagent.

Future work could involve further exploration of the mechanochemical activation of zero-valent metals and their application to organic synthesis, such as the use of zinc and 1,10-phenanthroline as a single-electron reducing agent.[46] Additionally, it could be of interest to utilise the alkene difunctionalisation protocol and apply this to more challenging systems, for example poorly soluble substrates or substrates that are unreactive in solution-phase processes, such as aryl and alkyl chlorides. Also of interest is further investigation into scaling up the process by TSE, using the preliminary extrusion experiment as a starting point.

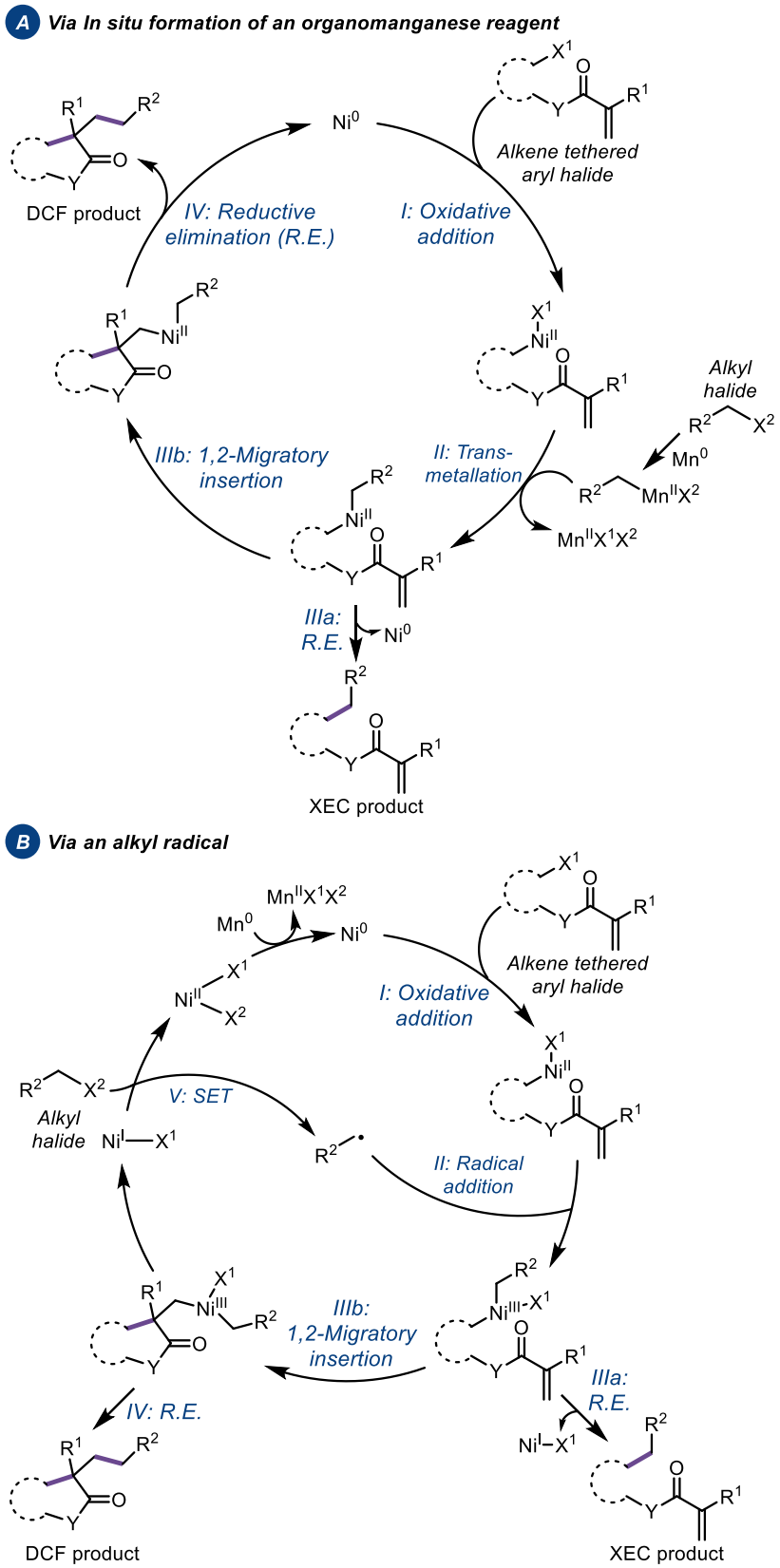

Scheme 4.2.5. Plausible reaction pathways, A) via an *in situ* generated organomanganese reagent; B) via an alkyl radical intermediate.

4.4. Bibliography

1 J. S. Zhang, L. Liu, T. Chen and L. B. Han, *Chem. Asian J.*, 2018, **13**, 2277–2291.

2 R. K. Dhungana, K. C. Shekhar, P. Basnet and R. Giri, *Chem. Rec.*, 2018, **18**, 1314–1340.

3 J. Derosa, O. Apolinar, T. Kang, V. T. Tran and K. M. Engle, *Chem. Sci.*, 2020, **11**, 4287–4296.

4 K. E. Poremba, S. E. Dibrell and S. E. Reisman, *ACS Catal.*, 2020, **10**, 8237–8246.

5 A. Vaupel and P. Knochel, *J. Org. Chem.*, 1996, **61**, 5743–5753.

6 J. W. Gu, Q. Q. Min, L. C. Yu and X. Zhang, *Angew. Chem. Int. Ed.*, 2016, **55**, 12270–12274.

7 T. Qin, J. Cornella, C. Li, L. R. Malins, J. T. Edwards, S. Kawamura, B. D. Maxwell, M. D. Eastgate and P. S. Baran, *Science*, 2016, **352**, 801–805.

8 S. Maiti, J. H. Rhlee and S. Maiti, *Chem. Commun.*, 2021, **57**, 11346–11349.

9 L. Zhu, X. Meng, L. Xie, Q. Shen, W.-Y. Li, L. Zhang and C. Wang, *Org. Chem. Front.*, 2022, **9**, 3068–3074.

10 V. B. Phapale, E. Buñuel, M. García-Iglesias and D. J. Cárdenas, *Angew. Chem. Int. Ed.*, 2007, **46**, 8790–8795.

11 A. García-Domínguez, Z. Li and C. Nevado, *J. Am. Chem. Soc.*, 2017, **139**, 6835–6838.

12 W. Shu, A. García-Domínguez, M. T. Quirós, R. Mondal, D. J. Cárdenas and C. Nevado, *J. Am. Chem. Soc.*, 2019, **141**, 13812–13821.

13 X. Qi and T. Diao, *ACS Catal.*, 2020, **10**, 8542–8556.

14 Y. C. Luo, C. Xu and X. Zhang, *Chinese J. Chem.*, 2020, **38**, 1371–1394.

15 X. X. Wang, X. Lu, Y. Li, J. W. Wang and Y. Fu, *Sci. China Chem.*, 2020, **63**, 1586–1600.

16 Z. Q. Li, O. Apolinar, R. Deng and K. M. Engle, *Chem. Sci.*, 2021, **12**, 11038–11044.

17 Z. Zhang, S. Bera, C. Fan and X. Hu, *J. Am. Chem. Soc.*, 2022, **144**, 7015–7029.

18 L. M. Yin, M. C. Sun, X. J. Si, D. Yang, M. P. Song and J. L. Niu, *Org. Lett.*, 2022, **24**, 1083–1087.

19 H. Lv, H. Kang, B. Zhou, X. Xue, K. M. Engle and D. Zhao, *Nat. Commun.*, 2019, **10**, 5025.

20 F. Wang, D. Wang, X. Mu, P. Chen and G. Liu, *J. Am. Chem. Soc.*, 2014, **136**, 10202–10205.

21 L. Wu, F. Wang, X. Wan, D. Wang, P. Chen and G. Liu, *J. Am. Chem. Soc.*, 2017, **139**, 2904–2907.

22 L. Liao, R. Jana, K. B. Urkalan and M. S. Sigman, *J. Am. Chem. Soc.*, 2011, **133**, 5784–5787.

23 Z. Liu, T. Zeng, K. S. Yang and K. M. Engle, *J. Am. Chem. Soc.*, 2016, **138**, 15122–15125.

24 K. B. Urkalan and M. S. Sigman, *Angew. Chem. Int. Ed.*, 2009, **48**, 3146–3149.

25 K. Wang, Z. DIng, Z. Zhou and W. Kong, *J. Am. Chem. Soc.*, 2018, **140**, 12364–12368.

26 D. J. Triggle, J. M. Mitchell and R. Filler, *CNS Drug Rev.*, 1998, **4**, 87–136.

27 Y. Kamano, H. ping Zhang, Y. Ichihara, H. Kizu, K. Komiyama and G. R. Pettit, *Tetrahedron Lett.*, 1995, **36**, 2783–2784.

28 C. Schumacher, J. G. Hernández and C. Bolm, *Angew. Chem. Int. Ed.*, 2020, **59**, 16357–16360.

29 H. Lv, X. Xu, J. Li, X. Huang, G. Fang and L. Zheng, *Angew. Chem. Int. Ed.*, 2022, **61**, e202206420.

30 K. Fang, W. Huang, C. Shan, J. Qu and Y. Chen, *Org. Lett.*, 2021, **23**, 5523–5527.

31 X. Wu, B. Luan, W. Zhao, F. He, X.-Y. Wu, J. Qu and Y. Chen, *Angew. Chem. Int. Ed.*, 2022, **61**, e202111598.

32 Y. Li, Z. Ding, A. Lei and W. Kong, *Org. Chem. Front.*, 2019, **6**, 3305–3309.

33 T. Ma, Y. Chen, Y. Li, Y. Ping and W. Kong, *ACS Catal.*, 2019, **9**, 9127–9133.

34 J. Wu and C. Wang, *Org. Lett.*, 2021, **23**, 6407–6411.

35 Y. Feng, S. Zhao, G. Du, S. Zhang, D. Zhang, H. Liu, X. Li, Y. Dong and F. G. Sun, *Org. Chem. Front.*, 2021, **8**, 1149–1154.

36 H. Li, J. Chen, J. Dong and W. Kong, *Org. Lett.*, 2021, **23**, 6466–6470.

37 K. H. Min, N. Iqbal and E. J. Cho, *Org. Lett.*, 2022, **24**, 989–994.

38 Y. Jin and C. Wang, *Angew. Chem. Int. Ed.*, 2019, **58**, 6722–6726.

39 T. Y. Zhao, L. J. Xiao and Q. L. Zhou, *Angew. Chem. Int. Ed.*, 2022, **61**, e202115702.

40 J. B. Qiao, Y. Q. Zhang, Q. W. Yao, Z. Z. Zhao, X. Peng and X. Z. Shu, *J. Am. Chem. Soc.*, 2021, **143**, 12961–12967.

41 R. Schmidt, C. F. Burmeister, M. Baláž, A. Kwade and A. Stolle, *Org. Process Res. Dev.*, 2015, **19**, 427–436.

42 H. Kulla, F. Fischer, S. Benemann, K. Rademann and F. Emmerling, *CrystEngComm*, 2017, **19**, 3902–3907.

43 A. C. Jones, W. I. Nicholson, J. A. Leitch and D. L. Browne, *Org. Lett.*, 2021, **23**, 6337–6341.

44 W. I. Nicholson, F. Barreteau, J. A. Leitch, R. Payne, I. Priestley, E. Godineau, C. Battilocchio and D. L. Browne, *Angew. Chem. Int. Ed.*, 2021, **60**, 21868–21874.

45 A. Guijarro, D. M. Rosenberg and R. D. Rieke, *J. Am. Chem. Soc.*, 1999, **121**, 4155–4167.

46 M. Nambo, Y. Tahara, J. C. H. Yim, D. Yokogawa and C. M. Crudden, *Chem. Sci.*, 2021, **12**, 4866–4871.

Chapter 5: Experimental Procedures and Characterisation Data

5.1. General Information

Unless otherwise stated, all reagents were purchased from commercial sources and used without further purification.

Room temperature (rt) refers to 20 – 25 °C. Ice/water baths were used to obtain temperatures of 0 °C. All reactions involving heating were carried out using DrySyn blocks and a contact thermometer.

Analytical thin layer chromatography (TLC) was carried out using aluminium plates coated with silica (Kieselgel 60 F_{254} silica) and visualization was achieved using ultraviolet light (254 nm), followed by staining with a 1% aqueous $KMnO_4$ solution, unless otherwise stated. Flash column chromatography (FCC) used Kieselgel 60 silica in the solvent system stated. The petroleum ether (PE) utilised was in the 40 – 60 °C boiling range and the hexane used was HPLC grade (>95%).

Melting points (mp) were recorded on a Gallenkamp melting point apparatus and are reported corrected by linear calibration to benzophenone (47 – 49 °C) and benzoic acid (121 – 123 °C).

Infrared spectra were recorded on a Shimadzu IRAffinity-1 Fourier Transform ATIR spectrometer as thin films using a Pike MIRacle ATR accessory, with absorbance peaks quoted (v_{max}/cm^{-1}).

^{1}H, ^{13}C, ^{19}F NMR spectra were obtained on a Bruker Avance 300 (300 MHz ^{1}H, 75 MHz ^{13}C, 282 MHz ^{19}F), a Bruker Avance 400 (400 MHz ^{1}H, 101 MHz ^{13}C, 376 MHz ^{19}F) or a Bruker Avance 500 (500 MHz ^{1}H, 126 MHz ^{13}C, 471 MHz ^{19}F) spectrometer at rt in the solvent stated. ^{13}C experiments were run as attached proton tests (APT), where CH's and CH_3's are in positive mode and C's and CH_2's are in negative mode. Chemical shifts are reported in parts per million (ppm) relative to the residual solvent signal. All coupling constants, *J*, are quoted in Hertz (Hz). Multiplicities are reported based on their apparent appearance, with the following symbols: s = singlet, d = doublet, t = triplet, q = quartet, m = multiplet and multiples thereof. The notation br describes a broad signal. NMR assignments are given for representative compounds within a series.

High resolution mass spectral (HRMS) data were obtained on a Waters MALDI-TOF mx in Cardiff University.

The ball mill used was either an In Solido Technologies (IST) 500 mixer-mill or a Retsch Mixer Mill 400. Reactions were carried out using stainless steel milling jars and grinding balls. The maximum time these mixer-mills can be set to is 99 minutes, therefore, for reactions longer than this the milling was resumed until the desired time had elapsed.

Heated ball-mill experiments were carried out using a PID-controlled heating device, equipped with aluminium heating bands.

The planetary ball-mill used was a Fritsch Planetary Micro Mill model “Pulverisette 7” using 12 mL zirconium oxide grinding bowls containing 3 g, 10 mm ceramic grinding balls. The grinding cycle was set to 15 minutes and to alternate direction between cycles after a 1 minute pause, unless stated otherwise. The planetary mill was set to repeat these cycles until the reaction time had been reached.

Optical rotation measurements were taken on a Bellingham and Stanley ADP410 polarimeter at ambient temperature, using a LED light source filtered to 589.3 nm (sodium D-line) and are reported in concentrations of g/100 mL.

High-performance liquid chromatography (HPLC) analysis was conducted using either a Gilson HPLC consisting of a Gilson 305 pump, Gilson 306 pump, Gilson 811C dynamic mixer, Gilson 805 manometric module, Gilson 401C dilutor, Gilson 213XL sample injector and a Gilson 118 UV/vis detector, or a Shimadzu LC-10 AD coupled diode array-detector SPD-MA-10A-VP. A Daicel Chiralpak® column was used as the stationary phase.

The large-scale extrusion experiment was carried out using a Thermo Scientific™ Process 11 Twin-screw Extruder (TSE) with 7 controllable heating sections.

5.2. Mechanochemical Aza-Morita-Baylis-Hillman Reaction

5.2.1. Experimental and Characterization Data

5.2.2. Synthesis of Starting Materials

5.2.2.1. General Procedure A – Synthesis of Aldimines

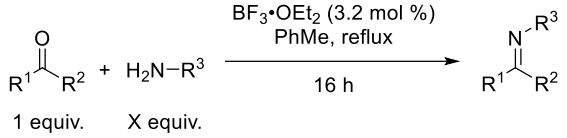

To a round-bottomed flask, equipped with a magnetic stirrer bar, was charged the appropriate aldehyde (1 equiv.) and amine (1 or 1.1 equiv.). Toluene (0.4 M) was added, followed by $BF_3.OEt_2$ (3.2 mol %). The flask was equipped with a Dean-Stark and condenser and heated to reflux for 16 hours. After this time had elapsed, the reaction mixture was allowed to cool to room temperature, where a precipitate formed which was collected by filtration. If no precipitate was formed upon cooling to room temperature, hexane was added, and the mixture was cooled to -20 °C to facilitate precipitation. The solid was then recrystallised from the stated solvent/solvent mixture.

***N*-benzylidene-4-methylbenzenesulfonamide (3a)**

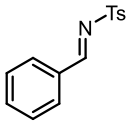

Prepared according to general procedure A from benzaldehyde (25 mmol) and 4-methylbenzenesulfonamide (25 mmol), followed by recrystallisation from 1:1 EtOAc/hexane to give the title compound as a white solid (3.84 g, 59%), with physical properties and spectroscopic data in accordance with the literature;[1] **R_f** = 0.49 (1.5:8.5 EtOAc/PE); **mp** 120 – 122 °C; **^{1}H NMR** (500 MHz, $CDCl_3$) δ_H: 9.03 (s, 1H, *H*C=N), 7.94 – 7.92 (m, 2H, Ph*H*), 7.91 – 7.88 (m, 2H, Ts*H*), 7.63 – 7.59 (m, 1H, Ph*H*), 7.51 – 7.46 (m, 2H, Ph*H*), 7.36 – 7.33 (m, 2H, Ts*H*), 2.44 (s, 3H, ArCH_3); **^{13}C {^{1}H} NMR** (101 MHz, $CDCl_3$) δ_C: 170.3 (*C*=N), 144.8 (Ar*C*), 135.3 (Ar*C*H), 135.1 (Ar*C*), 132.5 (Ar*C*H), 131.5 (Ar*C*H), 130.0 (Ar*C*H), 129.3 (Ar*C*H), 128.2 (Ar*C*H), 21.8 (Ar*C*H_3).

_N_-(4-fluorobenzylidene)-4-methylbenzenesulfonamide (3b)

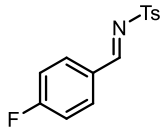

Prepared according to general procedure A from 4-fluorobenzaldehyde (10 mmol) and 4-methylbenzenesulfonamide (10 mmol), followed by recrystallisation from 2:2:1 EtOAc/hexane/toluene to give the title compound as a white solid (1.36 g, 49%) with physical and spectroscopic data in accordance with the literature;[1] **R_f** = 0.45 (1.5:8.5 EtOAc/PE); **mp** 126 – 118 °C; **^{1}H NMR** (500 MHz, $CDCl_3$) δ_H: 8.99 (s, 1H), 7.99 – 7.93 (m, 2H), 7.91 – 7.86 (m, 2H), 7.38 – 7.33 (m, 2H), 7.21 – 7.13 (m, 2H), 2.44 (s, 3H); **^{13}C {^{1}H} NMR** (101 MHz, $CDCl_3$) δ_C: 168.7, 167.0 (d, *J* = 259.6), 144.8, 135.2, 133.9 (d, *J* = 9.1), 130.0, 128.9 (d, *J* = 3.0), 128.3, 116.8 (d, *J* = 23.2), 21.80; **^{19}F {^{1}H} NMR** (376 MHz, $CDCl_3$) δ_F: -101.1.

_N_-(4-chlorobenzylidene)-4-methylbenzenesulfonamide (3c)

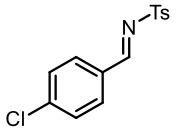

Prepared according to general procedure A from 4-chlorobenzaldehyde (10 mmol) and 4-methylbenzenesulfonamide (10 mmol), followed by recrystallisation from 2:2:1 EtOAc/hexane/toluene to give the title compound as a white solid (1.44 g, 49%) with physical and spectroscopic data in accordance with the literature;[1] **R_f** = 0.50 (1.5:8.5 EtOAc/PE); **mp** 185 – 187 °C; **^{1}H NMR** (500 MHz, $CDCl_3$) δ_H: 8.99 (s, 1H), 7.91 – 7.84 (m, 4H), 7.49 – 7.44 (m, 2H), 7.38 – 7.33 (m, 2H), 2.44 (s, 3H); **^{13}C {^{1}H} NMR** (126 MHz, $CDCl_3$) δ_C: 168.8, 144.9, 141.6, 135.1, 132.5, 131.0, 130.0, 129.8, 128.3, 21.8.

_N_-(4-bromobenzylidene)-4-methylbenzenesulfonamide (3d)

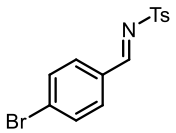

Prepared according to general procedure A from 4-bromobenzaldehyde (5 mmol) and 4-methylbenzenesulfonamide (5 mmol), followed by recrystallisation from 2:2:1 EtOAc/hexane/toluene to give the title compound as a white solid (0.93 g, 55%) with physical and spectroscopic data in accordance with the literature;[1] **R_f** = 0.50 (1.5:8.5

EtOAc/PE); **mp** 201 – 203 °C; **^{1}H NMR** (500 MHz, $CDCl_3$) δ_H: 8.98 (s, 1H), 7.92 – 7.84 (m, 2H), 7.82 – 7.74 (m, 2H), 7.68 – 7.60 (m, 2H), 7.39 – 7.31 (m, 2H), 2.44 (s, 3H); **^{13}C {^{1}H} NMR** (126 MHz, $CDCl_3$) δ_C: 168.9, 145.0, 135.0, 132.8, 132.5, 131.4, 130.4, 130.0, 128.3, 21.8.

***N*-(4-iodobenzylidene)-4-methylbenzenesulfonamide (3e)**

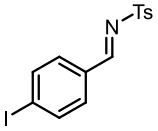

Prepared according to general procedure A from 4-iodobenzaldehyde (10 mmol) and 4-methylbenzenesulfonamide (10 mmol), followed by recrystallisation from 2:2:1 EtOAc/hexane/toluene to give the title compound as a white solid (2.73 g, 71%); **R_f** = 0.48 (1.5:8.5 EtOAc/PE); **mp** 208 – 210 °C; **ν_{max}/cm^{-1}** (film): 1602, 1583, 1552, 1315, 1290, 1278, 1159, 1088, 1051, 1007, 1000, 867, 811, 797, 780, 704, 676, 639; **^{1}H NMR** (400 MHz, $CDCl_3$) δ_H: 8.96 (s, 1H), 7.91 – 7.83 (m, 4H), 7.67 – 7.58 (m, 2H), 7.39 – 7.32 (m, 2H), 2.44 (s, 3H); **^{13}C {^{1}H} NMR** (126 MHz, $CDCl_3$) δ_C: 169.2, 145.0, 138.7, 135.0, 132.3, 131.9, 130.0, 128.3, 103.4, 21.8; **HRMS** (ES) calculated for $[C_{14}H_{13}NO_2SI]^+$ $(M+H)^+$: m/z 385.9713 found 385.9712 (-0.3 ppm).

***N*-([1,1'-biphenyl]-4-ylmethylene)-4-methylbenzenesulfonamide (3f)**

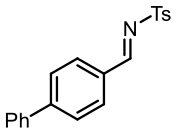

Prepared according to general procedure A from biphenyl-4-carboxaldehyde (11 mmol) and 4-methylbenzenesulfonamide (10 mmol), followed by recrystallisation from 2:2:1 EtOAc/hexane/toluene to give the title compound as a white solid (2.35 g, 70%) with physical and spectroscopic data in accordance with the literature;[2] **R_f** = 0.48 (1:4 EtOAc/PE); **mp** 130 – 132 °C; **^{1}H NMR** (300 MHz, $CDCl_3$) δ_H: 9.07 (s, 1H), 8.00 (d, *J* = 8.2, 2H), 7.95 – 7.86 (m, 2H), 7.71 (d, *J* = 8.2, 2H), 7.66 – 7.59 (m, 2H), 7.52 – 7.40 (m, 3H), 7.36 (d, *J* = 8.1, 2H), 2.44 (s, 3H); **^{13}C {^{1}H} NMR** (126 MHz, $CDCl_3$) δ_C: 169.8, 147.8, 144.7, 139.6, 135.4, 132.0, 131.4, 130.0, 129.2, 128.8, 128.2, 127.9, 127.4, 21.8.

4-methyl-*N*-(4-methylbenzylidene)benzenesulfonamide (3g)

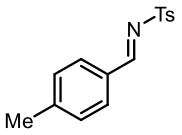

Prepared according to general procedure A from 4-methylbenzaldehyde (10 mmol) and 4-methylbenzenesulfonamide (10 mmol), followed by recrystallisation from 1:1 EtOAc/hexane to give the title compound as a white solid (1.12 g, 41%) with physical and spectroscopic data in accordance with the literature;[1] **R_f** = 0.38 (1:4 EtOAc/PE); **mp** 124 – 126 °C; **^{1}H NMR** (500 MHz, $CDCl_3$) δ_H: 8.99 (s, 1H), 7.91 – 7.86 (m, 2H), 7.85 – 7.79 (m, 2H), 7.37 – 7.32 (m, 2H), 7.31 – 7.27 (m, 2H), 2.44 – 2.42 (m , 6H); **^{13}C {^{1}H} NMR** (126 MHz, $CDCl_3$) δ_C: 170.1, 146.5, 144.6, 135.6, 131.6, 130.1, 130.0, 129.9, 128.2, 22.1, 21.8.

4-methyl-*N*-(4-nitrobenzylidene)benzenesulfonamide (3h)

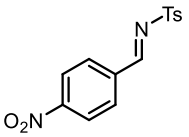

Prepared according to general procedure A from 4-nitrobenzaldehyde (25 mmol) and 4-methylbenzenesulfonamide (25 mmol), followed by recrystallisation from toluene to give the title compound as a beige solid (2.45 g, 32%), with physical properties and spectroscopic data in accordance with the literature;[1] **R_f** = 0.56 (1.5:8.5 EtOAc/PE); **mp** 215 - 217 °C; **^{1}H NMR** (500 MHz, $CDCl_3$) δ_H: 9.10 (s, 1H), 8.37 – 8.28 (m, 2H), 8.14 – 8.07 (m, 2H), 7.93 – 7.87 (m, 2H), 7.41 – 7.34 (m, 2H), 2.46 (s, 3H); **^{13}C {^{1}H} NMR** (101 MHz, $CDCl_3$) δ_C: 167.4, 151.3, 145.5, 137.6, 134.3, 132.0, 130.2, 128.6, 124.3, 21.9.

***N*-(4-cyanobenzylidene)-4-methylbenzenesulfonamide (3i)**

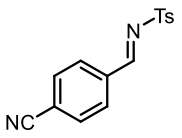

Prepared according to general procedure A from 4-cyanobenzaldehyde (11 mmol) and 4-methylbenzenesulfonamide (10 mmol), followed by recrystallisation from 1:1 EtOAc/hexane to give the title compound as a white solid (2.02 g, 71%) with physical and spectroscopic data in accordance with the literature;[1] **R_f** = 0.48 (1:4 EtOAc/PE);

mp 189 – 191 °C; **^{1}H NMR** (500 MHz, $CDCl_3$) δ_H: 9.05 (s, 1H), 8.06 – 8.00 (m, 2H), 7.92 – 7.86 (m, 2H), 7.81 – 7.75 (m, 2H), 7.40 – 7.34 (m, 2H), 2.45 (s, 3H); **^{13}C {^{1}H} NMR** (126 MHz, $CDCl_3$) δ_C: 167.9, 145.4, 136.1, 134.4, 132.9, 131.4, 130.1, 128.5, 117.8 (2C), 21.9.

4-methyl-*N*-(4-(trifluoromethyl)benzylidene)benzenesulfonamide (3j)

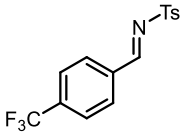

Prepared according to general procedure A from 4-(trifluoromethyl)benzaldehyde (10 mmol) and 4-methylbenzenesulfonamide (10 mmol), followed by recrystallisation from EtOAc to give the title compound as a white solid (0.24 g, 7%) with physical and spectroscopic data in accordance with the literature;[3] **R_f** = 0.50 (1:4 EtOAc/PE); **mp** 168 – 170 °C; **^{1}H NMR** (500 MHz, $CDCl_3$) δ_H: 9.07 (s, 1H), 8.05 (d, *J* = 8.0, 2H), 7.92 – 7.88 (m, 2H), 7.75 (d, *J* = 8.0, 2H), 7.39 – 7.35 (m, 2H), 2.45 (s, 3H); **^{13}C {^{1}H} NMR** (126 MHz, $CDCl_3$) δ_C: 168.5, 145.2, 136.0 (q, *J* = 40.3), 135.5, 134.7, 131.5, 130.1, 128.4, 126.3 (q, *J* = 3.8), 123.5 (q, *J* = 274.7), 21.9; **^{19}F {^{1}H} NMR** (376 MHz, $CDCl_3$) δ_F: -63.3.

Methyl-4-((tosylimino)methyl)benzoate (3k)

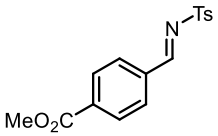

Prepared according to general procedure A from methyl-4-formylbenzoate (11 mmol) and 4-methylbenzenesulfonamide (10 mmol), followed by recrystallisation from toluene to give the title compound as a white solid (2.27 g, 72%) with physical and spectroscopic data in accordance with the literature;[4] **R_f** = 0.23 (1:4 EtOAc/PE); **mp** 191 – 192 °C; **^{1}H NMR** (500 MHz, $CDCl_3$) δ_H: 9.06 (s, 1H), 8.18 – 8.07 (m, 2H), 8.01 – 7.96 (m, 2H), 7.92 – 7.87 (m, 2H), 7.38 – 7.33 (m, 2H), 3.95 (s, 3H), 2.45 (s, 3H); **^{13}C {^{1}H} NMR** (126 MHz, $CDCl_3$) δ_C: 169.0, 166.0, 145.1, 136.0, 135.5, 134.8, 131.2, 130.3, 130.1, 128.4, 52.6, 21.8.

_N_-(4-methoxybenzylidene)-4-methylbenzenesulfonamide (3l)

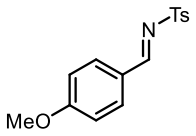

Prepared according to general procedure A from 4-methoxybenzaldehyde (20 mmol) and 4-methylbenzenesulfonamide (20 mmol), following by recrystallisation from 1:1 EtOAc/hexane to give the title compound as a white solid (3.02 g, 52%), with physical properties and spectroscopic data in accordance with the literature;[1] **R_f** = 0.47 (0.5:9.5 Acetone/Toluene); **mp** 123 - 125 °C; **^{1}H NMR** (400 MHz, $CDCl_3$) δ_H: 8.94 (s, 1H), 7.92 – 7.84 (m, 4H), 7.36 – 7.30 (m, 2H), 7.00 – 6.92 (m, 2H), 3.88 (s, 3H), 2.43 (s, 3H); **^{13}C {^{1}H} NMR** (126 MHz, $CDCl_3$) δ_C: 169.3, 165.4, 144.4, 135.9, 134.4, 129.9, 128.1, 125.4, 114.8, 55.8, 21.8.

_N_-(4-(dimethylamino)benzylidene)-4-methylbenzenesulfonamide (3m)

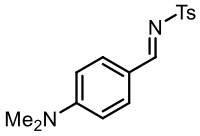

Prepared according to general procedure A from 4-(dimethylamino)benzaldehyde (5.5 mmol) and 4-methylbenzenesulfonamide (5 mmol), with no further purification required to give the title compound as a yellow solid (1.32 g, 87%), with physical and spectroscopic data in accordance with the literature;[1] **R_f** = 0.38 (1:4 EtOAc/PE); **mp** 183 – 185 °C; **^{1}H NMR** (300 MHz, $CDCl_3$) δ_H: 8.82 (s, 1H), 7.89 – 7.82 (m, 2H), 7.80 – 7.74 (m, 2H), 7.34 – 7.27 (m, 2H), 6.70 – 6.61 (m, 2H), 3.10 (s, 6H), 2.41 (s, 3H); **^{13}C {^{1}H} NMR** (126 MHz, $CDCl_3$) δ_C: 169.2, 155.0, 143.7, 137.0, 134.1, 129.7, 127.7, 120.1, 111.5, 40.3, 21.7.

_N_-(3-fluorobenzylidene)-4-methylbenzenesulfonamide (3n)

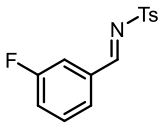

Prepared according to general procedure A from 3-fluorobenzaldehyde (11 mmol) and 4-methylbenzenesulfonamide (10 mmol), with no further purification required to give the title compound as a white solid (1.00 g, 36%), with physical and spectroscopic data in accordance with the literature;[3] **R_f** = 0.45 (1:4 EtOAc/PE); **mp** 103 – 105 °C; **^{1}H**

NMR (500 MHz, $CDCl_3$) δ_H: 9.00 (d, *J* = 1.3, 1H), 7.92 – 7.87 (m, 2H), 7.70 – 7.63 (m, 2H), 7.51 – 7.45 (m, 1H), 7.38 – 7.34 (m, 2H), 7.33 – 7.29 (m, 1H), 2.45 (s, 3H); **^{13}C {^{1}H} NMR** (126 MHz, $CDCl_3$) δ_C: 168.8 (d, *J* = 2.5), 163.0 *(J* = 249.5)*,* 145.0, 134.9, 134.7 (d, *J* = 7.6), 131.0 (d, *J* = 7.6), 130.0, 128.3, 128.0 (d, *J* = 3.8), 122.1 (d, *J* = 21.4), 116.8 (d, *J* = 21.4), 21.8; **^{19}F {^{1}H} NMR** (376 MHz, $CDCl_3$) δ_F: -110.9.

_N_-(3-chlorobenzylidene)-4-methylbenzenesulfonamide (3o)

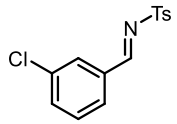

Prepared according to general procedure A from 3-chlorobenzaldehyde (11 mmol) and 4-methylbenzenesulfonamide (10 mmol), followed by recrystallisation from 1:1 EtOAc/hexane to give the title compound as a white solid (0.57 g, 19%) with physical and spectroscopic data in accordance with the literature;[5] **R_f** = 0.32 (1:4 EtOAc/PE); **mp** 96 – 98 °C; **^{1}H NMR** (300 MHz, $CDCl_3$) δ_H: 8.98 (s, 1H), 7.96 – 7.93 (m, 1H), 7.89 (d, *J* = 8.3, 2H), 7.82 – 7.73 (m, 1H), 7.62 – 7.52 (m, 1H), 7.44 (t, *J* = 7.8, 1H), 7.36 (d, *J* = 8.0, 2H), 2.45 (s, 3H); **^{13}C {^{1}H} NMR** (126 MHz, $CDCl_3$) δ_C: 168.7, 145.1, 135.6, 134.9, 134.8, 134.2, 130.6, 130.4, 130.0, 129.9, 128.4, 21.8.

4-methyl-_N_-(3-methylbenzylidene)benzenesulfonamide (3p)

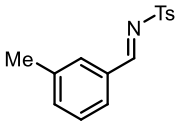

Prepared according to general procedure A from 3-methylbenzaldehyde (10 mmol) and 4-methylbenzenesulfonamide (10 mmol), followed by recrystallisation from 1:1 EtOAc/hexane to give the title compound as a white solid (0.98 g, 36%) with physical and spectroscopic data in accordance with the literature;[1] **R_f** = 0.50 (1.5:8.5 EtOAc/PE); **mp** 98 – 100 °C; **^{1}H NMR** (500 MHz, $CDCl_3$) δ_H: 9.00 (s, 1H), 7.90 – 7.87 (m, 2H), 7.76 (s, 1H), 7.73 – 7.68 (m, 1H), 7.44 – 7.41 (m, 1H), 7.39 – 7.33 (m, 3H), 2.44 (s, 3H), 2.39 (s, 3H); **^{13}C {^{1}H} NMR** (126 MHz, $CDCl_3$) δ_C: 170.5, 144.7, 139.3, 136.0, 135.4, 132.5, 131.5, 129.9, 129.2 (2C), 128.2, 21.8, 21.3.

_N_-(2-fluorobenzylidene)-4-methylbenzenesulfonamide (3q)

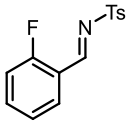

Prepared according to general procedure A from 2-fluorobenzaldehyde (11 mmol) and 4-methylbenzenesulfonamide (10 mmol), followed by recrystallisation from 2:2:1 EtOAc/hexane/toluene to give the title compound as a white solid (1.93 g, 70%) with physical and spectroscopic data in accordance with the literature;[3] **R_f** = 0.30 (1:4 EtOAc/PE); **mp** 147 – 149 °C; **^{1}H NMR** (500 MHz, $CDCl_3$) δ_H: 9.36 (s, 1H), 8.09 – 8.06 (m, 1H), 7.91 – 7.87 (m, 2H), 7.63 – 7.58 (m, 1H), 7.39 – 7.33 (m, 2H), 7.25 – 7.21 (m, 1H), 7.19 – 7.15 (m, 1H), 2.44 (s, 3H); **^{13}C {^{1}H} NMR** (126 MHz, $CDCl_3$) δ_C: 164.5 (d, *J* = 260.8), 163.8 (d, *J* = 6.3), 144.9, 137.1 (d, *J* = 10.1), 135.0, 130.0, 129.5 (d, *J* = 1.3), 128.4, 125.0 (d, *J* = 3.8), 120.7 (d, *J* = 8.8), 116.5 (d, *J* = 21.4), 21.8; **^{19}F {^{1}H} NMR** (376 MHz, $CDCl_3$) δ_F: -116.1.

_N_-(2-chlorobenzylidene)-4-methylbenzenesulfonamide (3r)

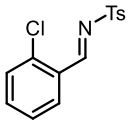

Prepared according to general procedure A from 2-chlorobenzaldehyde (10 mmol) and 4-methylbenzenesulfonamide (10 mmol), followed by recrystallisation from 1:1 EtOAc/hexane to give the title compound as a white solid (1.03 g, 35%) with physical and spectroscopic data in accordance with the literature;[6] **R_f** = 0.32 (1:4 EtOAc/PE); **mp** 145 – 147 °C; **^{1}H NMR** (300 MHz, $CDCl_3$) δ_H: 9.50 (s, 1H), 8.16 (d, *J* = 9.0, 1H), 7.95 – 7.86 (m, 2H), 7.56 – 7.45 (m, 2H), 7.38 – 7.31 (m, 3H), 2.45 (s, 3H); **^{13}C {^{1}H} NMR** (126 MHz, $CDCl_3$) δ_C: 166.9, 145.0, 139.1, 135.8, 134.9, 130.6, 130.4, 130.0 (2C), 128.4, 127.5, 21.8.

4-methyl-_N_-(2-methylbenzylidene)benzenesulfonamide (3s)

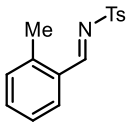

Prepared according to general procedure A from 2-tolualdehyde (10 mmol) and 4-methylbenzenesulfonamide (10 mmol), followed by recrystallisation from 1:1

EtOAc/hexane to give the title compound as a white solid (0.38 g, 14%) with physical and spectroscopic data in accordance with the literature;[1] **R_f** = 0.55 (1:4 EtOAc/PE); **mp** 104 – 106 °C; **^{1}H NMR** (500 MHz, $CDCl_3$) δ_H: 9.34 (s, 1H), 8.01 (dd, *J* = 7.8, 1.5, 1H), 7.93 – 7.87 (m, 2H), 7.47 (td, *J* = 7.5, 1.5, 1H), 7.38 – 7.32 (m, 2H), 7.30 – 7.25 (m, 2H), 2.61 (s, 3H), 2.44 (s, 3H); **^{13}C {^{1}H} NMR** (126 MHz, $CDCl_3$) δ_C: 168.8, 144.6, 142.4, 135.6, 134.7, 131.7, 130.8, 130.6, 129.9, 128.2, 126.8, 21.8, 19.8.

4-methyl-*N*-(2,4,6-trimethylbenzylidene)benzenesulfonamide (3t)

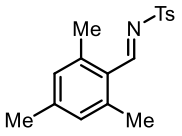

Prepared according to general procedure A from 2,4,6-trimethylbenzaldehyde (11 mmol) and 4-methylbenzenesulfonamide (10 mmol), followed by recrystallisation from 2:2:1 EtOAc/hexane/toluene to give the title compound as a white solid (1.78 g, 59%) with physical and spectroscopic data in accordance with the literature;[7] **R_f** = 0.48 (1.5:8.5 EtOAc/PE); **mp** 112 – 114 °C; **^{1}H NMR** (300 MHz, $CDCl_3$) δ_H: 9.46 (s, 1H), 7.92 – 7.85 (m, 2H), 7.37 – 7.29 (m, 2H), 6.92 (s, 2H), 2.53 (s, 6H), 2.43 (s, 3H), 2.31 (s, 3H); **^{13}C {^{1}H} NMR** (126 MHz, $CDCl_3$) δ_C: 169.2, 144.8, 144.3, 143.1, 136.2, 130.8, 129.9, 128.0, 126.3, 21.9, 21.8, 21.7.

4-methyl-*N*-((perfluorophenyl)methylene)benzenesulfonamide (3u)

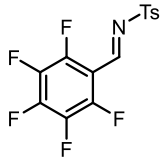

Prepared according to general procedure A from pentafluorobenzaldehyde (11 mmol) and 4-methylbenzenesulfonamide (10 mmol), followed by recrystallisation from 2:2:1 EtOAc/hexane/toluene to give the title compound as a white solid (2.20 g, 63%) with physical and spectroscopic data in accordance with the literature;[8] **R_f** = 0.45 (1:4 EtOAc/PE); **mp** 139 – 141 °C; **^{1}H NMR** (400 MHz, $CDCl_3$) δ_H: 9.21 (s, 1H), 7.89 (d, *J* = 8.0, 2H), 7.37 (d, *J* = 8.0, 2H), 2.46 (s, 3H); **^{13}C {^{1}H} NMR** (101 MHz, $CDCl_3$) δ_C: 158.7, 145.6, 134.0, 130.2, 128.6, 21.9 (unidentifiable signals between 135 – 150 ppm, due to broadening from multiple ^{13}C-^{19}F couplings); **^{19}F {^{1}H} NMR** (376 MHz, $CDCl_3$) δ_F: -135.59 – -136.09 (m), -142.16 – -142.33 (m), -159.34 – -159.75 (m).

_N_-(2-hydroxybenzylidene)-4-methylbenzenesulfonamide (3v)

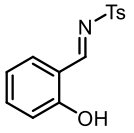

Prepared according to general procedure A from 2-hydroxybenzaldehyde (11 mmol) and 4-methylbenzenesulfonamide (10 mmol), with no further purification required to give the title compound as a pink solid (2.39 g, 87%), with physical and spectroscopic data in accordance with the literature;[9] **R_f** = 0.48 (1:4 EtOAc/PE); **mp** 120 – 122 °C; **ν_{max}/cm^{-1}** (film): 3052, 1623, 1594, 1556, 1489, 1457, 1362, 1318, 1303, 1273, 1153, 1084, 903, 845, 816, 701, 624, 569; **^{1}H NMR** (500 MHz, $CDCl_3$) δ_H: 10.82 (s, 1H), 9.09 (s, 1H), 7.91 – 7.82 (m, 2H), 7.54 – 7.48 (m, 2H), 7.37 – 7.34 (m, 2H), 7.03 – 6.99 (m, 2H), 2.44 (s, 3H); **^{13}C {^{1}H} NMR** (101 MHz, $CDCl_3$) δ_C: 171.6, 162.3, 145.2, 137.5, 135.6, 135.2, 130.2, 128.1, 120.4, 118.1, 116.8, 21.8; **HRMS** (ES) calculated for $[C_{14}H_{14}NO_3S]^+$ $(M+H)^+$: m/z 276.0683 found 276.0694 (-4.0 ppm).

4-methyl-_N_-(naphthalen-1-ylmethylene)benzenesulfonamide (3w)

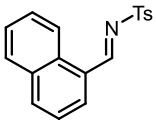

Prepared according to general procedure A from 1-naphthaldehyde (11 mmol) and 4-methylbenzenesulfonamide (10 mmol), followed by recrystallisation from 2:1 EtOAc/toluene to give the title compound as a pale yellow solid (2.22 g, 72%) with physical and spectroscopic data in accordance with the literature;[1] **R_f** = 0.33 (1:4 EtOAc/PE); **mp** 143 – 145 °C; **^{1}H NMR** (500 MHz, $CDCl_3$) δ_H: 9.61 (s, 1H), 8.99 (d, *J* = 8.5, 1H), 8.16 (dd, *J* = 7.3, 1.3, 1H), 8.10 (d, *J* = 8.2, 1H), 7.97 – 7.94 (m, 2H), 7.93 – 7.91 (m, 1H), 7.68 (ddd, *J* = 8.5, 6.9, 1.4, 1H), 7.61 – 7.56 (m, 2H), 7.37 – 7.34 (m, 2H), 2.44 (s, 3H); **^{13}C {^{1}H} NMR** (126 MHz, $CDCl_3$) δ_C: 169.9, 144.7, 136.3, 135.6, 135.3, 133.9, 132.0, 130.0, 129.2, 129.1, 128.2, 127.8, 127.1, 125.3, 124.4, 21.8.

4-methyl-*N*-(naphthalen-2-ylmethylene)benzenesulfonamide (3x)

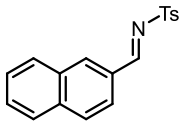

Prepared according to general procedure A from 2-naphthaldehyde (10 mmol) and 4-methylbenzenesulfonamide (10 mmol), followed by recrystallisation from 1:1 EtOAc/hexane to give the title compound as an off-white solid (1.35 g, 44%) with physical and spectroscopic data in accordance with the literature;[3] **R_f** = 0.50 (1.5:8.5 EtOAc/PE); **mp** 123 – 125 °C; **^{1}H NMR** (500 MHz, $CDCl_3$) δ_H: 9.17 (s, 1H), 8.36 – 8.32 (m, 1H), 8.03 (dd, *J* = 8.6, 1.7, 1H), 7.98 – 7.92 (m, 3H), 7.91 – 7.86 (m, 2H), 7.64 (ddd, *J* = 8.2, 6.9, 1.3, 1H), 7.58 (ddd, *J* = 8.1, 6.9, 1.3, 1H), 7.39 – 7.34 (m, 2H), 2.44 (s, 3H); **^{13}C {^{1}H} NMR** (126 MHz, $CDCl_3$) δ_C: 170.2, 144.7, 136.7, 136.3, 135.4, 132.8, 130.3, 130.0, 129.7, 129.6, 129.3, 128.3, 128.2, 127.4, 124.3, 21.8.

***N*-(furan-2-ylmethylene)-4-methylbenzenesulfonamide (3y)**

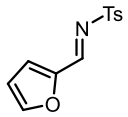

Prepared according to general procedure A from 2-furaldehyde (11 mmol) and 4-methylbenzenesulfonamide (10 mmol), followed by recrystallisation from 2:2:1 EtOAc/hexane/toluene to give the title compound as a dark brown solid (1.29 g, 52%) with physical and spectroscopic data in accordance with the literature;[10] **R_f** = 0.12 (1:4 EtOAc/PE); **mp** 111 – 113 °C; **^{1}H NMR** (500 MHz, $CDCl_3$) δ_H: 8.81 (s, 1H), 7.89 – 7.84 (m, 2H), 7.74 – 7.73 (m, 1H), 7.36 – 7.30 (m, 3H), 6.64 (dd, *J* = 3.6, 1.7, 1H), 2.42 (s, 3H); **^{13}C {^{1}H} NMR** (126 MHz, $CDCl_3$) δ_C: 155.8, 149.9, 149.2, 144.7, 135.3, 129.9, 128.2, 124.7, 113.8, 21.8.

4-methyl-*N*-(thiophen-2-ylmethylene)benzenesulfonamide (3z)

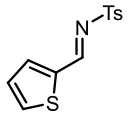

Prepared according to general procedure A from thiophene-2-carboxaldehyde (11 mmol) and 4-methylbenzenesulfonamide (10 mmol), with no further purification required to give the title compound as a grey solid (2.33 g, 88%), with physical and

spectroscopic data in accordance with the literature;[1] **R_f** = 0.21 (1:4 EtOAc/PE); **mp** 129 – 131 °C; **^{1}H NMR** (500 MHz, $CDCl_3$) δ_H: 9.11 – 9.10 (m, 1H), 7.90 – 7.84 (m, 2H), 7.79 – 7.74 (m, 2H), 7.35 – 7.31 (m, 2H), 7.22 – 7.19 (m, 1H), 2.43 (s, 3H); **^{13}C {^{1}H} NMR** (126 MHz, $CDCl_3$) δ_C: 162.3, 144.6, 139.1, 138.3, 136.8, 135.6, 129.9, 129.0, 128.1, 21.8.

_N_-((1_H_-pyrrol-2-yl)methylene)-4-methylbenzenesulfonamide (3aa)

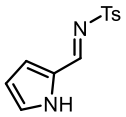

Prepared according to general procedure A from pyrrole-2-carboxaldehyde (11 mmol) and 4-methylbenzenesulfonamide (10 mmol), followed by recrystallisation from 2:2:1 EtOAc/hexane/toluene to give the title compound as a dark red solid (0.17 g, 7%) with physical and spectroscopic data in accordance with the literature;[11] **R_f** = 0.40 (1:4 EtOAc/PE); **mp** 128 – 130 °C; **^{1}H NMR** (500 MHz, $CDCl_3$) δ_H: 9.67 (br s, 1H), 8.72 (s, 1H), 7.84 – 7.78 (m, 2H), 7.30 – 7.27 (m, 2H), 7.21 – 7.17 (m, 1H), 7.04 – 7.02 (m, 1H), 6.39 (dt, *J* = 4.0, 2.4, 1H), 2.42 (s, 3H); **^{13}C {^{1}H} NMR** (126 MHz, $CDCl_3$) δ_C: 157.4, 144.1, 136.5, 129.8, 128.9, 127.7, 126.6, 125.0, 113.0, 21.7.

4-methyl-_N_-((_E_)-3-phenylallylidene)benzenesulfonamide (3ab)

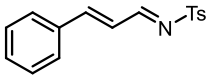

Prepared according to general procedure A from *trans*-cinnamaldehyde (11 mmol) and 4-methylbenzenesulfonamide (10 mmol), followed by recrystallisation from 2:2:1 EtOAc/hexane/toluene to give the title compound as a brown solid (0.56 g, 20%) with physical and spectroscopic data in accordance with the literature;[1] **R_f** = 0.30 (1:4 EtOAc/PE); **mp** 126 – 128 °C; **^{1}H NMR** (400 MHz, $CDCl_3$) δ_H: 8.78 (d, *J* = 9.4, 1H), 7.86 (d, *J* = 8.4, 2H), 7.57 – 7.53 (m, 2H), 7.49 (d, *J* = 15.8, 1H), 7.46 – 7.39 (m, 3H), 7.37 – 7.32 (m, 2H), 6.99 (dd, *J* = 15.8, 9.4, 1H), 2.44 (s, 3H); **^{13}C {^{1}H} NMR** (126 MHz, $CDCl_3$) δ_C: 171.0, 153.9, 144.7, 135.5, 134.3, 131.8, 130.0, 129.4, 128.8, 128.1, 124.9, 21.8.

_N_-benzylidenemethanesulfonamide (3ac)

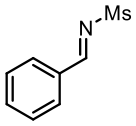

Prepared according to general procedure A from benzaldehyde (11 mmol) and methanesulfonamide (10 mmol), followed by recrystallisation from 1:1 EtOAc/hexane to give the title compound as a white solid (0.69 g, 38%) with physical and spectroscopic data in accordance with the literature;[12] **R_f** = 0.43 (3:7 EtOAc/PE); **mp** 70 – 72 °C; **^{1}H NMR** (300 MHz, $CDCl_3$) δ_H: 9.04 (s, 1H), 7.96 (d, *J* = 7.4, 2H), 7.67 (t, *J* = 7.7, 1H), 7.54 (t, *J* = 7.7, 2H), 3.15 (s, 3H); **^{13}C {^{1}H} NMR** (126 MHz, $CDCl_3$) δ_C: 171.8, 135.3, 132.2, 131.5, 129.4, 40.4.

_N_-(cyclohexylmethylene)-4-methylbenzenesulfonamide (3ad)

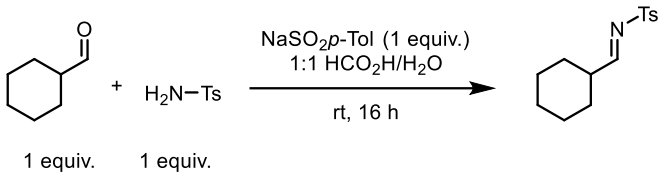

To a 250 mL round-bottomed flask, equipped with a magnetic stirrer bar, was charged cyclohexanecarboxaldehyde (1.21 mL, 10 mmol, 1 equiv.), 4-methylbenzenesulfonamide (1.71 g, 10 mmol, 1 equiv.), sodium 4-methylbenzenesulfinate (1.78 g, 10 mmol, 1 equiv.). Followed by the addition of formic acid (15 mL) and water (15 mL). The resulting mixture was stirred at room temperature for 16 hours. Upon completion, a precipitate had formed, which was filtered, washed with water (25 mL) and pentane (25 mL), and dissolved in dichloromethane (100 mL). Saturated aqueous sodium bicarbonate (70 mL) was added, and the mixture was stirred at room temperature for 2 hours. The mixture was transferred to a separatory funnel, where the organic phase was collected, the aqueous phase extracted one more time with dichloromethane (50 mL) and the combined organic phases were dried over magnesium sulfate. After concentrating the mixture in vacuo, the crude solid was recrystallised from a 1:1 mixture of ethyl acetate and hexane to give the title compound as a white solid (1.52 g, 57%), with physical and spectroscopic data in accordance with the literature;[3] **R_f** = 0.45 (1:4 EtOAc/PE); **mp** 114 – 116 °C; **^{1}H NMR** (300 MHz, $CDCl_3$) δ_H: 8.47 (d, *J* = 4.4, 1H), 7.84 – 7.76 (m, 2H), 7.33 (d, *J* = 8.1, 2H), 2.45 – 2.39

(m, 4H), 1.94 – 1.61 (m, 5H), 1.40 – 1.14 (m, 5H); **^{13}C {^{1}H} NMR** (126 MHz, $CDCl_3$) δ_C: 181.2, 144.7, 135.0, 129.9, 128.2, 43.8, 28.5, 25.8, 25.2, 21.8.

4-methyl-*N*-(1-phenylethylidene)benzenesulfonamide (3ae)

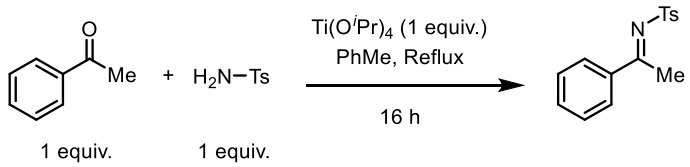

To a 100 mL round-bottomed flask, equipped with a magnetic stirrer bar, was charged acetophenone (2.4 mL, 20 mmol, 1 equiv.), 4-methylbenzenesulfonamide (3.42 g, 20 mmol, 1 equiv.), titanium (IV) isopropoxide (5.92 mL, 20 mmol, 1 equiv.) and toluene (40 mL). The resulting mixture was heated to reflux for 16 hours. Upon completion, the toluene was removed in vacuo and the crude residue was purified by FCC (1:9 EtOAc/PE) to give the title compound as a white solid (0.55 g, 10%), with physical and spectroscopic data in accordance with the literature;[13] **R_f** = 0.32 (1:4 EtOAc/PE); **mp** 82 – 84 °C; **^{1}H NMR** (500 MHz, $CDCl_3$) δ_H: 7.95 – 7.86 (m, 4H), 7.56 – 7.51 (m, 1H), 7.45 – 7.39 (m, 2H), 7.37 – 7.33 (m, 2H), 2.99 (s, 3H), 2.45 (s, 3H); **^{13}C {^{1}H} NMR** (126 MHz, $CDCl_3$) δ_C: 180.0, 143.7, 138.9, 137.7, 133.3, 129.6, 128.8, 128.4, 127.3, 21.7, 21.3.

***N*-(diphenylmethylene)-4-methylbenzenesulfonamide (3af)**

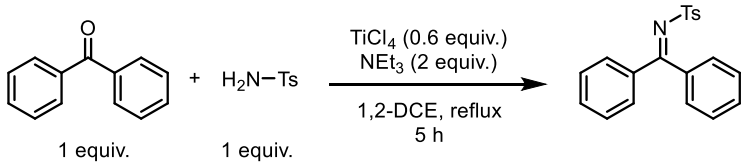

To a 100 mL round-bottomed flask, equipped with a magnetic stirrer bar, was charged benzophenone (1.82 g, 10 mmol, 1 equiv.), 4-methylbenzenesulfonamide (1.71 g, 10 mmol, 1 equiv.), triethylamine (2.79 mL, 20 mmol, 2 equiv.), and 1,2-dichloroethane (20 mL). Titanium (IV) tetrachloride (0.66 mL, 6 mmol, 0.6 equiv.) was added dropwise to the mixture and the resulting mixture was heated to reflux for 5 hours. Upon completion, the mixture was quenched with saturated aqueous sodium bicarbonate (25 mL) and transferred to a separatory funnel. The organic phase was collected, the aqueous phase extracted two more times with dichloromethane (2 x 25 mL) and the combined organic phases dried over magnesium sulfate. After concentrating in vacuo,

the crude solid was recrystallised from a 1:1 mixture of EtOAc/hexane to give the title compound as a beige solid (1.25 g, 37%), with physical and spectroscopic data in accordance with the literature;[14] **R_f** = 0.48 (1.5:8.5 EtOAc/PE); **mp** 110 – 112 °C; **^{1}H NMR** (500 MHz, $CDCl_3$) δ_H: 7.83 (d, *J* = 7.9, 2H), 7.66 – 7.34 (m, 10H), 7.29 (d, *J* = 8.0, 2H), 2.43 (s, 3H); **^{13}C {^{1}H} NMR** (126 MHz, $CDCl_3$) δ_C: 178.9, 143.5, 138.6, 129.5, 128.3 (4C), 127.5, 21.7.

5.2.3. Substrate Scope

5.2.3.1. General Procedure B -Mechanochemical Aza-MBH Reaction

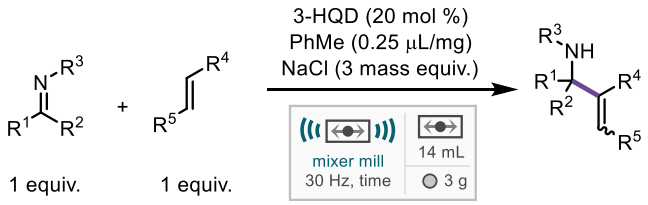

To a 14 mL stainless steel jar, equipped with a 3 g, 9 mm stainless steel ball, was charged the corresponding imine (0.25 mmol, 1 equiv.), Michael acceptor (0.28 mmol, 1.1 equiv.), 3-hydroxyquinuclidine (6.4 mg, 20 mol %, 0.05 mmol), toluene (0.25 μL/mg), and sodium chloride (3 mass equiv.). The jar was closed and placed on the mixer-mill, to be milled at 30 Hz for the stated time. Upon completion, the reaction mixture was transferred to a separatory funnel by washing the jar with EtOAc (25 mL) and water (25 mL). The organic layer was washed with 1 M HCl (15 mL), the organic phase was collected and the aqueous phase was extracted two more times with EtOAc (2 x 25 mL). The combined organic phases were washed with brine (15 mL), dried over magnesium sulfate and concentrated in vacuo. The crude product was purified by FCC to give the aza-MBH product.

Ethyl 2-(((4-methylphenyl)sulfonamido)(phenyl)methyl)acrylate (5a)

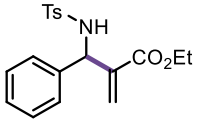

Prepared according to general procedure B from *N*-benzylidene-4-methylbenzenesulfonamide and ethyl acrylate, with a 99 minute reaction time, followed by purification by FCC (1.5:8.5 EtOAc/PE) to give the title compound as a white solid (76.3 mg, 85%), with physical and spectroscopic data in accordance with the literature;[15] **R_f** = 0.40 (1:4 EtOAc/PE); **mp** 108 – 110 °C; **^{1}H NMR** (500 MHz, $CDCl_3$) δ_H: 7.71 – 7.65 (m, 2H, Ts*H*), 7.26 – 7.18 (m, 5H, Ar*H*), 7.15 (m, 2H, Ar*H*), 6.21 (d, *J* = 0.9, 1H, H_2C=C), 5.80 (t, *J* = 0.9, 1H, H_2C=C), 5.65 (d, *J* = 8.9, 1H, N*H*), 5.30 (d, *J* = 8.9, 1H, N-C*H*), 4.05 (q, *J* = 7.1, 2H, OCH_2), 2.41 (s, 3H, ArCH_3), 1.14 (t, *J* = 7.1, 3H, CH_3); **^{13}C {^{1}H} NMR** (126 MHz, $CDCl_3$) δ_C: 165.4 (*C*=O), 143.5 ($C_{quaternary}$), 138.8 (2C, $C_{quaternary}$), 137.8 ($C_{quaternary}$), 129.6 (Ar*C*H), 128.7 (Ar*C*H), 127.9 (Ar*C*H), 127.8 (H_2C=C), 127.4 (Ar*C*H), 126.6 (Ar*C*H), 61.2 (O*C*H_2), 59.3 (N-*C*H), 21.7 (Ar*C*H_3), 14.1 (*C*H_3).

Ethyl 2-((4-fluorophenyl)((4-methylphenyl)sulfonamido)methyl)acrylate (5b)

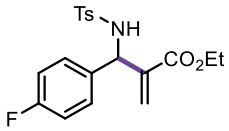

Prepared according to general procedure B from *N*-(4-fluorobenzylidene)-4-methylbenzenesulfonamide and ethyl acrylate, with a 3 h reaction time, followed by purification by FCC (1.5:8.5 EtOAc/PE) to give the title compound as a white solid (63.7 mg, 68%), with physical and spectroscopic data in accordance with the literature;[15] **R_f** = 0.33 (1.5:8.5 EtOAc/PE); **mp** 65 – 67 °C; **^{1}H NMR** (500 MHz, $CDCl_3$) δ_H: 7.68 – 7.65 (m, 2H), 7.25 – 7.21 (m, 2H), 7.16 – 7.10 (m, 2H), 6.95 – 6.89 (m, 2H), 6.19 (s, 1H), 5.77 (s, 1H), 5.65 (d, *J* = 9.0, 1H), 5.27 (d, *J* = 9.0, 1H), 4.06 (q, *J* = 7.1, 2H), 2.41 (s, 3H), 1.16 (t, *J* = 7.1, 3H); **^{13}C {^{1}H} NMR** (126 MHz, $CDCl_3$) δ_C: 165.3, 162.4 (d, *J* = 248.2), 143.6, 138.7, 137.8, 134.7 (d, *J* = 3.8), 129.7, 128.3 (d, *J* = 8.8), 127.9, 127.4, 115.5 (d, *J* = 21.4), 61.23, 58.8, 21.7, 14.1; **^{19}F {^{1}H} NMR** (376 MHz, $CDCl_3$) δ_F: -114.7.

Ethyl 2-((4-chlorophenyl)((4-methylphenyl)sulfonamido)methyl)acrylate (5c)

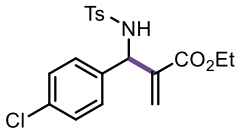

Prepared according to general procedure B from *N*-(4-chlorobenzylidene)-4-methylbenzenesulfonamide and ethyl acrylate, with a 3 h reaction time and 40 mol % catalyst, followed by purification by FCC (1.5:8.5 EtOAc/PE) to give the title compound as a white solid (59.8 mg, 61%), with physical and spectroscopic data in accordance with the literature;[15] **R_f** = 0.35 (1.5:8.5 EtOAc/PE); **mp** 93 – 95 °C ; **^{1}H NMR** (500 MHz, $CDCl_3$) δ_H: 7.68 – 7.61 (m, 2H), 7.24 – 7.16 (m, 4H), 7.13 – 7.07 (m, 2H), 6.19 (d, *J* = 0.7, 1H), 5.75 (t, *J* = 0.8, 1H), 5.69 (d, *J* = 9.2, 1H), 5.26 (d, *J* = 9.2, 1H), 4.09 – 4.03 (m, 2H), 2.41 (s, 3H), 1.16 (t, *J* = 7.1, 3H); **^{13}C {^{1}H} NMR** (126 MHz, $CDCl_3$) δ_C: 165.3, 143.7, 138.5, 137.7, 137.4, 133.7, 129.7, 128.8, 128.1, 128.0, 127.3, 61.3, 58.8, 21.7, 14.1.

Ethyl 2-((4-bromophenyl)((4-methylphenyl)sulfonamido)methyl)acrylate (5d)

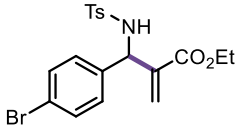

Prepared according to general procedure B from *N*-(4-bromobenzylidene)-4-methylbenzenesulfonamide and ethyl acrylate, with a 3 h reaction time and 40 mol % catalyst, followed by purification by FCC (1.5:8.5 EtOAc/PE) to give the title compound as a white solid (55.9 mg, 51%), with physical and spectroscopic data in accordance with the literature;[15] **R_f** = 0.34 (1.5:8.5 EtOAc/PE); **mp** 96 – 98 °C; **^{1}H NMR** (500 MHz, $CDCl_3$) δ_H: 7.67 – 7.63 (m, 2H), 7.37 – 7.33 (m, 2H), 7.25 – 7.22 (m, 2H), 7.06 – 7.02 (m, 2H), 6.19 (s, 1H), 5.76 (s, 1H), 5.70 (d, *J* = 9.2, 1H), 5.24 (d, *J* = 9.1, 1H), 4.11 – 4.02 (m, 2H), 2.41 (s, 3H), 1.17 (t, *J* = 7.1, 3H); **^{13}C {^{1}H} NMR** (126 MHz, $CDCl_3$) δ_C: 165.3, 143.7, 138.4, 138.0, 137.7, 131.7, 129.7, 128.3, 128.2, 127.3, 121.9, 61.3, 59.0, 21.67, 14.1.

Ethyl 2-((4-iodophenyl)((4-methylphenyl)sulfonamido)methyl)acrylate (5e)

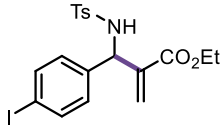

Prepared according to general procedure B from *N*-(4-iodobenzylidene)-4-methylbenzenesulfonamide and ethyl acrylate, with a 3 h reaction time and 40 mol % catalyst, followed by purification by FCC (1.5:8.5 EtOAc/PE) to give the title compound as a viscous, colourless oil (45.5 mg, 38%); $\mathbf{R_f}$ = 0.31 (1.5:8.5 EtOAc/PE); $\mathbf{\nu_{max}/cm^{-1}}$ (film): 2364, 1719, 1329, 1160, 1007, 668; **^{1}H NMR** (500 MHz, $CDCl_3$) δ_H: 7.66 – 7.62 (m, 2H), 7.57 – 7.52 (m, 2H), 7.25 – 7.21 (m, 2H), 6.93 – 6.89 (m, 2H), 6.19 (d, *J* = 0.7, 1H), 5.76 (t, *J* = 0.8, 1H), 5.67 (d, *J* = 9.2, 1H), 5.22 (d, *J* = 8.8, 1H), 4.09 – 4.03 (m, 2H), 2.42 (s, 3H), 1.17 (t, *J* = 7.1, 3H); **^{13}C {^{1}H} NMR** (126 MHz, $CDCl_3$) δ_C: 165.3, 143.7, 138.7, 138.4, 137.7, 137.6, 129.7, 128.6, 128.2, 127.3, 93.5, 61.4, 59.1, 21.7, 14.1; **HRMS** (ES) calculated for $[C_{19}H_{20}NO_4SINa]^+$ $(M+Na)^+$: m/z 508.0061 found 508.0055 (-1.2 ppm).

Ethyl 2-([1,1'-biphenyl]-4-yl((4-methylphenyl)sulfonamido)methyl)acrylate (5f)

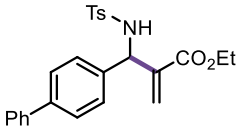

Prepared according to general procedure B from *N*-([1,1'-biphenyl]-4-ylmethylene)-4-methylbenzenesulfonamide and ethyl acrylate, with a 3 h reaction time, followed by purification by FCC (1.5:8.5 EtOAc/PE) to give the title compound as a white solid (72.3 mg, 66%); $\mathbf{R_f}$ = 0.31 (1:4 EtOAc/PE); **mp** 170 – 172 °C; $\mathbf{\nu_{max}/cm^{-1}}$ (film): 3265, 1709, 1320, 1280, 1180, 1072, 1027, 920, 823, 811, 767, 705, 690, 665, 563; **^{1}H NMR** (500 MHz, $CDCl_3$) δ_H: 7.72 – 7.66 (m, 2H), 7.55 – 7.50 (m, 2H), 7.48 – 7.39 (m, 4H), 7.36 – 7.32 (m, 1H), 7.25 – 7.21 (m, 4H), 6.24 (s, 1H), 5.84 (s, 1H), 5.71 (d, *J* = 9.0, 1H), 5.35 (d, *J* = 8.9, 1H), 4.08 (q, *J* = 7.1, 2H), 2.40 (s, 3H), 1.17 (t, *J* = 7.1, 3H); **^{13}C {^{1}H} NMR** (126 MHz, $CDCl_3$) δ_C: 165.5, 143.5, 140.8, 140.6, 138.8, 137.9, 137.8, 129.6, 128.9, 127.9, 127.6, 127.4 (2C), 127.2, 127.0, 61.2, 59.2, 21.7, 14.1; **HRMS** (ES^+) calculated for $[C_{25}H_{25}NO_4SNa]^+$ $(M+Na)^+$: m/z 458.1402 found 458.1402 (0.0 ppm).

Ethyl 2-(((4-methylphenyl)sulfonamido)(*p*-tolyl)methyl)acrylate (5g)

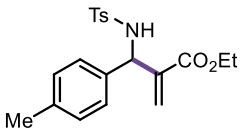

Prepared according to general procedure B from 4-methyl-*N*-(4-methylbenzylidene)benzenesulfonamide and ethyl acrylate, with a 3 h reaction time, followed by purification by FCC (1:4 EtOAc/PE) to give the title compound as a colourless, viscous oil (26.5 mg, 29%); $\mathbf{R_f}$ = 0.25 (1:4 EtOAc/PE); $\mathbf{\nu_{max}/cm^{-1}}$ (film): 3289, 1712, 1433, 1326, 1158, 1094, 813, 668; **^{1}H NMR** (500 MHz, $CDCl_3$) δ_H: 7.71 – 7.65 (m, 2H), 7.26 – 7.21 (m, 2H), 7.05 – 6.99 (m, 4H), 6.20 (s, 1H), 5.80 (s, 1H), 5.56 (d, *J* = 8.7 , 1H), 5.26 (d, *J* = 8.8, 1H), 4.05 (q, *J* = 7.1, 2H), 2.41 (s, 3H), 2.28 (s, 3H), 1.15 (t, *J* = 7.1, 3H); **^{13}C {^{1}H} NMR** (126 MHz, $CDCl_3$) δ_C: 165.5, 143.5, 139.0, 137.8, 137.6, 135.9, 129.6, 129.4, 127.5, 127.4, 126.5, 61.1, 59.1, 21.7, 21.1, 14.1; **HRMS** (ES) calculated for $[C_{20}H_{23}NO_4SNa]^+$ $(M+Na)^+$: m/z 396.1248 found 396.1245 (-0.8 ppm).

Ethyl 2-(((4-methylphenyl)sulfonamido)(4-nitrophenyl)methyl)acrylate (5h)

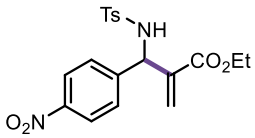

Prepared according to general procedure B from 4-methyl-*N*-(4-nitrobenzylidene)benzenesulfonamide and ethyl acrylate, with a 3 h reaction time, followed by purification by FCC (1.5:8.5 to 1:4 EtOAc/PE) to give the title compound as a viscous, colourless oil (47.7 mg, 47%), with physical properties and spectroscopic data in accordance with the literature;[15] $\mathbf{R_f}$ = 0.24 (1.5:8.5 EtOAc/PE); **^{1}H NMR** (500 MHz, $CDCl_3$) δ_H: 8.12 – 8.07 (m, 2H), 7.69 – 7.64 (m, 2H), 7.43 – 7.38 (m, 2H), 7.26 – 7.23 (m, 2H), 6.23 (d, *J* = 0.5, 1H), 5.92 (d, *J* = 9.5, 1H), 5.79 (s, 1H), 5.36 (d, *J* = 9.1, 1H), 4.13 – 4.01 (m, 2H), 2.41 (s, 3H), 1.17 (t, *J* = 7.1, 3H); **^{13}C {^{1}H} NMR** (126 MHz, $CDCl_3$) δ_C: 165.0, 147.4, 146.2, 143.9, 137.8, 137.6, 129.7, 129.0, 127.5, 127.2, 123.8, 61.6, 59.0, 21.6, 14.0.

Ethyl 2-((4-cyanophenyl)((4-methylphenyl)sulfonamido)methyl)acrylate (5i)

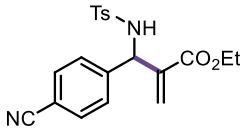

Prepared according to general procedure B from *N*-(4-cyanobenzylidene)-4-methylbenzenesulfonamide and ethyl acrylate, with a 3 h reaction time, followed by purification by FCC (1:4 EtOAc/PE) to give the title compound as a colourless, viscous oil (41.7 mg, 44%); $\mathbf{R_f}$ = 0.18 (1:4 EtOAc/PE); $\mathbf{\nu_{max}/cm^{-1}}$ (film): 3278, 2240, 1711, 1430, 1329, 1161, 1071, 815; **^{1}H NMR** (500 MHz, $CDCl_3$) δ_H: 7.68 – 7.64 (m, 2H), 7.56 – 7.52 (m, 2H), 7.37 – 7.32 (m, 2H), 7.26 – 7.22 (m, 2H), 6.21 (d, *J* = 0.6, 1H), 5.88 (d, *J* = 9.5, 1H), 5.76 (t, *J* = 0.6, 1H), 5.31 (d, *J* = 9.5, 1H), 4.12 – 4.01 (m, 2H), 2.42 (s, 3H), 1.16 (t, *J* = 7.1, 3H); **^{13}C {^{1}H} NMR** (126 MHz, $CDCl_3$) δ_C: 165.1, 144.3, 143.9, 137.8, 137.6, 132.4, 129.7, 129.0, 127.3, 127.3, 118.6, 111.7, 61.5, 59.2, 21.7, 14.0; **HRMS** (ES) calculated for $[C_{20}H_{20}N_2O_4SNa]^+$ $(M+Na)^+$: m/z 407.1049 found 407.1041 (-2.0 ppm).

Ethyl 2-(((4-methylphenyl)sulfonamido)(4-(trifluoromethyl)phenyl)methyl)acrylate (5j)

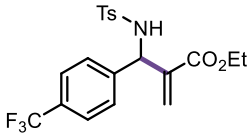

Prepared according to general procedure B from 4-methyl-*N*-(4-(trifluoromethyl)benzylidene)benzenesulfonamide and ethyl acrylate, with a 3 h reaction time, followed by purification by FCC (1:9 to 1:4 EtOAc/PE) to give the title compound as a white solid (61.3 mg, 57%), with physical properties and spectroscopic data in accordance with the literature;[15] $\mathbf{R_f}$ = 0.35 (1:4 EtOAc/PE); **mp** 79 – 81 °C (lit. 74 – 76 °C); **^{1}H NMR** (500 MHz, $CDCl_3$) δ_H: 7.64 (d, *J* = 8.1, 2H), 7.48 (d, *J* = 8.2, 2H), 7.31 (d, *J* = 8.1, 2H), 7.22 (d, *J* = 8.0, 2H), 6.22 (s, 1H), 5.82 (d, *J* = 9.3, 1H), 5.79 (s, 1H), 5.34 (d, *J* = 9.2, 1H), 4.10 – 4.04 (m, 2H), 2.40 (s, 3H), 1.17 (t, *J* = 7.1, 3H); **^{13}C {^{1}H} NMR** (126 MHz, $CDCl_3$) δ_C: 165.2, 143.7, 142.8, 138.2, 137.7, 130.1 (q, *J* = 32.8), 129.7, 128.6, 127.3, 127.0, 125.6 (q, *J* = 3.8), 124.1 (q, *J* = 268.4), 61.5, 59.3, 21.6, 14.1; **^{19}F {^{1}H} NMR** (376 MHz, $CDCl_3$) δ_F: -62.6.

Methyl 4-(2-(ethoxycarbonyl)-1-((4-methylphenyl)sulfonamido)allyl)benzoate (5k)

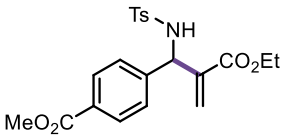

Prepared according to general procedure B from methyl-4-((tosylimino)methyl)benzoate and ethyl acrylate, with a 3 h reaction time and 40 mol % catalyst, followed by purification by FCC (3:7 EtOAc/PE) to give the title compound as a white solid (52.6 mg, 51%); **R_f** = 0.13 (1:4 EtOAc/PE); **mp** 102 – 104 °C; **ν_{max}/cm^{-1}** (film): 3286, 1719, 1436, 1329, 1282, 1161, 1112, 565; **^{1}H NMR** (500 MHz, $CDCl_3$) δ_H: 7.92 – 7.88 (m, 2H), 7.69 – 7.64 (m, 2H), 7.28 – 7.21 (m, 4H), 6.21 (s, 1H), 5.81 – 5.74 (m, 2H), 5.33 (d, *J* = 9.0, 1H), 4.00 (m, 2H), 3.89 (s, 3H), 2.40 (s, 3H), 1.14 (t, *J* = 7.1, 3H); **^{13}C {^{1}H} NMR** (126 MHz, $CDCl_3$) δ_C: 166.8, 165.2, 143.9, 143.7, 138.3, 137.7, 129.9, 129.7, 129.6, 128.5, 127.3, 126.6, 61.3, 59.3, 52.3, 21.6, 14.1; **HRMS** (ES) calculated for $[C_{21}H_{23}NO_6SNa]^+$ $(M+Na)^+$: m/z 440.1150 found 440.1144 (-1.4 ppm).

Ethyl 2-((4-methoxyphenyl)((4-methylphenyl)sulfonamido)methyl)acrylate (5l)

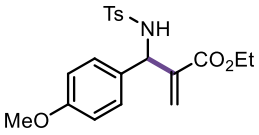

Prepared according to general procedure B from *N*-(4-methoxybenzylidene)-4-methylbenzenesulfonamide and ethyl acrylate, with a 3 h reaction time and 40 mol % catalyst, followed by purification by FCC (0.5:9.5 Acetone/Toluene) to give the title compound as a colourless oil (25.9 mg, 27%), with physical and spectroscopic data in accordance with the literature;[15] **R_f** = 0.32 (0.5:9.5 Acetone/Toluene); **^{1}H NMR** (500 MHz, $CDCl_3$) δ_H: 7.67 (d, *J* = 8.2, 2H), 7.23 (d, *J* = 8.2, 2H), 7.04 (d, *J* = 8.8, 2H), 6.75 (d, *J* = 8.6, 2H), 6.19 (s, 1H), 5.80 (s, 1H), 5.55 (t, *J* = 8.9, 1H), 5.24 (d, *J* = 8.6, 1H), 4.05 (q, *J* = 7.1, 2H), 3.75 (s, 3H), 2.41 (s, 3H), 1.15 (t, *J* = 7.1, 3H); **^{13}C {^{1}H} NMR** (126 MHz, $CDCl_3$) δ_C: 165.5, 159.2, 143.5, 139.1, 137.8, 130.9, 129.6, 127.9, 127.4, 127.3, 114.0, 61.1, 58.7, 55.4, 21.7, 14.1.

Ethyl 2-((3-fluorophenyl)((4-methylphenyl)sulfonamido)methyl)acrylate (5n)

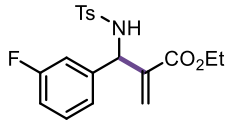

Prepared according to general procedure B from *N*-(3-fluorobenzylidene)-4-methylbenzenesulfonamide and ethyl acrylate, with a 3 h reaction time, followed by purification by FCC (1:4 EtOAc/PE) to give the title compound as a white solid (72.7 mg, 78%), with physical properties and spectroscopic data in accordance with the literature;[15] **R_f** = 0.19 (1:4 EtOAc/PE); **mp** 101 – 103 °C; **^{1}H NMR** (500 MHz, $CDCl_3$) δ_H: 7.70 – 7.63 (m, 2H), 7.24 (d, *J* = 7.9, 2H), 7.22 – 7.18 (m, 1H), 6.99 – 6.95 (m, 1H), 6.93 – 6.84 (m, 2H), 6.21 (d, *J* = 0.7, 1H), 5.77 (t, *J* = 0.8, 1H), 5.74 (d, *J* = 8.7, 1H), 5.27 (d, *J* = 9.3, 1H), 4.10 – 4.02 (m, 2H), 2.41 (s, 3H), 1.16 (t, *J* = 7.1, 3H); **^{13}C {^{1}H} NMR** (126 MHz, $CDCl_3$) δ_C: 165.1, 162.8 (d, *J* = 246.8), 143.6, 141.4 (d, *J* = 7.0), 138.2, 137.6, 130.1 (d, *J* = 8.2), 129.6, 128.3, 127.2, 122.0 (d, *J* = 2.9), 114.7 (d, *J* = 21.1), 113.6 (d, *J* = 22.9), 61.2, 58.9 (d, *J* = 2.1), 21.5, 13.9; **^{19}F {^{1}H} NMR** (376 MHz, $CDCl_3$) δ_F: -112.5.

Ethyl 2-((3-chlorophenyl)((4-methylphenyl)sulfonamido)methyl)acrylate (5o)

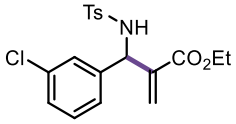

Prepared according to general procedure B from *N*-(3-chlorobenzylidene)-4-methylbenzenesulfonamide and ethyl acrylate, with a 3 h reaction time and 40 mol % catalyst, followed by purification by FCC (1:4 EtOAc/PE) to give the title compound as a white solid (69.1 mg, 70%); **R_f** = 0.19 (1:4 EtOAc/PE); **mp** 103 – 105 °C; **ν_{max}/cm^{-1}** (film): 3296, 2364, 1714, 1597, 1433, 1329, 1160, 1094, 814, 668; **^{1}H NMR** (500 MHz, $CDCl_3$) δ_H: 7.68 – 7.63 (m, 2H), 7.25 – 7.22 (m, 2H), 7.20 – 7.15 (m, 2H), 7.09 – 7.05 (m, 2H), 6.22 (d, *J* = 0.7, 1H), 5.78 (t, *J* = 0.8, 1H), 5.69 (d, *J* = 9.2, 1H), 5.26 (dd, *J* = 9.2, 0.6, 1H), 4.12 – 4.03 (m, 2H), 2.41 (s, 3H), 1.17 (t, *J* = 7.1, 3H); **^{13}C {^{1}H} NMR** (126 MHz, $CDCl_3$) δ_C: 165.2, 143.7, 140.9, 138.3, 137.7, 134.6, 129.9, 129.7, 128.4, 128.0, 127.3, 126.9, 124.7, 61.4, 59.0, 21.7, 14.1; **HRMS** (ES) calculated for $[C_{19}H_{20}NO_4S^{35}ClNa]^+$ $(M+Na)^+$: m/z 416.0698 found 416.0699 (+0.2 ppm).

Ethyl 2-(((4-methylphenyl)sulfonamido)(*m*-tolyl)methyl)acrylate (5p)

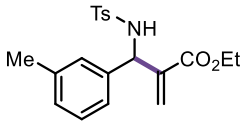

Prepared according to general procedure B from 4-methyl-*N*-(3-methylbenzylidene)benzenesulfonamide and ethyl acrylate, with a 3 h reaction time, followed by purification by FCC (1:4 EtOAc/PE) to give the title compound as a white solid (65.6 mg, 70%), with physical properties and spectroscopic data in accordance with the literature;[15] **R_f** = 0.36 (1.5:8.5 EtOAc/PE); **mp** 72 – 74 °C; **^{1}H NMR** (500 MHz, $CDCl_3$) δ_H: 7.69 – 7.64 (m, 2H), 7.25 – 7.21 (m, 2H), 7.11 (t, *J* = 7.6, 1H), 7.03 – 6.99 (m, 1H), 6.93 – 6.87 (m, 2H), 6.21 (d, *J* = 0.5, 1H), 5.81 (t, *J* = 0.9, 1H), 5.55 (d, *J* = 8.8, 1H), 5.26 (d, *J* = 8.7, 1H), 4.06 (q, *J* = 7.1, 2H), 2.41 (s, 3H), 2.24 (s, 3H), 1.15 (t, *J* = 7.1, 3H); **^{13}C {^{1}H} NMR** (126 MHz, $CDCl_3$) δ_C: 165.5, 143.4, 139.0, 138.7, 138.3, 137.8, 129.6, 128.6, 128.5, 127.6, 127.4, 127.3, 123.6, 61.1, 59.2, 21.6, 21.5, 14.1.

Ethyl 2-((2-fluorophenyl)((4-methylphenyl)sulfonamido)methyl)acrylate (5q)

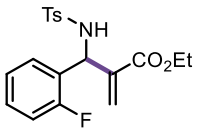

Prepared according to general procedure B from *N*-(2-fluorobenzylidene)-4-methylbenzenesulfonamide and ethyl acrylate, with a 3 h reaction time, followed by purification by FCC (1:4 EtOAc/PE) to give the title compound as a white solid (46.0 mg, 49%), with physical and spectroscopic data in accordance with the literature;[15] **R_f** = 0.12 (1:4 EtOAc/PE); **mp** 92 – 94 °C; **^{1}H NMR** (500 MHz, $CDCl_3$) δ_H: 7.66 – 7.61 (m, 2H), 7.22 (td, *J* = 7.7, 1.7, 1H), 7.19 – 7.13 (m, 3H), 6.98 (td, *J* = 7.6, 1.2, 1H), 6.89 (ddd, *J* = 10.6, 8.2, 1.2, 1H), 6.22 (d, *J* = 0.8, 1H), 5.87 – 5.86 (m, 1H), 5.76 (d, *J* = 9.4, 1H), 5.58 (d, *J* = 9.4, 1H), 4.08 (q, *J* = 7.1, 2H), 2.37 (s, 3H), 1.18 (t, *J* = 7.1, 3H); **^{13}C {^{1}H} NMR** (101 MHz, $CDCl_3$) δ_C: 165.4, 159.9 (d, *J* = 247.8), 143.4, 137.9 (d, *J* = 86.3), 129.6, 129.5 (2C), 128.8 (d, *J* = 3.3), 127.5, 127.2, 126.1 (d, *J* = 13.0), 124.2 (d, *J* = 3.5), 115.6 (d, *J* = 21.7), 61.2, 53.4 (d, *J* = 2.7), 21.6, 14.0; **^{19}F {^{1}H} NMR** (376 MHz, $CDCl_3$) δ_F: -116.8.

Ethyl 2-((2-chlorophenyl)((4-methylphenyl)sulfonamido)methyl)acrylate (5r)

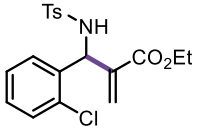

Prepared according to general procedure B from *N*-(2-chlorobenzylidene)-4-methylbenzenesulfonamide and ethyl acrylate, with a 3 h reaction time and 40 mol % catalyst, followed by purification by FCC (1:4 EtOAc/PE) to give the title compound as a white solid (55.8 mg, 57%); **R_f** = 0.16 (1:4 EtOAc/PE); **mp** 104 – 106 °C; **ν_{max}/cm^{-1}** (film): 3360, 2364, 2334, 1718, 1161, 913, 680; **^{1}H NMR** (500 MHz, $CDCl_3$) δ_H: 7.66 – 7.62 (m, 2H), 7.32 – 7.29 (m, 1H), 7.26 – 7.22 (m, 1H), 7.19 – 7.15 (m, 2H), 7.15 – 7.08 (m, 2H), 6.29 (s, 1H), 5.90 (s, 1H), 5.75 (d, *J* = 8.5, 1H), 5.67 (d, *J* = 8.6, 1H), 4.08 (q, *J* = 7.1, 2H), 2.37 (s, 3H), 1.18 (t, *J* = 7.1, 3H); **^{13}C {^{1}H} NMR** (126 MHz, $CDCl_3$) δ_C: 165.5, 143.5, 138.0, 137.5, 136.0, 133.1, 129.9, 129.5, 129.1 (2C), 128.6, 127.4, 127.0, 61.3, 56.0, 21.6, 14.1; **HRMS** (ES) calculated for $[C_{19}H_{20}NO_4S^{35}ClNa]^+$ $(M+Na)^+$: m/z 416.0701 found 416.0699 (-0.2 ppm).

Ethyl 2-(((4-methylphenyl)sulfonamido)(*o*-tolyl)methyl)acrylate (5s)

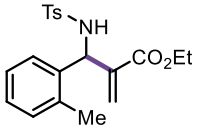

Prepared according to general procedure B from 4-methyl-*N*-(2-methylbenzylidene)benzenesulfonamide and ethyl acrylate, with a 3 h reaction time and 40 mol % catalyst, followed by purification by FCC (1:4 EtOAc/PE) to give the title compound as a white solid (43.7 mg, 47%); **R_f** = 0.33 (1:4 EtOAc/PE); **mp** 101 – 103 °C; **ν_{max}/cm^{-1}** (film): 3284, 2971, 1715, 1329, 1268, 1159, 1095, 1064, 815; **^{1}H NMR** (500 MHz, $CDCl_3$) δ_H: 7.68 – 7.63 (m, 2H), 7.24 – 7.20 (m, 2H), 7.14 – 7.09 (m, 1H), 7.09 – 7.03 (m, 3H), 6.30 (t, *J* = 0.9, 1H), 5.86 – 5.84 (m, 1H), 5.60 (d, *J* = 7.3, 1H), 5.01 (d, *J* = 7.2, 1H), 4.12 – 3.98 (m, 2H), 2.40 (s, 3H), 2.16 (s, 3H), 1.15 (t, *J* = 7.1, 3H); **^{13}C {^{1}H} NMR** (126 MHz, $CDCl_3$) δ_C: 165.7, 143.5, 139.7, 137.6, 136.9, 136.2, 130.9, 129.6, 128.1, 127.4, 126.7, 126.6, 126.4, 61.1, 54.7, 21.6, 19.2, 14.1; **HRMS** (ES) calculated for $[C_{20}H_{23}NO_4SNa]^+$ $(M+Na)^+$: m/z 396.1246 found 396.1245 (-0.3 ppm).

Ethyl 2-(((4-methylphenyl)sulfonamido)(perfluorophenyl)methyl)acrylate (5u)

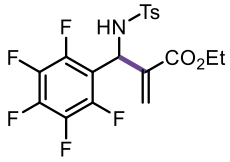

Prepared according to general procedure B from 4-methyl-*N*-((perfluorophenyl)methylene)benzenesulfonamide and ethyl acrylate, with a 3 h reaction time and 40 mol % catalyst, followed by purification by FCC (1:4 EtOAc/PE) to give the title compound as a white solid (35.4 mg, 31%); **R_f** = 0.29 (1:4 EtOAc/PE); **mp** 164 – 166 °C; **ν_{max}/cm^{-1}** (film): 3266, 1716, 1518, 1506, 1342, 1330, 1275, 1166, 1119, 1078, 994, 817, 764, 749, 714, 669, 554, 536; **^{1}H NMR** (400 MHz, $CDCl_3$) δ_H: 7.67 – 7.61 (m, 2H), 7.23 – 7.18 (m, 2H), 6.43 (s, 1H), 5.97 (s, 1H), 5.72 (d, *J* = 10.3, 1H), 5.55 (d, *J* = 10.4, 1H), 4.19 – 4.07 (m, 2H), 2.38 (s, 3H), 1.23 (t, *J* = 7.1, 3H); **^{13}C {^{1}H} NMR** (101 MHz, $CDCl_3$) δ_C: 164.6, 144.2, 136.9, 136.8, 129.6, 127.5, 127.2, 61.7, 48.8, 21.5, 14.0 (unidentifiable signals between 135 – 150 ppm, due to broadening from multiple ^{13}C-^{19}F couplings); **^{19}F {^{1}H} NMR** (376 MHz, $CDCl_3$) δ_F: -140.32 – -142.18 (m), -153.45 – -154.89 (m), -160.19 – -162.45 (m); **HRMS** (ES) calculated for $[C_{19}H_{16}NO_4F_5SNa]^+$ $(M+Na)^+$: m/z 472.0618 found 472.0618 (0.0 ppm).

Ethyl 2-(((4-methylphenyl)sulfonamido)(naphthalen-1-yl)methyl)acrylate (5w)

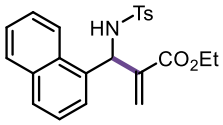

Prepared according to general procedure B from methyl-*N*-(naphthalen-1-ylmethylene)benzenesulfonamide and ethyl acrylate, with a 3 h reaction time and 40 mol % catalyst, followed by purification by FCC (1:4 EtOAc/PE) to give the title compound as a white solid (25.1 mg, 25%); **R_f** = 0.20 (1:4 EtOAc/PE); **mp** 167 – 169 °C; **ν_{max}/cm^{-1}** (film): 3284, 2984, 1715, 1325, 1275, 1158, 1093, 1069, 765, 671; **^{1}H NMR** (500 MHz, $CDCl_3$) δ_H: 7.85 – 7.78 (m, 2H), 7.74 (d, *J* = 7.8, 1H), 7.66 – 7.63 (m, 2H), 7.48 – 7.43 (m, 1H), 7.39 – 7.35 (m, 1H), 7.33 – 7.27 (m, 2H), 7.19 – 7.16 (m, 2H), 6.39 (s, 1H), 6.20 (d, *J* = 7.4, 1H), 5.94 (s, 1H), 5.12 (d, *J* = 7.4, 1H), 4.07 – 3.96 (m, 2H), 2.40 (s, 3H), 1.06 (t, *J* = 7.1, 3H); **^{13}C {^{1}H} NMR** (126 MHz, $CDCl_3$) δ_C: 165.7, 143.6, 139.8, 137.4, 134.6, 134.1, 130.6, 129.6, 129.1, 128.9, 127.5, 127.3, 126.7, 126.0, 125.2, 125.1, 123.1, 61.1, 54.2, 21.7, 14.0; **HRMS** (ES) calculated for $[C_{23}H_{23}NO_4SNa]^+$ $(M+Na)^+$: m/z 432.1249 found 432.1245 (-0.9 ppm).

Ethyl 2-(((4-methylphenyl)sulfonamido)(naphthalen-2-yl)methyl)acrylate (5x)

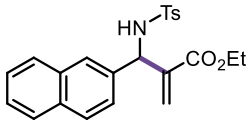

Prepared according to general procedure B from 4-methyl-*N*-(naphthalen-2-ylmethylene)benzenesulfonamide and ethyl acrylate, with a 3 h reaction time, followed by purification by FCC (1.5:8.5 EtOAc/PE) to give the title compound as a white solid (67.9 mg, 66%), with physical properties and spectroscopic data in accordance with the literature;[15] **R_f** = 0.35 (1.5:8.5 EtOAc/PE); **mp** 111 – 113 °C; **^{1}H NMR** (500 MHz, $CDCl_3$) δ_H: 7.79 – 7.74 (m, 1H), 7.72 – 7.65 (m, 4H), 7.57 – 7.54 (m, 1H), 7.47 – 7.42 (m, 2H), 7.25 (dd, *J* = 8.5, 1.9, 1H), 7.20 – 7.16 (m, 2H), 6.27 (d, *J* = 0.8, 1H), 5.88 (t, *J* = 0.9, 1H), 5.73 (d, *J* = 8.9, 1H), 5.47 (d, *J* = 8.8, 1H), 4.07 – 4.01 (m, 2H), 2.36 (s, 3H), 1.14 (t, *J* = 7.1, 3H); **^{13}C {^{1}H} NMR** (126 MHz, $CDCl_3$) δ_C: 165.5, 143.5, 138.9, 137.8, 136.1, 133.2, 132.9, 129.6, 128.5, 128.2, 127.8, 127.7, 127.4, 126.4, 126.3, 125.7, 124.6, 61.2, 59.4, 21.6, 14.1.

Ethyl 2-(furan-2-yl((4-methylphenyl)sulfonamido)methyl)acrylate (5y)

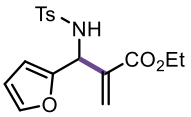

Prepared according to general procedure B from *N*-(furan-2-ylmethylene)-4-methylbenzenesulfonamide and ethyl acrylate, with a 3 h reaction time, followed by purification by FCC (1:4 EtOAc/PE) to give the title compound as a white solid (52.4 mg, 60%), with physical properties and spectroscopic data in accordance with the literature;[15] **R_f** = 0.18 (1:4 EtOAc/PE); **mp** 103 – 105 °C; **^{1}H NMR** (500 MHz, $CDCl_3$) δ_H: 7.71 – 7.65 (m, 2H), 7.25 – 7.22 (m, 2H), 7.20 (dd, *J* = 1.8, 0.9, 1H), 6.22 (s, 1H), 6.21 (dd, *J* = 3.3, 1.8, 1H), 6.05 (dt, *J* = 3.3, 0.9, 1H), 5.81 (s, 1H), 5.70 (d, *J* = 9.3, 1H), 5.38 (d, *J* = 9.3, 1H), 4.12 (q, *J* = 7.1, 2H), 2.40 (s, 3H), 1.21 (t, *J* = 7.1, 3H); **^{13}C {^{1}H} NMR** (126 MHz, $CDCl_3$) δ_C: 165.2, 151.4, 143.5, 142.3, 137.7, 137.2, 129.6, 128.2, 127.3, 110.7, 107.5, 61.3, 53.8, 21.7, 14.1.

Ethyl 2-(((4-methylphenyl)sulfonamido)(thiophen-2-yl)methyl)acrylate (5z)

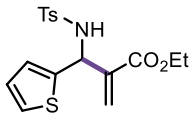

Prepared according to general procedure B from 4-methyl-*N*-(thiophen-2-ylmethylene)benzenesulfonamide and ethyl acrylate, with a 3 h reaction time and 40 mol % catalyst, followed by purification by FCC (0.5:9.5 Acetone/Toluene) to give the title compound as a white solid (32.3 mg, 35%), with physical properties and spectroscopic data in accordance with the literature;[15] **R_f** = 0.24 (1:4 EtOAc/PE); **mp** 117 – 119 °C; **^{1}H NMR** (500 MHz, $CDCl_3$) δ_H: 7.72 – 7.69 (m, 2H), 7.26 – 7.24 (m, 2H), 7.15 (dd, *J* = 5.1, 1.3, 1H), 6.85 (dd, *J* = 5.1, 3.6, 1H), 6.75 (dt, *J* = 3.6, 1.2, 1H), 6.20 (s, 1H), 5.86 (d, *J* = 9.4, 1H), 5.81 (s, 1H), 5.47 (d, *J* = 9.3, 1H), 4.10 (q, *J* = 7.1, 2H), 2.41 (s, 3H), 1.19 (t, *J* = 7.1, 3H); **^{13}C {^{1}H} NMR** (126 MHz, $CDCl_3$) δ_C: 165.3, 143.6, 143.3, 138.4, 137.7, 129.7, 128.0, 127.4, 127.2, 125.6, 125.1, 61.3, 56.1, 21.7, 14.1.

Ethyl (*E*)-2-methylene-3-((4-methylphenyl)sulfonamido)-5-phenylpent-4-enoate (5ab)

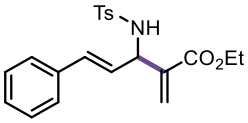

Prepared according to general procedure B from 4-methyl-*N*-((*E*)-3-phenylallylidene)benzenesulfonamide and ethyl acrylate, with a 3 h reaction time, followed by purification by FCC (1:4 EtOAc/PE) to give the title compound as a pale yellow solid (38.6 mg, 40%); **R_f** = 0.21 (1:4 EtOAc/PE); **mp** 126 – 128 °C; **ν_{max}/cm^{-1}** (film): 3292, 1709, 1323, 1286, 1161, 1138, 1091, 1041, 974, 956, 816, 755, 697, 669, 563, 543; **^{1}H NMR** (500 MHz, $CDCl_3$) δ_H: 7.73 – 7.69 (m, 2H), 7.28 – 7.16 (m, 7H), 6.33 (dd, *J* = 16.0, 1.4, 1H), 6.12 (d, *J* = 0.7, 1H), 6.03 (dd, *J* = 15.9, 6.5, 1H), 5.72 (t, *J* = 0.8, 1H), 5.62 (d, *J* = 9.5, 1H), 4.83 (dddd, *J* = 9.5, 6.6, 1.5, 0.7, 1H), 4.19 – 4.10 (m, 2H), 2.34 (s, 3H), 1.25 (t, *J* = 7.1, 3H); **^{13}C {^{1}H} NMR** (126 MHz, $CDCl_3$) δ_C: 165.5, 143.5, 138.6, 138.2, 136.1, 132.3, 129.6, 128.6, 128.1, 127.6, 127.4, 127.1, 126.7, 61.3, 58.7, 21.6, 14.2; **HRMS** (ES) calculated for $[C_{21}H_{23}NO_4SNa]^+$ $(M+Na)^+$: m/z 408.1245 found 408.1245 (0.0 ppm).

Ethyl 2-(methylsulfonamido(phenyl)methyl)acrylate (5ac)

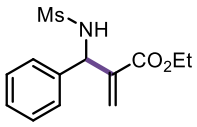

Prepared according to general procedure B from *N*-benzylidenemethanesulfonamide and ethyl acrylate, with a 3 h reaction time, followed by purification by FCC (3:7 EtOAc/PE) to give the title compound as a viscous, colourless oil (45.1 mg, 64%); $\mathbf{R_f}$ = 0.31 (3:7 EtOAc/PE); $\mathbf{\nu_{max}/cm^{-1}}$ (film): 3281, 1710, 1315, 1159, 1083, 1062, 978, 757, 698, 517; **^{1}H NMR** (500 MHz, $CDCl_3$) δ_H: 7.38 – 7.27 (m, 5H), 6.42 (s, 1H), 5.96 (s, 1H), 5.56 (d, *J* = 9.1, 1H), 5.47 (d, *J* = 9.0, 1H), 4.21 – 4.10 (m, 2H), 2.88 (s, 3H), 1.22 (t, *J* = 7.1, 3H); **^{13}C {^{1}H} NMR** (126 MHz, $CDCl_3$) δ_C: 165.6, 139.9, 139.0, 128.9, 128.1, 127.7, 126.7, 61.4, 59.3, 42.0, 14.1; **HRMS** (ES) calculated for $[C_{13}H_{18}NO_4S]^+$ $(M+H)^+$: m/z 284.0956 found 284.0957 (+0.4 ppm).

***N*-(2-cyano-1-phenylallyl)-4-methylbenzenesulfonamide (5ag)**

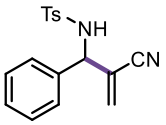

Prepared according to general procedure B from *N*-benzylidene-4-methylbenzenesulfonamide and acrylonitrile, with a 99 minute reaction time, followed by purification by FCC (1.5:8.5 to 3:7 EtOAc/PE) to give the title compound as a white solid (46.9 mg, 60%), with physical properties and spectroscopic data in accordance with the literature;[16] $\mathbf{R_f}$ = 0.26 (1.5:8.5 EtOAc/PE); **mp** 119 – 121 °C; **^{1}H NMR** (400 MHz, $CDCl_3$) δ_H: 7.73 – 7.69 (m, 2H), 7.34 – 7.27 (m, 5H), 7.14 – 7.08 (m, 2H), 6.08 (d, *J* = 1.4, 1H), 6.01 (d, *J* = 1.1, 1H), 5.05 (d, *J* = 7.0, 1H), 4.96 (d, *J* = 7.0, 1H), 2.44 (s, 3H); **^{13}C {^{1}H} NMR** (126 MHz, $CDCl_3$) δ_C: 144.3, 136.9, 136.3, 132.0, 129.9, 129.5, 129.3, 127.5, 127.0, 123.5, 116.6, 60.0, 21.7.

4-methyl-*N*-(2-methylene-3-oxo-1-phenylbutyl)benzenesulfonamide (5ah)

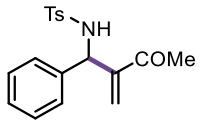

Prepared according to general procedure B from *N*-benzylidene-4-methylbenzenesulfonamide and methyl vinyl ketone, followed by purification by FCC (1.5:8.5 to 2.5:7.5 EtOAc/PE) to give the title compound as a white solid (25.6 mg, 31%), with physical properties and spectroscopic data in accordance with the literature;[17] **R_f** = 0.33 (2.5:7.5 EtOAc/PE); **mp** 109 – 111 °C (lit. 113 -114 °C); **^{1}H NMR** (500 MHz, $CDCl_3$) δ_H: 7.67 – 7.64 (m, 2H), 7.26 – 7.16 (m, 5H), 7.13 – 7.08 (m, 2H), 6.11 (s, 1H), 6.09 (d, *J* = 0.9, 1H), 5.61 (d, *J* = 8.6, 1H), 5.27 (d, *J* = 8.5, 1H), 2.41 (s, 3H), 2.16 (s, 3H); **^{13}C {^{1}H} NMR** (126 MHz, $CDCl_3$) δ_C: 199.0, 146.6, 143.5, 139.0, 137.7, 129.7, 128.7, 128.4, 127.8, 127.4, 126.5, 59.1, 26.5, 21.7.

***N*-(((4-methylphenyl)sulfonamido)(phenyl)methyl)acrylamide (5ai)**

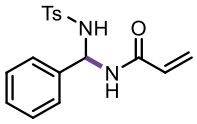

Prepared according to general procedure B from *N*-benzylidene-4-methylbenzenesulfonamide and acrylamide, with a 3 h reaction time, followed by purification by FCC (1:4 to 2:3 EtOAc/PE) to give the title compound as a white solid (19.2 mg, 23%); **R_f** = 0.43 (1:1 EtOAc/PE); **mp** 160 – 162 °C; **ν_{max}/cm^{-1}** (film): 3351, 3274, 1662, 1625, 1529, 1495, 1451, 1439, 1407, 1158, 1078, 1057, 981, 895, 817, 802, 694, 677, 577, 540; **^{1}H NMR** (500 MHz, $(CD_3)_2SO$) δ_H: 8.70 (d, *J* = 8.8, 1H), 8.57 (d, *J* = 8.4, 1H), 7.65 (d, *J* = 8.1, 2H), 7.35 – 7.23 (m, 7H), 6.32 (t, *J* = 8.5, 1H), 6.11 (dd, *J* = 17.1, 10.0, 1H), 6.00 (dd, *J* = 17.1, 2.3, 1H), 5.54 (dd, *J* = 10.0, 2.4, 1H), 2.35 (s, 3H); **^{13}C {^{1}H} NMR** (126 MHz,$(CD_3)_2SO$) δ_C: 163.4, 142.4, 139.3, 138.6, 131.0, 129.3, 128.3, 127.9, 126.6, 126.3, 126.0, 60.9, 21.0; **HRMS** (ES) calculated for $[C_{17}H_{18}N_2O_3SNa]^+$ $(M+Na)^+$: m/z 353.0936 found 353.0936 (0.0 ppm).

Ethyl 2-(hydroxy(4-nitrophenyl)methyl)acrylate (6a)

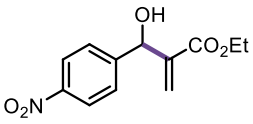

Prepared according to general procedure B from 4-nitrobenzaldehyde and ethyl acrylate, with a 99 minute reaction time, followed by purification by FCC (1:4 EtOAc/PE) to give the title compound as a pale yellow oil (35.5 mg, 57%), with physical properties and spectroscopic data in accordance with the literature;[18] **R_f** = 0.25 (2.5:7.5 EtOAc/PE); **^{1}H NMR** (400 MHz, $CDCl_3$) δ_H: 8.24 – 8.17 (m, 2H), 7.64 – 7.53 (m, 2H), 6.40 – 6.39 (m, 1H), 5.84 (t, *J* = 1.0, 1H), 5.62 (d, *J* = 5.2, 1H), 4.19 (q, *J* = 7.1, 2H), 3.34 (d, *J* = 6.3, 1H), 1.27 (t, *J* = 7.1, 3H); **^{13}C {^{1}H} NMR** (126 MHz, $CDCl_3$) δ_C: 166.1, 148.8, 147.6, 141.3, 127.5, 127.3, 123.8, 73.1, 61.5, 14.2.

5.2.4. Scale Up Reaction

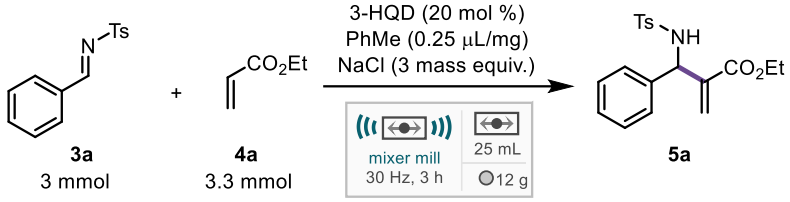

To a 25 mL stainless steel jar, equipped with a 12 g, 14 mm stainless steel ball, was charged *N*-benzylidene-4-methylbenzenesulfonamide (778 mg, 3 mmol, 1 equiv.), ethyl acrylate (360 µL, 3.3 mmol, 1.1 equiv.), 3-HQD (76 mg, 0.6 mmol, 20 mol %), toluene (300 µL), and sodium chloride (3 g, 3.0 mass equiv.). The jar was closed and placed on the mixer-mill to be milled at 30 Hz for 3 hours. Upon completion, the reaction mixture was transferred to a separatory funnel by washing the jar with EtOAc (30 mL) and water (30 mL). The organic layer was washed with 1 M HCl (20 mL) and the aqueous phase was extracted two more times with EtOAc (2 x 30 mL). The combined organic phases were washed with brine (15 mL), dried over magnesium sulfate and concentrated in vacuo. The crude product was purified by FCC (1:4 EtOAc/PE) to yield **5a** as a white solid (0.86 g, 80%).

5.2.5. Asymmetric Studies

5.2.5.1. Synthesis of Catalysts

β-Isocupreidine

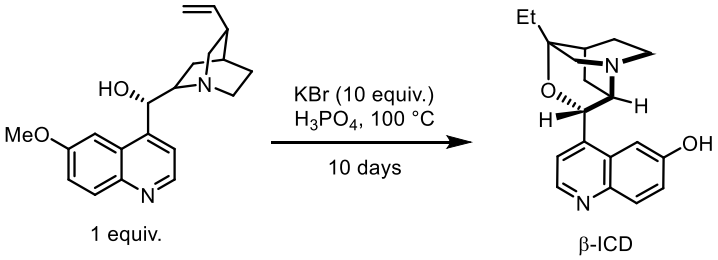

1 equiv. β-ICD

To a 50 mL round-bottomed flask, equipped with a magnetic stirrer bar, was charged quinidine (1 g, 3.1 mmol, 1 equiv.), potassium bromide (3.69 g, 31 mmol, 10 equiv.), and phosphoric acid (15 mL, 85 wt % in water). The resulting mixture was heated at 100 °C for 10 days. Upon completion, the reaction was allowed to cool to room temperature and the pH was adjusted to 8 using a cooled solution of 25% potassium hydroxide. The mixture was transferred to a separatory funnel and extracted with chloroform (50 mL). The organic phase was washed with brine and dried over potassium carbonate. After concentrating in vacuo, the crude compound was purified by FCC (1:9 to 1.5:8.5 MeOH/$CHCl_3$) to give the title compound as an off-white solid (0.47 g, 49%), with physical properties and spectroscopic data in accordance with the literature;[19] **R_f** = 0.47 (1.5:8.5 MeOH/$CHCl_3$); **mp** 172 – 174 °C; $[\boldsymbol{\alpha}]_{\boldsymbol{D}}^{\boldsymbol{20}}$ = -3.0 (c = 1, $CHCl_3$); **^{1}H NMR** (500 MHz, $CDCl_3$) δ_H: 8.73 (d, *J* = 4.4, 1H), 8.07 (s, 1H), 7.97 (d, *J* = 9.0, 1H), 7.64 (dd, *J* = 4.4, 0.9, 1H), 7.28 – 7.25 (m, 1H), 6.05 (s, 1H), 3.81 (d, *J* = 13.5, 1H), 3.60 (d, *J* = 5.9, 1H), 3.29 – 3.20 (m, 1H), 3.13 – 3.06 (m, 1H), 2.84 (d, *J* = 13.5, 1H), 2.30 – 2.22 (m, 1H), 1.90 (ddd, *J* = 12.8, 6.6, 2.0, 1H), 1.83 – 1.62 (m, 4H), 1.32 – 1.23 (m, 1H), 1.06 (t, *J* = 7.5, 3H); **^{13}C {^{1}H} NMR** (126 MHz, $CDCl_3$) δ_C: 156.6, 147.0, 143.4, 141.5, 131.5, 127.2, 122.4, 119.1, 106.3, 77.0, 72.5, 56.8, 54.0, 46.5, 32.9, 27.5, 23.2, 23.1, 7.4.

α-Isocupreine

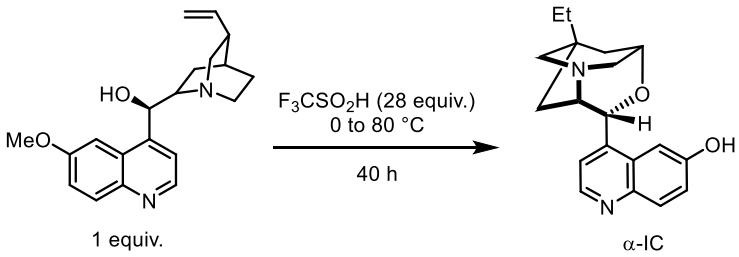

To a 25 mL round-bottomed flask, equipped with a magnetic stirrer bar, was charged quinine (1.02 g, 3.1 mmol, 1 equiv.) and triflic acid (7.7 mL, 86.6 mmol, 28 equiv.) at 0 °C. The resulting mixture was heated at 50 °C for 24 hours, then at 80 °C for a further 16 hours. Upon completion, the reaction was allowed to cool to room temperature and the pH was adjusted to 8 using a cooled solution of aqueous sodium carbonate. The mixture was transferred to a separatory funnel and extracted with chloroform (50 mL). The organic phase was washed with brine and dried over potassium carbonate. After concentrating in vacuo, the crude compound was purified by FCC (0.5:9.5 to 1:9 MeOH/$CHCl_3$) to give the title compound as an off-white solid (0.37 g, 38%), with physical properties and spectroscopic data in accordance with the literature;[20] **R_f** = 0.48 (1:9 MeOH/$CHCl_3$); **mp** 229 – 231 °C (decomposition); $[\boldsymbol{\alpha}]_{\boldsymbol{D}}^{\boldsymbol{20}}$ = -8.5 (c = 1, $CHCl_3$); **^{1}H NMR** (500 MHz, $CDCl_3$) δ_H: 8.72 (d, *J* = 4.4, 1H), 7.96 (d, *J* = 9.0, 1H), 7.86 (d, *J* = 2.5, 1H), 7.56 (dd, *J* = 4.4, 0.7, 1H), 7.24 (dd, *J* = 9.0, 2.5, 1H), 5.91 (s, 1H), 4.45 (s, 1H), 4.10 (d, *J* = 14.5, 1H), 4.04 (d, *J* = 9.9, 1H), 3.01 – 2.92 (m, 2H), 2.90 – 2.84 (m, 1H), 2.06 – 1.99 (m, 1H), 1.94 – 1.84 (m, 2H), 1.49 – 1.36 (m, 2H), 1.23 – 1.15 (m, 1H), 0.90 (t, *J* = 7.5, 3H); **^{13}C {^{1}H} NMR** (126 MHz, $CDCl_3$) δ_C: 156.6, 147.2, 143.3, 142.8, 131.5, 127.0, 122.1, 118.5, 106.1, 69.8, 68.2, 66.9, 64.3, 53.3, 43.0, 41.8, 37.1, 29.2, 9.5.

5.2.5.2. Asymmetric Aza-MBH Reaction

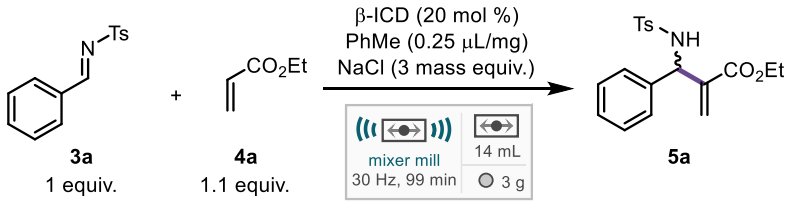

To a 14 mL stainless steel jar, equipped with a 3 g, 9 mm stainless steel ball, was charged *N*-benzylidene-4-methylbenzenesulfonamide (64.8 mg, 0.25 mmol, 1 equiv.), ethyl acrylate (30.5 µL, 0.28 mmol, 1.1 equiv.), β-isocupreidine (15.5 mg, 0.05 mmol,

20 mol %), toluene (25 µL), sodium chloride (300 mg, 3.0 mass equiv.). The jar was closed and placed on the mixer-mill to be milled at 30 Hz for 99 minutes. Upon completion, the reaction mixture was transferred to a separatory funnel by washing the jar with EtOAc (30 mL) and water (30 mL). The organic layer was washed with 1 M HCl (20 mL) and the aqueous phase was extracted two more times with EtOAc (2 x 30 mL). The combined organic phases were washed with brine (15 mL), dried over magnesium sulfate and concentrated in vacuo. The crude product was purified by FCC (1:4 EtOAc/PE) to give **5a** as a white solid (17.8 mg, 20%, 64% ee), Chiral HPLC (Chiralpak IA, 10:90 IPA/hexane, 1 mL/min, 211 nm, 25 °C); t_R = 22 min, t_R = 24 min.

5.2.5.3. Asymmetric Solution Comparison

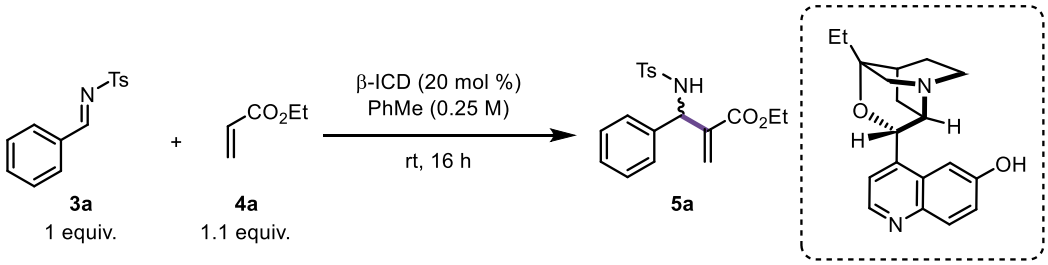

To a 5 mL microwave vial, equipped with a magnetic stirrer bar, was charged *N*-benzylidene-4-methylbenzenesulfonamide (64.8 mg, 0.25 mmol, 1 equiv.), ethyl acrylate (30.5 µL, 0.28 mmol, 1.1 equiv.), β-isocupreidine (15.5 mg, 0.05 mmol, 20 mol %) and toluene (1 mL). A rubber septum was used to seal the vial and the mixture was stirred at room temperature for 16 hours. Upon completion, the reaction mixture was transferred to a separatory funnel using EtOAc (10 mL) and water (10 mL). The organic layer was washed with 1 M HCl (10 mL) and the aqueous phase was extracted two more times with EtOAc (2 x 10 mL). The combined organic phases were washed with brine (10 mL), dried over magnesium sulfate and concentrated in vacuo. The crude product was purified by FCC (1:4 EtOAc/PE) to give **5a** as a white solid (21.7 mg, 24%, 78% ee), Chiral HPLC (Chiralpak IA, 10:90 IPA/hexane, 1 mL/min, 211 nm, 25 °C); t_R = 22 min, t_R = 24 min.

5.2.6. One-Pot Procedure

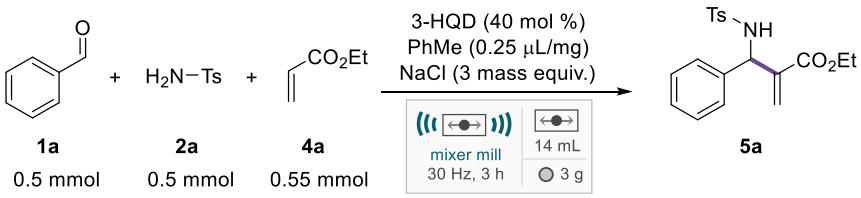

To a 14 mL stainless steel jar, equipped with a 3 g, 9 mm stainless steel ball, was charged benzaldehyde (50.8 µL, 0.5 mmol, 1 equiv.), 4-methylbenzenesulfonamide (85.6 mg, 0.5 mmol, 1 equiv.), ethyl acrylate (60.0 mg, 0.55 mmol, 1.1 equiv.), 3-HQD (25.4 mg, 0.4 mmol, 40 mol %), toluene (50 µL), sodium chloride (600 mg, 3.0 mass equiv.). The jar was closed and placed on the mixer-mill to be milled at 30 Hz for 3 hours. Upon completion, the reaction mixture was transferred to a separatory funnel by washing the jar with EtOAc (30 mL) and water (30 mL). The organic layer was washed with 1 M HCl (20 mL) and the aqueous phase was extracted two more times with EtOAc (2 x 30 mL). The combined organic phases were washed with brine (15 mL), dried over magnesium sulfate and concentrated in vacuo. The crude product was purified by FCC (1:4 EtOAc/PE) to give **5a** as a white solid (49.4 mg, 27%).

5.2.7. Solution-Phase and Neat-Stirred Comparisons

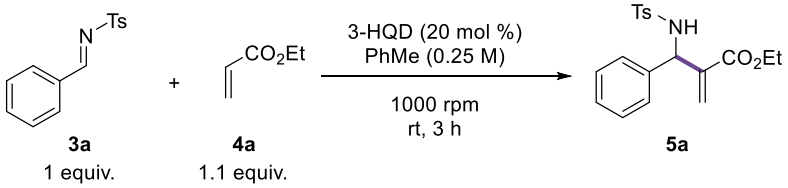

To a 5 mL microwave vial, equipped with a magnetic stirrer bar, was charged *N*-benzylidene-4-methylbenzenesulfonamide (64.8 mg, 0.25 mmol, 1 equiv.), ethyl acrylate (30.5 µL, 0.28 mmol, 1.1 equiv.), 3-HQD (6.4 mg, 0.05 mmol, 20 mol %), and toluene (1 mL) for the solution-phase experiments. The mixture was stirred at room temperature, at 1000 rpm, for up to 3 hours. For analysis, 1 M HCl (1 mL), EtOAc (1 mL), and mesitylene were added and the mixture was stirred for 2 minutes. The phases were allowed to settle, and an aliquot of the organic phase was taken for ^{1}H NMR analysis.

5.3. Mechanochemical Cross-Electrophile Coupling of Heteroaryl Halides and Alkyl Halides

5.3.1. Experimental and Characterisation Data

5.3.2. General Procedure C – Synthesis of Amidine Ligands

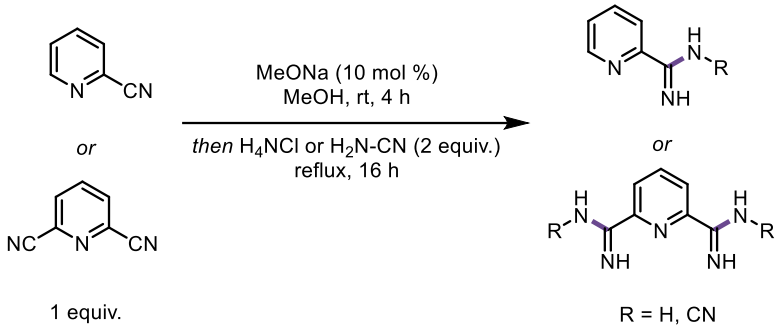

To a round-bottomed flask, equipped with a magnetic stirrer, was charged 2-pyridinecarbontrile or 2,6-pyridinecarbonitrile (1 equiv.) and methanol (0.5 M), under a nitrogen atmosphere. Sodium methoxide (0.5 M solution in methanol, 0.1 equiv.) was added, and the resulting mixture was stirred at room temperature for 4 hours. Ammonium chloride or cyanamide (2 equiv.) was then added in one portion and the reaction mixture was heated to reflux and stirred for 16 hours. After cooling to room temperature, the formed precipitate was filtered under suction, which, in the case of using cyanamide was spectroscopically pure product. When using ammonium chloride, the filtrate was concentrated in vacuo and the resulting crude compound was heated in ethanol (1 mL/mmol), then filtered while hot to yield the product.

Picolinimidamide hydrogen chloride (L8)

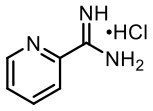

Prepared according to general procedure C from 2-pyridinecarbonitrile (20 mmol) and ammonium chloride, to give the title compound as a white solid (3.14 g, >98%), with physical and spectroscopic data in accordance with the literature;[21] **mp** 90 – 92 °C; **^{1}H NMR** (500 MHz, $(CD_3)SO$) δ_H: 8.82 (d, *J* = 4.2, 1H), 8.51 (br s, 4H), 8.43 (d, *J* = 7.9, 1H), 8.16 (td, *J* = 7.8, 1.4, 1H), 7.79 (dd, *J* = 7.3, 4.8, 1H); **^{13}C {^{1}H} NMR** (126 MHz, $(CD_3)SO$) δ_C: 162.2, 150.0, 144.0, 138.4, 128.6, 123.6.

_N_-cyanopicolinimidamide (L9)

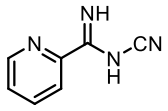

Prepared according to general procedure C from 2-pyridinecarbonitrile (9.6 mmol) and cyanamide, to give the title compound as a white solid (0.36 g, 26%), with physical and spectroscopic data in accordance with the literature;[21] **mp** 194 – 196 °C; **^{1}H NMR** (500 MHz, $(CD_3)SO$) δ_H: 9.11 (br s, 2H), 8.71 (dd, *J* = 4.7, 0.6, 1H), 8.13 (d, *J* = 7.9, 1H), 8.00 (td, *J* = 7.8, 1.7, 1H), 7.67 (ddd, *J* = 7.6, 4.8, 1.1, 1H); **^{13}C {^{1}H} NMR** (126 MHz, $(CD_3)SO$) δ_C: 165.7, 149.1, 148.1, 138.0, 127.5, 122.5, 116.3.

Pyridine-2,6-bis(carboximidamide) dihydrogen chloride (L10)

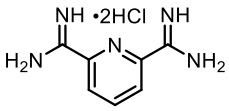

Prepared according to general procedure C from 2,6-pyridinecarbonitrile (7.7 mmol) and ammonium chloride, to give the title compound as a pale yellow solid (1.83 g, >98%), with physical and spectroscopic data in accordance with the literature;[21] **mp** >300 °C (decomposition); **^{1}H NMR** (500 MHz, $(CD_3)SO$) δ_H: 9.79 (br s, 8H), 8.81 (d, *J* = 8.0, 2H), 8.53 (t, *J* = 8.0, 1H); **^{13}C {^{1}H} NMR** (126 MHz, $(CD_3)SO$) δ_C: 160.4, 144.1, 140.8, 127.3.

_N_^{2},_N_^{6}-dicyanopyridine-2,6-bis(carboximidamide) (L11)

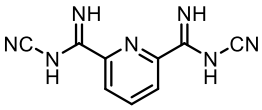

Prepared according to general procedure C from 2,6-pyridinecarbonitrile (7.7 mmol) and cyanamide, to give the title compound as a white solid (1.35 g, 81%), with physical and spectroscopic data in accordance with the literature;[22] **mp** >300 °C (decomposition); **^{1}H NMR** (500 MHz, $(CD_3)SO$) δ_H: 9.94 (br s, 2H), 9.16 (br s, 2H), 8.36 (d, *J* = 7.9, 2H), 8.17 (t, *J* = 7.9, 1H); **^{13}C {^{1}H} NMR** (126 MHz, $(CD_3)SO$) δ_C: 164.6, 147.4, 140.0, 125.8, 116.3.

5.3.3. General Procedure D – Mechanochemical Cross-Electrophile Coupling

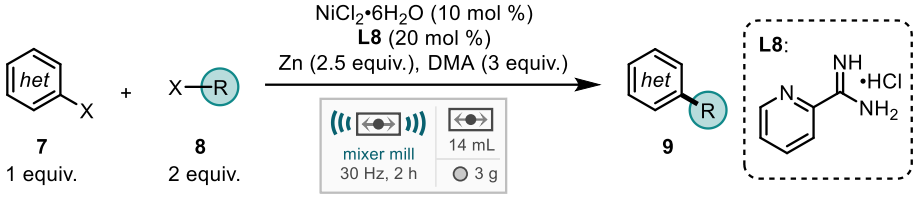

To a 14 mL stainless steel jar, equipped with a 3 g stainless steel ball, was charged nickel chloride hexahydrate (7.1 mg, 0.03 mmol, 10 mol %), amidine ligand **L8** (9.5 mg, 0.06 mmol, 20 mol %), zinc granular 20 – 30 mesh (49.0 mg, 0.75 mmol, 2.5 equiv.), followed by heteroaryl halide (0.3 mmol, 1 equiv.), alkyl halide (0.6 mmol, 2 equiv.) and *N*,*N*-dimethylacetamide (83.7 µL, 0.9 mmol, 3 equiv.). The jar was closed and placed on the mixer mill, to be milled at 30 Hz for 2 hours. Upon completion, the reaction mixture was transferred to a separatory funnel using ethyl acetate (50 mL) and water (50 mL), and the organic phase was washed twice with a 5% solution of ammonium hydroxide (2 x 20 mL). The aqueous phase was extracted once more with ethyl acetate (50 mL) and the combined organic phases were washed with brine (20 mL), then dried over magnesium sulfate and filtered. After concentrating in vacuo, the crude material was purified by FCC, in the stated solvent system, to give the cross-coupled product.

N.B. For coupling with alkyl bromides, 2 equivalents of sodium iodide were used.

3-octylpyridine (9a)

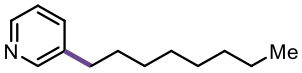

Prepared according to general procedure D from 3-bromopyridine and 1-iodooctane, followed by purification by FCC (0.5:9.5 EtOAc/hexane) to give the title compound as a pale yellow oil (27.6 mg, 48%), with physical and spectroscopic data in accordance with the literature;[23] $\mathbf{R_f}$ = 0.16 (0.5:9.5 EtOAc/hexane); **^{1}H NMR** (500 MHz, $CDCl_3$) δ_H: 8.46 – 8.41 (m, 2H, Ar*H*), 7.50 – 7.46 (m, 1H, Ar*H*), 7.20 (dd, *J* = 7.7, 4.8, 1H, Ar*H*), 2.64 – 2.54 (m, 2H, ArC*H*$_2$), 1.60 (dt, *J* = 15.3, 7.6, 2H, C*H*$_2$), 1.37 – 1.19 (m, 10H, C*H*$_2$), 0.87 (t, *J* = 7.0, 3H, C*H*$_3$); **^{13}C {^{1}H} NMR** (126 MHz, $CDCl_3$) δ_C: 150.1 (Ar*C*H), 147.3 (Ar*C*H), 138.1 (Ar*C*), 135.9 (Ar*C*H), 123.4 (Ar*C*H), 33.2 (Ar-*C*H$_2$), 32.0 (*C*H$_2$), 31.3 (*C*H$_2$), 29.5 (*C*H$_2$), 29.4 (*C*H$_2$), 29.3 (*C*H$_2$), 22.8 (*C*H$_2$), 14.3 (*C*H$_3$).

2-octylpyridine (9b)

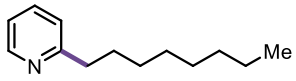

Prepared according to general procedure D from 2-bromopyridine and 1-iodooctane, followed by purification by FCC (0.5:9.5 EtOAc/hexane) to give the title compound as a pale yellow oil (41.1 mg, 72%), with physical and spectroscopic data in accordance with the literature;[24] **R_f** = 0.14 (0.5:9.5 EtOAc/hexane); **^{1}H NMR** (500 MHz, $CDCl_3$) δ_H: 8.53 – 8.50 (m, 1H), 7.57 (td, *J* = 7.6, 1.8, 1H), 7.13 (d, *J* = 7.8, 1H), 7.11 – 7.05 (m, 1H), 2.80 – 2.73 (m, 2H), 1.74 – 1.67 (m, 2H), 1.39 – 1.22 (m, 10H), 0.86 (t, *J* = 7.0, 3H); **^{13}C {^{1}H} NMR** (126 MHz, $CDCl_3$) δ_C: 162.9, 149.3, 136.4, 122.8, 121.0, 38.6, 32.0, 30.1, 29.6 (2C), 29.4, 22.8, 14.3.

2-(3-phenylpropyl)pyridine (9d)

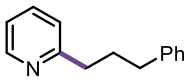

Prepared according to general procedure D from 2-bromopyridine and 1-bromo-3-phenylpropane, followed by purification by FCC (1:4 EtOAc/hexane) to give the title compound as a yellow oil (33.1 mg, 56%), with physical and spectroscopic data in accordance with the literature;[22] **R_f** = 0.16 (1:4 EtOAc/hexane); **^{1}H NMR** (500 MHz, $CDCl_3$) δ_H: 8.54 – 8.52 (m, 1H), 7.58 (td, *J* = 7.7, 1.9, 1H), 7.31 – 7.26 (m, 2H), 7.22 – 7.16 (m, 3H), 7.15 – 7.12 (m, 1H), 7.10 (ddd, *J* = 7.5, 4.9, 1.1, 1H), 2.86 – 2.79 (m, 2H), 2.72 – 2.64 (m, 2H), 2.12 – 2.03 (m, 2H); **^{13}C {^{1}H} NMR** (126 MHz, $CDCl_3$) δ_C: 162.1, 149.4, 142.3, 136.4, 128.6, 128.4, 125.9, 122.9, 121.1, 38.0, 35.7, 31.6.

5-octylpyrimidine (9e)

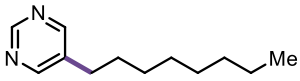

Prepared according to general procedure D from 5-bromopyrimidine and 1-iodooctane, followed by purification by FCC (1:4 EtOAc/hexane) to give the title compound as a colourless oil (24.8 mg, 43%), with physical and spectroscopic data in accordance with the literature;[25] **R_f** = 0.20 (1:4 EtOAc/hexane); **^{1}H NMR** (500 MHz, $CDCl_3$) δ_H: 9.06 (s, 1H), 8.57 (s, 2H), 2.64 – 2.55 (m, 2H), 1.66 – 1.59 (m, 2H), 1.38 – 1.20 (m, 10H), 0.87 (t, *J* = 7.0, 3H); **^{13}C {^{1}H} NMR** (126 MHz, $CDCl_3$) δ_C: 156.8, 156.7, 135.7, 31.9, 30.9, 30.5, 29.4, 29.3, 29.2, 22.8, 14.2.

5-methyl-2-octylpyridine (9f)

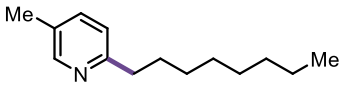

Prepared according to general procedure D from 2-bromo-5-methylpyridine and 1-iodooctane, followed by purification by FCC (0.5:9.5 EtOAc/hexane) to give the title compound as a colourless oil (40.3 mg, 65%); **R_f** = 0.15 (0.5:9.5 EtOAc/hexane); **ν_{max}/cm^{-1}** (film): 2922, 2853, 1603, 1568, 1487, 1381, 1030, 824, 723, 646, 559, 407; **^{1}H NMR** (500 MHz, $CDCl_3$) δ_H: 8.34 (s, 1H), 7.38 (dd, *J* = 7.9, 1.8, 1H), 7.02 (d, *J* = 7.9, 1H), 2.76 – 2.68 (m, 2H), 2.28 (s, 3H), 1.72 – 1.65 (m, 2H), 1.38 – 1.18 (m, 10H), 0.86 (t, *J* = 7.0, 3H); **^{13}C {^{1}H} NMR** (126 MHz, $CDCl_3$) δ_C: 159.7, 149.6, 137.0, 130.1, 122.2, 38.1, 32.0, 30.2, 29.6 (2C), 29.4, 22.8, 18.2, 14.3; **HRMS** (CI) calculated for $[C_{14}H_{24}N]^+$ $(M+H)^+$: m/z 206.1903 found 206.1904 (+0.2 ppm).

5-fluoro-2-octylpyridine (9g)

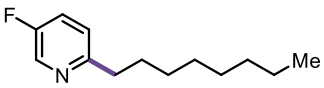

Prepared according to general procedure D from 2-bromo-5-fluoropyridine and 1-iodooctane, followed by purification by FCC (0.3:9.7 EtOAc/hexane) to give the title compound as a colourless oil (42.5 mg, 68%); **R_f** = 0.29 (0.5:9.5 EtOAc/hexane); **ν_{max}/cm^{-1}** (film): 2924, 2855, 1585, 1483, 1468, 1339, 1225, 1020, 908, 829; **^{1}H NMR** (400 MHz, $CDCl_3$) δ_H: 8.37 (d, *J* = 2.9, 1H), 7.29 (td, *J* = 8.5, 3.0, 1H), 7.12 (dd, *J* = 8.6, 4.4, 1H), 2.81 – 2.71 (m, 2H), 1.69 (quintet, *J* = 7.6, 2H), 1.39 – 1.18 (m, 10H), 0.87 (t, *J* = 6.9, 3H); **^{13}C {^{1}H} NMR** (126 MHz, $CDCl_3$) δ_C: 158.6 (d, *J* = 3.8), 158.1 (d, *J* = 25.3), 137.2 (d, *J* = 23.9), 123.4 (d, *J* = 3.8), 123.1 (d, *J* = 17.6), 37.7 (d, *J* = 1.3), 32.0, 30.1, 30.0, 29.4 (2C), 22.8, 14.2; **^{19}F {^{1}H} NMR** (376 MHz, $CDCl_3$) δ_F: -131.94; **HRMS** (CI) calculated for $[C_{13}H_{21}NF]^+$ $(M+H)^+$: m/z 210.1653 found 210.1651 (-0.5 ppm).

6-octylnicotinonitrile (9h)

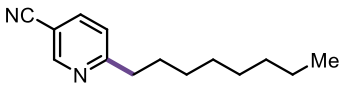

Prepared according to general procedure D from 6-bromonicotinonitrile and 1-iodooctane, followed by purification by FCC (0.3:9.7 EtOAc/hexane) to give the title compound as a colourless, viscous oil (29.2 mg, 46%); **R_f** = 0.06 (0.3:9.7 EtOAc/hexane); **ν_{max}/cm^{-1}** (film): 2924, 2855, 2232, 1593, 1553, 1481, 1452, 1379,

1092, 1024, 833; **^{1}H NMR** (500 MHz, $CDCl_3$) δ_H: 8.80 – 8.79 (m, 1H), 7.85 (dd, *J* = 8.1, 2.2, 1H), 7.28 – 7.26 (m, 1H), 2.89 – 2.80 (m, 2H), 1.78 – 1.66 (m, 2H), 1.39 – 1.19 (m, 10H), 0.87 (t, *J* = 7.0, 3H); **^{13}C {^{1}H} NMR** (126 MHz, $CDCl_3$) δ_C: 167.4, 152.3, 139.4, 122.9, 117.2, 107.2, 38.9, 32.0, 29.6, 29.5, 29.4, 29.3, 22.8, 14.2; **HRMS** (CI) calculated for $[C_{14}H_{21}N_2]^+$ $(M+H)^+$: m/z 217. 1699 found 217.1699 (+0.1 ppm).

2-octyl-5-(trifluoromethyl)pyridine (9i)

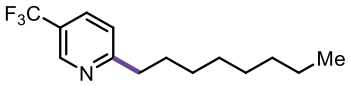

Prepared according to general procedure D from 2-bromo-5-(trifluoromethyl)pyridine and 1-iodooctane, followed by purification by FCC (0.5:9.5 EtOAc/hexane) to give the title compound as a colourless oil (38.9 mg, 50%); **R_f** = 0.47 (1:9 EtOAc/hexane); **ν_{max}/cm^{-1}** (film): 2926, 2857, 1609, 1574, 1325, 1161, 1126, 1078, 1016; **^{1}H NMR** (400 MHz, $CDCl_3$) δ_H: 8.78 (s, 1H), 7.81 (dd, *J* = 8.2, 2.2, 1H), 7.26 (d, *J* = 8.2, 1H), 2.91 – 2.78 (m, 2H), 1.80 – 1.67 (m, 2H), 1.40 – 1.19 (m, 10H), 0.87 (t, *J* = 6.9, 3H); **^{13}C {^{1}H} NMR** (126 MHz, $CDCl_3$) δ_C: 166.8, 146.3 (q, *J* = 3.8), 133.4 (q, *J* = 3.8), 123.9 (q, *J* = 272.2), 124.1 (q, *J* = 32.8), 122.5, 38.6, 32.0, 29.8, 29.5 (2C), 29.3, 22.8, 14.2; **^{19}F {^{1}H} NMR** (376 MHz, $CDCl_3$) δ_F: -62.22; **HRMS** (CI) calculated for $[C_{14}H_{21}NF_3]^+$ $(M+H)^+$: m/z 260.1621 found 260.1625 (+1.8 ppm).

5-Chloro-2-octylpyridine (9j)

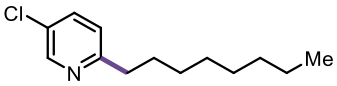

Prepared according to general procedure D from 2-bromo-5-chloropyridine and 1-iodooctane, followed by purification by FCC (0.5:9.5 EtOAc/hexane) to give the title compound as a colourless oil (41.7 mg, 62%); **R_f** = 0.47 (1:9 EtOAc/hexane); **ν_{max}/cm^{-1}** (film): 2923, 2855, 1580, 1560, 1468, 1376, 1112, 1013; **^{1}H NMR** (500 MHz, $CDCl_3$) δ_H: 8.48 – 8.46 (m, 1H), 7.55 (dd, *J* = 8.3, 2.5, 1H), 7.09 (d, *J* = 8.3, 1H), 2.79 – 2.71 (m, 2H), 1.72 – 1.65 (m, 2H), 1.38 – 1.19 (m, 10H), 0.87 (t, *J* = 7.0, 3H); **^{13}C {^{1}H} NMR** (126 MHz, $CDCl_3$) δ_C: 160.9, 148.1, 136.1, 129.3, 123.6, 37.9, 32.0, 30.0, 29.6, 29.4 (2C), 22.8, 14.2; **HRMS** (ES) calculated for $[C_{13}H_{21}N^{35}Cl]^+$ $(M+H)^+$: m/z 226.1356 found 226.1363 (+3.1 ppm).

6-octylpyridin-3-ol (9k)

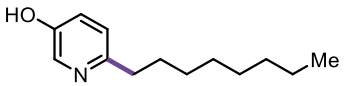

Prepared according to general D procedure from 2-bromo-5-hydroxypyridine and 1-iodooctane, followed by purification by FCC (1:3 EtOAc/hexane) to give the title compound as a pale yellow oil (21.3 mg, 34%); $\mathbf{R_f}$ = 0.15 (1:3 EtOAc/hexane); $\mathbf{\nu_{max}/cm^{-1}}$ (film): 2980, 2970, 2957, 2924, 2853, 2627, 1572, 1495, 1460, 1275, 833, 739, 654; **^{1}H NMR** (500 MHz, $CDCl_3$) δ_H: 8.18 (d, *J* = 2.1, 1H), 7.24 (dd, *J* = 8.5, 2.6, 1H), 7.10 (d, *J* = 8.5, 1H), 2.79 – 2.67 (m, 2H), 1.69 – 1.57 (m, 2H), 1.36 – 1.13 (m, 10H), 0.86 (t, *J* = 7.0, 3H); **^{13}C {^{1}H} NMR** (126 MHz, $CDCl_3$) δ_C: 153.2, 152.8, 135.7, 125.8, 124.3, 36.5, 32.0, 30.5, 29.5, 29.4 (2C), 22.8, 14.3; **HRMS** (ES) calculated for $[C_{13}H_{22}NO]^+$ $(M+H)^+$: m/z 208.1700 found 208.1701 (+0.5 ppm).

5-methoxy-2-octylpyridine (9l)

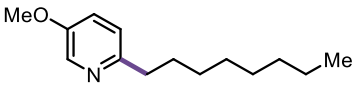

Prepared according to general procedure D from 2-bromo-5-methoxypyridine and 1-iodooctane, followed by purification by FCC (1:9 EtOAc/hexane) to give the title compound as a colourless oil (37.4 mg, 56%); $\mathbf{R_f}$ = 0.14 (1:9 EtOAc/hexane); $\mathbf{\nu_{max}/cm^{-1}}$ (film): 2980, 2970, 2957, 2922, 2853, 1572, 1495, 1483, 1464, 1395, 1034, 824; **^{1}H NMR** (500 MHz, $CDCl_3$) δ_H: 8.22 (d, *J* = 2.9, 1H), 7.12 (dd, *J* = 8.5, 3.0, 1H), 7.05 (d, *J* = 8.5, 1H), 3.83 (s, 3H), 2.74 – 2.68 (m, 2H), 1.72 – 1.61 (m, 2H), 1.38 – 1.15 (m, 10H), 0.87 (t, *J* = 7.0, 3H); **^{13}C {^{1}H} NMR** (126 MHz, $CDCl_3$) δ_C: 154.8, 153.9, 136.4, 122.8, 121.4, 55.7, 37.6, 32.0, 30.3, 29.6, 29.5, 29.4, 22.8, 14.3; **HRMS** (CI) calculated for $[C_{14}H_{24}ON]^+$ $(M+H)^+$: m/z 222.1852 found 222.1856 (+1.5 ppm).

6-octylpyridin-3-amine (9m)

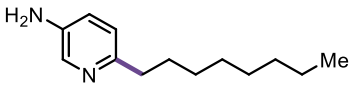

Prepared according to general procedure D from 5-amino-2-bromopyridine and 1-iodooctane, followed by purification by FCC (1:1 to 3:2 EtOAc/hexane) to give the title compound as an orange oil (25.0 mg, 40%); $\mathbf{R_f}$ = 0.12 (1:1 EtOAc/hexane); $\mathbf{\nu_{max}/cm^{-1}}$ (film): 3337, 3204, 2980, 2970, 2922, 2853, 1632, 1572, 1493, 1260, 1138, 829; **^{1}H NMR** (500 MHz, $CDCl_3$) δ_H: 8.04 (t, *J* = 1.7, 1H), 6.94 – 6.93 (m, 2H), 3.58 (br s, 2H), 2.72 – 2.61 (m, 2H), 1.71 – 1.60 (m, 2H), 1.37 – 1.15 (m, 10H), 0.87 (t, *J* = 7.0, 3H);

^{13}C {^{1}H} NMR (126 MHz, $CDCl_3$) δ_C: 152.7, 140.2, 136.7, 122.9, 122.8, 37.4, 32.0, 30.4, 29.6, 29.5, 29.4, 22.8, 14.3; **HRMS** (CI) calculated for $[C_{13}H_{23}N_2]^+$ $(M+H)^+$: m/z 207.1856 found 207.1859 (+1.4 ppm).

***N*-(6-octylpyridin-3-yl)acetamide (9n)**

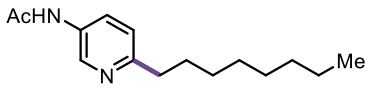

Prepared according to general procedure D from 5-acetamido-2-bromopyridine and 1-iodooctane, followed by purification by FCC (7:3 EtOAc/hexane) to give the title compound as an off-white solid (33.9 mg, 46%); **R_f** = 0.11 (7:3 EtOAc/hexane); **mp** 77 – 79 °C; **ν_{max}/cm^{-1}** (film): 3254, 2980, 2922, 2855, 1670, 1491, 1383, 1302, 750; **^{1}H NMR** (500 MHz, $CDCl_3$) δ_H: 8.41 (d, *J* = 2.5, 1H), 8.06 (dd, *J* = 8.4, 2.6, 1H), 7.63 (br s, 1H), 7.11 (d, *J* = 8.4, 1H), 2.77 – 2.69 (m, 2H), 2.19 (s, 3H), 1.72 – 1.62 (m, 2H), 1.38 – 1.16 (m, 10H), 0.86 (t, *J* = 7.0, 3H); **^{13}C {^{1}H} NMR** (126 MHz, $CDCl_3$) δ_C: 168.9, 158.4, 140.6, 132.5, 128.3, 122.8, 37.8, 32.0, 30.1, 29.6, 29.5, 29.4, 24.5, 22.8, 14.2; **HRMS** (CI) calculated for $[C_{15}H_{25}ON_2]^+$ $(M+H)^+$: m/z 249.1961 found 249.1964 (+1.1 ppm).

Ethyl 4-(pyridin-2-yl)butanoate (9p)

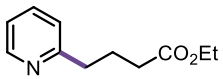

Prepared according to general procedure D from 2-bromopyridine and ethyl 4-bromobutyrate, followed by purification by FCC (2:3 EtOAc/hexane) to give the title compound as a yellow oil (41.8 mg, 72%), with physical and spectroscopic data in accordance with the literature;[26] **R_f** = 0.25 (2:3 EtOAc/hexane); **^{1}H NMR** (500 MHz, $CDCl_3$) δ_H: 8.52 – 8.50 (m, 1H), 7.58 (td, *J* = 7.7, 1.9, 1H), 7.14 (d, *J* = 7.8, 1H), 7.10 (ddd, *J* = 7.5, 4.9, 1.1, 1H), 4.11 (q, *J* = 7.1, 2H), 2.85 – 2.78 (m, 2H), 2.35 (t, *J* = 7.5, 2H), 2.10 – 2.02 (m, 2H), 1.24 (t, *J* = 7.1, 3H); **^{13}C {^{1}H}** NMR (126 MHz, $CDCl_3$) δ_C: 173.5, 161.3, 149.4, 136.5, 123.0, 121.3, 60.4, 37.5, 33.8, 25.0, 14.4.

Ethyl 4-(pyridin-3-yl)butanoate (9q)

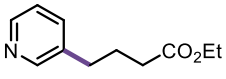

Prepared according to general procedure D from 3-bromopyridine and ethyl 4-bromobutyrate, followed by purification by FCC (2:3 EtOAc/hexane) to give the title compound as a yellow oil (28.7 mg, 49%), with physical and spectroscopic data in

accordance with the literature;[27] **R_f** = 0.18 (2:3 EtOAc/hexane); **^{1}H NMR** (500 MHz, $CDCl_3$) δ_H: 8.47 – 8.41 (m, 2H), 7.53 – 7.48 (m, 1H), 7.21 (ddd, *J* = 7.8, 4.8, 0.7, 1H), 4.12 (q, *J* = 7.1, 2H), 2.68 – 2.61 (m, 2H), 2.32 (t, *J* = 7.4, 2H), 1.99 – 1.90 (m, 2H), 1.25 (t, *J* = 7.1, 3H); **^{13}C {^{1}H} NMR** (126 MHz, $CDCl_3$) δ_C: 173.3, 150.0, 147.6, 136.9, 136.1, 123.5, 60.6, 33.6, 32.3, 26.3, 14.4.

Ethyl 4-(pyridin-4-yl)butanoate (9r)

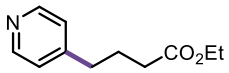

Prepared according to general procedure D from 4-bromopyridine hydrogen chloride and ethyl 4-bromobutyrate, followed by purification by FCC (2:3 EtOAc/hexane) to give the title compound as a yellow oil (14.5 mg, 25%), with physical and spectroscopic data in accordance with the literature;[26] **R_f** = 0.12 (2:3 EtOAc/hexane); **^{1}H NMR** (500 MHz, $CDCl_3$) δ_H: 8.50 – 8.48 (m, 2H), 7.12 – 7.10 (m, 2H), 4.13 (q, *J* = 7.1, 2H), 2.68 – 2.61 (m, 2H), 2.32 (t, *J* = 7.4, 2H), 2.00 – 1.92 (m, 2H), 1.25 (t, *J* = 7.1, 3H); **^{13}C {^{1}H} NMR** (126 MHz, $CDCl_3$) δ_C: 173.2, 150.5, 149.9, 124.1, 60.6, 34.5, 33.6, 25.5, 14.4.

Ethyl 4-(pyrimidin-5-yl)butanoate (9s)

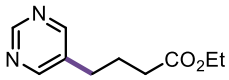

Prepared according to general procedure D from 5-bromopyrimidine and ethyl 4-bromobutyrate, followed by purification by FCC (2:3 to 1:1 EtOAc/hexane) to give the title compound as a colourless oil (38.9 mg, 67%); **R_f** = 0.09 (1:1 EtOAc/hexane); **ν_{max}/cm^{-1}** (film): 2980, 1728, 1560, 1410, 1182, 727, 633; **^{1}H NMR** (400 MHz, $CDCl_3$) δ_H: 9.07 (s, 1H), 8.58 (s, 2H), 4.13 (q, *J* = 7.1, 2H), 2.71 – 2.61 (m, 2H), 2.35 (t, *J* = 7.2, 2H), 2.02 – 1.90 (m, 2H), 1.25 (t, *J* = 7.1, 3H); **^{13}C {^{1}H} NMR** (101 MHz, $CDCl_3$) δ_C: 172.9, 157.1, 156.9, 134.5, 60.9, 33.4, 29.8, 25.9, 14.4; **HRMS** (CI) calculated for $[C_{10}H_{15}O_2N_2]^+$ $(M+H)^+$: m/z 195.1128 found 195.1127 (-0.3 ppm).

Ethyl 4-(pyrimidin-2-yl)butanoate (9t)

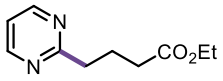

Prepared according to general procedure D from 2-bromopyrimidine and ethyl 4-bromobutyrate, followed by purification by FCC (1:1 EtOAc/hexane) to give the title compound as a yellow oil (24.4 mg, 42%); $\mathbf{R_f}$ = 0.16 (1:1 EtOAc/hexane); $\mathbf{\nu_{max}/cm^{-1}}$ (film): 2980, 1728, 1560, 1423, 1239, 1163, 635; **^{1}H NMR** (500 MHz, $CDCl_3$) δ_H: 8.66 (d, *J* = 4.9, 2H), 7.13 (t, *J* = 4.9, 1H), 4.12 (q, *J* = 7.1, 2H), 3.05 – 2.97 (m, 2H), 2.40 (t, *J* = 7.6, 2H), 2.21 – 2.13 (m, 2H), 1.24 (t, *J* = 7.1, 3H); **^{13}C {^{1}H} NMR** (126 MHz, $CDCl_3$) δ_C: 173.4, 170.7, 157.2, 118.7, 60.5, 38.7, 33.9, 23.7, 14.4; **HRMS** (CI) calculated for $[C_{10}H_{15}O_2N_2]^+$ $(M+H)^+$: m/z 195.1128 found 195.1129 (+0.5 ppm).

Ethyl 4-(pyrazin-2-yl)butanoate (9u)

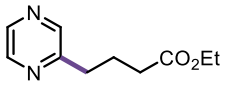

Prepared according to general procedure D from 2-bromopyrazine and ethyl 4-bromobutyrate, followed by purification by FCC (2:3 to 1:1 EtOAc/hexane) to give the title compound as a yellow oil (13.4 mg, 23%); $\mathbf{R_f}$ = 0.16 (1:1 EtOAc/hexane); $\mathbf{\nu_{max}/cm^{-1}}$ (film): 2980, 1728, 1402, 1375, 1161, 1016, 759; **^{1}H NMR** (400 MHz, $CDCl_3$) δ_H: 8.49 (dd, *J* = 2.5, 1.6, 1H), 8.46 (d, *J* = 1.3, 1H), 8.41 (d, *J* = 2.5, 1H), 4.13 (q, *J* = 7.1, 2H), 2.90 – 2.83 (m, 2H), 2.38 (t, *J* = 7.4, 2H), 2.15 – 2.05 (m, 2H), 1.25 (t, *J* = 7.1, 3H); **^{13}C {^{1}H} NMR** (101 MHz, $CDCl_3$) δ_C: 173.2, 156.9, 144.8, 144.3, 142.5, 60.6, 34.6, 33.9, 24.5, 14.4; **HRMS** (CI) calculated for $[C_{10}H_{15}O_2N_2]^+$ $(M+H)^+$: m/z 195.1128 found 195.1130 (+1.2 ppm).

Ethyl 4-(quinolin-3-yl)butanoate (9v)

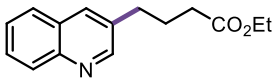

Prepared according to general procedure D from 3-bromoquinoline and ethyl 4-bromobutyrate, followed by purification by FCC (3:7 EtOAc/hexane) to give the title compound as a yellow oil (41.7 mg, 57%), with physical and spectroscopic data in accordance with the literature;[28] $\mathbf{R_f}$ = 0.31 (2:3 EtOAc/hexane); **^{1}H NMR** (500 MHz, $CDCl_3$) δ_H: 8.78 (d, *J* = 2.2, 1H), 8.10 – 8.04 (m, 1H), 7.93 (d, *J* = 1.3, 1H), 7.79 – 7.74 (m, 1H), 7.66 (ddd, *J* = 8.4, 6.9, 1.5, 1H), 7.52 (ddd, *J* = 8.1, 6.9, 1.2, 1H), 4.13 (q, *J* = 7.1, 2H), 2.90 – 2.79 (m, 2H), 2.38 (t, *J* = 7.4, 2H), 2.11 – 2.00 (m, 2H), 1.25 (t, *J* =

7.1, 3H); **^{13}C {^{1}H} NMR** (126 MHz, $CDCl_3$) δ_C: 173.3, 152.0, 147.0, 134.6, 134.2, 129.3, 128.9, 128.2, 127.5, 126.8, 60.6, 33.6, 32.5, 26.3, 14.4.

Ethyl 4-(1*H*-indol-7-yl)butanoate (9w)

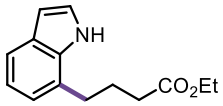

Prepared according to general procedure D from 7-bromoindole and ethyl 4-bromobutyrate, followed by purification by FCC (1:9 EtOAc/hexane) to give the title compound as a colourless, viscous oil (19.7 mg, 28%); **R_f** = 0.28 (1:9 EtOAc/hexane); **ν_{max}/cm^{-1}** (film): 3393, 2980, 1711, 1213, 908, 723; **^{1}H NMR** (500 MHz, $CDCl_3$) δ_H: 9.39 (br s, 1H), 7.52 (d, *J* = 7.8, 1H), 7.29 – 7.26 (m, 1H), 7.04 (dd, *J* = 7.8, 7.1, 1H), 6.99 – 6.95 (m, 1H), 6.55 (dd, *J* = 3.1, 2.1, 1H), 4.23 (q, *J* = 7.1, 2H), 2.91 – 2.82 (m, 2H), 2.49 – 2.42 (m, 2H), 2.07 – 1.98 (m, 2H), 1.32 (t, *J* = 7.1, 3H); **^{13}C {^{1}H} NMR** (126 MHz, $CDCl_3$) δ_C: 175.1, 135.4, 127.9, 124.7, 124.4, 121.5, 119.8, 119.0, 102.6, 60.9, 33.2, 31.3, 25.0, 14.4; **HRMS** (CI) calculated for $[C_{14}H_{17}O_2N]^+$ $(M+H)^+$: m/z 231.1254 found 231.1255 (+0.5 ppm).

3-(3-phenylpropyl)pyridine (9ab)

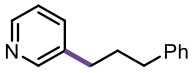

Prepared according to general procedure D from 3-bromopyridine and (3-bromopropyl)benzene, followed by purification by FCC (1:4 EtOAc/hexane) to give the title compound as a yellow oil (23.7 mg, 40%), with physical and spectroscopic data in accordance with the literature;[22] **R_f** = 0.23 (1:4 EtOAc/hexane); **^{1}H NMR** (500 MHz, $CDCl_3$) δ_H: 8.49 – 8.42 (m, 2H), 7.53 – 7.46 (m, 1H), 7.32 – 7.27 (m, 2H), 7.23 – 7.16 (m, 4H), 2.70 – 2.61 (m, 4H), 2.02 – 1.92 (m, 2H); **^{13}C {^{1}H} NMR** (126 MHz, $CDCl_3$) δ_C: 150.1, 147.5, 141.9, 137.5, 136.0, 128.6, 128.5, 126.1, 123.4, 35.4, 32.8, 32.6.

2-(3-(pyridin-2-yl)propyl)isoindoline-1,3-dione (9ac)

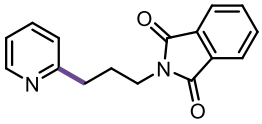

Prepared according to general procedure D from 2-bromopyridine and *N*-(3-iodopropyl)phthalimide, followed by purification by FCC (2:3 EtOAc/hexane) to give the title compound as a viscous yellow oil (50.7 mg, 63%); $\mathbf{R_f}$ = 0.15 (2:3 EtOAc/hexane); $\mathbf{\nu_{max}/cm^{-1}}$ (film): 2980, 1707, 1395, 1265, 733, 718, 702; **^{1}H NMR** (500 MHz, $CDCl_3$) δ_H: 8.48 – 8.46 (m, 1H), 7.86 – 7.77 (m, 2H), 7.74 – 7.66 (m, 2H), 7.56 (td, *J* = 7.7, 1.9, 1H), 7.17 (d, *J* = 7.8, 1H), 7.06 (ddd, *J* = 7.5, 4.9, 1.0, 1H), 3.78 (t, *J* = 7.0, 2H), 2.89 – 2.80 (m, 2H), 2.20 – 2.10 (m, 2H); **^{13}C {^{1}H} NMR** (126 MHz, $CDCl_3$) δ_C: 168.5, 160.9, 149.4, 136.5, 134.0, 132.3, 123.3, 123.0, 121.3, 37.8, 35.7, 28.5; **HRMS** (CI) calculated for $[C_{16}H_{15}O_2N_2]^+$ $(M+H)^+$: m/z 267.1128 found 267.1132 (+1.3 ppm).

2-(4-fluorophenethyl)pyridine (9ad)

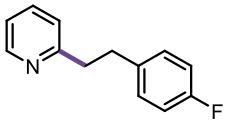

Prepared according to general procedure D from 2-bromopyridine and 1-(2-bromoethyl)-4-fluorobenzene, followed by purification by FCC (1:4 EtOAc/hexane) to give the title compound as a pale yellow oil (32.7 mg, 54%); $\mathbf{R_f}$ = 0.18 (1:4 EtOAc/hexane); $\mathbf{\nu_{max}/cm^{-1}}$ (film): 1590, 1569, 1508, 1475, 1435, 1276, 1218, 1157, 1051; **^{1}H NMR** (500 MHz, $CDCl_3$) δ_H: 8.57 – 8.54 (m, 1H), 7.56 (td, *J* = 7.6, 1.9, 1H), 7.15 – 7.08 (m, 3H), 7.05 (dt, *J* = 7.8, 1.0, 1H), 6.97 – 6.91 (m, 2H), 3.09 – 2.99 (m, 4H); **^{13}C {^{1}H} NMR** (126 MHz, $CDCl_3$) δ_C: 161.4 (d, *J* = 244.4), 161.1, 149.5, 137.3 (d, *J* = 3.8), 136.4, 129.9 (d, *J* = 7.6), 123.2, 121.4, 115.2 (d, *J* = 21.4), 40.4, 35.3; **^{19}F {^{1}H} NMR** (376 MHz, $CDCl_3$) δ_F: -117.58; **HRMS** (EI) calculated for $[C_{13}H_{11}NF]^+$ $(M-H)^+$: m/z 200.0870 found 200.0870 (+0.2 ppm).

2-(pyridin-2-yl)ethyl benzoate (9ae)

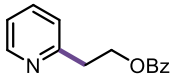

Prepared according to general procedure D from 2-bromopyridine and ethyl 2-bromobenzoate, followed by purification by FCC (1:4 to 2:3 EtOAc/hexane) to give the title compound as a colourless oil (18.1 mg, 27%); $\mathbf{R_f}$ = 0.21 (2:3 EtOAc/hexane); $\mathbf{\nu_{max}/cm^{-1}}$ (film): 1714, 1591, 1570, 1475, 1452, 1437, 1315, 1270, 1177, 1150, 1112, 1071, 1050; **^{1}H NMR** (400 MHz, $CDCl_3$) δ_H: 8.61 – 8.54 (m, 1H), 8.02 – 7.94 (m, 2H), 7.62 (td, *J* = 7.7, 1.8, 1H), 7.57 – 7.50 (m, 1H), 7.45 – 7.36 (m, 2H), 7.25 (d, *J* = 8.7, 1H), 7.16 (ddd, *J* = 7.4, 4.9, 0.9, 1H), 4.71 (t, *J* = 6.7, 2H), 3.26 (t, *J* = 6.7, 2H); **^{13}C {^{1}H} NMR** (101 MHz, $CDCl_3$) δ_C: 166.6, 158.3, 149.7, 136.6, 133.0, 130.4, 129.7, 128.5, 123.6, 121.8, 64.3, 37.7; **HRMS** (ES) calculated for $[C_{14}H_{14}NO_2]^+$ $(M+H)^+$: m/z 228.1027 found 228.1025 (-0.9 ppm).

***Tert*-butyl (2-(pyridin-2-yl)ethyl)carbamate (9af)**

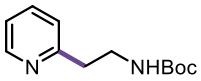

Prepared according to general procedure D from 2-bromopyridine and *tert*-butyl (2-bromoethyl)carbamate, followed by purification by FCC (3:2 EtOAc/hexane) to give the title compound as a pale yellow oil (15.9 mg, 24%); $\mathbf{R_f}$ = 0.15 (3:2 EtOAc/hexane); $\mathbf{\nu_{max}/cm^{-1}}$ (film): 3337, 2977, 1693, 1594, 1569, 1476, 1436, 1392, 1365, 1275, 1267, 1166, 1051; **^{1}H NMR** (500 MHz, $CDCl_3$) δ_H: 8.54 – 8.52 (m, 1H), 7.61 (td, *J* = 7.7, 1.8, 1H), 7.19 – 7.12 (m, 2H), 5.13 (br s, 1H), 3.56 – 3.51 (m, 2H), 3.00 – 2.95 (m, 2H), 1.42 (s, 9H); **^{13}C {^{1}H} NMR** (126 MHz, $CDCl_3$) δ_C: 159.6, 156.1, 149.3, 136.8, 123.7, 121.7, 79.2, 40.1, 37.9, 28.6; **HRMS** (ES) calculated for $[C_{12}H_{19}N_2O_2]^+$ $(M+H)^+$: m/z 223.1450 found 223.1447 (-1.3 ppm).

2-cyclohexylpyridine (9ag)

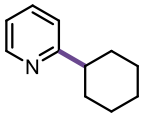

Prepared according to general procedure D from 2-bromopyridine and 1-iodocyclohexane, followed by purification by FCC (1:9 to 1:4 Et_2O/pentane) to give the title compound as a colourless oil (14.3 mg, 30%), with physical and spectroscopic data in accordance with the literature;[24] $\mathbf{R_f}$ = 0.31 (1:4 Et_2O/pentane); **^{1}H NMR** (500

MHz, $CDCl_3$) δ_H: 8.53 – 8.51 (m, 1H), 7.59 (td, *J* = 7.7, 1.9, 1H), 7.16 – 7.11 (m, 1H), 7.08 (ddd, *J* = 7.5, 4.8, 1.0, 1H), 2.69 (tt, *J* = 11.9, 3.4, 1H), 1.98 – 1.90 (m, 2H), 1.89 – 1.81 (m, 2H), 1.79 – 1.70 (m, 1H), 1.58 – 1.47 (m, 2H), 1.46 – 1.35 (m, 2H), 1.33 – 1.22 (m, 1H); **^{13}C {^{1}H} NMR** (126 MHz, $CDCl_3$) δ_C: 166.7, 149.2, 136.5, 121.1 (2C), 46.7, 33.1, 26.7, 26.2.

3-(oxetan-3-yl)pyridine (9ah)

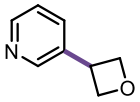

Prepared according to general procedure D from 3-bromopyridine and 3-bromooxetane, with a 4 h reaction time, followed by purification by FCC (1:4 EtOAc/hexane) to give the title compound as a pale yellow oil (12.8 mg, 32%); **R_f** = 0.11 (1:4 EtOAc/hexane); **ν_{max}/cm^{-1}** (film): 2349, 1275, 1267, 1262, 765, 750; **^{1}H NMR** (500 MHz, $CDCl_3$) δ_H: 8.63 – 8.50 (m, 2H), 7.88 – 7.82 (m, 1H), 7.34 (dd, *J* = 7.8, 4.7, 1H), 5.12 (dd, *J* = 8.3, 6.2, 2H), 4.75 (t, *J* = 6.4, 2H), 4.24 (tt, *J* = 8.3, 6.6, 1H); **^{13}C {^{1}H} NMR** (126 MHz, $CDCl_3$) δ_C: 148.8, 148.7, 137.1, 134.2, 142.0, 78.5, 38.0; **HRMS** (ES) calculated for $[C_8H_{10}NO]^+$ $(M+H)^+$: m/z 136.0759 found 136.0762 (+2.2 ppm).

***N*-(6-(but-3-en-1-yl)pyridin-3-yl)acetamide (9ai)**

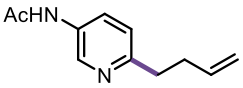

Prepared according to general procedure D from 5-acetamido-2-bromopyridine and 4-bromobut-1-ene, followed by purification by FCC (4:1 EtOAc/hexane) to give the title compound as an off-white solid (12.6 mg, 22%); **R_f** = 0.14 (7:3 EtOAc/hexane); **mp** 102 – 104 °C; **ν_{max}/cm^{-1}** (film): 2939, 1689, 1641, 1611, 1587, 1539, 1486, 1373, 1286, 1242, 1100; **^{1}H NMR** (500 MHz, $CDCl_3$) δ_H: 8.42 (d, *J* = 2.5, 1H), 8.08 (dd, *J* = 8.4, 2.6, 1H), 7.36 (br s, 1H), 7.13 (d, *J* = 8.4, 1H), 5.89 – 5.80 (m, 1H), 5.06 – 5.04 (m, 1H), 5.00 – 4.94 (m, 1H), 2.88 – 2.82 (m, 2H), 2.50 – 2.42 (m, 2H), 2.20 (s, 3H); **^{13}C {^{1}H} NMR** (126 MHz, $CDCl_3$) δ_C: 168.8, 157.3, 140.6, 137.8, 132.6, 128.2, 122.9, 115.4, 37.1, 33.9, 24.6; **HRMS** (ES) calculated for $[C_{11}H_{15}N_2O]^+$ $(M+H)^+$: m/z 191.1182 found 191.1184 (+1.0 ppm).

N-(6-neopentylpyridin-3-yl)acetamide (9aj)

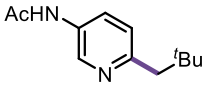

Prepared according to general procedure D from 5-acetamido-2-bromopyridine and neopentyl iodide, followed by purification by FCC (7:3 to 4:1 EtOAc/hexane) to give the title compound as a white solid (26.1 mg, 42%); **R_f** = 0.14 (7:3 EtOAc/hexane); **mp** 86 – 88 °C; **ν_{max}/cm^{-1}** (film): 3467, 2957, 2924, 1666, 1608, 1545, 1490, 1474, 1366, 1311, 1273, 1234, 1144, 1222, 1032; **^{1}H NMR** (500 MHz, $CDCl_3$) δ_H: 8.42 (d, *J* = 2.4, 1H), 8.09 (dd, *J* = 8.4, 2.6, 1H), 7.43 (br s, 1H), 7.09 (d, *J* = 8.4, 1H), 2.65 (s, 2H), 2.20 (s, 3H), 0.93 (s, 9H); **^{13}C {^{1}H} NMR** (126 MHz, $CDCl_3$) δ_C: 168.9, 156.1, 140.0, 132.6, 127.5, 124.8, 51.4, 32.2, 29.6, 24.6; **HRMS** (ES) calculated for $[C_{12}H_{19}N_2O]^+$ $(M+H)^+$: m/z 207.1498 found 207.1497 (-0.5 ppm).

5.3.3.1. Scale Up Experiment

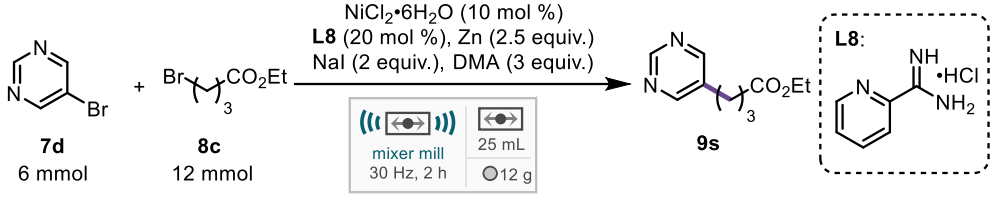

To a 25 mL stainless steel jar, equipped with a 12 g, 14 mm stainless steel ball, was charged nickel chloride hexahydrate (143 mg, 0.6 mmol, 10 mol %), amidine ligand **L8** (189 mg, 1.2 mmol, 20 mol %), zinc granular 20 – 30 mesh (981 mg, 15 mmol, 2.5 equiv.), sodium iodide (1.80 g, 12 mmol, 2 equiv.), and 5-bromopyrimidine (954 mg, 6 mmol, 1 equiv.). Followed by ethyl 4-bromobutyrate (1.72 mL, 12 mmol, 2 equiv.) and *N,N*-dimethylacetamide (1.67 mL, 18 mmol, 3 equiv.). The jar was closed and placed on the mixer mill, to be milled at 30 Hz for 2 hours. Upon completion, the reaction mixture was transferred to a separatory funnel using ethyl acetate (50 mL) and water (50 mL), and the organic phase was washed twice with a 5% solution of ammonium hydroxide (2 x 20 mL). The aqueous phase was extracted once more with ethyl acetate (50 mL) and the combined organic phases were washed with brine (50 mL), then dried over magnesium sulfate. After concentrating in vacuo, the crude material was purified by FCC (0.5:9.5 EtOAc/hexane) to give **9s** as a colourless oil (0.73 g, 62%).

5.3.4. Solution-Phase Comparisons

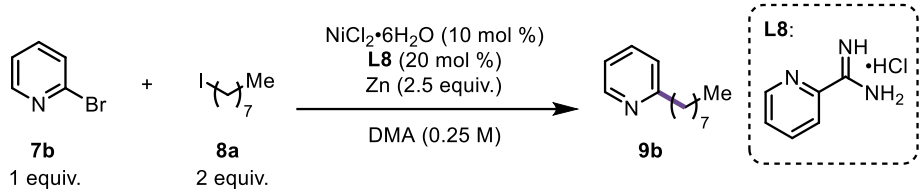

To a 5 mL microwave vial, equipped with a magnetic stirrer, was charged nickel chloride hexahydrate (7.1 mg, 0.03 mmol, 10 mol %), amidine ligand **L8** (9.5 mg, 0.06 mmol, 20 mol %), and zinc granular 20 – 30 mesh (49 mg, 0.75 mmol, 2.5 equiv.). The vial was capped and either left under an air atmosphere or a nitrogen inlet was introduced. Following this, 2-bromopyridine (28.6 µL, 0.3 mmol, 1 equiv.), 1-iodooctane (108.3 µL, 0.6 mmol, 2 equiv.), and *N,N*-dimethylacetamide (1.2 mL, 0.25 M) were added. The reaction mixture was stirred at either room temperature or 60 °C for 16 hours. Upon completion, the reaction mixture was quenched with a small volume of 5% ammonium hydroxide solution (2 mL). Ethyl acetate (2 mL) and internal standard (mesitylene) were added, and the mixture allowed to stir for a few minutes. The phases were allowed to settle, and an aliquot of the organic layer was taken for ^{1}H NMR analysis. NMR yields of **9b**: rt, under air 4%; rt, under N_2 31%; 60 °C, under N_2 67%.

5.3.5. Heated Ball-Mill Experiment

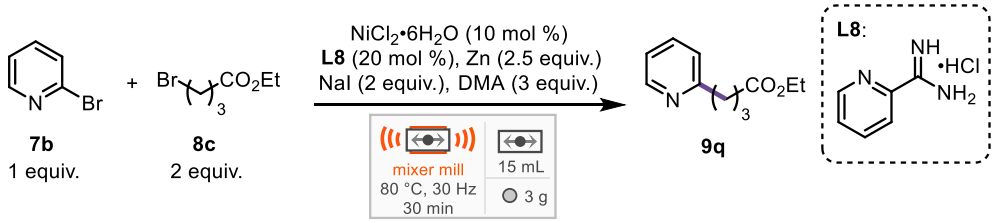

To a 15 mL stainless steel jar, equipped with a 3 g, 9 mm stainless steel ball, was charged nickel chloride hexahydrate (7.1 mg, 0.03 mmol, 10 mol %), amidine ligand **L8** (9.5 mg, 0.06 mmol, 20 mol %), zinc granular 20 – 30 mesh (49 mg, 0.75 mmol, 2.5 equiv.), and sodium iodide (89.9 mg, 0.6 mmol, 2 equiv.). Followed by 2-bromopyridine (28.6 µL, 0.3 mmol, 1 equiv.), ethyl 4-bromobutyrate (85.9 µL, 0.6 mmol, 2 equiv.) and *N,N*-dimethylacetamide (83.7 µL, 0.9 mmol, 3 equiv.). The jar was closed, placed on the mixer mill, and encased by a band heater. Heating to 80 °C and milling at 30 Hz were commenced simultaneously and continued for 30 minutes. Upon completion, the jar was allowed to cool, and the reaction mixture was transferred to a separatory funnel using ethyl acetate (25 mL) and water (25 mL). The organic phase was washed twice with a 5% solution of ammonium hydroxide (2 x 20 mL). The

aqueous phase was extracted once more with ethyl acetate (25 mL) and the combined organic phases were washed with brine (20 mL), then dried over magnesium sulfate. After concentrating in vacuo, the crude material was analysed by ^{1}H NMR using mesitylene as an internal standard. NMR yield of **9q**: 60%.

5.3.6. Mechanistic Studies

5.3.6.1. Stainless Steel Free Reaction in Planetary Ball-Mill

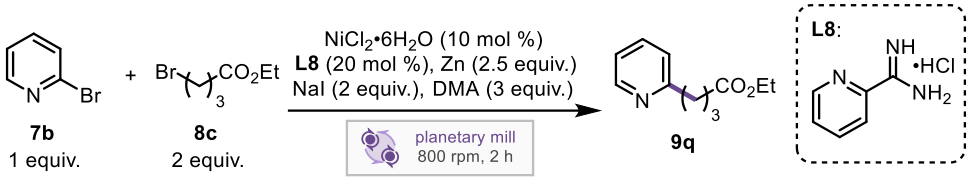

To a 12 mL zirconium oxide grinding bowl, equipped with 6, 3 g, 10 mm ceramic grinding balls, was charged nickel chloride hexahydrate (7.1 mg, 0.03 mmol, 10 mol %), amidine ligand **L8** (9.5 mg, 0.06 mmol, 20 mol %), zinc granular 20 – 30 mesh (49 mg, 0.75 mmol, 2.5 equiv.), and sodium iodide (89.9 mg, 0.6 mmol, 2 equiv.). Followed by 2-bromopyridine (28.6 µL, 0.3 mmol, 1 equiv.), ethyl 4-bromobutyrate (85.9 µL, 0.6 mmol, 2 equiv.) and *N,N*-dimethylacetamide (83.7 µL, 0.9 mmol, 3 equiv.). The lid was placed on the bowl and the bowl mounted on the central disc of the planetary mill. The reaction mixture was then milled at 800 rpm, for 2 hours (15 minute cycles, with reverse cycles and 1 minute pauses in between cycles). Upon completion, the reaction mixture was transferred to a separatory funnel using ethyl acetate (25 mL) and water (25 mL). The organic phase was washed twice with a 5% solution of ammonium hydroxide (2 x 20 mL). The aqueous phase was extracted once more with ethyl acetate (25 mL) and the combined organic phases were washed with brine (20 mL), then dried over magnesium sulfate. After concentrating in vacuo, the crude material was analysed by ^{1}H NMR using mesitylene as an internal standard. NMR yield of **9q**: 32%.

5.3.6.2. Radical Clock Experiment

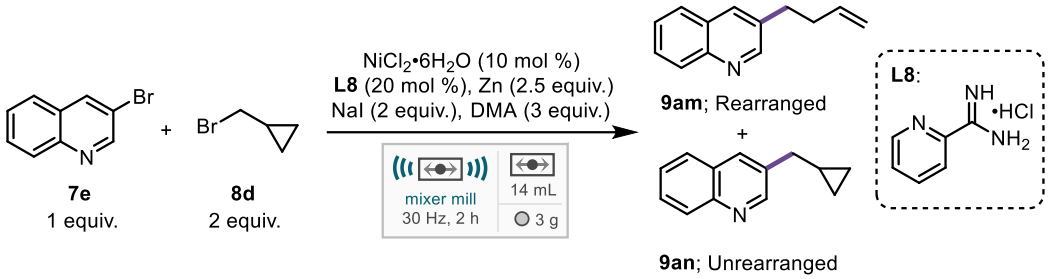

To a 14 mL stainless steel jar, equipped with a 3 g, 9 mm stainless steel ball, was charged nickel chloride hexahydrate (23.8 mg, 0.1 mmol, 10 mol %), amidine ligand L1 (31.5 mg, 0.2 mmol, 20 mol %), zinc granular 20 – 30 mesh (164 mg, 2.5 mmol, 2.5 equiv.), and sodium iodide (300 mg, 2 mmol, 2 equiv.). Followed by 3-bromoquinoline (135.7 µL, 1 mmol, 1 equiv.), (bromomethyl)cyclopropane (194 µL, 2 mmol, 2 equiv.), and *N,N*-dimethylacetamide (278 µL, 3 mmol, 3 equiv.). The jar was closed and placed on the mixer mill, to be milled at 30 Hz for 2 hours. Upon completion, the reaction mixture was transferred to a separatory funnel using ethyl acetate (50 mL) and water (50 mL), and the organic phase was washed twice with a 5% solution of ammonium hydroxide (2 x 20 mL). The aqueous phase was extracted once more with ethyl acetate (50 mL) and the combined organic phases were washed with brine (20 mL), then dried over magnesium sulfate. After concentrating in vacuo, the crude material was purified by FCC (1:9 EtOAc/hexane) to give the rearranged product **9am** as a yellow oil (90.6 mg, 49%); $\mathbf{R_f}$ = 0.37 (1:9 EtOAc/hexane); $\mathbf{\nu_{max}/cm^{-1}}$ (film): 2926, 1639, 1570, 1495, 1439, 1420, 1325, 1125, 1016, 957, 912, 899, 860; **^{1}H NMR** (500 MHz, $CDCl_3$) δ_H: 8.78 (d, *J* = 2.2, 1H), 8.10 – 8.05 (m, 1H), 7.91 (d, *J* = 1.4, 1H), 7.76 (dd, *J* = 8.1, 1.2, 1H), 7.65 (ddd, *J* = 8.4, 6.9, 1.4, 1H), 7.51 (ddd, *J* = 8.1, 6.9, 1.2, 1H), 5.93 – 5.81 (m, 1H), 5.10 – 5.03 (m, 1H), 5.03 – 4.99 (m, 1H), 2.93 – 2.86 (m, 2H), 2.52 – 2.44 (m, 2H); **^{13}C {^{1}H} NMR** (126 MHz, $CDCl_3$) δ_C: 152.2, 147.0, 137.2, 134.5, 134.4, 129.3, 128.7, 128.2, 127.5, 126.7, 115.9, 35.2, 32.7; **HRMS** (ES) calculated for $[C_{13}H_{14}N]^+$ $(M+H)^+$: m/z 184.1121 found 184.1120 (-0.17 ppm).

5.3.6.3. Organomanganese Formation Studies

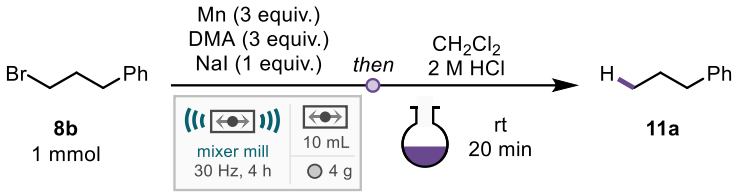

To a 10 mL stainless steel jar, equipped with a 4 g, 10 mm stainless steel ball, was charged 1-bromo-3-phenylpropane (152.0 µL, 1 mmol, 1 equiv.), manganese powder (164.8 mg, 3 mmol, 3 equiv.), sodium iodide (149.9 mg, 1 mmol, 1 equiv.), and *N,N*-dimethylacetamide (278.0 µL, 3 mmol, 3 equiv.). The jar was closed and placed on the mixer mill, to be milled at 30 Hz for 4 hours. Upon completion, the reaction mixture was transferred to a conical flask, equipped with a stirrer bar, using CH_2Cl_2 (20 mL). 2 M HCl (20 mL) was then added, and the resulting mixture was stirred at room temperature for 20 minutes to quench any organomanganese compounds. After this period, the mixture was transferred to a separatory funnel and the phases separated. The aqueous phase was extracted once more using CH_2Cl_2 (20 mL) and the combined organic phases were washed with brine and dried over magnesium sulfate. After concentrating in vacuo, the crude compound was analysed by ^1H NMR, using mesitylene as an internal standard. NMR yields of **11a**: without NaI 31%; with NaI 60%.

5.3.6.4. Radical Trapping Experiments

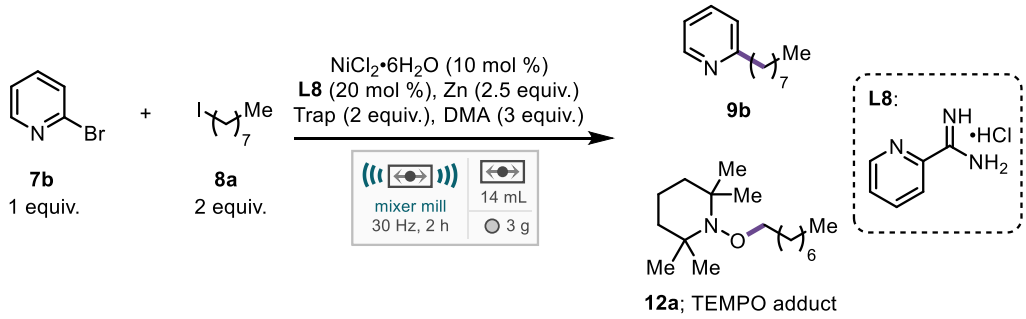

To a 14 mL stainless steel jar, equipped with a 3 g, 9 mm stainless steel ball, was charged nickel chloride hexahydrate (23.8 mg, 0.1 mmol, 10 mol %), amidine ligand **L8** (31.5 mg, 0.2 mmol, 20 mol %), zinc granular 20 – 30 mesh (164 mg, 2.5 mmol, 2.5 equiv.), and either TEMPO (313 mg, 2 mmol, 2 equiv.) or BHT (440.7 mg, 2 mmol, 2 equiv.). Followed by 2-bromopyridine (95.2 µL, 1 mmol, 1 equiv.), 1-iodooctane (361 µL, 2 mmol, 2 equiv.) and *N,N*-dimethylacetamide (278 µL, 3 mmol, 3 equiv.). The jar

was closed and placed on the mixer mill, to be milled at 30 Hz for 2 hours. Upon completion, the reaction mixture was transferred to a separatory funnel using ethyl acetate (50 mL) and water (50 mL), and the organic phase was washed twice with a 5% solution of ammonium hydroxide (2 x 20 mL). The aqueous phase was extracted once more with ethyl acetate (50 mL) and the combined organic phases were washed with brine (20 mL), then dried over magnesium sulfate. After concentrating in vacuo, the crude material was analysed by ^{1}H NMR and LR-MS to determine the presence of **9b** and/or TEMPO adduct(s). NMR yields of **9b**: with TEMPO <2%; with BHT 54%.

5.4. Mechanochemical Intramolecular Alkene Difunctionalisation

5.4.1. Experimental and Characterisation Data

5.4.2. General Procedure E – Synthesis of Alkene Tethered Aryl Halides

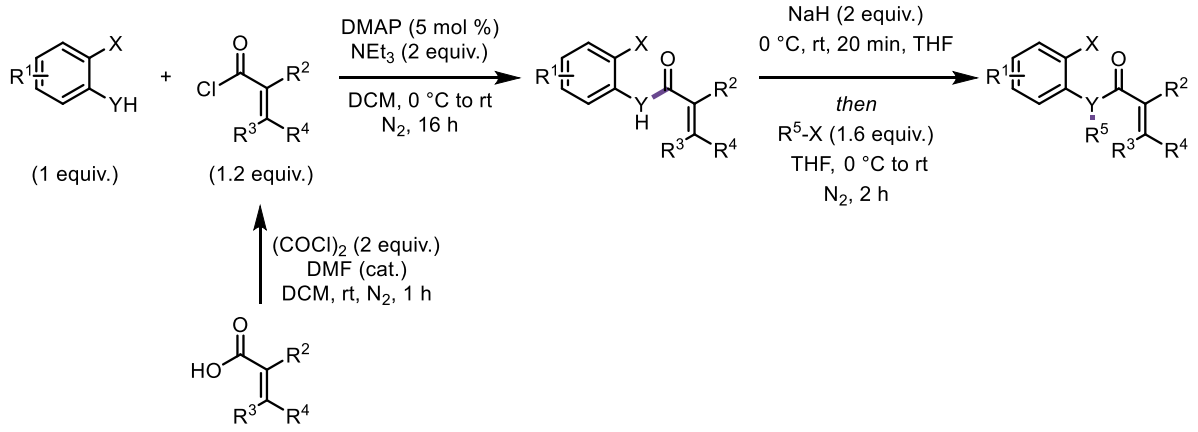

This procedure was adapted from a literature report.[29]

Acid chloride synthesis

To a round-bottomed flask, equipped with a magnetic stirrer bar, was charged acrylic acid derivative (1 equiv.) and a few drops of *N,N*-dimethylformamide under a nitrogen atmosphere. Dichloromethane (0.25 M) was added, followed by dropwise addition of oxalyl chloride (2 equiv.) at 0 °C. The resulting mixture was then allowed to warm to room temperature and stirred for an hour, or until gas evolution ceased. Upon completion, the mixture was concentrated in vacuo and used in the next step without further purification.

Acylation procedure

To a round-bottomed flask, equipped with a magnetic stirrer bar, was charged aromatic nucleophile (1 equiv.), 4-(dimethylamino)-pyridine (5 mol %), and triethylamine (2 equiv.), in DCM (0.25 M), under a nitrogen atmosphere. This was followed by dropwise addition of the appropriate acid chloride (1.2 equiv.) at 0 °C. The resulting mixture was then allowed to warm to room temperature and stirred for an additional 16 hours. Upon completion, the reaction mixture was quenched with saturated aqueous $NaHCO_3$. The phases were separated, and the aqueous layer was extracted two more times with DCM. The combined organic phases were washed with brine and dried over magnesium sulfate. The mixture was concentrated in vacuo and used in the next step without further purification.

Alkylation procedure

To a stirred solution of the crude acylated product, in tetrahydrofuran (0.25 M), was charged sodium hydride (60% in paraffin oil, 2 equiv.) portion wise at 0 °C, under a nitrogen atmosphere. The resulting mixture was stirred at 0 °C for 20 minutes, then the appropriate alkyl halide (1.6 equiv.) was added dropwise at 0 °C. Following this, the reaction mixture was allowed to warm to room temperature and stirred for an additional 2 hours. Upon completion, the reaction was quenched with slow addition of water at 0 °C, and extracted two times with ethyl acetate. The combined organic phases were washed with brine, dried over magnesium sulfate, and concentrated in vacuo. The crude compound was purified by FCC in the stated solvent system, to yield the alkylated product.

_N_-(2-bromo-4-fluorophenyl)-_N_-methylmethacrylamide (13a)

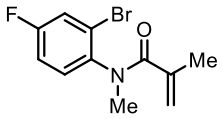

Prepared according to general procedure E, starting from 2-bromo-4-fluoroaniline (137 mmol) and methacryloyl chloride, followed by purification of the tertiary amide by FCC (1:4 EtOAc/PE) to give the title compound as an off-white solid (17.91 g, 58%); $\mathbf{R_f}$ = 0.31 (1:4 EtOAc/PE); **mp** 54 – 56 °C; $\mathbf{\nu_{max}/cm^{-1}}$ (film): 1655, 1626, 1487, 1452, 1362, 1315, 1259, 1236, 1204, 1121, 1053, 1028, 918, 895, 854, 826, 750; **^{1}H NMR** (300 MHz, $CDCl_3$) δ_H: 7.36 (dd, *J* = 7.8, 2.8, 1H, Ar*H*), 7.17 (dd, *J* = 8.5, 5.5, 1H, Ar*H*), 7.03

(td, *J* = 8.2, 2.6, 1H, Ar*H*), 4.99 (s, 2H, C=CH_2), 3.22 (s, 3H, N-CH_3), 1.81 (s, 3H, C-CH_3); **^{13}C {^{1}H} NMR** (126 MHz, $CDCl_3$) δ_C: 172.1 (*C*=O), 161.3 (d, *J* = 253.3, Ar*C*F), 140.2 (*C*=CH_2), 140.1 (Ar*C*), 130.9 (d, *J* = 7.1, Ar*C*H), 123.6 (d, *J* = 8.1, Ar*C*), 121.0 (d, *J* = 20.2, Ar*C*H), 118.8 (C=*C*H_2), 115.7 (d, *J* = 18.2, Ar*C*H), 36.6 (N-*C*H_3), 20.4 (C-*C*H_3); **^{19}F {^{1}H} NMR** (376 MHz, $CDCl_3$) δ_F: -111.26; **HRMS** (ES) calculated for $[C_{11}H_{12}NOF^{79}Br]^+$ $(M+H)^+$: m/z 272.0086 found 272.0089 (+1.1 ppm).

***N*-(4-fluoro-2-iodophenyl)-*N*-methylmethacrylamide (13aa)**

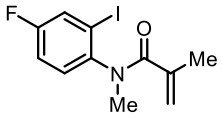

Prepared according to general procedure E, starting from 2-iodo-4-fluoroaniline (30 mmol) and methacryloyl chloride, followed by purification of the tertiary amide by FCC (1:9 to 1:4 EtOAc/PE) to give the title compound as an off-white solid (6.76 g, 71%), with physical and spectroscopic data in accordance with the literature;[30] **R_f** = 0.30 (1:4 EtOAc/PE); **mp** 69 – 71 °C; **^{1}H NMR** (500 MHz, $CDCl_3$) δ_H: 7.58 (dd, *J* = 7.7, 2.8, 1H), 7.18 – 7.11 (m, 1H), 7.11 – 7.03 (m, 1H), 5.04 – 5.00 (m, 2H), 3.21 (s, 3H), 1.82 (s, 3H); **^{13}C {^{1}H} NMR** (126 MHz, $CDCl_3$) δ_C: 171.9, 160.9 (d, *J* = 253.3), 143.5 (d, *J* = 2.5), 140.2, 130.0 (d, *J* = 7.6), 127.1 (d, *J* = 25.2), 119.2, 116.5 (d, *J* = 22.7), 99.1 (d, *J* = 7.6), 37.0, 20.7; **^{19}F {^{1}H} NMR** (376 MHz, $CDCl_3$) δ_F: -112.04.

***N*-(2-chloro-4-fluorophenyl)-*N*-methylmethacrylamide (13ab)**

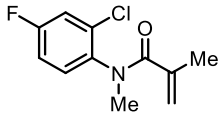

Prepared according to general procedure E, starting from 2-chloro-4-fluoroaniline (10 mmol) and methacryloyl chloride, followed by purification of the tertiary amide by FCC (1:4 EtOAc/PE) to give the title compound as an off-white solid (1.78 g, 78%); **R_f** = 0.11 (1:4 EtOAc/PE); **mp** 61 – 63 °C; **ν_{max}/cm^{-1}** (film): 1655, 1626, 1580, 1493, 1452, 1400, 1364, 1315, 1275, 1259, 1238, 1207, 1121, 907, 860, 750; **^{1}H NMR** (400 MHz, $CDCl_3$) δ_H: 7.21 – 7.12 (m, 2H), 6.98 (td, *J* = 8.5, 2.7, 1H), 5.01 – 4.93 (m, 2H), 3.22 (s, 3H), 1.80 (s, 3H); **^{13}C {^{1}H} NMR** (126 MHz, $CDCl_3$) δ_C: 172.2, 161.5 (d, *J* = 252.0), 140.2, 138.6 (d, *J* = 2.5), 133.7 (d, *J* = 11.3), 130.8 (d, *J* = 10.1), 118.6, 118.0 (d, *J* = 26.5), 115.2 (d, *J* = 22.7), 36.4, 20.3; **^{19}F {^{1}H} NMR** (376 MHz, $CDCl_3$) δ_F: -111.07;

HRMS (ES) calculated for $[C_{11}H_{12}NOF^{35}Cl]^+$ $(M+H)^+$: m/z 228.0591 found 228.0590 (-0.4 ppm).

***N*-(2-bromophenyl)-*N*-methylmethacrylamide (13b)**

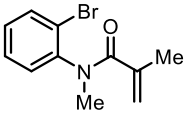

Prepared according to general procedure E, starting from 2-bromoaniline (30 mmol) and methacryloyl chloride, followed by purification of the tertiary amide by FCC (1:4 EtOAc/PE) to give the title compound as pale yellow solid (5.68 g, 75%), with physical and spectroscopic data in accordance with the literature;[31] **R_f** = 0.14 (1:4 EtOAc/PE); **mp** 52 – 54 °C; **^{1}H NMR** (500 MHz, $CDCl_3$) δ_H: 7.64 – 7.59 (m, 1H), 7.31 (t, *J* = 7.4, 1H), 7.21 – 7.14 (m, 2H), 5.01 (s, 1H), 4.97 (s, 1H), 3.25 (s, 3H), 1.81 (s, 3H); **^{13}C {^{1}H} NMR** (126 MHz, $CDCl_3$) δ_C: 172.1, 143.7, 140.3, 133.9, 130.1, 129.3, 128.6, 123.1, 118.8, 36.6, 20.4.

***N*-(2-bromo-4-methylphenyl)-*N*-methylmethacrylamide (13c)**

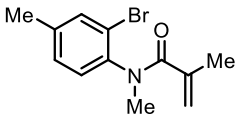

Prepared according to general procedure E, starting from 2-bromo-4-methylaniline (10 mmol) and methacryloyl chloride, followed by purification of the tertiary amide by FCC (1:4 EtOAc/PE) to give the title compound as an orange oil (2.16 g, 80%), with physical and spectroscopic data in accordance with the literature;[30] **R_f** = 0.17 (1:4 EtOAc/PE); **^{1}H NMR** (500 MHz, $CDCl_3$) δ_H: 7.43 (s, 1H), 7.11 – 7.04 (m, 2H), 5.02 (s, 1H), 4.96 (s, 1H), 3.22 (s, 3H), 2.34 (s, 3H), 1.81 (s, 3H); **^{13}C {^{1}H} NMR** (126 MHz, $CDCl_3$) δ_C: 172.2, 141.0, 140.4, 139.7, 134.2, 129.6, 129.3, 122.7, 118.6, 36.6, 20.9, 20.5.

***N*-(2-bromo-3-methylphenyl)-*N*-methylmethacrylamide (13d)**

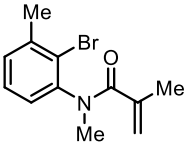

Prepared according to general procedure E, starting from 2-bromo-3-methylaniline (10 mmol) and methacryloyl chloride, followed by purification of the tertiary amide by FCC (1:4 EtOAc/PE) to give the title compound as an off-white solid (1.38 g, 52%); **R_f** =

0.32 (1:4 EtOAc/PE); **mp** 56 – 58 °C; **ν_{max}/cm^{-1}** (film): 1653, 1626, 1574, 1468, 1362, 1315, 1275, 1261, 1173, 1144, 1098, 1063, 1032, 750; **^{1}H NMR** (500 MHz, $CDCl_3$) δ_H: 7.20 – 7.15 (m, 2H), 7.04 – 6.99 (m, 1H), 5.02 (s, 1H), 4.94 (s, 1H), 3.23 (s, 3H), 2.44 (s, 3H), 1.81 (s, 3H); **^{13}C {^{1}H} NMR** (126 MHz, $CDCl_3$) δ_C: 172.1, 144.0, 140.5, 140.4, 130.1, 127.8, 127.3, 125.7, 118.45, 36.6, 23.9, 20.5; **HRMS** (ES) calculated for $[C_{12}H_{15}NO^{79}Br]^+$ $(M+H)^+$: m/z 268.0337 found 268.0336 (-0.4 ppm).

***N*-(2-bromo-4-(*tert*-butyl)phenyl)-*N*-methylmethacrylamide (13e)**

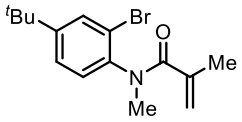

Prepared according to general procedure E, starting from 2-bromo-4-(*tert*-butyl)aniline (10 mmol) and methacryloyl chloride, followed by purification of the tertiary amide by FCC (1:4 EtOAc/PE) to give the title compound as a white solid (2.22 g, 72%); **R_f** = 0.21 (1:4 EtOAc/PE); **mp** 78 – 80 °C; **ν_{max}/cm^{-1}** (film): 2963, 2349, 1655, 1628, 1493, 1452, 1423, 1362, 1315, 1275, 750; **^{1}H NMR** (400 MHz, $CDCl_3$) δ_H: 7.58 (d, *J* = 1.9, 1H), 7.29 (dd, *J* = 8.2, 1.8, 1H), 7.09 (d, *J* = 8.2, 1H), 5.03 (s, 1H), 4.98 (s, 1H), 3.23 (s, 3H), 1.81 (s, 3H), 1.31 (s, 9H); **^{13}C {^{1}H} NMR** (126 MHz, $CDCl_3$) δ_C: 172.2, 153.0, 140.9, 140.3, 130.8, 129.4, 125.7, 122.6, 118.8, 36.6, 34.9, 31.3, 20.4; **HRMS** (ES) calculated for $[C_{15}H_{21}NO^{79}Br]^+$ $(M+H)^+$: m/z 310.0807 found 310.0800 (-2.3 ppm).

***N*-(2-bromo-4-chlorophenyl)-*N*-methylmethacrylamide (13f)**

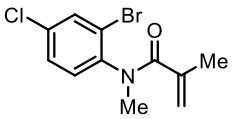

Prepared according to general procedure E, starting from 2-bromo-4-chloroaniline (10 mmol) and methacryloyl chloride, followed by purification of the tertiary amide by FCC (1:4 EtOAc/PE) to give the title compound as a pale yellow oil (1.77 g, 61%), with physical and spectroscopic data in accordance with the literature;[29] **R_f** = 0.15 (1:4 EtOAc/PE); **^{1}H NMR** (500 MHz, $CDCl_3$) δ_H: 7.63 (d, *J* = 2.2, 1H), 7.29 (dd, *J* = 8.3, 1.6, 1H), 7.12 (d, *J* = 8.2, 1H), 5.00 (s, 2H), 3.22 (s, 3H), 1.82 (s, 3H); **^{13}C {^{1}H} NMR** (126 MHz, $CDCl_3$) δ_C: 171.9, 142.5, 140.1, 134.3, 133.6, 130.7, 128.9, 123.6, 119.1, 36.5, 20.4.

Methyl 3-bromo-4-(*N*-methylmethacrylamido)benzoate (13g)

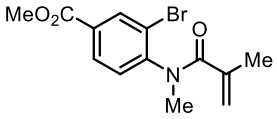

Prepared according to general procedure E, starting from methyl 4-amino-3-bromobenzoate (10 mmol) and methacryloyl chloride, followed by purification of the tertiary amide by FCC (1:4 EtOAc/PE) to give the title compound as a yellow solid (0.89 g, 28%); **R_f** = 0.07 (1:4 EtOAc/PE); **mp** 54 – 56 °C; **ν_{max}/cm^{-1}** (film): 1722, 1655, 1626, 1593, 1435, 1399, 1358, 1281, 1246, 1111, 1055, 768; **^{1}H NMR** (500 MHz, $CDCl_3$) δ_H: 8.28 (d, *J* = 1.8, 1H), 7.96 (dd, *J* = 8.1, 1.6, 1H), 7.24 (d, *J* = 8.1, 1H), 4.98 (s, 2H), 3.91 (s, 3H), 3.25 (s, 3H), 1.82 (s, 3H); **^{13}C {^{1}H} NMR** (126 MHz, $CDCl_3$) δ_C: 171.7, 165.1, 147.8, 140.0, 135.2, 131.0, 129.8 (2C), 123.0, 119.4, 52.7, 36.5, 20.3; **HRMS** (ES) calculated for $[C_{13}H_{15}NO_3{}^{79}Br]^+$ $(M+H)^+$: m/z 312.0235 found 312.0244 (+2.9 ppm).

***N*-(2-bromo-4-(trifluoromethyl)phenyl)-*N*-methylmethacrylamide (13h)**

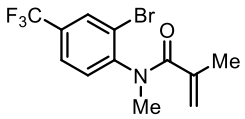

Prepared according to general procedure E, starting from 2-bromo-4-(trifluoromethyl)aniline (10 mmol) and methacryloyl chloride, followed by purification of the tertiary amide by FCC (1:4 EtOAc/PE) to give the title compound as a yellow oil (1.18 g, 37%); **R_f** = 0.19 (1:4 EtOAc/PE); **ν_{max}/cm^{-1}** (film): 1659, 1630, 1358, 1319, 1258, 1171, 1123, 1078, 1055, 920; **^{1}H NMR** (500 MHz, $CDCl_3$) δ_H: 7.89 (d, *J* = 1.4, 1H), 7.58 (d, *J* = 7.8, 1H), 7.31 (d, *J* = 7.9, 1H), 5.04 (s, 1H), 5.00 (s, 1H), 3.26 (s, 3H), 1.85 (s, 3H); **^{13}C {^{1}H}** NMR (126 MHz, $CDCl_3$) δ_C: 171.8, 147.2, 139.9, 131.4 (q, *J* = 34.0), 131.2 (q, *J* = 3.8), 130.4, 125.7 (q, *J* = 2.5), 123.5, 122.0 (q, *J* = 273.4), 119.6, 36.5, 20.3; **^{19}F {^{1}H} NMR** (376 MHz, $CDCl_3$) δ_F: -62.65; **HRMS** (ES) calculated for $[C_{12}H_{12}NOF_3{}^{79}Br]^+$ $(M+H)^+$: m/z 322.0054 found 322.0053 (-0.3 ppm).

_N_-(2-bromo-4-cyanophenyl)-_N_-methylmethacrylamide (13i)

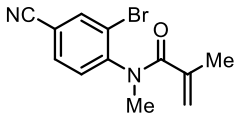

Prepared according to general procedure E, starting from 4-amino-3-bromo-benzonitrile (10 mmol) and methacryloyl chloride, followed by purification of the tertiary amide by FCC (3:7 to 2:3 EtOAc/PE) to give the title compound as an off-white solid (1.22 g, 44%), with physical and spectroscopic data in accordance with the literature;[29] **R_f** = 0.14 (2:3 EtOAc/PE); **mp** 96 – 98 °C; **^{1}H NMR** (500 MHz, $CDCl_3$) δ_H: 7.93 (s, 1H), 7.62 (d, *J* = 8.1, 1H), 7.30 (d, *J* = 8.1, 1H), 5.08 (s, 1H), 4.99 (s, 1H), 3.26 (s, 3H), 1.87 (s, 3H); **^{13}C {^{1}H} NMR** (126 MHz, $CDCl_3$) δ_C: 171.5, 148.2, 139.8, 137.4, 132.3, 130.6, 123.7, 119.8, 116.7, 113.1, 36.6, 20.2.

_N_-(2-bromo-4-nitrophenyl)-_N_-methylmethacrylamide (13j)

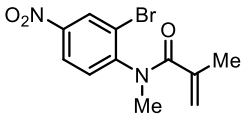

Prepared according to general procedure E, starting from 2-bromo-4-nitroaniline (10 mmol) and methacryloyl chloride, followed by purification of the tertiary amide by FCC (1:4 to 3:7 EtOAc/PE) to give the title compound as a yellow solid (1.22 g, 41%); **R_f** = 0.15 (3:7 EtOAc/PE); **mp** 88 – 90 °C; **ν_{max}/cm^{-1}** (film): 1656, 1628, 1580, 1524, 1477, 1344, 1275, 1261, 1229, 750; **^{1}H NMR** (500 MHz, $CDCl_3$) δ_H: 8.52 (d, *J* = 2.5, 1H), 8.20 (dd, *J* = 8.6, 2.4, 1H), 7.36 (d, *J* = 8.6, 1H), 5.10 (s, 1H), 5.02 (s, 1H), 3.29 (s, 3H), 1.89 (s, 3H); **^{13}C {^{1}H} NMR** (126 MHz, $CDCl_3$) δ_C: 171.5, 149.7, 147.0, 139.9, 130.4, 129.3, 123.8, 123.6, 119.9, 36.8, 20.2; **HRMS** (ES) calculated for $[C_{11}H_{12}N_2O_3{}^{79}Br]^+$ $(M+H)^+$: m/z 299.0031 found 299.0027 (-1.3 ppm).

_N_-(2-bromo-4-(trifluoromethoxy)phenyl)-_N_-methylmethacrylamide (13k)

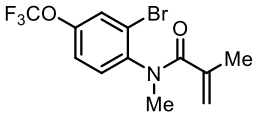

Prepared according to general procedure E, starting from 2-bromo-4-(trifluoromethoxy)aniline (10 mmol) and methacryloyl chloride, followed by purification of the tertiary amide by FCC (1:4 EtOAc/PE) to give the title compound as a pale

yellow oil (1.54 g, 46%), with physical and spectroscopic data in accordance with the literature;[29] **R_f** = 0.18 (1:4 EtOAc/PE); **^{1}H NMR** (400 MHz, $CDCl_3$) δ_H: 7.53 – 7.47 (m, 1H), 7.25 – 7.15 (m, 2H), 5.08 – 4.94 (m, 2H), 3.24 (s, 3H), 1.83 (s, 3H); **^{13}C {^{1}H} NMR** (126 MHz, $CDCl_3$) δ_C: 171.9, 148.4, 142.5, 140.1, 130.6, 126.3, 123.7, 120.9, 120.4 (q, *J* = 259.6) 119.3, 36.6, 20.4; **^{19}F {^{1}H} NMR** (376 MHz, $CDCl_3$) δ_F: -58.01.

***N*-(2-bromo-4-methoxyphenyl)-*N*-methylmethacrylamide (13l)**

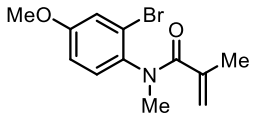

Prepared according to general procedure E, starting from 2-bromo-4-methoxyaniline (10 mmol) and methacryloyl chloride, followed by purification of the tertiary amide by FCC (1:4 EtOAc/PE) to give the title compound as a brown oil (1.94 g, 69%); **R_f** = 0.12 (1:4 EtOAc/PE); **ν_{max}/cm^{-1}** (film): 1653, 1626, 1601, 1493, 1452, 1440, 1364, 1285, 1223, 1124, 1032, 841; **^{1}H NMR** (300 MHz, $CDCl_3$) δ_H: 7.12 (d, *J* = 2.8, 1H), 7.08 (d, *J* = 8.7, 1H), 6.82 (dd, *J* = 8.7, 2.8, 1H), 5.01 (s, 1H), 4.96 (s, 1H), 3.79 (s, 3H), 3.20 (s, 3H), 1.79 (s, 3H); **^{13}C {^{1}H} NMR** (126 MHz, $CDCl_3$) δ_C: 172.3, 159.4, 140.5, 136.4, 130.3, 123.5, 118.6, 118.3, 114.3, 55.8, 36.7, 20.5; **HRMS** (ES) calculated for $[C_{12}H_{15}NO_2{}^{79}Br]^+$ $(M+H)^+$: m/z 284.0286 found 284.0284 (-0.7 ppm).

***N*-(3-bromopyridin-2-yl)-*N*-methylmethacrylamide (13m)**

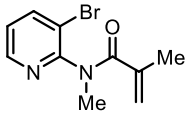

Prepared according to general procedure E, starting from 2-amino-3-bromopyridine (10 mmol) and methacryloyl chloride, followed by purification of the tertiary amide by FCC (2:3 EtOAc/PE) to give the title compound as a yellow oil (0.58 g, 23%); **R_f** = 0.19 (2:3 EtOAc/PE); **ν_{max}/cm^{-1}** (film): 1657, 1626, 1568, 1435, 1416, 1140, 1072, 1022, 796; **^{1}H NMR** (500 MHz, $CDCl_3$) δ_H: 8.43 (d, *J* = 4.6, 1H), 7.93 (d, *J* = 7.9, 1H), 7.12 (dd, *J* = 7.9, 4.7, 1H), 4.99 (s, 1H), 4.92 (s, 1H), 3.30 (s, 3H), 1.93 (s, 3H); **^{13}C {^{1}H} NMR** (126 MHz, $CDCl_3$) δ_C: 172.1, 155.6, 148.1, 142.6, 141.0, 124.1, 119.3, 118.8, 35.1, 20.1; **HRMS** (ES) calculated for $[C_{10}H_{12}N_2O^{79}Br]^+$ $(M+H)^+$: m/z 255.0133 found 255.0135 (+0.8 ppm).

_N_-benzyl-_N_-(2-bromo-4-fluorophenyl)methacrylamide (13n)

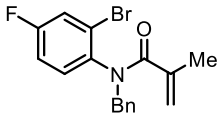

Prepared according to general procedure E, from 2-bromo-4-fluoroaniline (10 mmol) and methacryloyl chloride, followed by purification of the tertiary amide by FCC (1:9 EtOAc/PE) to give the title compound as a pale yellow oil (2.55 g, 73%); **R_f** = 0.31 (1:4 EtOAc/PE); **ν_{max}/cm^{-1}** (film): 1655, 1628, 1485, 1452, 1323, 1260, 1182, 1080, 1030, 750; **^{1}H NMR** (500 MHz, $CDCl_3$) δ_H: 7.36 (dd, *J* = 7.8, 2.8, 1H), 7.30 – 7.23 (m, 3H), 7.23 – 7.17 (m, 2H), 6.83 (td, *J* = 8.2, 2.8, 1H), 6.70 – 6.64 (m, 1H), 5.65 (d, *J* = 14.2, 1H), 5.00 (s, 2H), 4.14 (d, *J* = 14.3, 1H), 1.84 (s, 3H); **^{13}C {^{1}H} NMR** (126 MHz, $CDCl_3$) δ_C: 171.6, 161.4 (d, *J* = 254.5), 140.3, 137.7, 136.7, 132.6 (d, *J* = 8.8), 129.5, 128.6, 127.8, 124.1 (d, *J* = 10.1), 120.9 (d, *J* = 25.2), 118.6, 115.1 (d, *J* = 21.4), 51.6, 20.6; **^{19}F {^{1}H} NMR** (376 MHz, $CDCl_3$) δ_F: -111.11; **HRMS** (ES) calculated for $[C_{17}H_{16}NOF^{79}Br]^+$ $(M+H)^+$: m/z 348.0399 found 348.0399 (0.0 ppm).

***Tert*-butyl (2-bromo-4-fluorophenyl)(methacryloyl)carbamate (13o)**

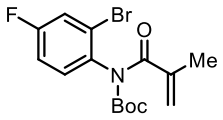

Prepared according to general procedure E, from 2-bromo-4-fluoroaniline (10 mmol) and methacryloyl chloride, followed by purification of the tertiary amide by FCC (0.5:9.5 EtOAc/PE) to give the title compound as a white solid (2.34 g, 65%); **R_f** = 0.40 (1:4 EtOAc/PE); **mp** 79 – 81 °C; **ν_{max}/cm^{-1}** (film): 2982, 1740, 1690, 1597, 1489, 1456, 1394, 1369, 1354, 1275, 1258, 1198, 1084, 764, 750; **^{1}H NMR** (500 MHz, $CDCl_3$) δ_H: 7.39 (dd, *J* = 7.9, 2.8, 1H), 7.19 (dd, *J* = 8.8, 5.4, 1H), 7.11 – 7.05 (m, 1H), 5.58 (s, 1H), 5.38 – 5.34 (m, 1H), 2.10 (s, 3H), 1.43 (s, 9H); **^{13}C {^{1}H} NMR** (126 MHz, $CDCl_3$) δ_C: 172.8, 161.8 (d, *J* = 253.3), 151.9, 142.4, 134.2 (d, *J* = 3.8), 131.2 (d, *J* = 8.8), 124.1 (d, *J* = 10.1), 120.7 (d, *J* = 25.2), 118.5, 115.5 (d, *J* = 22.7), 84.2, 27.9, 19.5; **^{19}F {^{1}H} NMR** (376 MHz, $CDCl_3$) δ_F: -111.10; **HRMS** (CI) calculated for $[C_{10}H_9NOF^{79}Br]^+$ $(M-C_5H_8O_2)^+$: m/z 256.9846 found 256.9847 (+0.5 ppm).

N-(2-bromo-4-fluorophenyl)methacrylamide (13p)

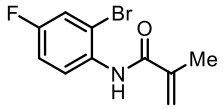

Prepared according to general procedure E, from 2-bromo-4-fluoroaniline (50 mmol) and methacryloyl chloride, followed by purification of the secondary amide by FCC (0.5:9.5 EtOAc/PE) to give the title compound as a white solid (8.84 g, 69%); **R_f** = 0.35 (1:9 EtOAc/PE); **mp** 64 – 66 °C; **ν_{max}/cm^{-1}** (film): 3277, 2349, 1659, 1622, 1593, 1516, 1479, 1385, 1373, 1275, 1256, 1190, 748; **^{1}H NMR** (300 MHz, $CDCl_3$) δ_H: 8.41 (dd, *J* = 9.2, 5.6, 1H), 8.00 (s, 1H), 7.31 (dd, *J* = 7.8, 2.9, 1H), 7.12 – 7.03 (m, 1H), 5.94 – 5.90 (m, 1H), 5.55 – 5.51 (m, 1H), 2.11 – 2.09 (m, 3H); **^{13}C {^{1}H} NMR** (126 MHz, $CDCl_3$) δ_C: 166.2, 158.6 (d, *J* = 249.5), 140.4, 132.3 (d, *J* = 3.8), 122.8 (d, *J* = 8.8), 121.2, 119.4 (d, *J* = 25.2), 115.4 (d, *J* = 21.4), 113.7 (d, *J* = 10.1), 18.7; **^{19}F {^{1}H} NMR** (376 MHz, $CDCl_3$) δ_F: -116.13; **HRMS** (ES) calculated for $[C_{10}H_{10}NOF^{79}Br]^+$ $(M+H)^+$: m/z 257.9930 found 257.9929 (-0.4 ppm).

N-(2-bromo-4-fluorophenyl)-*N*-methyl-2-phenylacrylamide (13q)

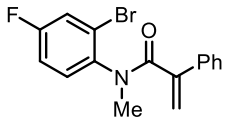

Prepared according to general procedure E, starting from 2-bromo-4-fluoroaniline (10 mmol) and 2-phenyl acrylic acid, followed by purification of the tertiary amide by FCC (1:4 EtOAc/PE) to give the title compound as a viscous yellow oil (2.22 g, 66%), in an approximately 9:1 mixture of rotamers, with physical and spectroscopic data in accordance with the literature;[32] **R_f** = 0.18 (1:4 EtOAc/PE); Data for major rotamer, **^{1}H NMR** (500 MHz, $CDCl_3$) δ_H: 7.24 – 7.16 (m, 4H), 7.15 – 7.08 (m, 2H), 6.77 – 6.67 (m, 2H), 5.56 (s, 1H), 5.38 – 5.34 (m, 1H), 3.27 (s, 3H); **^{13}C {^{1}H} NMR** (126 MHz, $CDCl_3$) δ_C: 170.6, 161.3 (d, *J* = 253.3), 145.8, 138.5 (d, *J* = 3.8), 136.8, 131.4 (d, *J* = 10.1), 128.5, 128.2, 126.1, 123.8 (d, *J* = 10.1), 120.5 (d, *J* = 25.2), 117.5, 115.0 (d, *J* = 22.7), 36.1; **^{19}F {^{1}H} NMR** (376 MHz, $CDCl_3$) δ_F: -111.14.

_N_-(2-bromo-4-fluorophenyl)-_N_-methylacrylamide (13r)

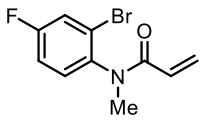

Prepared according to general procedure E, starting from 2-bromo-4-fluoroaniline (10 mmol) and acryloyl chloride, followed by purification of the tertiary amide by FCC (3:7 EtOAc/PE) to give the title compound as a white solid (1.33 g, 52%), with physical and spectroscopic data in accordance with the literature;[33] **R_f** = 0.08 (1:4 EtOAc/PE); **mp** 53 – 55 °C; **^{1}H NMR** (500 MHz, $CDCl_3$) δ_H: 7.42 (dd, *J* = 7.8, 2.8, 1H), 7.25 (dd, *J* = 8.7, 5.5, 1H), 7.10 (ddd, *J* = 8.7, 7.6, 2.8, 1H), 6.38 (dd, *J* = 16.7, 1.9, 1H), 5.85 (dd, *J* = 16.7, 10.3, 1H), 5.53 (dd, *J* = 10.4, 1.9, 1H), 3.24 (s, 3H); **^{13}C {^{1}H} NMR (**126 MHz, $CDCl_3$) δ_C: 165.9, 161.8 (d, *J* = 253.3), 138.7 (d, *J* = 3.8), 131.1 (d, *J* = 8.8), 128.6, 127.6, 124.3 (d, *J* = 10.1), 121.2 (d, *J* = 26.5), 116.1 (d, *J* = 22.7), 36.2; **^{19}F {^{1}H} NMR** (376 MHz, $CDCl_3$) δ_F: -110.28.

(*E*)-_N_-(2-bromo-4-fluorophenyl)-_N_,2-dimethylbut-2-enamide (13s)

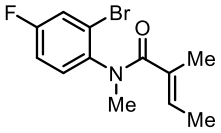

Prepared according to general procedure E, starting from 2-bromo-4-fluoroaniline (10 mmol) and tiglic acid, followed by purification of the tertiary amide by FCC (1.5:8.5 EtOAc/PE) to give the title compound as an off-white solid (0.72 g, 25%); **R_f** = 0.10 (1:4 EtOAc/PE); **mp** 62 – 64 °C; **ν_{max}/cm^{-1}** (film): 1661, 1636, 1489, 1358, 1121, 735; **^{1}H NMR** (300 MHz, $CDCl_3$) δ_H: 7.35 (dd, *J* = 7.9, 2.8, 1H), 7.17 – 7.08 (m, 1H), 7.06 – 6.97 (m, 1H), 5.85 – 5.62 (m, 1H), 3.21 (s, 3H), 1.62 (s, 3H), 1.48 (s, 3H); **^{13}C {^{1}H} NMR** (126 MHz, $CDCl_3$) δ_C: 173.6, 161.1 (d, *J* = 253.3), 140.4, 132.1, 130.9 (d, *J* = 8.8), 130.2, 123.4 (d, *J* = 10.1), 120.9 (d, *J* = 25.2), 115.6 (d, *J* = 21.4), 36.8, 14.0, 13.5; **^{19}F {^{1}H} NMR** (376 MHz, $CDCl_3$) δ_F: -111.87; **HRMS** (ES) calculated for $[C_{12}H_{14}NOF^{79}Br]^+$ $(M+H)^+$: m/z 286.0243 found 286.0245 (+0.7 ppm).

_N_-(2-bromo-4-fluorophenyl)-_N_-methylcyclohex-1-ene-1-carboxamide (13t)

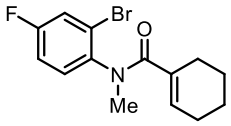

Prepared according to general procedure E, starting from 2-bromo-4-fluoroaniline (10 mmol) and 1-cyclohexene-1-carboxylic acid, followed by purification of the tertiary amide by FCC (1:4 EtOAc/PE) to give the title compound as a white solid (2.31 g, 74%); **R_f** = 0.14 (1:4 EtOAc/PE); **mp** 87 – 89 °C; **ν_{max}/cm^{-1}** (film): 2932, 1659, 1636, 1489, 1306, 1259, 858; **^{1}H NMR** (300 MHz, $CDCl_3$) δ_H: 7.35 (dd, *J* = 7.9, 2.8, 1H), 7.18 – 7.11 (m, 1H), 7.02 (ddd, *J* = 8.7, 7.7, 2.8, 1H), 5.92 – 5.74 (m, 1H), 3.20 (s, 3H), 2.14 – 1.98 (m, 2H), 1.96 – 1.76 (m, 2H), 1.59 – 1.30 (m, 4H); **^{13}C {^{1}H} NMR** (126 MHz, $CDCl_3$) δ_C: 172.7, 161.1 (d, *J* = 253.3), 140.4, 134.1, 132.2, 130.9 (d, *J* = 8.8), 123.4 (d, *J* = 10.1), 120.9 (d, *J* = 25.2), 115.5 (d, *J* = 21.4), 36.7, 25.9, 25.0, 22.1, 21.5; **^{19}F {^{1}H} NMR** (376 MHz, $CDCl_3$) δ_F: -111.81; **HRMS** (ES) calculated for $[C_{14}H_{16}NOF^{79}Br]^+$ $(M+H)^+$: m/z 312.0399 found 312.0404 (+1.6 ppm).

2-bromo-4-fluorophenyl methacrylate (13u)

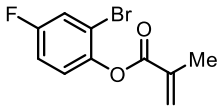

Prepared according to general procedure E, from 2-bromo-4-fluorophenol (10 mmol) and methacryloyl chloride, followed by purification of the ester by FCC (0.5:9.5 EtOAc/PE) to give the title compound as a white solid (2.32 g, 89%); **R_f** = 0.54 (1:4 EtOAc/PE); **mp** 48 – 50 °C; **ν_{max}/cm^{-1}** (film): 1740, 1597, 1483, 1180, 1109, 750; **^{1}H NMR** (500 MHz, $CDCl_3$) δ_H: 7.36 (dd, *J* = 7.8, 2.8, 1H), 7.16 (dd, *J* = 8.9, 5.1, 1H), 7.09 – 7.02 (m, 1H), 6.43 (s, 1H), 5.81 (s, 1H), 2.09 (s, 3H); **^{13}C {^{1}H} NMR** (126 MHz, $CDCl_3$) δ_C: 165.1, 160.0 (d, *J* = 249.5), 144.9 (d, *J* = 2.5), 135.3, 128.4, 124.6 (d, *J* = 8.8), 120.5 (d, *J* = 26.5), 116.6 (d, *J* = 10.1), 115.5 (d, *J* = 22.7), 18.6; **^{19}F {^{1}H} NMR** (376 MHz, $CDCl_3$) δ_F: -114.65; **HRMS** (CI) calculated for $[C_{10}H_8O_2F^{79}Br]^+$ $(M)^+$: m/z 257.9686 found 257.9687 (+0.4 ppm).

S-(2-bromophenyl) 2-methylprop-2-enethioate (13v)

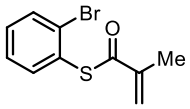

Prepared according to general procedure E, starting from 2-bromo-thiophenol (10 mmol) and methacryloyl chloride, followed by purification of the thioester by FCC (0.2:9.8 EtOAc/PE) to give the title compound as a colourless oil (0.74 g, 29%); **R_f** = 0.54 (1:4 EtOAc/PE); **ν_{max}/cm^{-1}** (film): 1678, 1449, 1277, 1261, 1018, 764, 750; **^{1}H NMR** (300 MHz, $CDCl_3$) δ_H: 7.74 – 7.68 (m, 1H), 7.57 – 7.52 (m, 1H), 7.37 (td, *J* = 7.5, 1.5, 1H), 7.32 – 7.25 (m, 1H), 6.26 (q, *J* = 0.9, 1H), 5.75 (q, *J* = 1.5, 1H), 2.02 (dd, *J* = 1.5, 0.9, 3H); **^{13}C {^{1}H} NMR** (126 MHz, $CDCl_3$) δ_C: 190.0, 143.4, 137.6, 133.7, 131.3, 130.1, 129.5, 128.1, 124.6, 18.3; **HRMS** (APCI) calculated for $[C_{10}H_{10}SO^{79}Br]^+$ $(M+H)^+$: m/z 256.9636 found 256.9633 (-1.2 ppm).

5.4.3. Substrate Scope

5.4.3.1. General Procedure F – Mechanochemical Intramolecular Alkene Difunctionalisation

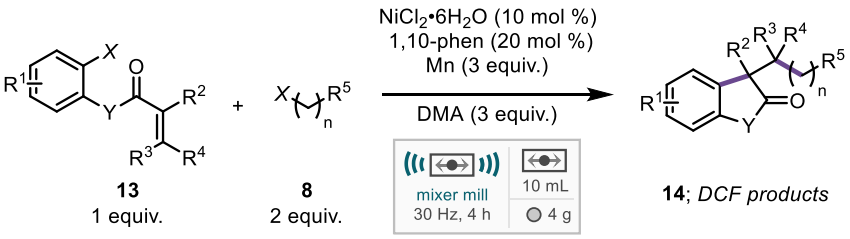

To a 10 mL stainless-steel jar, equipped with a 4 g, 10 mm stainless-steel ball, was charged the appropriate alkene tethered aryl halide (1 mmol, 1 equiv.), alkyl halide (2 mmol, 2 equiv.), nickel chloride hexahydrate (23.8 mg, 0.1 mmol, 10 mol %), 1,10-phenanthroline (36.0 mg, 0.2 mmol, 20 mol %), manganese powder (164.8 mg, 3 mmol, 3 equiv.), and *N,N*-dimethylacetamide (278.0 µL, 3 mmol, 3 equiv.). The jar was closed and placed on the mixer mill for 4 hours, at 30 Hz. Upon completion, the reaction mixture was transferred to a separatory funnel using EtOAc (50 mL) and water (50 mL). 1 M HCl (50 mL) was added, and the phases were separated. The aqueous phase was extracted two more times with EtOAc (2 x 50 mL) and the combined organic phases were washed with brine (30 mL). The organic phase was dried over

magnesium sulfate and concentrated in vacuo. The crude compound was purified by FCC, in the stated solvent system, to yield the corresponding product.

N.B. Sodium iodide (1 equiv.) was used for coupling with alkyl bromides.

5-fluoro-1,3-dimethyl-3-nonylindolin-2-one (3a)

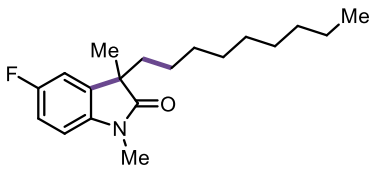

Prepared according to general procedure F, from *N*-(2-bromo-4-fluorophenyl)-*N*-methylmethacrylamide and 1-iodooctane, followed by purification by FCC (1:9 EtOAc/hexane) to give the title compound as a yellow oil (206.1 mg, 67%); **R_f** = 0.38 (1:4 EtOAc/PE); **ν_{max}/cm^{-1}** (film): 2926, 2855, 1707, 1493, 1268, 1277, 1350, 1275, 1117, 907, 729; **^{1}H NMR** (500 MHz, $CDCl_3$) δ_H: 6.96 (ddd, *J* = 9.3, 8.5, 2.6, 1H, Ar*H*), 6.91 (dd, *J* = 8.0, 2.6, 1H, Ar*H*), 6.74 (dd, *J* = 8.4, 4.1, 1H, Ar*H*), 3.20 (s, 3H, N-CH_3), 1.93 – 1.84 (m, 1H, C*H*), 1.73 – 1.64 (m, 1H, C*H*), 1.34 (s, 3H, C-CH_3), 1.31 – 1.09 (m, 14H, CH_2), 1.01 – 0.91 (m, 1H, C*H*), 0.90 – 0.75 (m, 4H, CH_3+C*H*); **^{13}C {^{1}H} NMR** (126 MHz, $CDCl_3$) δ_C: 180.6 (*C*=O), 159.5 (d, *J* = 240.7, Ar*C*F), 139.4 (d, *J* = 1.3, Ar*C*), 136.2 (d, *J* = 7.6, Ar*C*), 113.8 (d, *J* = 22.7, Ar*C*H), 110.8 (d, *J* = 23.9, Ar*C*H), 108.4 (d, *J* = 8.8, Ar*C*H), 49.1 (d, *J* = 2.5, *$C_{quaternary}$*), 38.6 (*C*H_2), 32.0 (*C*H_2), 29.8 (*C*H_2), 29.6 (*C*H_2), 29.4 (2C, *C*H_2), 26.4 (N-*C*H_3), 24.6 (*C*H_2), 23.9 (C-*C*H_3), 22.8 (*C*H_2), 14.2 (CH_2*C*H_3); **^{19}F {^{1}H}** NMR (376 MHz, $CDCl_3$) δ_F: -121.01; **HRMS** (ES) calculated for $[C_{19}H_{29}NOF]^+$ $(M+H)^+$: m/z 306.2233 found 306.2241 (+2.6 ppm).

5-fluoro-3-hexyl-1,3-dimethylindolin-2-one (14b)

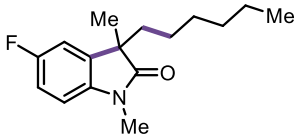

Prepared according to general procedure F, from *N*-(2-bromo-4-fluorophenyl)-*N*-methylmethacrylamide and 1-iodopentane, followed by purification by FCC (1.5:8.5 EtOAc/hexane) to give the title compound as a yellow oil (168.6 mg, 64%); **R_f** = 0.26 (1:4 EtOAc/PE); **ν_{max}/cm^{-1}** (film): 2957, 2928, 2867, 1709, 1493, 1466, 1443, 1377, 1348, 1275, 1242, 1180, 1115, 912, 806; **^{1}H NMR** (500 MHz, $CDCl_3$) δ_H: 6.95 (ddd, *J* = 9.2, 8.5, 2.6, 1H), 6.91 (dd, *J* = 8.0, 2.6, 1H), 6.74 (dd, *J* = 8.4, 4.1, 1H), 3.19 (s, 3H), 1.94 – 1.84 (m, 1H), 1.72 – 1.64 (m, 1H), 1.33 (s, 3H), 1.22 – 1.08 (m, 6H), 1.01 – 0.87

(m, 1H), 0.87 – 0.75 (m, 4H); **^{13}C {^{1}H} NMR** (126 MHz, $CDCl_3$) δ_C: 180.6, 159.5 (d, *J* = 240.7), 139.4 (d, *J* = 2.5), 136.2 (d, *J* = 7.6), 113.9 (d, *J* = 23.9), 110.8 (d, *J* = 25.2), 108.4 (d, *J* = 7.6), 49.1 (d, *J* = 1.3), 38.6, 31.6, 29.5, 26.4, 24.5, 23.9, 22.7, 14.1; **^{19}F NMR** (471 MHz, $CDCl_3$) δ_F: -120.99 – -121.03 (m); **HRMS** (ES) calculated for $[C_{16}H_{23}NOF]^+$ $(M+H)^+$: m/z 264.1764 found 264.1768 (+0.4 ppm).

3-(3,3-dimethylbutyl)-5-fluoro-1,3-dimethylindolin-2-one (14c)

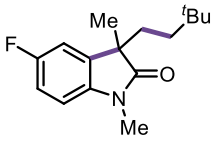

Prepared according to general procedure F, from *N*-(2-bromo-4-fluorophenyl)-*N*-methylmethacrylamide and neopentyl iodide, followed by purification by FCC (1:9 EtOAc/hexane) to give the title compound as a pale yellow oil (200.7 mg, 76%); **R_f** = 0.24 (1:4 EtOAc/hexane); **ν_{max}/cm^{-1}** (film): 2953, 1709, 1493, 1468, 1443, 1364, 1348, 1277, 1260, 899, 868, 750; **^{1}H NMR** (500 MHz, $CDCl_3$) δ_H: 6.98 – 6.92 (m, 1H), 6.89 (dd, *J* = 8.0, 2.6, 1H), 6.74 (dd, *J* = 8.5, 4.1, 1H), 3.20 (s, 3H), 1.88 (td, *J* = 13.1, 4.6, 1H), 1.67 (td, *J* = 13.2, 3.8, 1H), 1.34 (s, 3H), 0.91 – 0.83 (m, 1H), 0.78 (s, 9H), 0.68 – 0.60 (m, 1H); **^{13}C {^{1}H} NMR** (126 MHz, $CDCl_3$) δ_C: 180.5, 159.5 (d, *J* = 240.7), 139.4 (d, *J* = 2.5), 136.2 (d, *J* = 8.8), 113.8 (d, *J* = 22.7), 110.7 (d, *J* = 23.9), 108.4 (d, *J* = 7.6), 48.9 (d, *J* = 1.3), 37.9, 33.5, 30.0, 29.3, 26.4, 24.1; **^{19}F {^{1}H} NMR** (376 MHz, $CDCl_3$) δ_F: -120.95; **HRMS** (ES) calculated for $[C_{16}H_{23}NOF]^+$ $(M+H)^+$: m/z 264.1764 found 264.1756 (-3.0 ppm).

3-(cyclohexylmethyl)-5-fluoro-1,3-dimethylindolin-2-one (14d)

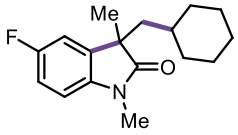

Prepared according to general procedure F, from *N*-(2-bromo-4-fluorophenyl)-*N*-methylmethacrylamide and 1-iodocyclohexane, followed by purification by FCC (1.5:8.5 EtOAc/hexane) to give the title compound as a pale yellow oil (150.1 mg, 55%), with physical and spectroscopic data in accordance with the literature;[34] **R_f** = 0.24 (1:4 EtOAc/hexane); **^{1}H NMR** (500 MHz, $CDCl_3$) δ_H: 6.98 – 6.93 (m, 1H), 6.90 (dd, *J* = 8.0, 2.6, 1H), 6.75 (dd, *J* = 8.4, 4.1, 1H), 3.20 (s, 3H), 1.93 (dd, *J* = 14.1, 7.0, 1H), 1.72 – 1.65 (m, 1H), 1.55 – 1.44 (m, 3H), 1.37 – 1.27 (m, 4H), 1.24 – 1.17 (m,

1H), 1.03 – 0.88 (m, 4H), 0.87 – 0.69 (m, 2H); **^{13}C {^{1}H} NMR** (126 MHz, $CDCl_3$) δ_C: 180.9, 159.5 (d, *J* = 240.7), 139.2 (d, *J* = 2.5), 136.3 (d, *J* = 7.6), 113.8 (d, *J* = 23.9), 111.0 (d, *J* = 23.9), 108.5 (d, *J* = 7.6), 48.5 (d, *J* = 1.3), 45.5, 34.9, 34.6, 33.6, 26.5, 26.3, 26.2 (2C) 26.1; **^{19}F {^{1}H} NMR** (376 MHz, $CDCl_3$) δ_F: -120.98.

Ethyl 5-(5-fluoro-1,3-dimethyl-2-oxoindolin-3-yl)pentanoate (14h)

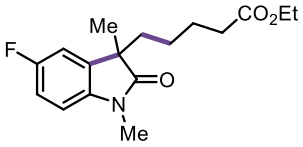

Prepared according to general procedure F, from *N*-(2-bromo-4-fluorophenyl)-*N*-methylmethacrylamide and ethyl 4-bromobutyrate, followed by purification by FCC (1:4 to 3:7 EtOAc/hexane) to give the title compound as a yellow oil (172.6 mg, 56%); **R_f** = 0.19 (3:7 EtOAc/hexane); **ν_{max}/cm^{-1}** (film): 2927, 1707, 1493, 1466, 1371, 1348, 1271, 1180, 1109, 808; **^{1}H NMR** (400 MHz, $CDCl_3$) δ_H: 6.95 (ddd, *J* = 9.2, 8.5, 2.6, 1H), 6.90 (dd, *J* = 7.9, 2.5, 1H), 6.74 (dd, *J* = 8.4, 4.1, 1H), 4.05 (q, *J* = 7.1, 2H), 3.19 (s, 3H), 2.20 – 2.13 (m, 2H), 1.96 – 1.85 (m, 1H), 1.75 – 1.65 (m, 1H), 1.58 – 1.42 (m, 2H), 1.33 (s, 3H), 1.19 (t, *J* = 7.1, 3H), 1.07 – 0.93 (m, 1H), 0.92 – 0.78 (m, 1H); **^{13}C {^{1}H} NMR** (126 MHz, $CDCl_3$) δ_C: 180.3, 173.5, 159.5 (d, *J* = 240.7), 139.3 (d, *J* = 1.3), 135.9 (d, *J* = 7.6), 114.0 (d, *J* = 22.7), 110.8 (d, *J* = 25.2), 108.5 (d, *J* = 8.8), 60.3, 49.0 (d, *J* = 1.3), 38.1, 34.1, 26.4, 25.1, 24.1, 23.9, 14.3; **^{19}F {^{1}H} NMR** (376 MHz, $CDCl_3$) δ_F: -120.79; **HRMS** (CI) calculated for $[C_{17}H_{22}NO_3F]^+$ $(M)^+$: m/z 307.1578 found 307.1580 (+0.44 ppm).

5-fluoro-3-(4-methoxybutyl)-1,3-dimethylindolin-2-one (14i)

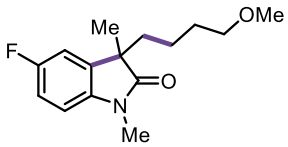

Prepared according to general procedure F, from *N*-(2-bromo-4-fluorophenyl)-*N*-methylmethacrylamide and 1-bromo-3-methoxypropane, followed by purification by FCC (3:7 EtOAc/hexane) to give the title compound as a yellow oil (132.5 mg, 50%); **R_f** = 0.15 (3:7 EtOAc/hexane); **ν_{max}/cm^{-1}** (film): 2930, 1705, 1493, 1275, 1113, 750; **^{1}H NMR** (400 MHz, $CDCl_3$) δ_H: 6.98 – 6.88 (m, 2H), 6.74 (dd, *J* = 8.4, 4.1, 1H), 3.27 – 3.20 (m, 5H), 3.19 (s, 3H), 1.91 (td, *J* = 12.8, 4.7, 1H), 1.71 (td, *J* = 12.8, 4.6, 1H), 1.54 – 1.38 (m, 2H), 1.33 (s, 3H), 1.07 – 0.84 (m, 2H); **^{13}C {^{1}H} NMR** (101 MHz, $CDCl_3$) δ_C:

180.4, 159.5 (d, *J* = 241.4), 139.3 (d, *J* = 2.0), 135.9 (d, *J* = 8.1), 113.9 (d, *J* = 24.2), 110.9 (d, *J* = 25.3), 108.4 (d, *J* = 8.1), 72.5, 58.6, 49.1 (d, *J* = 2.0), 38.4, 29.8, 26.4, 23.9, 21.3; **^{19}F {^{1}H} NMR** (376 MHz, $CDCl_3$) δ_F: -120.86; **HRMS** (APCI) calculated for $[C_{15}H_{21}NO_2F]^+$ $(M+H)^+$: m/z 266.1556 found 266.1560 (+1.5 ppm).

5-fluoro-1,3-dimethyl-3-(4-phenylbutyl)indolin-2-one (14j)

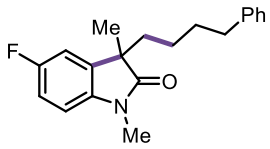

Prepared according to general procedure F, from *N*-(2-bromo-4-fluorophenyl)-*N*-methylmethacrylamide and (3-bromopropyl)benzene, followed by purification by FCC (1:9 to 1:4 EtOAc/hexane) to give the title compound as a pale yellow oil (137.8 mg, 44%); **R_f** = 0.26 (3:7 EtOAc/hexane); **ν_{max}/cm^{-1}** (film): 2930, 2857, 1707, 1493, 1377, 1348, 1273, 1188, 1113, 748, 698; **^{1}H NMR** (500 MHz, $CDCl_3$) δ_H: 7.25 – 7.20 (m, 2H), 7.17 – 7.12 (m, 1H), 7.10 – 7.05 (m, 2H), 6.99 – 6.94 (m, 1H), 6.91 (dd, *J* = 7.9, 2.6, 1H), 3.19 (s, 3H), 2.48 (t, *J* = 8.0, 2H), 1.99 – 1.90 (m, 1H), 1.80 – 1.69 (m, 1H), 1.57 – 1.42 (m, 2H), 1.35 (s, 3H), 1.11 – 0.99 (m, 1H), 0.96 – 0.86 (m, 1H); **^{13}C {^{1}H} NMR** (126 MHz, $CDCl_3$) δ_C: 180.50, 159.5 (d, *J* = 240.7), 142.5, 139.3 (d, *J* = 1.3), 136.0 (d, *J* = 7.6), 128.4 (d, *J* = 3.8), 125.8, 113.9 (d, *J* = 23.9), 110.9 (d, *J* = 23.9), 108.4 (d, *J* = 7.6), 49.1 (d, *J* = 1.3), 38.3, 35.7, 31.7, 26.4, 24.3, 23.8; **^{19}F {^{1}H} NMR** (376 MHz, $CDCl_3$) δ_F: -120.85; **HRMS** (ES) calculated for $[C_{20}H_{23}NOF]^+$ $(M+H)^+$: m/z 312.1764 found 312.1760 (-1.3 ppm).

8-(5-fluoro-1,3-dimethyl-2-oxoindolin-3-yl)octanenitrile (14k)

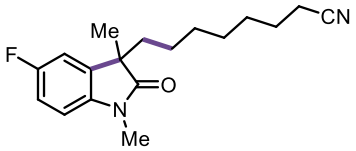

Prepared according to general procedure F, from *N*-(2-bromo-4-fluorophenyl)-*N*-methylmethacrylamide and 7-bromoheptanenitrile, followed by purification by FCC (1:4 to 3:7 EtOAc/hexane) to give the title compound as a pale orange oil (131.9 mg, 44%); **R_f** = 0.11 (3:7 EtOAc/hexane); **ν_{max}/cm^{-1}** (film): 2930, 2245, 1705, 1493, 1275, 1113, 750; **^{1}H NMR** (500 MHz, $CDCl_3$) δ_H: 6.99 – 6.93 (m, 1H), 6.91 (dd, *J* = 7.9, 2.5, 1H), 6.75 (dd, *J* = 8.4, 4.1, 1H), 3.20 (s, 3H), 2.28 (t, *J* = 7.1, 2H), 1.89 (td, *J* = 12.8, 4.7, 1H), 1.68 (td, *J* = 12.9, 4.3, 1H), 1.63 – 1.54 (m, 2H), 1.37 – 1.29 (m, 5H), 1.22 –

1.12 (m, 4H), 1.01 – 0.90 (m, 1H), 0.88 – 0.76 (m, 1H); **^{13}C {^{1}H} NMR** (126 MHz, $CDCl_3$) δ_C: 180.5, 159.5 (d, *J* = 240.7), 139.4 (d, *J* = 2.5), 136.0 (d, *J* = 7.6), 119.9, 113.9 (d, *J* = 23.9), 110.8 (d, *J* = 25.2), 108.4 (d, *J* = 8.8), 49.1 (d, *J* = 1.3), 38.4, 29.4, 28.6, 28.5, 26.4, 25.4, 24.4, 23.9, 17.2; **^{19}F NMR** (471 MHz, $CDCl_3$) δ_F: -120.84 – -120.91 (m); **HRMS** (ES) calculated for $[C_{18}H_{24}N_2OF]^+$ $(M+H)^+$: m/z 303.1873 found 303.1874 (+0.3 ppm).

5-fluoro-3-(3-(4-fluorophenyl)propyl)-1,3-dimethylindolin-2-one (14l)

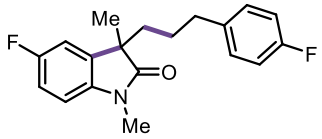

Prepared according to general procedure F, from *N*-(2-bromo-4-fluorophenyl)-*N*-methylmethacrylamide and 1-(2-bromoethyl)-4-fluorobenzene, followed by purification by FCC (1:9 to 1.5:8.5 EtOAc/hexane) to give the title compound as a pale yellow oil (78.3 mg, 25%); **R_f** = 0.29 (3:7 EtOAc/hexane); **ν_{max}/cm^{-1}** **(**film): 2930, 1705, 1661, 1508, 1491, 1377, 1350, 1275, 1219, 750; **^{1}H NMR** (500 MHz, $CDCl_3$) δ_H: 7.01 – 6.93 (m, 3H), 6.93 – 6.88 (m, 2H), 6.86 (dd, *J* = 7.9, 2.6, 1H), 6.73 (dd, *J* = 8.5, 4.1, 1H), 3.19 (s, 3H), 2.55 – 2.37 (m, 2H), 1.99 – 1.90 (m, 1H), 1.75 – 1.67 (m, 1H), 1.33 (s, 3H), 1.32 – 1.24 (m, 1H), 1.15 – 1.05 (m, 1H); **^{13}C {^{1}H} NMR** (126 MHz, $CDCl_3$) δ_C: 180.3, 161.4 (d, *J* = 244.4), 159.5 (d, *J* = 240.1), 139.3 (d, *J* = 1.3), 137.4 (d, *J* = 3.8), 135.8 (d, *J* = 7.6), 129.8 (d, *J* = 7.6), 115.2 (d, *J* = 20.2), 114.0 (d, *J* = 23.9), 110.8 (d, *J* = 23.9), 108.5 (d, *J* = 7.6), 49.0 (d, *J* = 2.5), 38.0, 35.2, 26.6, 26.4, 24.0; **^{19}F {^{1}H} NMR** (376 MHz, $CDCl_3$) δ_F: -117.67, -120.74; **HRMS** (ES) calculated for $[C_{19}H_{20}NOF_2]^+$ $(M+H)^+$: m/z 316.1513 found 316.1503 (-3.2 ppm).

3-(2-cyclobutylethyl)-5-fluoro-1,3-dimethylindolin-2-one (14m)

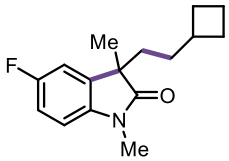

Prepared according to general procedure F, from *N*-(2-bromo-4-fluorophenyl)-*N*-methylmethacrylamide and (bromomethyl)cyclobutane, followed by purification by FCC (1:9 EtOAc/hexane) to give the title compound as a pale yellow oil (188.0 mg, 72%); **R_f** = 0.30 (1:4 EtOAc/hexane); **ν_{max}/cm^{-1}** (film): 2967, 2928, 1707, 1493, 1275, 1115, 750; **^{1}H NMR** (400 MHz, $CDCl_3$) δ_H: 6.99 – 6.93 (m, 1H), 6.90 (dd, *J* = 8.0, 2.5,

1H), 6.74 (dd, *J* = 8.4, 4.1, 1H), 3.20 (s, 3H), 2.15 – 2.02 (m, 1H), 2.00 – 1.87 (m, 2H), 1.84 – 1.63 (m, 3H), 1.56 (td, *J* = 12.9, 4.2, 1H), 1.52 – 1.37 (m, 2H), 1.32 (s, 3H), 1.11 – 0.99 (m, 1H), 0.93 – 0.81 (m, 1H); **^{13}C {^{1}H} NMR** (101 MHz, $CDCl_3$) δ_C: 180.5, 159.5 (d, *J* = 240.4), 139.4 (d, *J* = 2.0), 136.2 (d, *J* = 8.1), 113.8 (d, *J* = 23.2), 110.8 (d, *J* = 24.2), 108.4 (d, *J* = 9.1), 48.9 (d, *J* = 1.0), 36.0, 35.9, 31.6, 28.1 (2C), 26.4, 23.8, 18.4; **^{19}F {^{1}H} NMR** (376 MHz, $CDCl_3$) δ_F: -120.94; **HRMS** (APCI) calculated for $[C_{16}H_{21}NOF]^+$ $(M+H)^+$: m/z 262.1607 found 262.1618 (+4.2 ppm).

3-(2-cyclohexylethyl)-5-fluoro-1,3-dimethylindolin-2-one (14n)

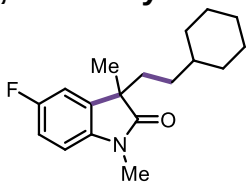

Prepared according to general procedure F, from *N*-(2-bromo-4-fluorophenyl)-*N*-methylmethacrylamide and (bromomethyl)cyclohexane, followed by purification by FCC (1:9 EtOAc/hexane) to give the title compound as a pale yellow oil (148.0 mg, 51%); **R_f** = 0.24 (1:4 EtOAc/hexane); **ν_{max}/cm^{-1}** (film): 2922, 1711, 1493, 1275, 750; **^{1}H NMR** (400 MHz, $CDCl_3$) δ_H: 6.98 – 6.92 (m, 1H), 6.91 – 6.86 (m, 1H), 6.74 (dd, *J* = 8.4, 4.1, 1H), 3.19 (s, 3H), 1.89 (td, *J* = 12.9, 4.6, 1H), 1.75 – 1.65 (m, 1H), 1.64 – 1.54 (m, 5H), 1.33 (s, 3H), 1.21 – 0.98 (m, 4H), 0.90 – 0.59 (m, 4H); **^{13}C {^{1}H} NMR** (101 MHz, $CDCl_3$) δ_C: 180.6, 159.5 (d, *J* = 241.4), 139.4 (d, *J* = 2.0), 136.2 (d, *J* = 8.1), 113.8 (d, *J* = 23.2), 110.8 (d, *J* = 24.2), 108.3 (d, *J* = 9.1), 49.0 (d, *J* = 2.0), 37.9, 36.0, 33.3, 33.1, 31.8, 26.7, 26.4 (3C), 23.9; **^{19}F {^{1}H} NMR** (376 MHz, $CDCl_3$) δ_F: -120.98; **HRMS** (ES) calculated for $[C_{18}H_{25}NOF]^+$ $(M+H)^+$: m/z 290.1920 found 290.1925 (+1.7 ppm).

3-(cyclopentylmethyl)-5-fluoro-1,3-dimethylindolin-2-one (14o)

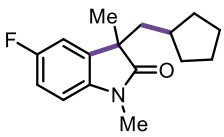

Prepared according to general procedure F, from *N*-(2-bromo-4-fluorophenyl)-*N*-methylmethacrylamide and 1-bromocyclopentane, followed by purification by FCC (1:9 EtOAc/hexane) to give the title compound as a pale yellow solid (122.4 mg, 47%); **R_f** = 0.26 (1:4 EtOAc/hexane); **mp** 63 – 65 °C; **ν_{max}/cm^{-1}** (film): 2949, 2866, 2349, 1707, 1493, 1468, 1375, 1350, 1275, 1113, 1049, 750; **^{1}H NMR** (500 MHz, $CDCl_3$) δ_H:

6.98 – 6.93 (m, 1H), 6.91 (dd, *J* = 8.0, 2.5, 1H), 6.74 (dd, *J* = 8.4, 4.1, 1H), 3.20 (s, 3H), 2.07 (dd, *J* = 13.8, 7.2, 1H), 1.85 (dd, *J* = 13.8, 6.0, 1H), 1.52 – 1.37 (m, 3H), 1.35 – 1.20 (m, 7H), 1.05 – 0.95 (m, 1H), 0.88 – 0.77 (m, 1H); **^{13}C {^{1}H} NMR** (126 MHz, $CDCl_3$) δ_C: 180.8, 159.5 (d, *J* = 240.7), 139.3 (d, *J* = 2.5), 136.3 (d, *J* = 7.6), 113.8 (d, *J* = 22.7), 111.2 (d, *J* = 23.9), 108.3 (d, *J* = 8.8), 49.2 (d, *J* = 1.3), 44.5, 37.3, 33.9, 32.9, 26.5, 25.4, 25.0 (2C); **^{19}F {^{1}H} NMR** (376 MHz, $CDCl_3$) δ_F: -121.10; **HRMS** (ES) calculated for $[C_{16}H_{21}NOF]^+$ $(M+H)^+$: m/z 262.1607 found 262.1607 (0.0 ppm).

3-((*R*)-4,8-dimethylnon-7-en-1-yl)-5-fluoro-1,3-dimethylindolin-2-one (14p)

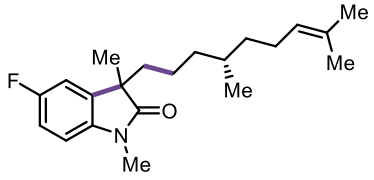

Prepared according to general procedure F, from *N*-(2-bromo-4-fluorophenyl)-*N*-methylmethacrylamide and (*S*)-(+)-citronellyl bromide, followed by purification by FCC (1:4 EtOAc/hexane) to give the title compound as a pale yellow oil (170.1 mg, 51%), as an approximately 1:1 mixture of diastereomers; **R_f** = 0.27 (1:4 EtOAc/hexane); **ν_{max}/cm^{-1}** (film): 2926, 1713, 1495, 1275, 750; **^{1}H NMR** (400 MHz, $CDCl_3$) δ_H: 6.99 – 6.93 (m, 1H), 6.91 (dd, *J* = 8.0, 2.5, 1H), 6.75 (dd, *J* = 8.4, 4.1, 1H), 5.03 (t, *J* = 7.1, 1H), 3.20 (s, 3H), 1.96 – 1.78 (m, 3H), 1.72 – 1.62 (m, 4H), 1.56 (s, 3H), 1.33 (s, 3H), 1.31 – 1.09 (m, 4H), 1.09 – 0.91 (m, 3H), 0.76 – 0.69 (m, 3H); **^{13}C {^{1}H} NMR** (101 MHz, $CDCl_3$) δ_C: 180.6, 159.5 (d, *J* = 241.4), 139.4, 139.3, 136.2 (d, *J* = 8.1), 131.2 (2C), 125.0, 113.8 (d, *J* = 23.2), 110.8 (d, *J* = 24.2), 108.4 (d, *J* = 8.1), 49.1, 38.8 (2C), 37.2, 37.1, 37.0 (2C), 32.2, 32.1, 26.4, 25.8, 25.6 (2C), 23.9 (2C), 22.0, 21.9, 19.6, 19.5, 17.7; **^{19}F {^{1}H} NMR** (376 MHz, $CDCl_3$) δ_F: -120.95, -120.96; **HRMS** (APCI) calculated for $[C_{21}H_{31}NOF]^+$ $(M+H)^+$: m/z 322.2390 found 322.2392 (+0.6 ppm).

3-(3,3-dimethylbutyl)-1,3-dimethylindolin-2-one (14v)

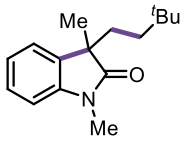

Prepared according to general procedure F, from *N*-(2-bromophenyl)-*N*-methylmethacrylamide and neopentyl iodide, followed by purification by FCC (1:9 EtOAc/hexane) to give the title compound as a pale yellow oil (147.7 mg, 60%); **R_f** = 0.27 (1:4 EtOAc/hexane); **ν_{max}/cm^{-1}** (film): 2953, 1709, 1612, 1493, 1470, 1452, 1377,

1364, 1346, 1125, 1099, 746; **^{1}H NMR** (500 MHz, $CDCl_3$) δ_H: 7.28 – 7.24 (m, 1H), 7.16 – 7.13 (m, 1H), 7.06 (td, *J* = 7.5, 1.0, 1H), 6.84 (d, *J* = 7.7, 1H), 3.21 (s, 3H), 1.87 (td, *J* = 13.0, 4.7, 1H), 1.71 (td, *J* = 13.1, 3.8, 1H), 1.35 (s, 3H), 0.89 (td, *J* = 13.0, 4.7, 1H), 0.77 (s, 9H), 0.65 (td, *J* = 12.9, 3.8, 1H); **^{13}C {^{1}H} NMR** (126 MHz, $CDCl_3$) δ_C: 181.0, 143.5, 134.4, 127.7, 122.6, 122.5, 108.0, 48.4, 37.9, 33.5, 30.0, 29.3, 26.3, 24.2; **HRMS** (ES) calculated for $[C_{16}H_{24}NO]^+$ $(M+H)^+$: m/z 246.1858 found 246.1860 (+0.8 ppm).

3-(3,3-dimethylbutyl)-1,3,5-trimethylindolin-2-one (14w)

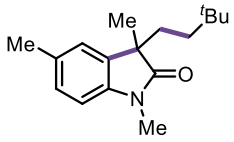

Prepared according to general procedure F, from *N*-(2-bromo-4-methylphenyl)-*N*-methylmethacrylamide and neopentyl iodide, followed by purification by FCC (1:9 EtOAc/hexane) to give the title compound as a pale yellow oil (169.1 mg, 65%); **R_f** = 0.27 (1:4 EtOAc/hexane); **ν_{max}/cm^{-1}** (film): 2953, 1709, 1499, 1468, 1364, 1346, 804; **^{1}H NMR** (500 MHz, $CDCl_3$) δ_H: 7.07 – 7.04 (m, 1H), 6.97 – 6.94 (m, 1H), 6.72 (d, *J* = 7.8, 1H), 3.19 (s, 3H), 2.35 (s, 3H), 1.86 (td, *J* = 13.0, 4.6, 1H), 1.68 (td, *J* = 13.1, 3.9, 1H), 1.33 (s, 3H), 0.91 – 0.85 (m, 1H), 0.78 (s, 9H), 0.67 (td, *J* = 13.0, 3.9, 1H); **^{13}C {^{1}H} NMR** (126 MHz, $CDCl_3$) δ_C: 180.9, 141.2, 134.5, 132.0, 127.9, 123.4, 107.7, 48.4, 37.9, 33.5, 30.0, 29.3, 26.3, 24.2, 21.3; **HRMS** (CI) calculated for $[C_{17}H_{26}NO]^+$ $(M+H)^+$: m/z 260.2009 found 260.2015 (+2.5 ppm).

5-(*tert*-butyl)-3-(3,3-dimethylbutyl)-1,3-dimethylindolin-2-one (14x)

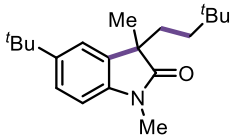

Prepared according to general procedure F, from *N*-(2-bromo-4-(*tert*-butyl)phenyl)-*N*-methylmethacrylamide and neopentyl iodide, followed by purification by FCC (1:9 EtOAc/hexane) to give the title compound as a pale yellow solid (155.8 mg, 52%); **R_f** = 0.44 (1:4 EtOAc/hexane); **mp** 49 – 51 °C; **ν_{max}/cm^{-1}** (film): 2955, 1713, 1275, 1261, 764, 750; **^{1}H NMR** (500 MHz, $CDCl_3$) δ_H: 7.28 (d, *J* = 8.1, 1H), 7.18 (s, 1H), 6.76 (d, *J* = 8.1, 1H), 3.19 (s, 3H), 1.87 (td, *J* = 12.9, 5.0, 1H), 1.69 (td, *J* = 13.0, 3.1, 1H), 1.36 (s, 3H), 1.32 (s, 9H), 0.95 – 0.87 (m, 1H), 0.76 (s, 9H), 0.59 (td, *J* = 12.8, 3.1, 1H); **^{13}C**

{^{1}H} NMR (126 MHz, $CDCl_3$) δ_C: 181.1, 145.8, 141.2, 134.1, 124.0, 119.8, 107.2, 48.6, 37.9, 34.7, 33.5, 31.8, 30.0, 29.2, 26.3, 24.2; **HRMS** (ES) calculated for $[C_{20}H_{32}NO]^+$ $(M+H)^+$: m/z 302.2484 found 302.2475 (-3.0 ppm).

Methyl 3-(3,3-dimethylbutyl)-1,3-dimethyl-2-oxoindoline-5-carboxylate (14y)

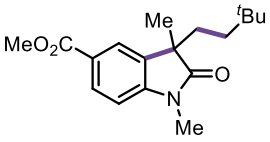

Prepared according to general procedure F, from methyl 3-bromo-4-(*N*-methylmethacrylamido)benzoate and neopentyl iodide, followed by purification by FCC (1:9 EtOAc/hexane) to give the title compound as an off-white solid (150.0 mg, 49%); **R_f** = 0.18 (1:4 EtOAc/hexane); **mp** 86 – 88 °C; **ν_{max}/cm^{-1}** (film): 2955, 1707, 1616, 1275, 907, 748, 727; **^{1}H NMR** (500 MHz, $CDCl_3$) δ_H: 8.02 (dd, *J* = 8.2, 1.2, 1H), 7.82 (d, *J* = 1.0, 1H), 6.87 (d, *J* = 8.2, 1H), 3.92 (s, 3H), 3.24 (s, 3H), 1.90 (td, *J* = 13.1, 4.4, 1H), 1.75 (td, *J* = 13.1, 3.9, 1H), 1.37 (s, 3H), 0.84 (td, *J* = 13.0, 4.4, 1H), 0.77 (s, 9H), 0.64 (td, *J* = 13.0, 3.9, 1H); **^{13}C {^{1}H} NMR** (126 MHz, $CDCl_3$) δ_C: 181.2, 167.2, 147.7, 134.4, 130.6, 124.6, 123.8, 107.6, 52.2, 48.3, 37.9, 33.5, 30.0, 29.3, 26.5, 24.1; **HRMS** (ES) calculated for $[C_{18}H_{26}NO_3]^+$ $(M+H)^+$: m/z 304.1913 found 304.1909 (-1.3 ppm).

3-(3,3-dimethylbutyl)-1,3-dimethyl-5-(trifluoromethyl)indolin-2-one (14z)

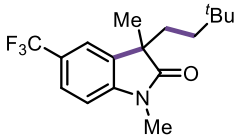

Prepared according to general procedure F, from *N*-(2-bromo-4-(trifluoromethyl)phenyl)-*N*-methylmethacrylamide and neopentyl iodide, followed by purification by FCC (0.5:9.5 to 1:9 EtOAc/hexane) to give the title compound as a pale yellow solid (216.3 mg, 69%); **R_f** = 0.24 (1:4 EtOAc/hexane); **mp** 65 – 67 °C; **ν_{max}/cm^{-1}** (film): 2957, 1719, 1622, 1504, 1460, 1327, 1283, 1115, 820, 750; **^{1}H NMR** (500 MHz, $CDCl_3$) δ_H: 7.55 (d, *J* = 8.0, 1H), 7.37 (s, 1H), 6.90 (d, *J* = 7.9, 1H), 3.24 (s, 3H), 1.91 (td, *J* = 13.0, 3.0, 1H), 1.72 (td, *J* = 13.1, 2.4, 1H), 1.38 (s, 3H), 0.92 – 0.83 (m, 1H), 0.77 (s, 9H), 0.62 (td, *J* = 12.9, 2.4, 1H); **^{13}C {^{1}H} NMR** (126 MHz, $CDCl_3$) δ_C: 180.8, 146.5, 135.0, 125.6 (q, *J* = 3.8), 124.8 (q, *J* = 32.8), 124.7 (q, *J* = 272.2), 119.5 (q, *J* = 3.8), 107.7, 48.4, 37.9, 33.5, 30.0, 29.2, 26.4, 24.0; **^{19}F {^{1}H} NMR** (376 MHz,

$CDCl_3$) δ_F: -61.31; **HRMS** (ES) calculated for $[C_{17}H_{23}NOF_3]^+$ $(M+H)^+$: m/z 314.1732 found 314.1730 (-0.6 ppm).

3-(3,3-dimethylbutyl)-1,3-dimethyl-2-oxoindoline-5-carbonitrile (14aa)

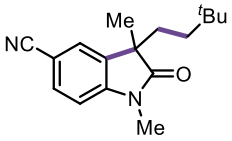

Prepared according to general procedure F, from *N*-(2-bromo-4-cyanophenyl)-*N*-methylmethacrylamide and neopentyl iodide, followed by purification by FCC (1:9 EtOAc/hexane) to give the title compound as a white solid (130.4 mg, 48%); **R_f** = 0.16 (1:4 EtOAc/hexane); **mp** 142 – 144 °C; **ν_{max}/cm^{-1}** (film): 2955, 2222, 1717, 1612, 1497, 1366, 1340, 1260, 820, 750; **^{1}H NMR** (500 MHz, $CDCl_3$) δ_H: 7.61 (d, *J* = 8.1, 1H), 7.39 (s, 1H), 6.90 (d, *J* = 8.1, 1H), 3.24 (s, 3H), 1.89 (td, *J* = 13.1, 4.5, 1H), 1.71 (td, *J* = 13.2, 3.8, 1H), 1.37 (s, 3H), 0.84 (td, *J* = 13.0, 4.5, 1H), 0.78 (s, 9H), 0.62 (td, *J* = 13.0, 3.8, 1H); **^{13}C {^{1}H} NMR** (126 MHz, $CDCl_3$) δ_C: 180.5, 147.4, 135.5, 133.3, 125.9, 119.6, 108.5, 105.7, 48.3, 37.9, 33.4, 30.0, 29.2, 26.5, 23.9; **HRMS** (APCI) calculated for $[C_{17}H_{23}N_2O]^+$ $(M+H)^+$: m/z 271.1810 found 271.1810 (0.0 ppm).

5-chloro-3-(3,3-dimethylbutyl)-1,3-dimethylindolin-2-one (14ab)

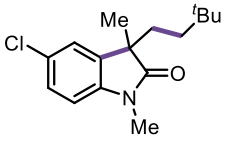

Prepared according to general procedure F, from *N*-(2-bromo-4-chlorophenyl)-*N*-methylmethacrylamide and neopentyl iodide, followed by purification by FCC (0.5:9.5 to 0.7:9.3 EtOAc/hexane) to give the title compound as a pale yellow oil (180.5 mg, 65%); **R_f** = 0.30 (1:4 EtOAc/hexane); **ν_{max}/cm^{-1}** (film): 2955, 1713, 1609, 1489, 1364, 1343, 808, 750; **^{1}H NMR** (500 MHz, $CDCl_3$) δ_H: 7.23 (dd, *J* = 8.2, 2.1, 1H), 7.12 (d, *J* = 2.1, 1H), 6.75 (d, *J* = 8.3, 1H), 3.19 (s, 3H), 1.87 (td, *J* = 13.1, 4.5, 1H), 1.68 (td, *J* = 13.1, 3.9, 1H), 1.34 (s, 3H), 0.86 (td, *J* = 13.0, 4.5, 1H), 0.78 (s, 9H), 0.66 (td, *J* = 13.0, 3.9, 1H); **^{13}C {^{1}H} NMR** (126 MHz, $CDCl_3$) δ_C: 180.4, 142.1, 136.2, 128.0, 127.7, 123.1, 108.9, 48.7, 37.9, 33.5, 30.0, 29.3, 26.4, 24.1; **HRMS** (ES) calculated for $[C_{16}H_{23}NO^{35}Cl]^+$ $(M+H)^+$: m/z 280.1468 found 280.1468 (0.0 ppm).

3-(3,3-dimethylbutyl)-5-methoxy-1,3-dimethylindolin-2-one (14ac)

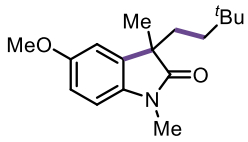

Prepared according to general procedure F, from *N*-(2-bromo-4-methoxyphenyl)-*N*-methylmethacrylamide and neopentyl iodide, followed by purification by FCC (1:9 EtOAc/hexane) to give the title compound as a pale yellow solid (195.1 mg, 71%); **R_f** = 0.19 (1:4 EtOAc/hexane); **mp** 71 – 73 °C; **ν_{max}/cm^{-1}** (film): 2953, 1707, 1277, 1261, 750; **^{1}H NMR** (500 MHz, $CDCl_3$) δ_H: 6.81 – 6.70 (m, 3H), 3.80 (s, 3H), 3.19 (s, 3H), 1.87 (td, *J* = 13.0, 4.6, 1H), 1.67 (td, *J* = 13.1, 3.8, 1H), 1.34 (s, 3H), 0.88 (td, *J* = 13.1, 4.7, 1H), 0.78 (s, 9H), 0.66 (td, *J* = 13.0, 3.8, 1H); **^{13}C {^{1}H} NMR** (126 MHz, $CDCl_3$) δ_C: 180.6, 156.1, 137.1, 135.9, 111.4, 110.3, 108.2, 55.9, 48.8, 37.9, 33.5, 30.0, 29.3, 26.4, 24.3; **HRMS** (ES) calculated for $[C_{17}H_{26}NO_2]^+$ $(M+H)^+$: m/z 276.1964 found 276.1970 (+2.2 ppm).

3-(3,3-dimethylbutyl)-1,3-dimethyl-5-(trifluoromethoxy)indolin-2-one (14ad)

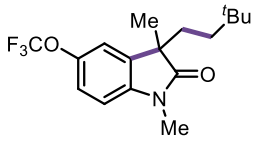

Prepared according to general procedure F, from *N*-(2-bromo-4-(trifluoromethoxy)phenyl)-*N*-methylmethacrylamide and neopentyl iodide, followed by purification by FCC (1:9 EtOAc/hexane) to give the title compound as a pale yellow solid (184.0 mg, 56%); **R_f** = 0.25 (1:4 EtOAc/hexane); **mp** 67 – 69 °C; **ν_{max}/cm^{-1}** (film): 2957, 1715, 1497, 1250, 1215, 1161, 748; **^{1}H NMR** (500 MHz, $CDCl_3$) δ_H: 7.16 – 7.11 (m, 1H), 7.03 (d, *J* = 1.3, 1H), 6.81 (d, *J* = 8.4, 1H), 3.22 (s, 3H), 1.89 (td, *J* = 13.1, 4.8, 1H), 1.69 (td, *J* = 13.1, 3.7, 1H), 1.36 (s, 3H), 0.92 – 0.84 (m, 1H), 0.77 (s, 9H), 0.60 (td, *J* = 12.9, 3.7, 1H); **^{13}C {^{1}H} NMR** (126 MHz, $CDCl_3$) δ_C: 180.6, 144.9, 142.1, 135.9, 120.9, 120.7 (q, *J* = 255.8) 116.7, 108.3, 48.8, 37.8, 33.4, 30.0, 29.2, 26.4, 24.0; **^{19}F {^{1}H} NMR** (376 MHz, $CDCl_3$) δ_F: -58.47; **HRMS** (ES) calculated for $[C_{17}H_{23}NO_2F_3]^+$ $(M+H)^+$: m/z 330.1681 found 330.1678 (-0.9 ppm).

3-(3,3-dimethylbutyl)-1,3,4-trimethylindolin-2-one (14ae)

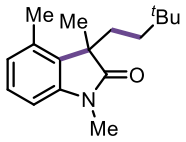

Prepared according to general procedure F, from *N*-(2-bromo-3-methylphenyl)-*N*-methylmethacrylamide and neopentyl iodide, followed by purification by FCC (0.5:9.5 EtOAc/hexane) to give the title compound as a colourless oil (92.0 mg, 35%); **R_f** = 0.28 (1:4 EtOAc/hexane); **ν_{max}/cm^{-1}** (film): 2955, 1707, 1609, 1468, 1275, 1261, 907, 764, 750; **^{1}H NMR** (500 MHz, $CDCl_3$) δ_H: 7.16 (t, *J* = 7.8, 1H), 6.82 (d, *J* = 7.8, 1H), 6.68 (d, *J* = 7.7, 1H), 3.20 (s, 3H), 2.35 (s, 3H), 1.98 – 1.93 (m, 2H), 1.43 (s, 3H), 0.78 (s, 9H), 0.76 – 0.70 (m, 1H), 0.55 – 0.48 (m, 1H); **^{13}C {^{1}H} NMR** (126 MHz, $CDCl_3$) δ_C: 180.9, 143.8, 134.1, 130.8, 127.5, 125.1, 105.8, 49.5, 38.5, 31.6, 30.0, 29.3, 26.3, 22.8, 18.2; **HRMS** (ES) calculated for $[C_{17}H_{26}NO]^+$ $(M+H)^+$: m/z 260.2014 found 260.2011 (-1.2 ppm).

3-(3,3-dimethylbutyl)-1,3-dimethyl-1,3-dihydro-2*H*-pyrrolo[2,3-*b*]pyridin-2-one (14af)

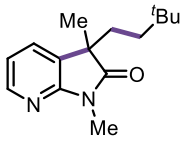

Prepared according to general procedure F, from *N*-(3-bromopyridin-2-yl)-*N*-methylmethacrylamide and neopentyl iodide, followed by purification by FCC (1:9 to 1.5:8.5 EtOAc/hexane) to give the title compound as a colourless oil (138.1 mg, 56%); **R_f** = 0.20 (1:4 EtOAc/hexane); **ν_{max}/cm^{-1}** (film): 2953, 1717, 1607, 1593, 1468, 1344, 750; **^{1}H NMR** (500 MHz, $CDCl_3$) δ_H: 8.17 (dd, *J* = 5.3, 1.6, 1H), 7.37 (dd, *J* = 7.2, 1.6, 1H), 6.96 (dd, *J* = 7.2, 5.3, 1H), 3.29 (s, 3H), 1.88 (td, *J* = 13.1, 4.6, 1H), 1.71 (td, *J* = 13.2, 3.9, 1H), 1.36 (s, 3H), 0.90 (td, *J* = 13.1, 4.6, 1H), 0.77 (s, 9H), 0.67 (td, *J* = 13.0, 3.8, 1H); **^{13}C {^{1}H} NMR** (126 MHz, $CDCl_3$) δ_C: 180.6, 157.0, 146.6, 129.9, 128.7, 118.2, 48.1, 37.9, 33.1, 30.0, 29.2, 25.4, 23.5; **HRMS** (ES) calculated for $[C_{15}H_{23}N_2O]^+$ $(M+H)^+$: m/z 247.1810 found 247.1814 (+1.6 ppm).

1-Benzyl-3-(3,3-dimethylbutyl)-5-fluoro-3-methylindolin-2-one (14ag)

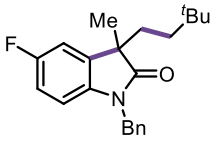

Prepared according to general procedure F, from *N*-benzyl-*N*-(2-bromo-4-fluorophenyl)methacrylamide and neopentyl iodide, followed by purification by FCC (0.5:9.5 EtOAc/hexane) to give the title compound as a yellow oil (212.7 mg, 63%); $\mathbf{R_f}$ = 0.38 (1:4 EtOAc/hexane); $\mathbf{\nu_{max}/cm^{-1}}$ (film): 2955, 1707, 1489, 1277, 1167, 750; **^{1}H NMR** (300 MHz, $CDCl_3$) δ_H: 7.35 – 7.22 (m, 5H), 6.90 (dd, *J* = 8.0, 2.6, 1H), 6.83 (ddd, *J* = 9.3, 8.5, 2.6, 1H), 6.61 (dd, *J* = 8.5, 4.2, 1H), 5.01 (d, *J* = 15.7, 1H), 4.81 (d, *J* = 15.7, 1H), 1.97 (td, *J* = 13.0, 4.7, 1H), 1.72 (td, *J* = 13.1, 3.8, 1H), 1.41 (s, 3H), 0.95 (td, *J* = 12.9, 4.7, 1H), 0.79 (s, 9H), 0.66 (td, *J* = 12.9, 3.8, 1H); **^{13}C {^{1}H} NMR** (126 MHz, $CDCl_3$) δ_C: 180.6, 159.5 (d, *J* = 240.7), 138.4 (d, *J* = 2.5), 136.1 (d, *J* = 7.6), 136.0, 128.9, 127.8, 127.4, 113.8 (d, *J* = 23.9), 110.7 (d, *J* = 23.9), 109.5 (d, *J* = 8.8), 48.9 (d, *J* = 1.3), 43.8, 38.2, 33.6, 30.0, 29.2, 24.4; **^{19}F {^{1}H} NMR** (376 MHz, $CDCl_3$) δ_F: -120.81; **HRMS** (ES) calculated for $[C_{22}H_{27}NOF]^+$ $(M+H)^+$: m/z 340.2077 found 340.2070 (-0.7 ppm).

3-(3,3-dimethylbutyl)-5-fluoro-1-methyl-3-phenylindolin-2-one (14ah)

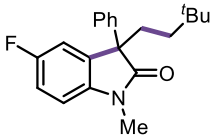

Prepared according to general procedure F, from *N*-(2-bromo-4-fluorophenyl)-*N*-methyl-2-phenylacrylamide and neopentyl iodide, followed by purification by FCC (1:9 EtOAc/hexane) to give the title compound as a yellow oil (110.5 mg, 34%); $\mathbf{R_f}$ = 0.20 (1:4 EtOAc/hexane); $\mathbf{\nu_{max}/cm^{-1}}$ (film): 2955, 1709, 1495, 1275, 750; **^{1}H NMR** (300 MHz, $CDCl_3$) δ_H: 7.38 – 7.21 (m, 5H), 7.08 – 7.01 (m, 1H), 7.01 – 6.96 (m, 1H), 6.83 (dd, *J* = 8.5, 4.2, 1H), 3.22 (s, 3H), 2.34 (td, *J* = 12.9, 4.8, 1H), 2.17 (td, *J* = 13.0, 3.8, 1H), 1.02 (td, *J* = 12.9, 4.8, 1H), 0.83 (s, 9H), 0.74 (td, *J* = 12.8, 3.8, 1H); **^{13}C {^{1}H} NMR** (126 MHz, $CDCl_3$) δ_C: 178.5, 159.4 (d, *J* = 240.7), 140.0 (d, *J* = 2.5), 139.9, 134.1 (d, *J* = 8.8), 128.7, 127.6, 126.9, 114.5 (d, *J* = 23.9), 112.9 (d, *J* = 23.9), 108.8 (d, *J* = 8.8), 57.0 (d, *J* = 1.3), 37.9, 33.1, 30.2, 29.3, 26.7; **^{19}F NMR** (471 MHz, $CDCl_3$) δ_F: -120.36 – -120.45 (m); **HRMS** (ES) calculated for $[C_{21}H_{25}NOF]^+$ $(M+H)^+$: m/z 326.1920 found 326.1920 (+0.0 ppm).

3-(4,4-dimethylpentan-2-yl)-5-fluoro-1,3-dimethylindolin-2-one (14ai)

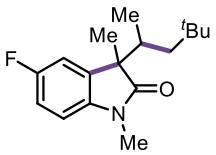

Prepared according to general procedure F, from (*E*)-*N*-(2-bromo-4-fluorophenyl)-*N*,2-dimethylbut-2-enamide and neopentyl iodide, followed by purification by FCC (1:9 EtOAc/hexane) to give the title compound as a pale yellow oil (44.9 mg, 16%), as an approximately 3:1 mixture of diastereomers; **R_f** = 0.28 (1:4 EtOAc/hexane); **ν_{max}/cm^{-1}** (film): 2953, 1709, 1495, 1275, 1117, 750; Data for major diastereomer, **^{1}H NMR** (300 MHz, $CDCl_3$) δ_H: 7.01 – 6.88 (m, 2H), 6.79 – 6.70 (m, 1H), 3.20 (s, 3H), 1.92 – 1.79 (m, 1H), 1.72 – 1.59 (m, 1H), 1.34 (s, 4H), 1.14 – 0.85 (m, 6H), 0.83 (s, 3H), 0.82 – 0.75 (m, 1H), 0.73 (s, 9H); **^{13}C {^{1}H} NMR** (126 MHz, $CDCl_3$) δ_C: 180.6, 159.5 (d, *J* = 240.7), 139.3 (d, *J* = 1.3), 136.2 (d, *J* = 7.6), 113.8 (d, *J* = 22.7), 110.8 (d, *J* = 23.8), 108.4 (d, *J* = 7.6), 49.2 (d, *J* = 1.3), 39.3, 36.6, 30.4, 30.2, 29.4, 26.4, 24.0; **^{19}F NMR** (471 MHz, $CDCl_3$) δ_F: -120.93 – -120.98 (m), -121.10 – -121.14 (m); **HRMS** (ES) calculated for $[C_{17}H_{25}NOF]^+$ $(M+H)^+$: m/z 278.1920 found 278.1919 (-0.4 ppm).

3-benzyl-5-fluoro-1,3-dimethylindolin-2-one (14aq)

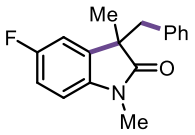

Prepared according to general procedure F, from *N*-(2-bromophenyl)-*N*-methylmethacrylamide and bromobenzene, followed by purification by FCC (1:9 EtOAc/hexane) to give the title compound as an off-white solid (30.5 mg, 11%), with physical and spectroscopic data in accordance with the literature;[35] **R_f** = 0.18 (1:4 EtOAc/hexane); **mp** 104 – 106 °C; **^{1}H NMR** (400 MHz, $CDCl_3$) δ_H: 7.12 – 7.04 (m, 3H), 6.91 – 6.83 (m, 4H), 6.52 (dd, *J* = 9.2, 4.2, 1H), 3.13 (d, *J* = 13.0, 1H), 3.01 – 2.94 (m, 4H), 1.47 (s, 3H); **^{13}C {^{1}H} NMR** (101 MHz, $CDCl_3$) δ_C: 179.7, 159.2 (d, *J* = 240.4), 139.2 (d, *J* = 2.0), 135.9, 134.9 (d, *J* = 8.1), 129.9, 127.8, 126.7, 114.0 (d, *J* = 24.2), 111.6 (d, *J* = 25.3), 108.3 (d, *J* = 8.1), 50.6 (d, *J* = 2.0), 44.6, 26.2, 22.8; **^{19}F {^{1}H} NMR** (376 MHz, $CDCl_3$) δ_F: -121.09.

_N_-(4-fluoro-2-octylphenyl)-_N_-methylmethacrylamide (15a)

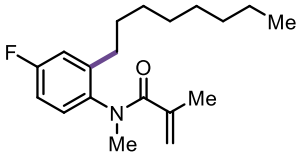

Prepared according to general procedure F, from *N*-(2-bromo-4-fluorophenyl)-*N*-methylmethacrylamide and 1-iodooctane, on a 0.3 mmol scale using zinc as the reductant, followed by purification by FCC (1:9 EtOAc/hexane) to give the title compound as a yellow oil (20.6 mg, 22%); $\mathbf{R_f}$ = 0.28 (1:4 EtOAc/PE); $\mathbf{\nu_{max}/cm^{-1}}$ (film): 2924, 2855, 1653, 1626, 1495, 1454, 1420, 1364, 1217, 1150, 1119, 910, 870; **^{1}H NMR** (500 MHz, $CDCl_3$) δ_H: 7.02 (dd, *J* = 8.6, 5.4, 1H), 6.97 (dd, *J* = 9.7, 2.9, 1H), 6.86 (td, *J* = 8.2, 2.9, 1H), 4.96 (s, 1H), 4.89 (s, 1H), 3.21 (s, 3H), 2.58 – 2.41 (m, 2H), 1.72 (s, 3H), 1.65 – 1.55 (m, 3H), 1.42 – 1.19 (m, 12H), 0.88 (t, *J* = 6.9, 3H); **^{13}C {^{1}H} NMR** (126 MHz, $CDCl_3$) δ_C: 172.3, 162.0 (d, *J* = 248.2), 142.3 (d, *J* = 7.6), 140.5, 138.9 (d, *J* = 3.8), 129.9 (d, *J* = 8.8), 118.8, 116.2 (d, *J* = 22.7), 113.7 (d, *J* = 22.7), 37.7, 32.0, 30.7, 29.9 (2C), 29.6, 29.3, 22.8, 20.6, 14.2; **^{19}F {^{1}H} NMR** (376 MHz, $CDCl_3$) δ_F: -113.57; **HRMS** (ES) calculated for $[C_{19}H_{29}NOF]^+$ $(M+H)^+$: m/z 306.2233 found 306.2236 (+0.3 ppm).

5-fluoro-1,3,3-trimethylindolin-2-one (16a)

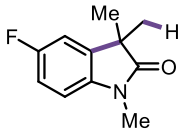

Prepared according to general procedure F, from *N*-(2-bromophenyl)-*N*-methylmethacrylamide, with no alkyl halide and sodium iodide (1 equiv.) as an additive, followed by purification by FCC (1:4 EtOAc/hexane) to give the title compound as a yellow solid (92.6 mg, 48%), with physical and spectroscopic data in accordance with the literature;[36] $\mathbf{R_f}$ = 0.15 (1:4 EtOAc/hexane); **mp** 86 – 88 °C; **^{1}H NMR** (500 MHz, $CDCl_3$) δ_H: 6.99 – 6.91 (m, 2H), 6.77 – 6.72 (m, 1H), 3.20 (s, 3H), 1.36 (s, 6H); **^{13}C {^{1}H} NMR** (126 MHz, $CDCl_3$) δ_C: 181.1, 159.5 (d, *J* = 240.7), 138.7 (d, *J* = 2.5), 137.6 (d, *J* = 7.6), 113.9 (d, *J* = 23.9), 110.7 (d, *J* = 25.2), 108.5 (d, *J* = 8.8), 44.8 (d, *J* = 2.5), 26.5, 24.4; **^{19}F {^{1}H} NMR** (376 MHz, $CDCl_3$) δ_F: -120.91.

5.4.3.2. Reaction Scale Up

5.4.3.2.1. Scale Up by Ball-Milling

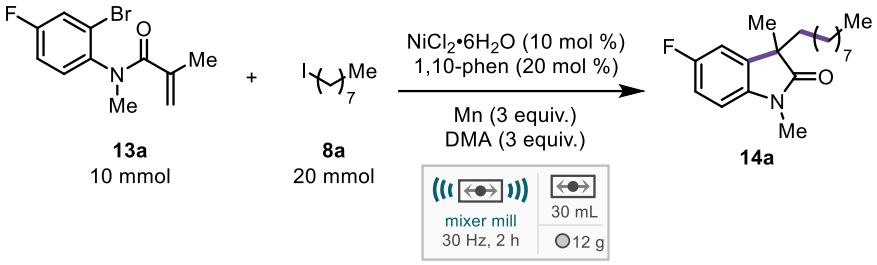

To a 30 mL stainless-steel jar, equipped with a 12 g, 14 mm stainless-steel ball, was charged **13a** (2.72 g, 10 mmol, 1 equiv.), 1-iodooctane (3.61 mL, 20 mmol, 2 equiv.), nickel chloride hexahydrate (237.7 mg, 1 mmol, 10 mol %), 1,10-phenanthroline (360.4 mg, 2 mmol, 20 mol %), manganese powder (1.65 g, 30 mmol, 3 equiv.), and *N,N*-dimethylacetamide (2.78 mL, 3 mmol, 3 equiv.). The jar was closed and placed on the mixer mill for 2 hours, at 30 Hz. Upon completion, the reaction mixture was transferred to a separatory funnel using EtOAc (50 mL) and water (50 mL). 1 M HCl (50 mL) was added, and the phases were separated. The aqueous phase was extracted two more times with EtOAc (2 x 50 mL) and the combined organic phases were washed with brine (30 mL). The organic phase was dried over magnesium sulfate and concentrated in vacuo. The crude compound was purified by FCC in 1:9 EtOAc/hexane to give **14a** as a pale-yellow oil (1.60 g, 52%).

5.4.3.2.2. Heated Ball-Mill Experiments

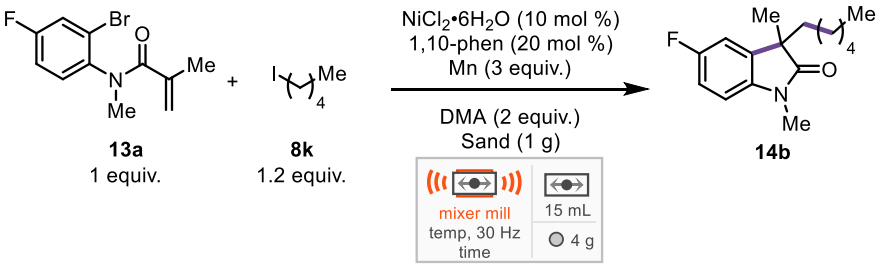

To a 15 mL stainless steel jar, equipped with a 4 g, 10 mm stainless steel ball, was charged **13a** (272.1 mg, 1 mmol, 1 equiv.), 1-iodopentane (156.7 µL, 1.2 mmol, 1.2 equiv.), nickel chloride hexahydrate (23.8 mg, 0.1 mmol, 10 mol %), 1,10-phenanthroline (36.0 mg, 0.2 mmol, 20 mol %), manganese powder (164.8 mg, 3 mmol, 3 equiv.), *N,N*-dimethylacetamide (185.4 µL, 2 mmol, 2 equiv.), and sand (1 g, 1 g/mmol). The jar was closed, placed on the mixer mill, and encased by a band heater. Heating to 50, 75, or 100 °C and milling at 30 Hz were commenced

simultaneously and continued for 30 minutes. Upon completion, the jar was allowed to cool, and the reaction mixture was transferred to a separatory funnel using EtOAc (50 mL) and water (50 mL). 1 M HCl (50 mL) was added, and the phases were separated. The aqueous phase was extracted two more times with EtOAc (2 x 50 mL) and the combined organic phases were washed with brine (30 mL). The organic phase was dried over magnesium sulfate and concentrated in vacuo. After concentrating in vacuo, the crude material was analysed by ^{19}F NMR using (trifluoromethyl)benzene as an internal standard. NMR yields of **14b**: 50 °C 13%, 75 °C 25%, 100 °C 35%.

5.4.3.2.3. Scale Up by Extrusion

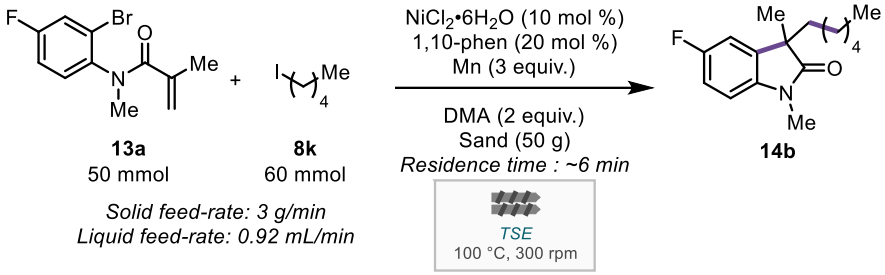

To a mortar and pestle was charged **13a** (13.61 g, 50 mmol, 1 equiv.), nickel chloride hexahydrate (1.19 g, 5 mmol, 10 mol %), 1,10-phenanthroline (1.80 g, 10 mmol, 20 mol %), manganese powder (8.24 g, 150 mmol, 3 equiv.), and sand (50 g, 50 g/mmol). The pestle was used break up large chunks and a spatula used to mix the solids together. The mixture was added to the gravimetric feeder situated at the first port of the extruder, with a feed rate of 3 g/min (calibrated *ex situ*). 1-Iodopentane (7.83 mL, 60 mmol, 1.2 equiv.) and *N,N*-dimethylacetamide (9.27 mL, 100 mmol, 2 equiv.) were added via syringe pump through the second port of the extruder at a rate of 0.92 mL/min. The TSE was set to 300 rpm and each of the 7 heating zones were set to 100 °C. The extrudate was collected in a beaker placed at the end of the barrel, containing EtOAc (100 mL) and 1 M HCl (100 mL). Once all the materials had passed through the extruder, the mixture was transferred to a separatory funnel and the phases were separated. The aqueous phase was extracted two more times with EtOAc (2 x 100 mL) and the combined organic phases were washed with brine (100 mL). The organic phase was dried over magnesium sulfate and concentrated in vacuo. The crude compound was analysed by ^{19}F NMR using (trifluoromethyl)benzene as an internal standard. NMR yield of **14b**: <2% (98% recovered **13a**).

5.4.3.3. Solution-Phase Comparisons

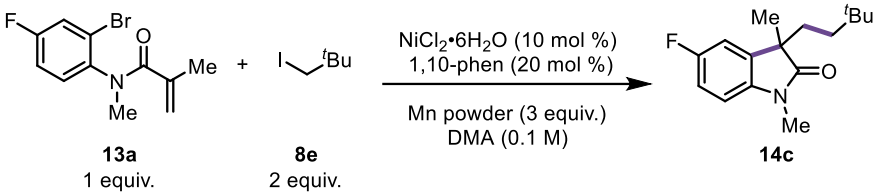

13a 1 equiv. **8e** 2 equiv. **14c**

To a 20 mL microwave vial, under a nitrogen atmosphere and equipped with a magnetic stirrer bar, was charged **13a** (272.1 mg, 1 mmol, 1 equiv.), neopentyl iodide (265.1 µL, 2 mmol, 2 equiv.), nickel chloride hexahydrate (23.8 mg, 0.1 mmol, 10 mol %), 1,10-phenanthroline (36.0 mg, 0.2 mmol, 20 mol %), manganese powder (164.8 mg, 3 mmol, 3 equiv.), and *N,N*-dimethylacetamide (10 mL, 0.1 M). The mixture was stirred at room temperature or 80 °C for 16 hours. Upon completion, the reaction mixture was quenched with 1 M HCl (5 mL) and diluted with EtOAc (5 mL). (Trifluoromethyl)benzene was added and the mixture was allowed to stir for 5 minutes. The phases were allowed to settle, and an aliquot of the organic layer was taken for ^{19}F NMR analysis. NMR yields of **9c**: rt, under N_2 <2%; 80 °C, under N_2 11%; Mn pre-mill for 5 min, then 80 °C, under N_2 40%.

5.4.3.4. Asymmetric Studies

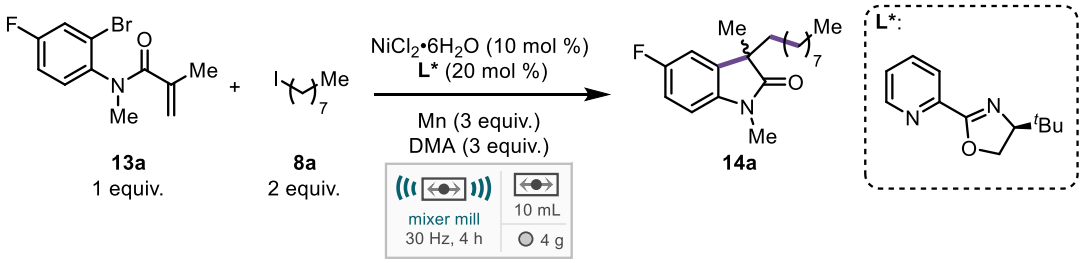

13a 1 equiv. **8a** 2 equiv. **14a**

To a 10 mL stainless-steel jar, equipped with a 4 g, 10 mm stainless-steel ball, was charged **13a** (272.1 mg, 1 mmol, 1 equiv.), 1-iodooctane (361.1 µL, 2 mmol, 2 equiv.), nickel chloride hexahydrate (23.8 mg, 0.1 mmol, 10 mol %), **L*** (40.9 mg, 0.2 mmol, 20 mol %), manganese powder (164.8 mg, 3 mmol, 3 equiv.), and *N,N*-dimethylacetamide (278.0 µL, 3 mmol, 3 equiv.). The jar was closed and placed on the mixer mill for 4 hours, at 30 Hz. Upon completion, the reaction mixture was transferred to a separatory funnel using EtOAc (50 mL) and water (50 mL). 1 M HCl (50 mL) was added, and the phases were separated. The aqueous phase was extracted two more times with EtOAc (2 x 50 mL) and the combined organic phases were washed with brine (30 mL). The organic phase was dried over magnesium sulfate and concentrated in vacuo. The crude compound was purified by FCC in 1:9

EtOAc/hexane to give **14a** as a pale-yellow oil (105.0 mg, 34%, 46% ee); $[\alpha]_D^{20}$ = -0.6 (c = 0.9, $CHCl_3$); Chiral HPLC (Chiralpak IA, 1:99 IPA/hexane, 1 mL/min, 254 nm, 25 °C); t_R = 8.4 min, t_R = 9.1 min.

5.4.3.5. Synthesis of Starting Material in Ball-Mill

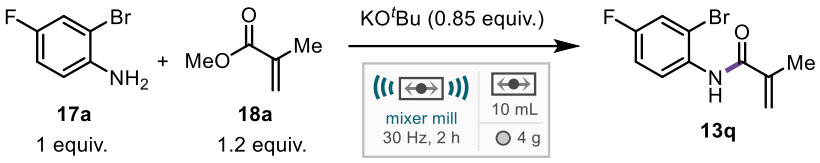

This procedure was adapted from a previous report.[37] To a 10 mL stainless-steel jar, equipped with a 4 g, 10 mm stainless-steel ball, was charged 2-bromo-4-fluoroaniline (113.8 µL, 1 mmol, 1 equiv.), methyl methacrylate (128.4 µL, 1.2 mmol, 1.2 equiv.), and potassium *tert*-butoxide (95.4 mg, 0.85 mmol, 0.85 equiv.). The jar was closed and placed on the mixer mill for 2 hours, at 30 Hz. Upon completion, the reaction mixture was diluted with a small amount of EtOAc (3 mL) and brine was added (3 mL), the jar was closed again and shaken a few times by hand. The mixture was transferred to a separatory funnel and the phases were separated. The aqueous phase was extracted one more time with EtOAc (5 mL) and the combined organic phases were dried over magnesium sulfate and concentrated in vacuo. The crude compound was purified by FCC (1:9 EtOAc/hexane) to give **13q** as a white solid (84.7 mg, 33%).

5.4.3.6. Mechanistic Studies

5.4.3.6.1. Stainless Steel Free Reaction in a Planetary Ball-Mill

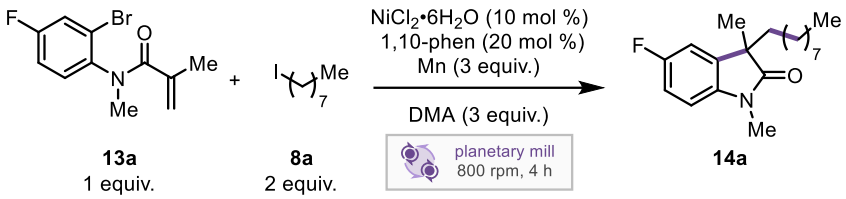

To a 12 mL zirconium oxide grinding bowl, equipped with 6, 3 g, 10 mm ceramic grinding balls, was charged **13a** (272.1 mg, 1 mmol, 1 equiv.), 1-iodooctane (361.1 µL, 2 mmol, 2 equiv.), nickel chloride hexahydrate (23.8 mg, 0.1 mmol, 10 mol %), 1,10-phenanthroline (36.0 mg, 0.2 mmol, 20 mol %), manganese powder (164.8 mg, 3 mmol, 3 equiv.), and *N,N*-dimethylacetamide (278.0 µL, 3 mmol, 3 equiv.). The lid was placed on the bowl and the bowl mounted on the central disc of the planetary mill. The reaction mixture was then milled at 800 rpm, for 2 hours (15 minute cycles, with

reverse cycles and 1 minute pauses in between cycles). Upon completion, the reaction mixture was transferred to a separatory funnel using EtOAc (50 mL) and water (50 mL). 1 M HCl (50 mL) was added, and the phases were separated. The aqueous phase was extracted two more times with EtOAc (2 x 50 mL) and the combined organic phases were washed with brine (30 mL). The organic phase was dried over magnesium sulfate and concentrated in vacuo. After concentrating in vacuo, the crude material was analysed by ^{19}F NMR using (trifluoromethyl)benzene as an internal standard. NMR yield of **14a**: 48%.

5.4.3.6.2. Radical Clock Experiment

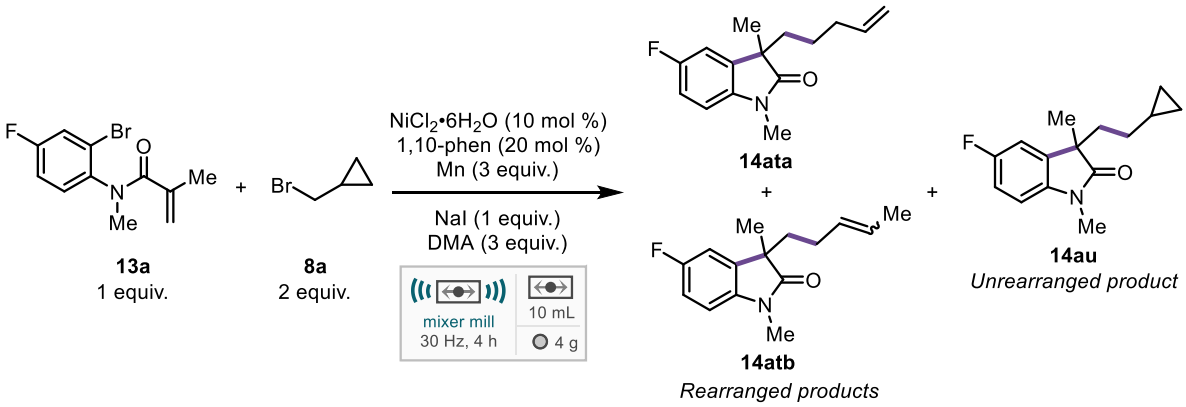

To a 10 mL stainless-steel jar, equipped with a 4 g, 10 mm stainless-steel ball, was charged **13a** (272.1 mg, 1 mmol, 1 equiv.), (bromomethyl)cyclopropane (194.2 µL, 2 mmol, 2 equiv.), nickel chloride hexahydrate (23.8 mg, 0.1 mmol, 10 mol %), 1,10-phenanthroline (36.0 mg, 0.2 mmol, 20 mol %), manganese powder (164.8 mg, 3 mmol, 3 equiv.), sodium iodide (149.9 mg, 1 mmol, 1 equiv.), and *N,N*-dimethylacetamide (278.0 µL, 3 mmol, 3 equiv.). The jar was closed and placed on the mixer mill for 4 hours, at 30 Hz. Upon completion, the reaction mixture was transferred to a separatory funnel using EtOAc (50 mL) and water (50 mL). 1 M HCl (50 mL) was added, and the phases were separated. The aqueous phase was extracted two more times with EtOAc (2 x 50 mL) and the combined organic phases were washed with brine (30 mL). The organic phase was dried over magnesium sulfate and concentrated in vacuo. The crude compound was purified by FCC (1:9 EtOAc/hexane) to give the rearranged products **14ata** and **14atb** as a yellow oil, as an inseparable mixture, in an approximately 3:1 ratio (104.1 mg, 42%) $\mathbf{R_f}$ = 0.20 (1:4 EtOAc/hexane); $\mathbf{\nu_{max}/cm^{-1}}$ (film): 2930, 1705, 1493, 1468, 1443, 1348, 1180, 1115, 966, 907, 868; Data for major isomer (**14ata**), **^{1}H NMR** (300 MHz, $CDCl_3$) δ_H: 7.00 – 6.88 (m, 2H), 6.74 (ddd, *J* = 8.3, 4.1, 2.5, 1H), 5.64 (ddt, *J* = 17.0, 10.2, 6.7, 1H), 4.95

– 4.86 (m, 2H), 3.19 (s, 3H), 2.06 – 1.82 (m, 2H), 1.77 – 1.64 (m, 1H), 1.56 – 1.49 (m, 1H), 1.34 (s, 3H), 1.16 – 0.82 (m, 2H); **^{13}C {^{1}H} NMR** (101 MHz, $CDCl_3$) δ_C: 180.5, 159.5 (d, *J* = 241.4), 139.4 (d, *J* = 2.0), 138.2, 136.0 (d, *J* = 8.1), 115.0, 113.9 (d, *J* = 23.2), 110.8 (d, *J* = 24.2), 108.4 (d, *J* = 8.1), 49.0 (d, *J* = 2.0), 38.0, 33.8, 26.4, 23.9, 23.8; **^{19}F {^{1}H} NMR** (376 MHz, $CDCl_3$) δ_f: -120.86; Selected data for minor isomer (**14atb**), **^{13}C {^{1}H} NMR** (101 MHz, $CDCl_3$) δ_C: 130.0, 125.6, 110.9 (d, *J* = 25.3), 49.0 (d, *J* = 2.0), 38.1, 28.0, 24.1, 18.0; **^{19}F {^{1}H} NMR** (376 MHz, $CDCl_3$) δ_f: -120.97; **HRMS** (ES) calculated for $[C_{15}H_{19}NOF]^+$ $(M+H)^+$: m/z 248.1451 found 248.1450 (-0.4 ppm).

5.4.3.6.3. Radical Trapping Experiments

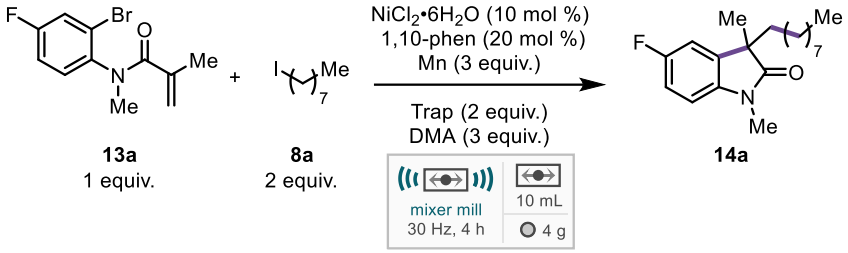

To a 10 mL stainless-steel jar, equipped with a 4 g, 10 mm stainless-steel ball, was charged **13a** (272.1 mg, 1 mmol, 1 equiv.), 1-iodooctane (361.1 µL, 2 mmol, 2 equiv.), nickel chloride hexahydrate (23.8 mg, 0.1 mmol, 10 mol %), 1,10-phenanthroline (36.0 mg, 0.2 mmol, 20 mol %), manganese powder (164.8 mg, 3 mmol, 3 equiv.), either TEMPO (313 mg, 2 mmol, 2 equiv.) or BHT (440.7 mg, 2 mmol, 2 equiv.), and *N,N*-dimethylacetamide (278.0 µL, 3 mmol, 3 equiv.). The jar was closed and placed on the mixer mill for 4 hours, at 30 Hz. Upon completion, the reaction mixture was transferred to a separatory funnel using EtOAc (50 mL) and water (50 mL). 1 M HCl (50 mL) was added, and the phases were separated. The aqueous phase was extracted two more times with EtOAc (2 x 50 mL) and the combined organic phases were washed with brine (30 mL). The organic phase was dried over magnesium sulfate and concentrated in vacuo. After concentrating in vacuo, the crude material was analysed by ^{19}F NMR and LR-MS to detect any products or radical trapped adducts. NMR yields of **14a**: with TEMPO <2%; with BHT 45%.

5.5. Bibliography

1 D. Huang, X. Wang, X. Wang, W. Chen, X. Wang and Y. Hu, *Org. Lett.*, 2016, **18**, 604–607.

2 J. M. Shikora and S. R. Chemler, *Org. Lett.*, 2018, **20**, 2133–2137.

3 W. W. Yao, R. Li, J. F. Li, J. Sun and M. Ye, *Green Chem.*, 2019, **21**, 2240–2244.

4 D. M. Barber, H. Sanganee and D. J. Dixon, *Chem. Commun.*, 2011, **47**, 4379–4381.

5 T. Jin, M. Yu, L. Liu, Y. Zhao and T. Li, *Synth. Commun.*, 2006, **36**, 2339–2344.

6 J. Kraïem, D. Ghedira and T. Ollevier, *Green Chem.*, 2016, **18**, 4859–4864.

7 J. K. Laha, K. P. Jethava, K. S. S. Tummalapalli and S. Sharma, *Eur. J. Org. Chem.*, 2017, **2017**, 4617–4624.

8 S. Cinar, B. Temelli and C. Unaleroglu, *Tetrahedron Lett.*, 2014, **55**, 544–547.

9 T. Jin, G. Feng, M. Yang and T. Li, *Synth. Commun.*, 2004, **34**, 1277–1283.

10 P. F. Koh, P. Wang, J. M. Huang and T. P. Loh, *Chem. Commun.*, 2014, **50**, 8324–8327.

11 J. H. Wynne, S. E. Price, J. R. Rorer and W. M. Stalick, *Synth. Commun.*, 2003, **33**, 341–352.

12 D. Chen, X. Chen, T. Du, L. Kong, R. Zhen, S. Zhen, Y. Wen and G. Zhu, *Tetrahedron Lett.*, 2010, **51**, 5131–5133.

13 R. Matsubara, F. Berthiol and S. Kobayashi, *J. Am. Chem. Soc.*, 2008, **130**, 1804–1805.

14 R. N. Ram and A. A. Khan, *Synth. Commun.*, 2001, **31**, 841–846.

15 I. Khan, M. Manzotti, G. J. Tizzard, S. J. Coles, R. L. Melen and L. C. Morrill, *ACS Catal.*, 2017, **7**, 7748–7752.

16 M. Winkler, L. Martínková, A. C. Knall, S. Krahulec and N. Klempier,

Tetrahedron, 2005, **61**, 4249–4260.

17 M. Shi and Y. M. Xu, *Eur. J. Org. Chem.*, 2002, **2002**, 696–701.

18 V. S. Silva, T. A. Tolentino, T. C. A. F. Rodrigues, F. F. M. Santos, D. F. S. Machado, W. A. Silva, H. C. B. De Oliveira and A. H. L. Machado, *Org. Biomol. Chem.*, 2019, **17**, 4498–4511.

19 Y. Iwabuchi, M. Nakatani, N. Yokoyama and S. Hatakeyama, *J. Am. Chem. Soc.*, 1999, **121**, 10219–10220.

20 Y. Nakamoto, F. Urabe, K. Takahashi, J. Ishihara and S. Hatakeyama, *Chem. Eur. J.*, 2013, **19**, 12653–12656.

21 E. C. Hansen, D. J. Pedro, A. C. Wotal, N. J. Gower, J. D. Nelson, S. Caron and D. J. Weix, *Nat. Chem.*, 2016, **8**, 1126–1130.

22 E. C. Hansen, C. Li, S. Yang, D. Pedro and D. J. Weix, *J. Org. Chem.*, 2017, **82**, 7085–7092.

23 Y. Sumida, T. Sumida and T. Hosoya, *Synthesis*, 2017, **49**, 3590–3601.

24 D. A. Everson, J. A. Buonomo and D. J. Weix, *Synlett*, 2014, **25**, 233–238.

25 L. L. Anka-Lufford, K. M. M. Huihui, N. J. Gower, L. K. G. Ackerman and D. J. Weix, *Chem. Eur. J.*, 2016, **22**, 11564–11567.

26 Y. L. Su, G. X. Liu, J. W. Liu, L. Tram, H. Qiu and M. P. Doyle, *J. Am. Chem. Soc.*, 2020, **142**, 13846–13855.

27 O. Vechorkin, V. Proust and X. Hu, *J. Am. Chem. Soc.*, 2009, **131**, 9756–9766.

28 G. Dilauro, C. S. Azzollini, P. Vitale, A. Salomone, F. M. Perna and V. Capriati, *Angew. Chem. Int. Ed.*, 2021, **60**, 10632–10636.

29 Y. Hu, Z. Wang, H. Luo, H. Jin, Y. Liu and B. Zhou, *Org. Biomol. Chem.*, 2021, **19**, 3834–3837.

30 X. Liu, B. Li and Z. Gu, *J. Org. Chem.*, 2015, **80**, 7547–7554.

31 Y. Feng, S. Yang, S. Zhao, D. P. Zhang, X. Li, H. Liu, Y. Dong and F. G. Sun, *Org. Lett.*, 2020, **22**, 6734–6738.

32 M. Pørez-Gómez and J.-A. García-López, *Angew. Chem. Int. Ed.*, 2016, **55**, 14389–14393.

33 D. Shukla and S. A. Babu, *Adv. Synth. Catal.*, 2019, **361**, 2075–2093.

34 J. Du, X. Wang, H. Wang, J. Wei, X. Huang, J. Song and J. Zhang, *Org. Lett.*, 2021, **23**, 5631–5635.

35 K. Wang, Z. DIng, Z. Zhou and W. Kong, *J. Am. Chem. Soc.*, 2018, **140**, 12364–12368.

36 P. Kilaru, S. P. Acharya, P. Zhao, *Chem. Commun.*, 2018, **54**, 924–927.

37 W. I. Nicholson, F. Barreteau, J. A. Leitch, R. Payne, I. Priestley, E. Godineau, C. Battilocchio and D. L. Browne, *Angew. Chem. Int. Ed.*, 2021, **60**, 21868–21874.